University of Leuven, Belgium
Group Biomedical Sciences
Doctoral school of Mechanisms of Human Diseases
Department of Development and Regeneration
Cluster "Organ systems", Research Unit
Female Pelvic Floor Disorders

&

Charles University in Prague, Czech Republic
Third Faculty of Medicine
Doctoral school of Experimental Surgery
Institute for the Care of Mother and Child

MODERN TECHNOLOGIES IN THE ASSESSMENT AND TREATMENT OF PELVIC ORGAN PROLAPSE
–
EXPERIMENTAL AND CLINICAL STUDIES

Iva URBANKOVA

Jury:
Promoters: Prof. Dr. Jan Deprest
                  Doc. MUDr. Ladislav Krofta, CSc.

Chair: Prof. Dr. Dirk Timmerman
                  Prof. Dr. Tania Roskams
Secretary: Prof. Dr. Frank Van der Aa
Jury members: Prof. Dr. André D´Hoore
                  Prof. Dr. Laurent de Landsheere
                  Prof. Dr. Stefano Salvatore
                  Prof. MUDr. Jaromír Mašata CSc.
                  Prof. BSc. Sheila MacNeil
                  Prof. MUDr. David Kachlík, PhD

Leuven, 18.9.2017

Doctoral thesis in medical sciences

This thesis was submitted as partial fulfillment of the requirements for the degree of 'Doctor in Medical Sciences'.

For Charles University in Prague

For KU Leuven

Personal contribution: Personal contribution is identified in each chapter (experiment). Data in clinical part (Chapter 2) were mostly collected by research nurses, and I evaluated the data, performed statistical analysis and wrote the manuscript, In the experimental part (Chapters 3 – 7) I designed the experiment under the supervision of my promoter Prof. Jan Deprest. Majority of experiments was carried out and evaluated with help of research fellows quoted as co-authors in individual chapters and with help of lab technicians. I have written all the manuscripts included in the thesis as well as the introduction and discussion. My promoters and co-authors edited the manuscript and individual chapters, respectively.

Conflict of interest: Conflicts of interest are quoted in each chapter. There were several financial supporters including unconditional grants or Europe Union funding. Providers did not interfere with study designs, data collection or data interpretation.

In Leuven, 18.9.2017

Urbankova Iva

PDF version could be downloaded:

TABLE OF CONTENTS

LIST OF ABBREVIATIONS

α-SMA	smooth muscle actin α
AC	anal canal
ACM	acellular collagen matrix
AI	anal incontinence
ATLA	*arcus tendineus levatoris ani*
B	bladder
BMI	body mass index
BSA	bovine serum albumin
C	cervix
CM	coccygeus muscle
CVe	constrictor vestibuli
EAS	external anal sphincter
ECM	extracellular matrix
EDA	epidural analgesia
EDTA	Ethylene-diamine-tetraacetic acid
EOM	external obturator muscle
ER-α	Estrogen receptor α
ESA	effective surface area
FBGC	foreign body giant cells
FDA	Food and Drug Administration
GRC	graft-related complication
GAD	glutaraldehyde
H&E	hematoxylin-eosin
HRT	hormonal replacement therapy
IAS	internal anal canal
ICIQ-SF	International Consultation on Incontinence Questionnaire
ICS	International Continence Society
IOM	internal obturator muscle
IQR	interquartile range
IUGA	International UroGynecological Association
IUS	internal urethral sphincter
LAM	levator ani muscle
LMR	longitudinal muscle of the rectum
MHD	modified Hausdorff distance
MR	magnetic resonance
OVX	ovariectomy
P	pubis
PAS	periodic acid-Shiff
PB	perineal body
PBS	phosphate buffered saline
PFD	pelvic floor dysfunction
PFT	pelvic floor physiotherapy
PISQ-12	Pelvic Organ Prolapse/Urinary Incontinence Sexual Questionnaire
PMN	polymorphonuclear
POP	pelvic organ prolapse
PP	polypropylene
PVDF	polyvinylidene fluoride
R	rectum
RE	rectal epithelium
RMDS	rood mean square difference
RVP	rectovaginal pouch
RVS	rectovaginal septum
S	spine

SCENIHR Scientific Committee on Emerging and Newly Identified Health Risks
SUI   stress urinary incontinence
U   urethra
UH   uterine horn
UI   urinary incontinence
Ur   urethral muscle
Ut   uterus
V   vagina
VEX   vacuum extraction

CHAPTER 1: INTRODUCTION AND STUDY AIMS

ANATOMY OF THE PELVIC FLOOR

The normal position and configuration of the pelvic organs are maintained by a complex system and dynamic interactions of muscles and connective tissue attachments that create the pelvic floor, with the bony pelvis. Skeletal support is provided by a pair of hip bones joined by the cartilaginous *symphysis pubis*, and to the sacrum and coccyx. The pelvis is further stabilized with a pair of *sacrotuberous* and *sacrospinous* ligaments [1]. The inner surface of the pelvis is covered with the dorsally located *piriformis* muscle and by the *internal obturator* muscle. The latter is attached to the obturator membrane and on the surrounding parts of the ilium and ischium (Figure 1, 2).

Figure 1. Attachments of the pelvic fascia to the pubic bone (A), anterior perineal membrane (B), superior fascia of the levator ani muscle (C), and perineal body (D). PS, pubic symphysis; ATLA, arcus tendineus levator ani; ATFP, arcus tendineus fasciae pelvis; ATFR, arcus tendineus fasciae rectovaginalis; OIM, obturator internus muscle; LA, levator ani muscle; IS, ischial spine; PM, piriformis muscle; U, urethral outlet; V, vaginal outlet; PB, perineal body; R, rectal outlet; CM, coccygeus muscle.
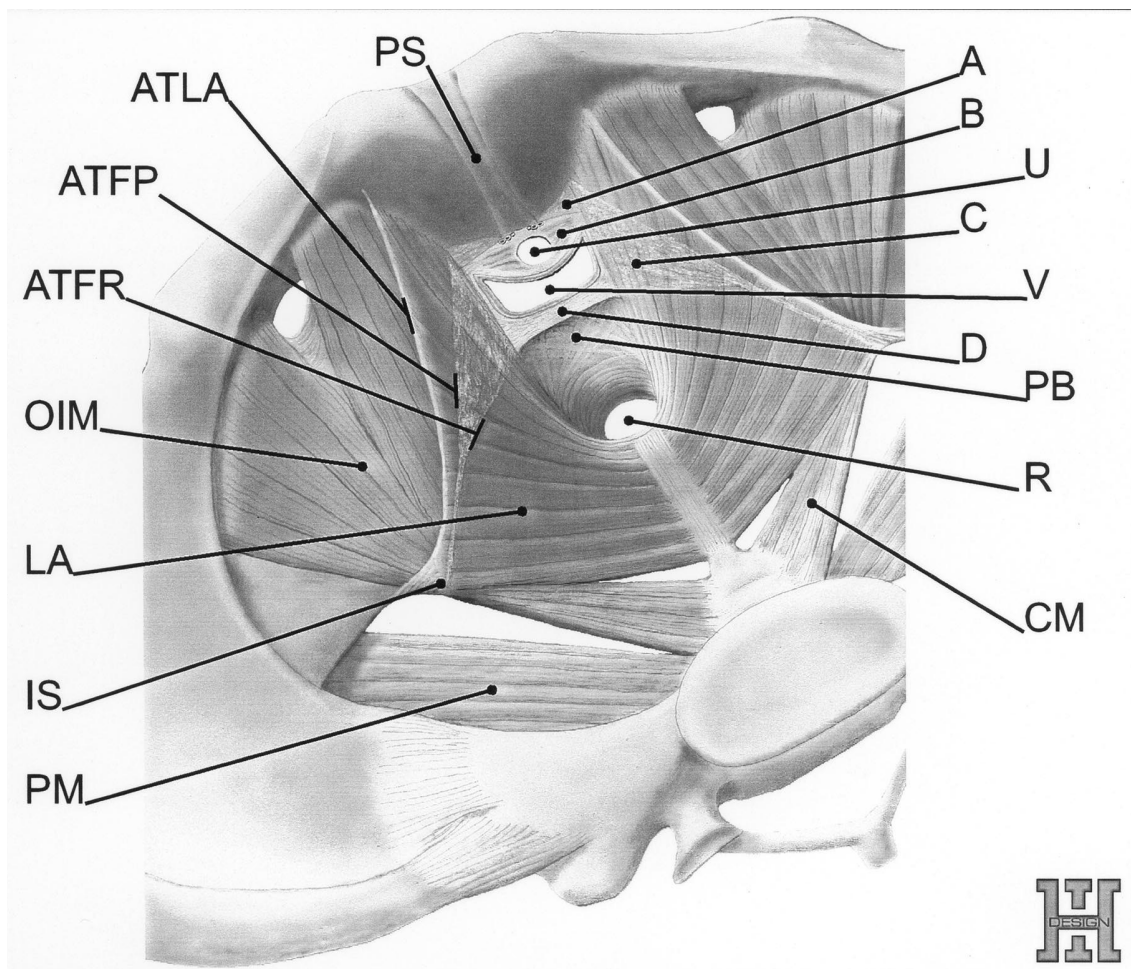
Figure 2. *Left lateral view from above the female pelvis. The vagina, endopelvic fascia, and levator ani muscle are cut in the sagittal plane. Urethra, urinary bladder, and rectum have been removed. OIM, obturator internus muscle; PCF, pubocervical fascia; ATLA, arcus tendineus levator ani; LA, levator ani muscle; ATFP, arcus tendineus fasciae pelvis; PS, pubic symphysis; VW, vaginal wall; RVF, rectovaginal fascia; ATFR, arcus tendineus fasciae rectovaginalis; PM, perineal membrane; PB, perineal body; EAS, external anal sphincter; SC, space of Courtney; ACR, anococcygeal raphe; ACL, anococcygeal ligament; PM, piriformis muscle; CL, cardinal ligament; USL, uterosacral ligament; C, cervix of the uterus; CM, coccygeus muscle; Co, coccyx; SP, sacral plexus.*
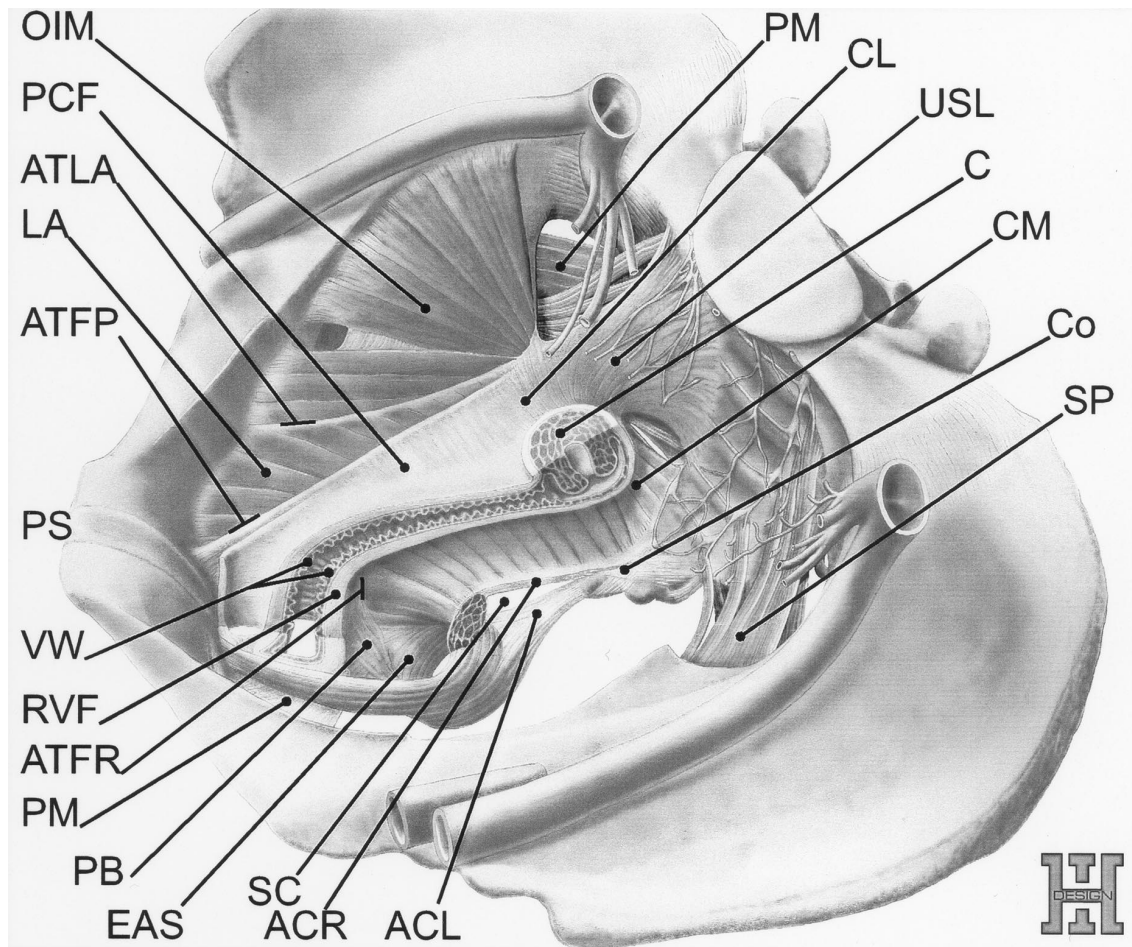
Table 1. *Subdivisions of the levator ani muscle and their attachments and insertion points [3, 4].*

Subdivision	Ventrolateral attachment	Dorso-medial insertion
Pubovaginalis	Dorsal aspect of the pubis	Vaginal wall
Puboperinealis		Perineal body
Puboanalis		Intersphincteric insertion
Puborectalis	Dorsolateral aspect of the pubis	Sling around the rectum
Iliococcygeus	Fascia obturatoria, ischium	Iliococcygeal raphe (coccyx)

The pelvic floor diaphragm is the muscular support. It comprises of the dorsally located *ischiococcygeus*, which has in humans minimal function, yet in quadrupeds, it is well developed and responsible for tail movement. The main constituent is the *levator ani* muscle (LAM) complex. The LAM has three major parts; the *iliococcygeus, puborectalis*, and *pubococcygeus*, which is often further dived in three subdivisions; *pubovaginalis, puboperinealis*, and *puboanalis* (Table 1) [3]. The most ventral pubococcygeus provides an additional support to the urethra, vagina, and anus, and narrowing the urogenital hiatus. The U-shaped *puborectalis* forms a sling encircling the anorectal junction. Its basal tonus determines the anorectal angle and contributes to fecal continence. Finally, the *iliococcygeus* is medially attached to the coccyx and to the anococcygeal raphe. It forms a horizontally oriented shelf or the "levator plate" on which the rectum, upper vagina and the uterus rest.

The fascial support is a complex system with disunited nomenclature [5]. The visceral fascia covering pelvic organs continually transforms into the parietal fascia while covering structures on pelvic sidewalls such as the supplying vessels, nerves or lymphatics [5, 6]. The visceral part also called the endopelvic fascia, is firmly attached to the adventitia of individual organs. This three-dimensional structure embeds pelvic floor structures and organs, but typical fascia has not been histologically identified yet. The surgically separated tissue used for plication during prolapse surgery is actually the fibromuscular part of the vagina [7].

The transition of the endopelvic fascia to the pelvic side wall is attaching the rectum, vagina, and bladder by the rectovaginal, pubo/vesicovaginal fascia and by ligamentous structures such as the uterosacral or the cardinal ligaments. These mesentery-like structures contain vessels, nerves, smooth muscle cells, areolar and extracellular connective tissue (collagen, elastin etc.) [5]. Therefore they are not true ligaments but they still provide support to the genital system. The parietal fascia has several condensations serving as the lateral attachments for the endopelvic fascia (i.e. tendinous arch of the rectovaginal and pelvic fascias) and for the levator ani (tendinous arch of the levator ani – ATLA).

This complex supportive system was divided by DeLancey into three levels supporting the vaginal compartments and the uterus [8].

Level I: this level provides support to the apical compartment, which includes the cervix and proximal third of the vagina. Main support is provided by the cardinal and uterosacral ligaments. The cardinal ligaments or transversal cervical ligaments are laterally attached to posterolateral pelvic sidewall adjacent to the origin of the internal iliac artery. They are basically thick connective mesenteries caudally to the ureters enveloping the uterine artery, venous root draining the perivisceral venous plexus into the iliac vein, and pelvic plexus [6]. The uterosacral ligaments point in a posterolateral direction and their fibrous attachments extend from the muscular fasciae and presacral fascia corresponding to S1 – S4 vertebra [2]. The uterosacral ligaments contain fibrous attachments, autonomic nerve fibers from the inferior hypogastric plexus, hypogastric nerve and visceral branches of iliac vessels [6]. Additional support is provided by the rectovaginal and pubocervical fascia. Their cranial aspects and both pairs of ligaments form together a "pericervical ring" and provide support also to the upper vagina.

Level II: The middle part of the vagina is supported by the pubocervical and rectovaginal fascias. At this level, each fascia has its own attachment line (tendinous arch of the tendinous rectovaginal/pelvic fascias resp.) on the superior fascia of the LAM. Separated attachments of the anterior and posterior vaginal wall are reflected in the H-shaped cross section at this level. Cranially, both fascias and their attachments are merged giving a flat appearance to the vagina. Additionally, these fascias also support the bladder and rectum.

Level III: The most distal third of the vagina receives support via fusion of the pubocervical and rectovaginal fascia with the LAM, perineal body and perineal membrane. The perineal membrane is a 3-dimensional tissue structure surrounding the vagina and urethra. The ventral portion is a continuation of the para-urethral and paravaginal connective tissue that is laterally attached to the pubic bone nearby the insertion of the *arcus tendinous fascia pelvis*. It contains the *compressor urethrae* and urethrovaginal sphincter. On its cranial side of the ventral portion, the *pubococcygeal* part of the LAM is attached. The dorsal portion of the perineal membrane spans laterally from the perineal body and lateral vaginal wall to the *ischiopubic rami*. Its dorsal margin is parallel with the course of the superficial transverse perineal muscle.

EVOLUTION OF THE PELVIC FLOOR ACROSS SPECIES

The complex supportive system of the pelvic floor is crucial to the upright position in bipeds. In quadrupeds and occasional bipeds, the ischioccygeus is responsible for tail movements and the levator ani for retraction of the anus. During the evolution of human species, the LAM significantly changed its shape, attachments, and function. In quadrupeds, the main weight of the body was oriented perpendicular to the spine. Correspondingly in the pelvis, the main support for pelvic organs is the bony "pelvic floor" (pointing to what we consider pelvic bones) formed by the pubic bones and ischia [9]. Evolution of bipedalism shifted the load of the body weight parallels to the spine. The spine, pelvis, and hips adapted accordingly. The spine became curved and the *erector spine* hypertrophic. The pelvis shortened, widened and became more vertical and curved. Lastly, the cortical bone in the femoral neck reduced [10]. As a result, the pelvic floor became horizontal and critical for assisting incontinence and prevention of pelvic organ prolapse. Compared to quadrupeds the human pelvic floor and the LAM are extremely well developed, which is mirrored by the size and orientation of the ischial spines that serve as the attachment for the tendinous arc of the endopelvic fascia [10].

Following the adaptation for bipedalism, the brain size progressively increased from about 500,000 years ago. This so-called encephalization necessitated dramatic changes in the birth mechanics including molding of the fetal head and intra-pelvic rotation [11]. There are no other primates or mammals whose birth mechanism is so complex. These evolutionary advantages are probably the origins of traumatic birth injuries seen today [11].

Differences in the evolution between bi- and quadrupeds are important for understanding the anatomical and functional variation between human and animals models used for research. Since there are no other bipedal mammals one has to accept certain differences between the experimental and clinical setup. The most appropriate animal model would be to use other primates; however, in Europe, their use is ethically not accepted – unless of vital importance.

PELVIC FLOOR TROUGH THE LIFESPAN

In early adulthood, the pelvic floor reaches its maximal functional capacity based on the genetic background, nutrition, and environment. As the subject ages, the quality of the pelvic floor gradually declines (Figure 3). Three important factors are taken into consideration by this model. One is the initial background, second is vaginal birth and third are later inciting factors, all along the timeline of aging. Some predisposed women with lesser initial pelvic floor function may become symptomatic during their lives without any vaginal delivery or additional inciting factors [12].

Figure 3. *The lifespan model, adapted from De Lancey et al.* [12]
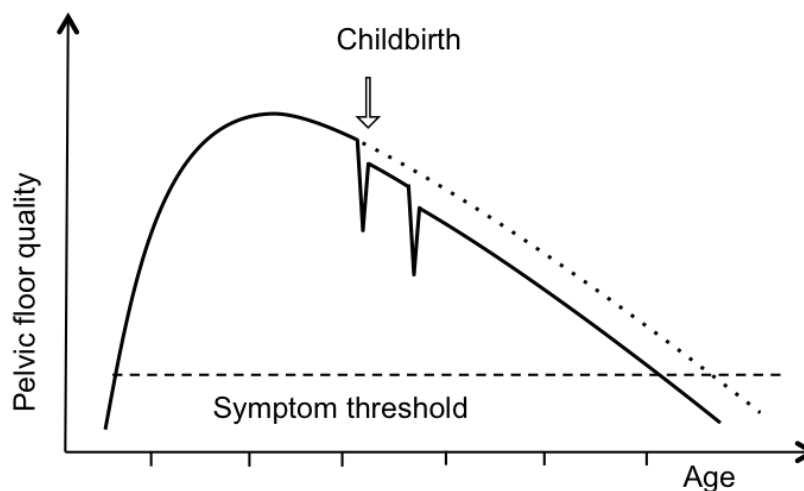
The inciting factors such as pregnancy and childbirth induce the most serious alteration to the pelvic floor. While pregnancy on itself plays a role, vaginal childbirth and more importantly its second stage is associated with a dramatic and dynamic change of the pelvic floor that may cause a varying degree of structural and functional changes [13, 14]. The degree of recovery varies among individuals. In the worst cases, the pelvic floor dysfunction is symptomatic shortly after delivery and may never recover. The risk of serious pelvic floor damage can be increased by several factors which are summarized in Table 2. On the long-term, additional vaginal deliveries will accumulate changes in the pelvic floor and thus increase the risk of PFD [15].

Following the reproductive period, the pelvic floor is expected to provide sufficient function for next 40 – 50 years. Aging is not the only cause of functional decline. Other intervening factors include increased stress and strain (i.e. occupational lifting, chronic cough, chronic constipation, obesity), chronic steroid use, disuse muscular atrophy, and in some high-impact aerobics or diabetic peripheral neuropathy [12]. The individual speed of decline and threshold level beyond which the pelvic floor disorder becomes symptomatic, explain why some women are symptomatic only in their 50's or later.

Table 2. Inciting factors for PFD development.

Predisposing maternal-fetal factors	Pelvic floor shape and size
	Macrosomic infant
	Fetal head position – occipito-posterior
Obstetrical interventions	Forceps
	Prolonged second stage of delivery
Mechanisms of injury	Muscle avulsion
	Connective tissue rupture
	Nerve avulsion
	Nerve compression

PREGNANCY INDUCED CHANGES IN PELVIC FLOOR

During pregnancy, hormones affect the biochemical and structural composition of the extracellular matrix and tissues of the pelvic floor. As a result, the viscoelastic properties of pelvic floor structures are changed to allow gradual stretching during fetal head descent during the second stage of labour. Increased relaxation of the pelvic floor could be observed clinically as a more descending uterus yet mainly larger genital hiatus [16]. Hormonal and biochemical pathways are not yet fully understood. Experimental observations in animal models have shown decreased vaginal wall stiffness and smooth muscle contractility, elongation of the LAM fibrils with an increase in collagen V content, extracellular matrix degradation followed by reconstitution after delivery [17–20]. These changes occur irrespective of the delivery mode and only part of the adaptations is restored to the pre-pregnancy status. The degree of recovery is dependent on species with almost complete restoration observed only in rodents [19].

The permanent changes in experimental animals include mainly increased vaginal capacity, collagen and changes in its organization [20–22]. For women, the pelvic floor anatomy is far more affected by the vaginal delivery; these being detailed below.

VAGINAL DELIVERY INDUCED CHANGES IN THE PELVIC FLOOR

In the second stage, the pelvic floor is exposed to extremely high pressure and is being stretched. The process by itself and its duration result in several mechanisms of injury, i.e. muscle avulsion, connective tissue rupture, nerve avulsion or compression resulting in hypoxia-reperfusion injury.

Avulsion of the LAM occurs in 13 – 36% of primiparous women [14]. Typically, the pubococcygeus muscle origin is torn from its bony origin on the pubis and ATLA [13, 23]. At the time of delivery, avulsion is rarely detected, not possible to treat and it also does not heal over time [24]. Based on finite element modeling, the LAM is stretched during the crowning of the head and deflection up to 3.5-fold of its initial length [25–27].

There is no agreement on the exact location of a maximal stretch, but there is no doubt that it stretches beyond what can be physiologically tolerated. We recently processed unique images from a vaginal delivery imaged by MR and calculated that the posterior medial aspect of the LAM is stretched by 248% [28]. In experimental conditions, muscle stretch by up to 1.5 already induces a significant posttraumatic force deficit [14].

Extreme distension of the LAM may also result in serious micro traumatisation followed by fibrosis and malfunction. Clinically, this corresponds to so-called "ballooning", which is a term for an oversized genital hiatus during Valsalva. Increased genital hiatus dimensions increase the risk of prolapse and prolapse recurrence after the primary surgical procedure [29–31].

The overstretch affects also the connective tissue comprising the endopelvic fascia, the rectovaginal and vesicovaginal septum. Resulting ruptures predispose women to develop various types of pelvic organ prolapse or stress urinary incontinence due to a hypermobile urethral-vesical junction.

Lastly, vaginal delivery interferes with pelvic floor innervation. The combination of stretch, compression, and ischemia may result in a neuropathic injury, which is detectable by electromyography of the LAM in one-quarter of women after a single vaginal delivery. Up to 40% of women display increased pudendal nerve terminal motor latency that may recover within two-thirds of them. The urethral rhabdosphincter is too small for reliable electromyography; nonetheless, a reduction in urethral closure pressure after vaginal delivery has been shown [14].

AGE AND MENOPAUSE INDUCED CHANGES

Changes in the pelvic floor induced by aging and menopause are difficult to discern as PFD usually become obvious in women over 60 years of age [32]. Apart from them, individual lifestyle and health significantly contribute to the quality of the pelvic floor. Heavy lifting, chronic cough or overweight may lead to PFD even without a single pregnancy or delivery [33].

Age-induced changes observed in other tissues including progressive molecular and cell transformation induced by free radicals, non-enzymatic glycosylation, and apoptosis, were also identified in the pelvic floor [34]. As a result of progressive changes, extracellular matrix (ECM) proteins such as elastin or collagen may be compromised by the accumulation of pathological cross-links leading to the increase in tissue stiffness [35]. There are fewer satellite cells and mitochondria in the LAM that document compromised tissue regeneration [34]. The effect of aging with the subtraction of the effect of delivery has been documented in nulliparous women, showing a gradual decrease in urethral closure pressure [36].

Apart from its role in reproduction, estrogen is involved in tissue metabolism and cell growth [37, 38]. Estrogen receptors are widely expressed

by cells in the vagina, rectum, bladder, urethra and in the supportive structures such as the sacrouterine ligament, LAM or in the endopelvic fascia [38]. They are involved in the synthesis and metabolism of collagen, elastin, hyaluronic acid, epithelial and smooth muscle proliferation and increase the blood flow. Lack of estrogens manifests as the genitourinary syndrome, which includes a broad spectrum of subjective complaints and objective findings, such as vulvar atrophy, POP, urinary incontinence or vaginal and introital stenosis [37]. Lack of estrogens accelerates or promote changes induced by aging [34, 39]. However, some yet not all symptoms improve with estrogen administration [37].

PELVIC ORGAN PROLAPSE

Pelvic organ prolapse (POP) is defined as any abnormal descent of pelvic organs through the vagina [40]. It may involve the anterior or posterior vaginal wall, as well as the uterus (cervix) or, when the uterus is absent, the apex of the vagina (vaginal vault). Our work focuses on POP. POP is however only one of many clinical conditions, encompassed by the term pelvic floor dysfunction, including also urinary incontinence, voiding, defecation and sexual dysfunction [40]. All of them are associated physical symptoms that have a significant emotional and body image impact, resulting in psychosocial distress, social isolation, anxiety, and depression (Table 3) [41, 42]. The impact on quality of life is comparable to that of stroke, dementia, tension-type headaches or Parkinson disease [43–45]. The symptoms of women presenting with POP are displayed in table 3. As one can see, they extend further than complaints typical for the vaginal descent, yet involve urinary, bowel and sexual function. Recent epidemiologic studies have demonstrated how intimately these problems are related and cluster in certain patterns [46].

Table 3: Typical symptoms of women with pelvic organ prolapse [47]

Vaginal/sexual	Urinary	Bowel
Sensation or protrusion of vaginal bulge	Incontinence	Incontinence of flatus or stool
Seeing or feeling vaginal bulge or protrusion	Frequency and urgency	Urgency to defecate
Pressure	Weak or prolonged urinary stream	Strain during defecation
Heaviness	Hesitancy	Digital evacuation to complete defecation
Dyspareunia	Feeling of incomplete emptying	Feeling of incomplete emptying
	Manual reduction of prolapse to start or to complete voiding	Splinting, or pushing on or around the vagina or perineum, to start or complete defecation
	Position change to start or to complete voiding	Feeling of blockage or obstruction during defecation

SURGICAL REPAIR OF POP

Symptomatic patients may seek therapy. Pelvic floor muscle training can be prescribed which has shown to slow the progression of anterior prolapse in older women [48]. Another non-surgical option is to use a pessary. Pessaries come in various shapes and sizes, and about two women in three will better, yet there are several limitations to these as well [49]. The mainstay of therapy is a surgery.

In last 50 years, the age-adjusted rate for POP surgical procedures in the US has decreased from 2.93 per in 1979 to 1.52 in 2006 per 1000 women. This drop is apparent mainly among those below 50 years of age [50]. Among older women, the age-adjusted rate is stable around 2.8 per 1000 [50]. The rate of surgical procedures is decreasing together with changes in obstetrical practice. For instance, use of a mid pelvic forceps was highly correlated with prolapse surgery 10 years later [51]. Such instruments are much less used now. While the Caesarean section rate is increasing, vaginal extraction procedures have dropped to 3.9 per 1000 women. However, it is not clear yet what will bring the increasing age at first delivery, a more sedentary lifestyle and the pandemic of obesity, diabetes and civilization diseases, longer life expectancy, higher demands on the quality of life and increased activity in the elder [52, 53].

As the elder population is growing, the absolute numbers of surgical procedures are still high. In 2016, 19.2% of the EU-28-population was over 65 years (5.4 % >80 years), and by 2030 that will be 23.9 % (7.2 %, >80 years) [53]. The lifetime risk for undergoing a surgical procedure is increasing with age reaching 18.7% by the age of 80 [54]. POP surgery rate of POP surgery peaks among women between 45-50 and 70-75 years of age [51]. Typical time to symptomatic presentation of POP is around 33 years after first delivery [55]. Shorter time to the presentation is typical for women who had forceps delivery and are older at the time of the first delivery [55]. According to current prediction models based on women demanding care for some type of PFD, we can expect an up to 35% growth in demand in any therapy in the upcoming decades [56, 57].

Surgery essentially involves suspension of the prolapsed vagina to restore normal anatomy hence also function. Reconstruction of the vaginal support using endogenous (native) tissues is the most common strategy. Prolapse surgery may be done by either abdominal or vaginal approach. In the vaginal approach procedures typically include anterior and posterior colporrhaphy for mid-vaginal anterior and posterior vaginal prolapse. When there is prolapse in the middle compartment, the cervix or vaginal vault is fixed either to the uterosacral ligaments, the sacrospinous ligament or to the anterior longitudinal ligament over the sacrum (sacrocolpopexy). For the latter typically a synthetic mesh is used. More rare operations suspend it to the iliopectineal ligament or iliococcygeal muscle.

TRENDS IN PROLAPSE SURGERY

The efficacy of different prolapse surgeries hence their respective indications are a matter of ongoing debate. There is evidence that vaginal reconstructive surgeries including vaginal colporrhaphy and apical suspension, that use native tissues, are prone to recurrence. 29-40% of patients were reported to have undergone reoperation within the first 3 years of these traditional surgeries [58, 59]. To reduce recurrence, use of synthetic meshes, similar to the ones used in hernia repair, showed promise and were approved for use by the FDA in 2004 for transvaginal repair [60, 61]. There was quite some confidence in those implant materials in the gynecologic community, as synthetic implants were already used for sacrocolpopexy, and were very successful when used as tapes for stress incontinence.

The contemporary concept of use of meshes and tapes is based on the "integral theory" and aims to restore the original pelvic floor anatomy by reinforcing and re-attaching ligaments and fascias to their original insertion points [62]. The reinforcement material could be synthetic (durable and resorbable, derived from various species (both xenografts or allografts), or obtained from the patients from a different anatomical location such as *fascia lata*. In terms of long-term efficacy, biological grafts and absorbable synthetic implants do not provide any advantage as we know today [63]. Neither do the autologous grafts, which in addition increase surgical morbidity at the donor location [64]. Synthetic implants were most widely used, and on a review of that literature, its benefit has been shown for the anterior and central compartments [63]. This comes however at a price.

A wide spectrum of permanent synthetic implants has been available but none of them seems ideal. Their employment is associated with graft-related complications (GRC) in 10 – 20 % of women including i.e. mesh exposure, pain, or dyspareunia [64]. The GRC rate varies according to the product and anatomical location. Moreover, augmented vaginal tissue is often atrophic, devascularized and thus structurally compromised. Inferior tissue quality is at higher risk of poor tissue ingrowths into the graft and suboptimal healing which may result in graft exposure (wrongly referred to, yet better known as erosion) to the vagina or erosion into adjacent viscera.

GRC and complications related to the insertion techniques have led up to thousands of lawsuits against surgeons and manufacturers. As a result, many transvaginal meshes have been removed from the market and also from the clinical practice. The available ones are mostly made from a lightweight large porous polypropylene, which showed the least risky profile. They are recommended mainly for the treatment of recurrent prolapse or in women with increased risk of recurrence such as those having obesity, at a younger age, chronically increased intra-abdominal pressure or levator ani avulsion – the list remaining very controversial [65, 66]. Currently, implants are available from several manufacturers but many do not have a sufficiently established safety and efficacy [63, 67].

As a response, international authorities recommended further research into current techniques, materials, novel products and pathophysiology of GRC development [40, 68, 69]. To provide clinically applicable results, it was recommended that research should be performed in models that mimic as closely as possible the human vagina, test the biocompatibility of implants and their effect on the biomechanical behavior of grafted tissue.

ANIMAL MODELS FOR TRANSVAGINAL SURGERY

Since one of the surgical approaches is transvaginal repair, and one would like to test materials or procedures experimentally, animal models are required that are sufficiently large to perform vaginal implantation and obtain sufficiently large specimens for biomechanical, histological or biochemical testing. Animal models suggested for this type of experiments include rabbits, non-human primates and lately also sheep.

Rabbits allow vaginal implantation yet their vaginal anatomy, healing and immune response significantly differ from humans [70]. The ideal model animals intuitively are non-human primates. There is an extensive research done in countries that allow their employment, like the United States of America. Surgical procedures however mostly include transabdominal implantation on the vagina to mimic sacrocolpopexy. To our knowledge, no vaginal surgery has been described in these species. However, pelvic floor changes induced by pregnancy, delivery, and aging have documented similarities to what is observed in humans [21, 71–73]. Moreover, some primates naturally develop pelvic organ prolapse [74]. Their utilization is extremely expensive and in Europe, research on primates is ethically and legally considered as unacceptable. This is also the case at the KU Leuven, unless under very strict indications.

A more recently employed model is sheep, they are widely available and relatively easy to handle. Sheep are used in other fields, like sexually transmittable diseases, orthopedics, cardiac surgery, fetal surgery because their size, anatomy, inner vaginal environment, placentation and fetal development are sufficiently similar to human [75–77]. We, therefore, considered the ewe as a suitable model to explore its use in our studies.

SPECIFIC STUDY AIMS AND HYPOTHESIS

The clinical study was completed in the Institute for the Care of Mother and Child, Third Faculty of Medicine of the Charles University in Prague, Czech Republic. This prospective cohort study aims:

- Aim: To determine the occurrence of, and major risk factors for pelvic floor dysfunction among primiparous women one year after delivery.
  Hypothesis: First pregnancy and vaginal delivery have an adverse effect on the pelvic floor function one year postpartum. Women at higher risk of pelvic floor dysfunction could be identified before and shortly after the first delivery

Experimental worked was done at the Centre for Surgical Technologies of the Group Biomedical Sciences, KU Leuven, Belgium and was dedicated to the description of, and experiments in a large animal model for vaginal surgery. These studies more specifically aimed to:

- Aim: To characterize the pelvic floor anatomy of the virgin ewe and compared it to that of women.
  Hypothesis: Sheep pelvic have to a certain extent similar to the female pelvis and therefore could be used as a model for prolapse and vaginal surgery.

- Aim: To document the effects of certain key events in the lifespan of women, such as their first delivery and menopause or while under its replacement therapy.
  Hypothesis: Lifespan events such as first delivery, ovariectomy, and hormonal replacement therapy changes morphology and biomechanical properties of the ovine vaginal wall.

- Aim: To compare biocompatibility of an acellular collagen matrix as an alternative to a polypropylene flat mesh augmented transvaginal repair.
  Hypothesis: Biocompatibility of an acellular collagen matrix derived from the bovine pericardium is comparable to polypropylene implant.

- Aim: To establish an ovine model for trocar guided transvaginal insertion of mesh with anchors, representative of the procedures clinically used.
  Hypothesis: The ovine model can be used for trocar guided mesh insertion in the ovine rectovaginal septum.

- Aim: To document the in vivo deformation of anchored implants as compared to flat meshes using a magnetic resonance imaging and computerized image analysis.
  Hypothesis: In vivo behavior, deformation and position of arm anchored implant inserted in the ovine rectovaginal septum is similar to a rectangular mesh secured with interrupted sutures to the underlying tissue

REFERENCES:

1. Hammer N, Steinke H, Slowik V, et al. (2009) The sacrotuberous and the sacrospinous ligament - A virtual reconstruction. Ann Anat 191:417–425. doi: 10.1016/j.aanat.2009.03.001

2. Otcenasek M, Baca V, Krofta L, Feyereisl J (2008) Endopelvic Fascia in Women Shape and Relation to Parietal Pelvic Structures. Obs Gynecol 111:622–33.

3. Kearney R, Sawhney R, DeLancey JOL (2004) Levator Ani Muscle Anatomy Evaluated by Origin-Insertion Pairs. Obstet Gynecol 104:168–173. doi: 10.1016/j.micinf.2011.07.011.Innate

4. Urbankova I, Vdoviakova K, Rynkevic R, et al. (2017) Comparative anatomy of the ovine and female pelvis. Gynecol Obstet Invest. doi: 10.1159/000454771

5. Ercoli A, Delmas V, Fanfani F, et al. (2005) Terminologia Anatomica versus unofficial descriptions and nomenclature of the fasciae and ligaments of the female pelvis: a dissection-based comparative study. Am J Obstet Gynecol 193:1565–73. doi: 10.1016/j.ajog.2005.05.007

6. Ramanah R, Berger MB, Parratte BM, Delancey JOL (2012) Anatomy and histology of apical support: a literature review concerning cardinal and uterosacral ligaments. Int Urogynecol J 23:1483–94. doi: 10.1007/s00192-012-1819-7

7. Zimmerman CW (2011) New Techniques in Genital Prolapse Surgery. 1–5. doi: 10.1007/978-1-84882-136-1

8. DeLancey JOL (1993) Anatomy and Biomechanics of Genital Prolapse. Clin Obstet Gynecol 36:897–909.

9. König H, Liebich H (2003) Anatomie domacich savcu, 2. dil, 2nd ed. Hájko & Hájková, Bratislava

10. Hogervorst T, Bouma HW, Vos J De (2009) Evolution of the hip and pelvis. Acta Orthop 80:1–38.

11. Wittman AB, Wall LL (2007) the Human Obstetric Dilemma. 62:739–748.

12. DeLancey JOL, Kane Low L, Miller JM, et al. (2008) Graphic integration of causal factors of pelvic floor disorders: an integrated life span model. Am J Obstet Gynecol 199:610.e1-5. doi: 10.1016/j.ajog.2008.04.001

13. Dietz HP, Wilson PD (2005) Childbirth and pelvic floor trauma. Best Pract Res Clin Obstet Gynaecol 19:913–924. doi: 10.1016/j.bpobgyn.2005.08.009

14. Callewaert G, Albersen M, Janssen K, et al. (2015) The impact of vaginal delivery on pelvic floor function - delivery as a time point for secondary prevention: A commentary. BJOG An Int J Obstet Gynaecol 678–681. doi: 10.1111/1471-0528.13505

15. Mant J, Painter R, Vessey M (1997) Epidemiology of genital prolapse: observations from the Oxford Family Planning Association study. BJOG An Int J Obstet Gynaecol 104:579–585. doi: 10.1111/j.1471-0528.1997.tb11536.x

16. Oliphant SS, Nygaard IE, Zong W, et al. (2014) Maternal adaptations in preparation for parturition predict uncomplicated spontaneous delivery outcome. Am J Obstet Gynecol 211:630.e1-630.e7. doi: 10.1016/j.ajog.2014.06.021

17. Lowder JLJ, Debes KMK, Moon DK, et al. (2007) Biomechanical adaptations of the rat vagina and supportive tissues in pregnancy to accommodate delivery. Obstet Gynecol 109:136–43. doi: 10.1097/01.AOG.0000250472.96672.6c

18. Alperin M, Lawley DM, Esparza MC, Lieber RL (2015) Pregnancy-induced adaptations in the intrinsic structure of rat pelvic floor muscles. Am J Obstet Gynecol 213:191.e1-7. doi: 10.1016/j.ajog.2015.05.012

19. Feola A, Moalli P, Alperin M, et al. (2011) Impact of pregnancy and vaginal delivery on the passive and active mechanics of the rat vagina. Ann Biomed Eng 39:549–58. doi: 10.1007/s10439-010-0153-9

20. Ulrich D, Edwards SL, Su K, et al. (2014) Influence of reproductive status on tissue composition and biomechanical properties of ovine vagina. PLoS One 9:e93172. doi: 10.1371/journal.pone.0093172

21. Feola A, Abramowitch S, Jones K, et al. (2010) Parity negatively impacts vaginal mechanical properties and collagen structure in rhesus macaques. Am J Obstet Gynecol 203:595.e1-8. doi: 10.1016/j.ajog.2010.06.035

22. Ayen E, Noakes DE, Baker SJ (1998) Changes in the capacity of the vagina and the compliance of the vaginal wall in ovariectomized, normal cyclical and pregnant ewes, before and after treatment with exogenous oestradiol and progesterone. Vet J 156:133–43.

23. Kearney R, Miller J, Asthno-Miller JA, DeLancey JOL (2006) Obstetrical factors associated with levator ani muscle injury after vaginal birth. Obstet Gynecol 107:144–149. doi: 10.1097/01.AOG.0000194063.63206.1c.Obstetrical

24. Shek KL, Chantarasorn V, Langer S, Dietz HP (2012) Does the levator trauma heal? medicine.inonu.edu.tr. doi: 10.1002/uog.11203.Copyright

25. Parente MPL, Jorge RMN, Mascarenhas T, et al. (2008) Deformation of the pelvic floor muscles during a vaginal delivery. Int Urogynecol J Pelvic Floor Dysfunct 19:65–71. doi: 10.1007/s00192-007-0388-7

26. Hoyte L, Damaser MS, Warfield SK, et al. (2008) Quantity and distribution of levator ani stretch during simulated vaginal childbirth. Am J Obstet Gynecol. doi: 10.1016/j.ajog.2008.04.027

27. Brooks S V, Zerba E, Faulkner JA (1995) Injury to muscle fibres after single stretches of passive and maximally stimulated muscles in mice. J Physiol 488:459–469. doi: 10.1113/jphysiol.1995.sp020980

28. Sindhwani N, Bamberg C, Famaey N, et al. (2017) In vivo evidence of significant levator ani muscle stretch on MR images of a live childbirth. Am J Obstet Gynecol 217:194.e1-194.e8. doi:

10.1016/j.ajog.2017.04.014

29. Dietz HP (2006) Why pelvic floor surgeons should utilize ultrasound imaging. Ultrasound Obstet Gynecol 28:629–634. doi: 10.1002/uog.3828

30. Khunda A, Shek KL, Dietz HP (2012) Can ballooning of the levator hiatus be determined clinically? Am J Obstet Gynecol 206:17–18. doi: 10.1016/j.ajog.2011.10.876

31. Dietz HP, Shek C, De Leon J, Steensma AB (2008) Ballooning of the levator hiatus. Ultrasound Obstet Gynecol 31:676–680. doi: 10.1002/uog.5355

32. Tinelli A, Malvasi A, Rahimi S, et al. (2010) Age-related pelvic floor modifications and prolapse risk factors in postmenopausal women. Menopause 17:204–12. doi: 10.1097/gme.0b013e3181b0c2ae

33. O'Dell KK, Morse AN (2008) It's not all about birth: biomechanics applied to pelvic organ prolapse prevention. J Midwifery Womens Health 53:28–36. doi: 10.1016/j.jmwh.2007.08.015

34. Rizk DEE, Fahim M a. (2008) Ageing of the female pelvic floor: Towards treatment a la carte of the "geripause." Int Urogynecol J Pelvic Floor Dysfunct 19:455–458. doi: 10.1007/s00192-008-0576-0

35. Sherratt MJ (2009) Tissue elasticity and the ageing elastic fibre. Age (Omaha) 31:305–325. doi: 10.1007/s11357-009-9103-6

36. Trowbridge ER, Wei JT, Fenner DE, et al. (2007) Effects of aging on lower urinary tract and pelvic floor function in nulliparous women. Obstet Gynecol 109:715–720. doi: 10.1097/01.AOG.0000257074.98122.69

37. Gandhi J, Chen A, Dagur G, et al. (2016) Genitourinary syndrome of menopause: evaluation, sequelae, and management. Am J Obstet Gynecol 1–8. doi: 10.1016/j.ajog.2016.07.045

38. Mannella P, Palla G, Bellini M, Simoncini T (2013) The female pelvic floor through midlife and aging. Maturitas 76:230–4. doi: 10.1016/j.maturitas.2013.08.008

39. Rizk DEE, Fahim M a., Hassan H a., et al. (2007) The effect of ovariectomy on biomarkers of urogenital ageing in old versus young adult rats. Int Urogynecol J Pelvic Floor Dysfunct 18:1077–1085. doi: 10.1007/s00192-006-0278-4

40. Haylen BT, de Ridder D, Freeman RM, et al. (2009) An international urogynecological association (IUGA)/international continence society (ICS) joint report on the terminology for female pelvic floor dysfunction. Neurourol Urodyn 29:n/a-n/a. doi: 10.1002/nau.20798

41. Jelovsek JE, Barber MD (2006) Women seeking treatment for advanced pelvic organ prolapse have decreased body image and quality of life. Am J Obstet Gynecol 194:1455–1461. doi: 10.1016/j.ajog.2006.01.060

42. Zielinski R, Miller J, Low LK, et al. (2012) The Relathionship between Pelvic Organ Prolapse, Genital Body Image and Sexual Health. Neurourol Urodyn 31:1145–1148. doi: 10.1002/nau.22205.The

43. Svihrova V, Svihra J, Luptak J, et al. (2014) Disability-adjusted life years (DALYs) in general population with pelvic organ prolapse: a study based on the prolapse quality-of-life questionnaire (P-QOL). Eur J Obstet Gynecol Reprod Biol 182:22–6. doi: 10.1016/j.ejogrb.2014.08.024

44. Murray CJL, Vos T, Lozano R, et al. (2012) Disability-adjusted life years (DALYs) for 291 diseases and injuries in 21 regions, 1990-2010: A systematic analysis for the Global Burden of Disease Study 2010. Lancet 380:2197–2223. doi: 10.1016/S0140-6736(12)61689-4

45. Hunskaar S, Vinsnes A (1991) The quality of life in women with urinary incontinence as measured by the sickness impact profile. J Am Geriatr Soc 40:976–7.

46. Gyhagen M, Åkervall S, Milsom I (2015) Clustering of pelvic floor disorders 20 years after one vaginal or one cesarean birth. Int Urogynecol J. doi: 10.1007/s00192-015-2663-3

47. Jelovsek JE, Maher C, Barber MD (2007) Pelvic organ prolapse. Lancet 369:1027–1038. doi: 10.1016/S0140-6736(07)60462-0

48. Li C, Gong Y, Wang B (2016) The efficacy of pelvic floor muscle training for pelvic organ prolapse: a systematic review and meta-analysis. Int Urogynecol J 27:981–992. doi: 10.1007/s00192-015-2846-y

49. Bugge C, Adams EJ, Gopinath D, Reid F (2013) Pessaries (mechanical devices) for pelvic organ prolapse in women. Cochrane Database Syst Rev 3–5. doi: 10.1002/14651858.CD004010.pub3

50. Jones K a, Shepherd JP, Oliphant SS, et al. (2010) Trends in inpatient prolapse procedures in the United States, 1979-2006. Am J Obstet Gynecol 202:501.e1-7. doi: 10.1016/j.ajog.2010.01.017

51. Lisonkova S, Lavery JA, Ananth C V., et al. (2016) Temporal trends in obstetric trauma and inpatient surgery for pelvic organ prolapse: an age-period-cohort analysis. Am J Obstet Gynecol 215:208.e1-208.e12. doi: 10.1016/j.ajog.2016.02.027

52. de Groot LCPMG, Verheijden MW, de Henauw S, et al. (2004) Lifestyle, nutritional status, health, and mortality in elderly people across Europe: a review of the longitudinal results of the SENECA study. J Gerontol A Biol Sci Med Sci 59:1277–84.

53. Eurostat (2017) Fertility statisctics. http://ec.europa.eu/eurostat/statistics-explained/index.php/Fertility_statistics.

54. Løwenstein E, Ottesen B, Gimbel H (2014) Incidence and lifetime risk of pelvic organ prolapse surgery in Denmark from 1977 to 2009. Int Urogynecol J. doi: 10.1007/s00192-014-2413-y

55. Thomas V, Shek KL, Guzmán Rojas R, Dietz HP (2015) Temporal latency between pelvic floor trauma and presentation for prolapse surgery: a retrospective observational study. Int Urogynecol J 1185–1189. doi: 10.1007/s00192-015-2677-x

56. Kirby AC, Luber KM, Menefee S a (2013) An update on the current and future demand for care of pelvic floor disorders in the United States. Am J Obstet Gynecol 209:584.e1-5. doi: 10.1016/j.ajog.2013.09.011

57. Mardon R, Halim S, Pawlson L., Haffer S. (2006) Management of Urinary Incontinence in Medicare Managed Care Beneficiaries Results From the 2004 Medicare Health Outcomes Survey. Arch Intern Med 166:1128–1133. doi: 10.1001/archinte.166.10.1128

58. Olsen AL, Smith VJ, Bergstrom JO, et al. (1997) Epidemiology of surgically managed Pelvic Organ Prolapse and Urinary Incontinence. Obstet Gynecol 89:520–506.

59. Clark AL, Gregory T, Smith VJ, Edwards R (2003) Epidemiologic evaluation of reoperation for surgically treated pelvic organ prolapse and urinary incontinence. Am J Obstet Gynecol 189:1261–1267. doi: 10.1067/S0002-9378(03)00829-9

60. Iglesia CB (2011) Synthetic vaginal mesh for pelvic organ prolapse. Curr Opin Obstet Gynecol 23:362–365. doi: 10.1097/GCO.0b013e32834a92ab

61. Maher C, Feiner B, Baessler K, et al. (2016) Transvaginal mesh or grafts compared with native tissue repair for vaginal prolapse. Cochrane Database Syst Rev. doi: 10.1002/14651858.CD012079

62. Petros, Peter E, Ulmsten U (1993) An integral theory and its method for the diagnosis and management of female urinary incontinence. Scand J Urol Nephrol 153:1–93.

63. Maher C, Feiner B, Baessler K, Schmid C (2013) Surgical management of pelvic organ prolapse in women (Review) Surgical management of pelvic organ prolapse in women. Cochrane Database Syst Rev. doi: 10.1002/14651858.CD004014.pub5.Copyright

64. Jakus SM, Shapiro A, Hall CD (2008) Biologic and synthetic graft use in pelvic surgery: a review. Obstet Gynecol Surv 63:253–266. doi: 10.1097/OGX.0b013e318166fb44

65. Vergeldt TFM, Weemhoff M, Inthout J, Kluivers KB Risk factors for pelvic organ prolapse and its recurrence: a systematic review. doi: 10.1007/s00192-015-2695-8

66. Dietz HP, Chantarasorn V, Shek KL (2010) Levator avulsion is a risk factor for cystocele recurrence. Ultrasound Obstet Gynecol 36:76–80. doi: 10.1002/uog.7678

67. Maher C, Feiner B, Baessler K, et al. (2016) Surgery for women with anterior compartment prolapse. Cochrane Database Syst Rev. doi: 10.1002/14651858.CD004014.pub6

68. FDA (2011) Urogynecologic Surgical Mesh : Update on the Safety and Effectiveness of Transvaginal Placement for Pelvic Organ Prolapse. Rev. Lit. Arts Am.

69. Reinier M, Groep G (2016) Final Opinion on the use of meshes in urogynecological surgery (SCENIHR- European Commission) Opinion on. doi: 10.13140/RG.2.1.5108.4883

70. Krause H, Goh J (2009) Sheep and rabbit genital tracts and abdominal wall as an implantation model for the study of surgical mesh. J Obstet Gynaecol Res 35:219–224. doi: 10.1111/j.1447-0756.2008.00930.x

71. Gilardi K V, Shideler SE, Valverde CR, et al. (1997) Characterization of the onset of menopause in the rhesus macaque. Biol Reprod 57:335–340. doi: 10.1095/biolreprod57.2.335

72. Liang R, Zong W, Palcsey S, et al. (2014) Impact of prolapse meshes on the metabolism of vaginal extracellular matrix in rhesus macaque. Am J Obstet Gynecol 212:174.e1-174.e7. doi: 10.1016/j.ajog.2014.08.008

73. Feola A, Abramowitch S, Jallah Z, et al. (2013) Deterioration in biomechanical properties of the vagina following implantation of a high-stiffness prolapse mesh. BJOG 120:224–32. doi: 10.1111/1471-0528.12077.

74. Otto L, Slayden DO, Clark A (2002) The rhesus macaque as an animal model for pelvic organ prolapse. Am J Obstet Gynecol 186:416–421. doi: 10.1067/mob.2002.121723

75. Vincent KL, Bourne N, Bell AB, et al. (2009) High resolution imaging of epithelial injury in the sheep cervicovaginal tract: a promising model for testing safety of candidate micorobicedes. Sex Transm Dis 36:312–318. doi: 10.1097/OLQ.0b013e31819496e4.HIGH

76. Vincent KL, Vargas G, Wei J, et al. (2013) Monitoring vaginal epithelial thickness changes noninvasively in sheep using optical coherence tomography. Am J Obstet Gynecol 208:282.e1-282.e7. doi: 10.1016/j.ajog.2013.01.025

77. Bryant HU (1997) OSTEOARTHRITIS CARTILAGE in o v a r i e c t o m i z e d s h e e p. 63–69.

CHAPTER 2

THE EFFECT OF THE FIRST VAGINAL BIRTH ON PELVIC FLOOR FUNCTION AND ANATOMY

Iva Urbankova, Klara Grohregin, Jiri Hanacek, Michal Krcmar, Jaroslav Feyereisl, Jan Deprest, Ladislav Krofta

Institute for the Care of Mother and Child and Third Faculty of Medicine, Charles University, Prague, Czech Republic

Department of Development and Regeneration, Organ systems cluster, Group Biomedical Sciences, and Pelvic Floor Unit, University Hospitals KU Leuven, Leuven, Belgium

Submitted to IUGJ; the format of this version is longer than in the submission as additional information is displayed in full in the text to facilitate your reading.

ABSTRACT

Introduction and hypothesis: Pregnancy and vaginal birth trauma, as well as maternal characteristics, are believed to relate to the risk later development of pelvic floor dysfunction, (PFD), including urinary incontinence (UI), urgency, anal incontinence (AI), pelvic organ prolapse (POP) and levator ani (LAM)-avulsion.

Methods: This is a single center prospective observational cohort study on healthy women in their first singleton pregnancy. All underwent clinical and transperineal ultrasound examination at 6 weeks and 12 months postpartum. Objective outcomes were POP-Q, presence or absence of LAM trauma. Functional outcomes were measured by the ICIQ-SF and PISQ 12. Multivariate regression was performed to determine delivery and maternal habitus related risk factors for UI, urgency, AI, dyspareunia, LAM-avulsion, and ballooning.

Results: 987 women were included. Risk factors for UI were maternal age (OR:1.088; 95%CI: 1.044–1.134; p=0.0001) and BMI before pregnancy (OR:1.081; 95%CI:1.035–1.130; p=0.001); for POP-stage-II+ maternal age (OR:1.082; 95%CI:1.082–1.144; p=0.005). Avulsion was more likely after forceps (OR:3.217; 95%CI:1.538–8.223; p=0.015) yet less likely after epidural analgesia (OR:0.576; 95%CI:0.370–0.898; p=0.015) and perineal rupture grade-I (OR:0.495; 95%CI:0.286–0.854; p=0.012). Ballooning was more likely at increased maternal age (OR:1.075;95%CI:2.022–1.131; p=0.005), epidural (OR:1.644; 95%CI:1.059–2.551; p=0.027) and perineal rupture grade-I (OR:1.788; 95%CI:1.103–2.899; p= 0.018)

Conclusion: Though maternal characteristics at delivery like age or BMI increase the risk for PFD, labour and delivery factors play a more important role.

Keywords: pelvic floor dysfunction, maternal age, BMI, forceps, epidural, perineal rupture

INTRODUCTION

Pelvic floor dysfunction (PFD) such as pelvic organ prolapse (POP), urinary (UI) and anal incontinence (AI) affect many women all over the world with millions of them undergoing corrective surgery at significant expense and personal suffering [1]. Many risk factors for development and symptom progression were identified and many of them are shared by different PFD [2]. According to the DeLancey's lifespan model, PFD becomes symptomatic when the pelvic floor function drops under a certain threshold level [3]. Following an initial drop caused by pregnancy and delivery, other risk factors such as lifestyle, smoking, overweight or chronically increased intra-abdominal pressure negatively affect its function. In most women, PFD becomes symptomatic after several decades, but women with severe pelvic floor trauma may become symptomatic shortly after their first delivery.

The most frequently shared risk factor for all PFD is vaginal delivery. Apart from the effects of pregnancy, vaginal delivery additionally interferes directly with all structures and tissues of the pelvic floor [4]. The detrimental nature of the effect of vaginal birth is even more outspoken in case of forceps extraction to complete the second stage of the labor [5]. Other obstetrical risk factors include high fetal birth weight, prolonged second stage of labor and higher BMI [6]. Some studies had also described higher maternal age at the time of first delivery but that is controversial [7, 8].

To contribute to the study of the effects of vaginal delivery, we set up a large prospectively cohort study of unselected nulliparous women which we followed up through their pregnancy, delivery and postpartum. Herein we correlate the demographic and obstetrical risk factors for the presence of PFD one year after the delivery. An additional goal was to identify the risk factors for levator ani trauma, as diagnosed by ultrasound, and if applicable, its contribution to the presence PFD.

MATERIAL AND METHODS

This is an ongoing single-center longitudinal study designed to recruit a large prospective cohort of healthy women in their first singleton pregnancy, and who deliver at or beyond 37 weeks. All women who were admitted to the labor suite between 5/2011 and 07/2013 were invited to participate. Exclusion criteria for entry were being minor, not speaking fluently Czech, non-Caucasians, and posthoc women becoming pregnant during follow-up.

Follow-up and outcome measures

Prior to discharge from the delivery unit, consenting patients were asked about the presence of involuntary leakage of urine, stools or pain during sexual intercourse. Study visits were arranged 6 weeks and 1 year after delivery. At these, they were asked about PFD and they were assessed by one out of four experienced nurses from the urogynaecological clinic. Patients filled out two validated questionnaires, i.e. the short form of International Consultation on Incontinence Questionnaire (ICIQ-SF) and Pelvic Organ Prolapse/Urinary Incontinence Sexual Questionnaire (PISQ 12) (Czech version) [9, 10]. Women were also specifically asked if they had any fecal and urinary incontinence and dyspareunia. The anatomical assessment was by the pelvic organ prolapse score (POP-Q) [11], pelvic floor muscle strength assessment by the Oxford scale [12]. Herein POP will be defined as the occurrence of prolapse stage II+ (leading point of the prolapse at least at POP-Q point 0 or further) [13]. Transperineal pelvic floor ultrasound (TPUS) was performed as described by Dietz et al. [14] (4.0 – 9.0 MHz probe, Voluson Expert E8, General Electric, Zipf, Austria). Briefly, the probe was placed vertically over the perineum. A 4D-loop including "squeeze – relaxation – Valsalva maneuver – relaxation" was recorded and stored for offline evaluation. The nurses had ≥ 3years of experience with TPUS and clinical assessment of PFD. Three other similarly qualified observers, not involved in the earlier clinical or ultrasound assessment, read the TPUS-volumes offline (4DView, GE). They measured the genital hiatal dimensions at minimal hiatal diameter during contraction, Valsalva and at rest; and scored for the presence of LAM-avulsion and ballooning [14]. Ballooning was defined as a genital hiatus area at Valsalva $>25cm^2$ [15].

Additional demographic, biometric and obstetric data were obtained from the medical records, including onset of labour, use of oxytocin during labour, epidural or other analgesics, length of the first and second stage, spontaneous or instrumental vaginal delivery, or if applicable, the use of caesarean section, cervical dilation at that moment and the leading indication, and if applicable, any trauma to the vagina, vulva or anal sphincter. Perineal trauma was categorized as grade I (perineal skin/vaginal mucosa), grade II (fascia, muscles, perineal body), grade III (idem + anal sphincter; irrespective of episiotomy) [16].

Labour and delivery management

At our institution, midwives essentially manage most of the first and second stage, yet under the supervision of a gynecologist. We adhere

to the principles of "active management of labor" [17, 18]. For pain relief, either nalbuphine (10mg/3hours, i.v.) or "delayed walking" epidural analgesia consisting of bupivacaine 0.5% and sufentanil (EDA) (i.e. cervical dilatation ≥ 4 cm) is offered [19, 20]. Following 30 min in a recumbent position, the parturient was advised to actively move and walk. If needed, EDA was reloaded every 2 hours. Following an uncomplicated first stage, the second stage is actively managed by encouraging pushing the head down to stage +3. During crowning, perineal protection includes manual support and controlling the passage of the head with the other hand [21]. Mediolateral episiotomy is performed when felt clinically indicated, yet there is no formal policy.

Pelvic floor muscle training (PFT)

During pregnancy, patients have access to prenatal pelvic floor physiotherapy (PFT) yet can use that at their discretion. In the postpartum, all were informed about how to do later PFT their selves during information sessions by physiotherapists in the ward. At the first follow-up visit, Kegel exercises were explained and women received a brochure on PFT. At the 6 and 12-months visit, women were encouraged to continue on PFT. Symptomatic women or those without palpable voluntary contraction were offered supervised PFT (three sessions) locally or at a physiotherapist of their choice. All prescribed PFT in the Czech Republic is covered by the national health insurance.

Statistical evaluation

This study was approved by the institutional ethics committee and all patients gave written informed consent.

Data were stored in a purpose designed database (Office Excel 2007, Microsoft corp., Redmond, WA, USA) and analyzed with SPSS 19.0 (SPSS Inc., Chicago, IL). Only data from women who delivered vaginally were used to determine maternal and obstetrical risk factors for LAM-avulsion and PFD 12-months postpartum. Univariate analysis was performed on maternal (age, BMI before pregnancy and at delivery from which the BMI change was calculated) and obstetrical (fetal weight, length of 1st and 2nd stage, type of analgesia, perineal injury, forceps delivery, breastfeeding) characteristics. Variables with $p < 0.250$ were taken into account for multivariate regression analysis, using a forward elimination of covariates according to the lack of significance. The risk for symptomatic stress UI and POP in women with LAM-avulsion was tested using a Chi-square test.

RESULTS

3648 subjects agreed to participate; 1359 women completed all study visits (drop out: 62.8%). From these, we excluded 24 who became pregnant again within one year and 348 (18.6%) who had a cesarean section. This left 987/3648 (27.0%) women who delivered vaginally. A comparison of demographic and obstetric characteristics of in- and excluded women is displayed in Table 1. Included women were elder (+ 0.8 yr) and more likely had labor induced (+ 6%).

Table 1: Demographical and obstetrical characteristics of non-responders, and responders.

	Non-responders	Responders	p
	N = 2313	**N = 1335**	
Demographics			
Age (mean ± SD)	30.0 ±4.0	30.8 ±3.5	**0.0001**
Height (mean ± SD; cm)	168.7 ±6.2	168.9 ±6.3	Ns
BMI before pregnancy (mean ± SD)	22.2 ±3.4	22.2 ±3.3	Ns
BMI at the delivery (mean ± SD)	27.4 ±3.9	27.3 ±3.7	Ns
BMI increase (mean ± SD)	5.2 ±1.8	5.1 ±1.7	Ns
Obstetrical characteristics			
Fetal weight (mean ± SD; g)	3357.1 ±419.1	3381.6 ±420.7	Ns
Length of the first stage (mean ± SD; hh:mm)	06:47 ±3:59	06:53 ±04:06	Ns
Length of the second stage (mean ± SD; hh:mm)	00:44 ±00:34	00:46 ±00:35	Ns
Elective caesarean section (N, %)	77 (3.3%)	50 (3.7%)	Ns
Acute caesarean section (N, %)	469 (20.3%)	297 (22.2%)	Ns
Forceps delivery (N, %)	37 (1.6%)	23 (1.7%)	Ns
Vacuum extraction (N, %)	4 (0.2%)	3 (0.2%)	Ns
Labour induction (N, %)	454 (19.6%)	312 (23.4%)	**0.004**
Epidural analgesia (N, %)	541 (23.4%)	304 (22.8%)	Ns
Oxytocin (N, %)	1545 (66.8%)	903 (67.6%)	Ns
Use of analgesics other than epidural (N, %)	864 (37.4%)	525 (39.3%)	Ns
Perineal rupture grade I (N, %)	228 (9.9%)	110 (8.2%)	Ns
Perineal rupture grade II (N, %)	115 (5.0%)	77 (5.8%)	Ns
Episiotomy (N, %)	1219 (52.7%)	703 (52.7%)	Ns
Perineal rupture grade III (N, %)	37 (1.6%)	30 (2.2%)	Ns

Table 2: *Objective and subjective outcomes in n=978 women in this study.*
The Oxford score was calculated as the average of right and left muscle strength.

POP Q	Mean	SD; range
Aa	-1.6	0.6; -3 - +1
Ba	-1.6	0.6; -3 - +1
C	-5.8	1.5; -7 - +1
Ap	-1.5	0.6; -2 - +1
Bp	-1.5	0.7; -3 - +1
Pb	3.7	0.4; 2 – 7
Gh	3.8	0.4; 2 – 5
TVL	8.8	0.5; 6 -10
Mean Oxford score	1.4	1.1; 0 – 5
Ultrasound findings	**Mean**	**SD; range**
Urogenital hiatus on relaxation	22.8	4.2; 8.8 – 37.0
on Valsalva	28.2	6.9; 8.22 – 49.7
during contraction	14.5	3.6; 6.6 – 30.5
Urethral gap	2.4	0.4;1.6 – 4.7
Questioners	**Median/Mean**	**IQR/ SD; range**
ICIQ SF (N=987)	1.9	4
ICIQ SF with UI (n=314)	5.9	4
-Amount of urine	2.0	0
-UI frequency	1	0
-UI visual analog scale	2	2
PISQ 12	38.8	4.0; 13 – 47

Levator muscles and degree of prolapse

Unilateral LAM-avulsion was diagnosed one year after delivery in 173 (18.1%). In 89 (9.0%) this was bilateral. LAM-avulsion was predominantly left (n = 109; 63%). Ballooning was present in 309 (31.3%) women, of which 165 (53.3%) without LAM-avulsion. The POP-Q, average Oxford score and subjective outcome are displayed in Table 2. Stage II prolapse in at least one compartment was present in 562 (56.9%) of which stage II+ was in 130 (23.1%) (Table 3).

Table 3: *Pelvic organ prolapse stage II (the leading point at the stage -1) and II+ (the leading point at stage 0 and +1). No prolapse stage III or IV were identified.*

	Anterior compartment	Central compartment	Posterior compartment
Prolapse stage II (-1)	259 (26.2%)	4 (0.4%)	317 (32.1%)
Prolapse stage II+ (hymen; +1)	90 (9.1%)	1 (0.1%)	109 (11.0%)

Urinary incontinence and urgency

UI before pregnancy was reported by 53 (5.4%) women. That number increased 6-fold during pregnancy to 29.7% of study participants (Figure 1). Of those, in one-third (23.4%) this resolved within six weeks after delivery, without reappearance within a year. However, after birth an additional 203 women previously not incontinent, reported UI: this is nearly as many women who developed UI in pregnancy. As a result, six weeks postpartum 40.6% (n = 401) were not dry. Later during that first year, UI resolved in 163 (- 40.6%), yet 76 (+19.0%) women developed *de novo* incontinence. As a result, in our cohort, 31.8% of women still report urinary incontinence after their first vaginal delivery. This population includes 66.0% (n = 35) of the women who reported UI before pregnancy, 41.7% (n = 100) of the women who developed UI during pregnancy, and 50% (n = 103) of the women who developed UI only duringthe postpartum. The type of incontinence as picked up by ICIQ SF only in these 314 women is displayed: three-quarters had stress incontinence, of which only a small fraction it was mixed with urge problems (Figure 2).

Urgency was reported by 24 (2.4%) women before pregnancy. Those had their problem persisting in pregnancy, yet their number increased to a four times (n = 96; 9.7%) (Figure 3). In half of them, the problem resolved in the postpartum, yet 23 women developed *de novo* urgency after vaginal delivery. By one year, the problem disappeared in half of the women. By one year, there were 4.8% of women who delivered vaginally reporting urgency, of which half developed this as a new problem.

Anal function

No women reported AI before or during pregnancy. Other dysfunctions were not quantified. At six weeks after delivery, 1.6% of women reported either faecal urgency (n = 2), flatus (n = 6) or stool (n = 8) incontinence (Figure 4). When adding the other forms anorectal dysfunctions 8.4% of women reported bother at 6-weeks (n = 83). Three-quarters of these dysfunctions resolved by one year. AI persisted in only one patient; yet 8 additional patients reported first AI between 6 weeks and one year after delivery (6 urgency, 2 flatus/stool incontinence). The number of women reporting de novo dyschezia was, however, three times higher (n = 24; 2.4%), which is half as many women reporting urgency incontinence.

Figure 1. *Development of urinary incontinence.*
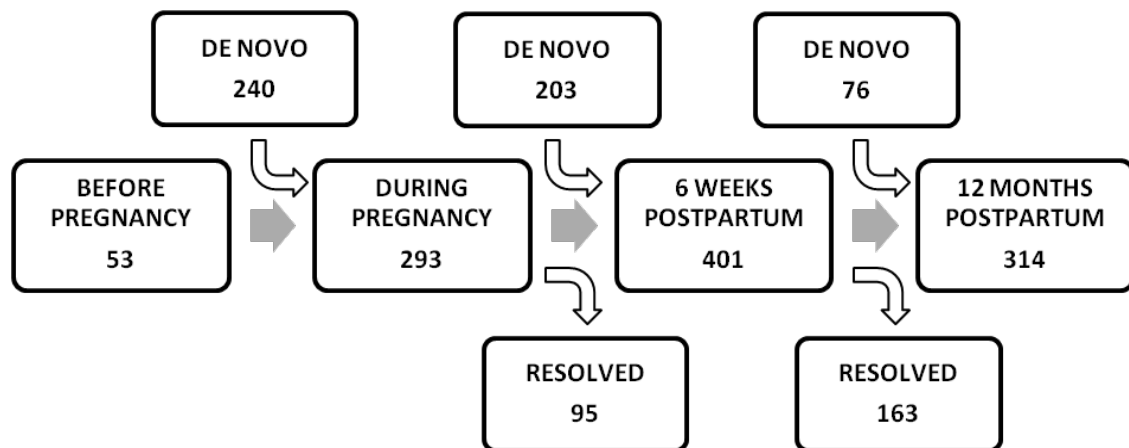
Figure 2: *Leakage types in 314 urinary incontinent women one year postpartum (Domain 6 - When does urine leak? ICIQ SF)*
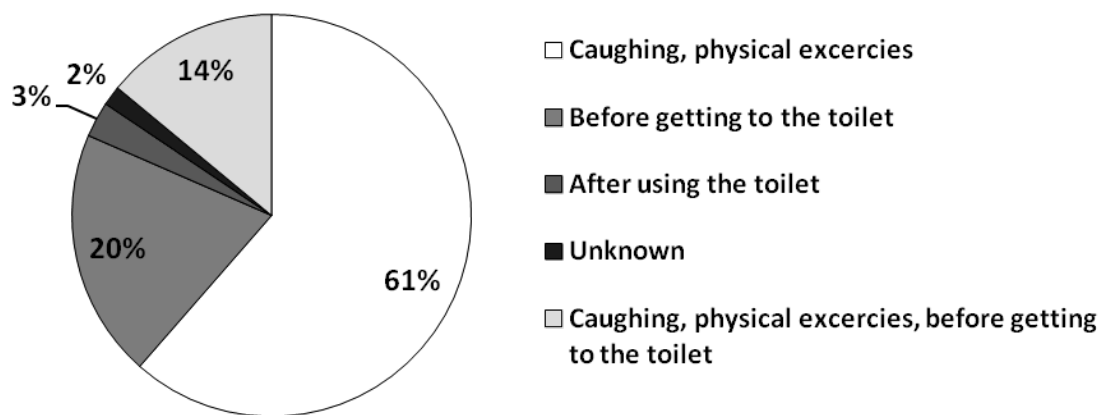
Figure 3. *Development of urgency*
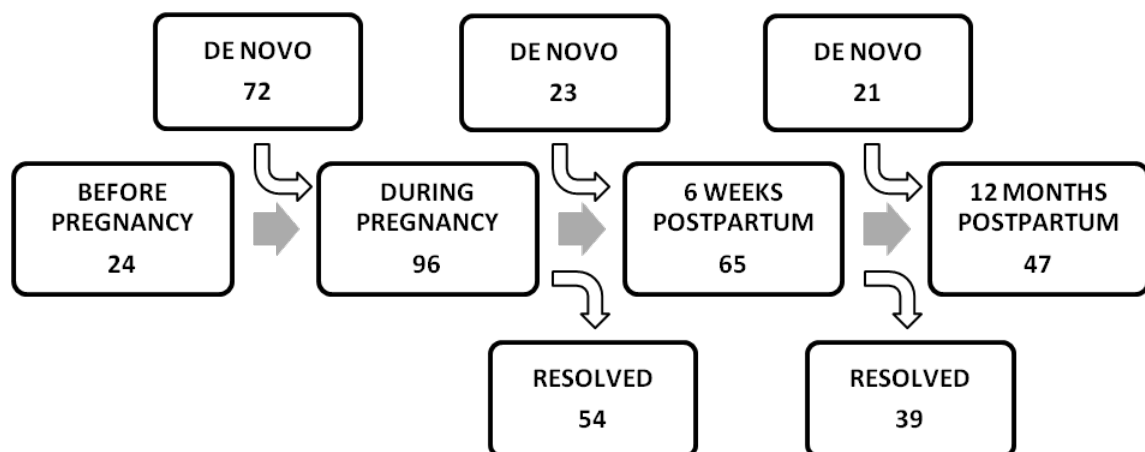
Figure 4 *Anal functions at 6weeks and 12 months*
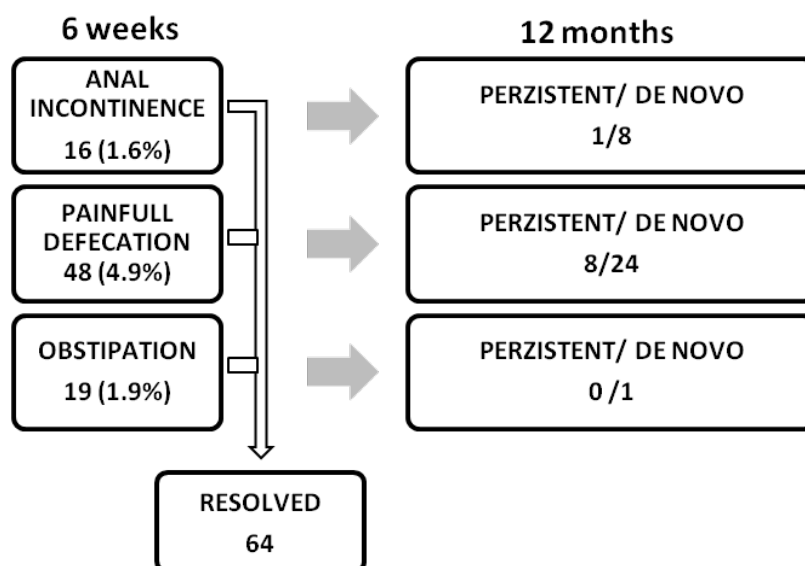
Sexual function

One-year postpartum 961 (97.5%) women were sexually active of which 169 (17.1%) reported dyspareunia. Women breastfeeding at one year (421, 42.6%) were more likely (OR: 1.449; 95% CI: 1.039 – 2.019, p = 0.033) to report dyspareunia.

Uni- and multivariate analysis

We performed univariate analysis of these factors effect of age, height, initial BMI, delivery BMI, BMI increase during pregnancy, fetal weight, forceps extraction; length of the first and second stage of labour; usage of oxytocin, epidural analgesia, other analgesics; perineal tear grade I, II and III, and episiotomy. Only variables with p < 0.250 are displayed in Tables 5 and 6. Five sets of analysis were performed for PFDs and LAM trauma at 12 months; the presence of urinary incontinence, pelvic organ prolapse stage II+, LAM avulsion and LAM ballooning. Analysis for fecal incontinence was not performed due to its low occurrence.

Urinary incontinence was 1.6 more likely in women with LAM avulsion (95%CI 1.175 – 2.127, p = 0.003). POP stage II+ was more likely in women with LAM avulsion (OR 2.588, 95%CI 1.764 – 3.797, p = 0.0001) and with ballooning (OR 2.144, 95%CI 1.396 – 3.293, p = 0.0001).

Figure 5: *Clustering of pelvic floor dysfunction*
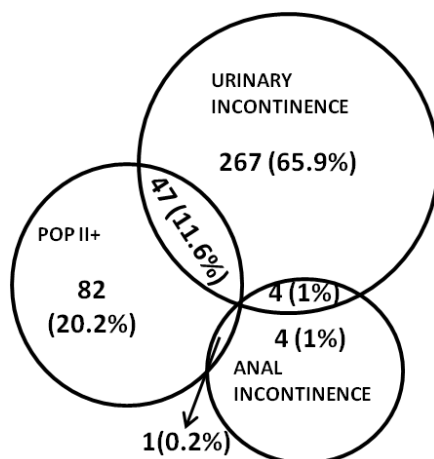
Table 4: *Uni- and multivariate regression analysis for the presence of urinary incontinence (UI) and pelvic organ prolapse stage II+ (POP II+). Results for variables with p >0.250 in univariate analysis are not showed.*

	Univariate analysis		Multivariate analysis	
	OR (95%CI)	p	OR (95% CI)	p
UI				
Age (per additional year of age)	1.084 (1.041 – 1.129)	**0.0001**	1.088 (1.044–1.134)	**0.0001**
Height (per additional cm)	0.978 (0.957 – 1.000)	**0.051**	0.976 (0.837 – 0.988)	**0.030**
BMI before pregnancy	1.071 (1.026 – 1.119)	**0.002**	1.081 (1.035–1.130)	**0.001**
BMI at delivery	1.029 (0.991 - 1.068)	**0.130**		Excl.
BMI increase	0.899 (0.8285 – 0.976)	**0.010**	0.902 (0.828–0.979)	**0.014**
POP II+				
Age	1.081 (1.023 – 1.143)	**0.006**	1.082 (1.024-1.144)	**0.005**
Duration of the first stage (per additional minute)	0.999 (0.998 – 1.000)	**0.035**	0.999 (0.098–1.000)	**0.032**
Duration of the second stage (per additional minute)	0.996 (0.990 – 1.002)	**0.238**		Excl.
Fetal weight (per additional gram)	1.000 (1.000 – 1.001)	**0.144**		Excl.
Use of analgesics other than epidural	0.792 (0.537 – 1.168)	**0.247**		Excl.

Table 5. Uni- and multivariate regression analysis for presence any levator ani avulsion (LAM avulsion) and ballooning without LAM avulsion. Results for variables with p >0.250 in univariate analysis are not showed.

	Univariate analysis		Multivariate analysis	
	OR (95%CI)	p	OR (95% CI)	p
LAM avulsion				
Age (per additional year of age)	1.038 (0.995 – 1.082)	**0.081**		Excl
Initial BMI	0.964 (0.917 – 1.014)	**0.152**		Excl
Delivery BMI	0.964 (0.924 – 1.006)	**0.093**	0.952 (0.910 – 0.996)	**0.032**
Duration of the second stage (per additional minute)	1.006 (1.002 – 1.011)	**0.007**	1.005 (1.000 – 1.009)	**0.044**
Fetal weight (per additional gram)	1.001 (1.000 – 1.001)	**0.003**	1.001 (1.000 – 1.001)	**0.007**
Forceps delivery	4.841 (2.006 – 11.679)	**0.0001**	3.217 (1.538 – 8.223)	**0.015**
Epidural analgesia	0.633 (0.410 – 0.978)	**0.042**	0.576 (0.370 – 0.898)	**0.015**
Episiotomy	1.271 (0.920 – 1.755)	**0.150**		Excl
Perineal rupture grade I	0.466 (0.272 – 0.798)	**0.004**	0.495 (0.286 – 0.854)	**0.012**
Ballooning without LAM avulsion				
Age (per additional year of age)	1.061 (1.010 – 1.115)	**0.019**	1.075 (2.022 – 1.131)	**0.005**
Initial BMI	1.059 (1.005 – 1.116)	**0.015**	1.066 (1.010 – 1.125)	**0.019**
Delivery BMI	1.033 (0.987 – 1.082)	**0.162**		Excl
Duration of the second stage (per additional minute)	0.993 (0.987 – 0.999)	**0.017**	0.992 (0.986 – 0.998)	**0.008**
Perineal rupture grade III	0.347 (0.082 – 1.475)	**0.208**		Excl
Epidural analgesia	1.564 (1.016 – 2.409)	**0.053**	1.644 (1.059 – 2.551)	**0.027**
Episiotomy	0.671 (0.470 – 0.956)	**0.030**		Excl
Perineal rupture grade I	1.739 (1.084 – 2.790)	**0.029**	1.788 (1.103 – 2.899)	**0.018**
Use of analgesics other than epidural	0.711 (0.498 – 1.016)	**0.065**		Excl

DISCUSSION

One year postpartum the most common PFD was the urinary incontinence reported by every third woman. Risk factors for its development were maternal age, BMI before pregnancy and its increase during pregnancy. Risk factors for POP II+ included mainly maternal age. LAM injuries were present in 43% of women. Muscle avulsion was 3.2 more likely in women who had forceps-assisted delivery. Surprisingly, there was an opposite effect of epidural analgesia and perineal rupture grade I on the LAM avulsion and ballooning.

The study cohort represents very well the population of nulliparous women delivering at the Institute that is older than the national reported average age (28.2 years of age). In the study cohort, 70% of women were administered oxytocin during labour. This probably results in the active labour management, according to which we advise usage of oxytocin if progression is less than 1 cm/hour [17, 18]. There were no details on the length and dosage used in individual patients, therefore we are not able to discern between a short-term administration at the end of the second stage and continuous application from the beginning of the first stage. However, higher maternal age (>35) was shown to increases twice the likely-hood of oxytocin administration compared to younger women (<19) [22]. Another strikingly high is the number of episiotomies (71%) that overshoots the nationally reported rates [23]. We are not able to identify the possible reasons. There was the relatively low rate of EDA (14%), forceps/VEX deliveries (2.6%) and third-degree perineal tears (3.0%) all of which correspond to the long-term institutional and national data [20, 24].

Our observation confirms that not only vaginal delivery severely interferes with pelvic floor function but also pregnancy has its impact. Every fourth woman reported stress UI only due to the pregnancy that persists in many of them until 1-year postpartum. As a result of delivery, more than one-third of asymptomatic women developed UI persisting in two-thirds of them beyond 1-year. Discern between the effects the pregnancy by itself and the effect of delivery is not possible in this cohort. Further evaluation of women who delivered via cesarean section may support findings of others who have shown an increased risk for UI compared to nulliparous women [25]. Similarly to others, the age at the first delivery was showed to be critical for the development of symptomatic UI [26]. However, its effect attenuates with the actual age and disappear after 50 years of age [27, 28].

Regression of UI during the observational period was also probably affected be physiotherapy that was strongly promoted by nurses in the urogynecological office. We did not collect more detail information on duration, intensity or type of PFT so we are not able to draw more conclusions. However, recent literature support PFT as an appropriate treatment for UI even though it may not have a long-lasting effect [29, 30].

For POP evaluation we chose the more strict criteria because we were lacking subjectively reported outcome [13, 31, 32]. POP (II+) was present by almost every eight women and likely hood was increased by 8% for each

additional year of age. Also, women who had LAM-avulsion or ballooning were more likely to have POPII+. We did not include this factor in the analysis since they only develop as a result of delivery. There is some evidence that mediolateral episiotomy protects whereas spontaneous perineal lacerations promote POP development [28]. We did not confirm this observation in the relation to the POP either due to high episiotomy rate or short observational period.

The underlying conditions for PFD development are direct and indirect injuries to the LAM and other soft tissues of the pelvic floor. We only investigated the muscular component. The avulsion was present in almost every third women and was 3-fold more likely in women with forceps, which is similar to current literature (OR 1.6 - 4.40) [5, 33, 34]. Unlike others, the unilateral avulsion was predominantly on the left side [35–37]. Ballooning was identified often in women with the LAM-avulsion, yet we only include ballooning in women without avulsion in the regression analysis. It is taught that ballooning is a result of the muscular over-distension, micro-traumatization, pudendal neuropathy and resulting healing [28]. LAM-avulsion and ballooning shared three common risk factors (the epidural analgesia, perineal rupture grade I and the length of the second stage of labour) yet with opposite effects. The likely hood of LAM-avulsion was halved in women who had EDA and who sustained grade I perineal tear. On the other side, the muscle is 1.6-fold and 1.8-fold more likely to become overstretched, respectively. Effect of EDA could be explained by its effect on muscle relaxation, which becomes less likely to tear from its insertion on the pubic bone but more likely be overstretched. Our observation could be supported BY studies showing a protective effect of EDA on third and fourth-degree perineal tears [38, 39]. On the other side, EDA prolongs the second stage of the labour and was previously linked with increased risk of UI [7, 40].

The role of perineal rupture grade I, which is a minor perineal trauma, could be explained by compliant pelvic floor and perineum that allow sufficient adaptation during crowning. Therefore the LAM-avulsion is less likely whereas overstretch (ballooning) is more likely. Since no prevention of perineal injury has been identified the explanation could be an individual's physiognomy and intrinsic tissue characteristics such as its composition, compliance, and elasticity [41]. Intrinsic tissue properties are partially inherited, affected by age, internal diseases etc [3, 42, 43]. Indeed, we and others have identified age as the risk factor increasing likely hood of LAM avulsion by 8 - 10% for each additional year [8].

There are several limitations to our study. The major limitation is the missing questioner on pelvic organ prolapse. In some women symptoms related to POP were noted in clinical report but they were not specifically asked about typical symptoms (vaginal bulge etc.) To overcome this, we considered for the analysis only the POP at least stage II+, that includes descent to the level of the hymen or beyond [44]. We also did not prospectively collect subjective complaints on dyspareunia, AI, UI, and urgency before and during the pregnancy, therefore these data may be

biased. This information is not reported during prenatal consultations and we invited women only at the time of delivery. We did not consider the collection of this data (questioners) at time of admission to the delivery suite inappropriate. It would be beneficial to obtain also 3D scans of the anal sphincter to identify the occult anal sphincter tears. We also did not use any standardized test to further categorize the type UI and only relied only on subjective reports.

The strengths include a large amount of unselected women included in the follow-up and its prospective design. It was possible due to a high volume center with more than 5000 deliveries per year. This cohort was also very homogeneous since it includes only Caucasian women and therefore very well represents local population. For the future, we are able to follow this cohort beyond the end of this study and collect data on their subsequent deliveries and pelvic floor function during their later lives. An additional benefit was an increase of general awareness on PFD among the populationof women invited to the study and their peers who often contacted the urogynecological office to consult or treat their problems.

CONCLUSION

It seems that we will never be able to completely prevent the development of PFD since part of their origin lays in the pregnancy and aging. We should try to minimise the harmful procedures i.e. forceps yet not on behalf of fetal safety. Moreover, women should be informed by care providers on their individual risks for PFD development as a result of pregnancy and delivery however it should not serve as a general excuse for performing a cesarean section. During the postpartum visit, women should be asked about PFD and if needed preventive approaches (pelvic floor muscle training, weight reduction etc.) should be recommended.

To a certain extent, we have contributed to the discussion on risk factors related to PFD. Maternal age and weight were again identified as important factors in the development of UI and POP. It seems that epidural analgesia may have a protective effect on levator avulsion but at the same time, it may contribute to its micro-traumatization and development of ballooning. To make a stronger conclusion on EDA it would need more research. The effect of perineal rupture grade I may represent a link between the intrinsic tissues properties that allow to some primiparous women deliver with only minor injuries yet predispose them to tissue overstretch.

Ethical approval: Ethical approval was given by the institutional ethical committee. All patients included in the study signed informed consent ahead.

Conflict of interest: none

Authors' contribution: I Urbankova data evaluation, manuscript writing, K Grohregin data collection and evaluation, M Krcmar and J Hanacek data evaluation, J Feyereisl and L Krofta study design, J Deprest manuscript writing. All authors contributed to manuscript editing.

REFERENCES:

1. Milsom I, Altman D, Lapitan MC, et al. (2009) Epidemiology of urinary (UI) and faecal (FI) incontinence and pelvic organ prolapse (POP). Health Publication Ltd, Paris

2. Bortolini MAT, Drutz HP, Lovatsis D, Alarab M (2010) Vaginal delivery and pelvic floor dysfunction: Current evidence and implications for future research. Int Urogynecol J Pelvic Floor Dysfunct 21:1025–1030. doi: 10.1007/s00192-010-1146-9

3. DeLancey JOL, Kane Low L, Miller JM, et al. (2008) Graphic integration of causal factors of pelvic floor disorders: an integrated life span model. Am J Obstet Gynecol 199:610.e1-5. doi: 10.1016/j.ajog.2008.04.001

4. Callewaert G, Albersen M, Janssen K, et al. (2015) The impact of vaginal delivery on pelvic floor function - delivery as a time point for secondary prevention: A commentary. BJOG An Int J Obstet Gynaecol 678–681. doi: 10.1111/1471-0528.13505

5. Memon HU, Blomquist JL, Dietz HP, et al. (2015) Comparison of levator ani muscle avulsion injury after forceps-assisted and vacuum-assisted vaginal childbirth. Obstet Gynecol 125:1080–7. doi: 10.1097/AOG.0000000000000825

6. Glazener C, Elders A, MacArthur C, et al. (2013) Childbirth and prolapse: Long-term associations with the symptoms and objective measurement of pelvic organ prolapse. BJOG An Int J Obstet Gynaecol 120:161–168. doi: 10.1111/1471-0528.12075

7. Rortveit G, Daltveit AK, Hannestad YS, Hunskaar S (2003) Vaginal delivery parameters and urinary incontinence: The Norwegian EPINCONT study. Am J Obstet Gynecol 189:1268–1274. doi: 10.1067/S0002-9378(03)00588-X

8. Dietz HP, Simpson JM (2007) Does delayed child-bearing increase the risk of levator injury in labour? Aust N Z J Obstet Gynaecol 47:491–5. doi: 10.1111/j.1479-828X.2007.00785.x

9. Avery K, Donovan J, Peters JF (2004) ICIQ: A brief and robust measure for evaluating the symptoms and impact of urinary incontinence. Neurourol Urodyn 23:322–30.

10. Rogers R, Coates K, Kammerer-Doak D, et al. (2003) A short form of the Pelvic Organ Prolapse/Urinary Incontinence Sexual Questionnaire, (PISQ-12). Int Urogynecol J Pelvic Floor Dysfunct 14:164–8. doi: 10.1007/s00192-003-1063-2

11. Bump RC, Mattiasson A, Bo K (1996) The standardization of terminology of fiale pelvic organ prolapse and pelvic floor dysfunction. Am J Obs Gynecol 175:10–7.

12. Bø K, Finckenhagen HB (2001) Vaginal palpation of pelvic floor muscle strength: inter-test reproducibility and comparison between palpation and vaginal squeeze pressure. Acta Obstet Gynecol Scand 80:883–883. doi: 10.1080/791200641

13. Wiegersma M, Panman CMCR, Kollen BJ, et al. (2017) Is the hymen a suitable cut-off point for clinically relevant pelvic organ prolapse? Maturitas 99:86–91. doi: 10.1016/j.maturitas.2017.02.012

14. Dietz HP (2004) Ultrasound imaging of the pelvic floor. Part II: Three-dimensional or volume imaging. Ultrasound Obstet Gynecol 23:615–625. doi: 10.1002/uog.1072

15. Dietz HP, Shek C, De Leon J, Steensma AB (2008) Ballooning of the levator hiatus. Ultrasound Obstet Gynecol 31:676–680. doi: 10.1002/uog.5355

16. ICS/IUJA Terminology Committees (2010) an International Urogynecological Association (IUGA) / International Continence Society (ICS) Joint Report on the Terminology.

17. O'Driscoll K, Stronge JM, Minogue M (1973) Active management of labour. Br Med J 3:135–137. doi: 10.1016/S0140-6736(87)90401-6

18. Sadler LC, Mccowan LME (2000) A randomised controlled trial and meta-analysis of active management of labour. 107:909–915.

19. Bl S, WI L, Zeng Y, et al. (2014) Early versus late initiation of epidural analgesia for labour (Review) Early versus late initiation of epidural analgesia for labour. 2–4. doi: 10.1002/14651858.CD007238.pub2.Copyright

20. Stourac P, Blaha J, Klozova R, et al. (2015) Anesthesia for cesarean delivery in the Czech Republic: A 2011 national survey. Anesth Analg 120:1303–1308. doi: 10.1213/ANE.0000000000000572

21. Jansova M, Kalis V, Rusavy Z, et al. (2014) Modeling manual perineal protection during vaginal delivery. Int Urogynecol J Pelvic Floor Dysfunct 25:65–71. doi: 10.1007/s00192-013-2164-1

22. Omih EE, Lindow S (2015) Impact of maternal age on delivery outcomes following spontaneous labour at term. J Perinat Med 2015:773–777. doi: 10.1515/jpm-2015-0128

23. Rogers R, Gilson GJ, Miller AC, et al. (1997) Active management of labor: does it make a difference? Am J Obs Gynecol 177:599–605. doi: S0002-9378(97)70152-2 [pii]

24. Velebil P (2012) Czech republic and obstetrical interventions. Entre Nuos 26–27.

25. Rortveit G, Daltveit AK, Hannestad YS, Hunskaar S (2003) Urinary Incontinence after Vaginal Delivery or Cesarean Section. N Engl J Med 348:900–907. doi: 10.1056/NEJMoa021788

26. Diez-Itza I, Aizpitarte I, Becerro a (2007) Risk factors for the recurrence of pelvic organ prolapse after vaginal surgery: a review at 5 years after surgery. Int Urogynecol J Pelvic Floor Dysfunct 18:1317–24. doi: 10.1007/s00192-007-0321-0

27. Rortveit G, Hunskaar S (2006) Urinary incontinence and age at the first and last delivery: The Norwegian HUNT/EPINCONT study. Am J Obstet Gynecol 195:433–438. doi: 10.1016/j.ajog.2006.01.023

28. Memon H, Handa VL (2012) Pelvic floor disorders following vaginal or cesarean delivery. Curr Opin Obstet Gynecol 24:349–354. doi: 10.1097/GCO.0b013e328357628b

29. Glazener CM a, MacArthur C, Hagen S, et al. (2014) Twelve-year follow-up of conservative management of postnatal urinary and faecal incontinence and prolapse outcomes: Randomised controlled trial. BJOG An Int J Obstet Gynaecol 121:112–119. doi: 10.1111/1471-0528.12473

30. Boyle R, Hay-Smith EJC, Cody JD, Mørkved S (2012) Pelvic floor muscle training for prevention and treatment of urinary and faecal incontinence in antenatal and postnatal women. Cochrane Database Syst Rev. doi: 10.1002/14651858.CD007471.pub2

31. Kassis NC, Hamner JJ, Takase-Sanchez MM, et al. (2017) If you could see what we see, would it bother you? Int Urogynecol J 28:59–64. doi: 10.1007/s00192-016-3073-x

32. Manonai J, Wattanayingcharoenchai R (2016) Relationship between pelvic floor symptoms and POP-Q measurements. Neurourol Urodyn 35:724–727. doi: 10.1002/nau.22786

33. Diez-Itza I, Arrue M, Ibañez L, et al. (2011) Influence of mode of delivery on pelvic organ support 6 months postpartum. Gynecol Obstet Invest 72:123–129. doi: 10.1159/000323682

34. Shek KL, Dietz HP (2010) Can levator avulsion be predicted antenatally? Am J Obstet Gynecol 202:586.e1-586.e6. doi: 10.1016/j.ajog.2009.11.038

35. Dietz HP, Garnham AP, Rojas RGG (2015) Is the levator???urethra gap helpful for diagnosing avulsion? Int Urogynecol J Pelvic Floor Dysfunct 1–5. doi: 10.1007/s00192-015-2909-0

36. Branham V, Thomas J, Jaffe T, et al. (2007) Levator ani abnormality 6 weeks after delivery persists at 6 months. Am J Obstet Gynecol 197:1–6. doi: 10.1016/j.ajog.2007.02.040

37. Krofta L, Otčenášek M, Kašíková E, Feyereisl J (2009) Pubococcygeus-puborectalis trauma after forceps delivery: Evaluation of the levator ani muscle with 3D/4D ultrasound. Int Urogynecol J Pelvic Floor Dysfunct. doi: 10.1007/s00192-009-0837-6

38. Hauckv YL, Lewis L, Nathan EA, et al. (2015) Risk factors for severe perineal trauma during vaginal childbirth: A Western Australian retrospective cohort study. Women and Birth 28:16–20.

39. Jangö H, Langhoff-Roos J, Rosthøj S, Sakse A (2014) Modifiable risk factors of obstetric anal sphincter injury in primiparous women: A population-based cohort study. Am J Obstet Gynecol 210:59.e1-59.e6. doi: 10.1016/j.ajog.2013.08.043

40. Serati M, Salvatore S, Khullar V, et al. (2008) Prospective study to assess risk factors for pelvic floor dysfunction after delivery. Acta Obstet Gynecol Scand 87:313–8. doi: 10.1080/00016340801899008

41. Aasheim V, Nilsen ABV, Reinar LM, Lukasse M (2017) Perineal techniques during the second stage of labour for reducing perineal trauma. Cochrane Database Syst Rev. doi: 10.1002/14651858.CD006672.pub3

42. Sherratt MJ (2009) Tissue elasticity and the ageing elastic fibre. Age (Omaha) 31:305–325. doi: 10.1007/s11357-009-9103-6

43. Durnea CM, Khashan a. S, Kenny LC, et al. (2014) Prevalence, etiology and risk factors of pelvic organ prolapse in premenopausal primiparous women. Int Urogynecol J 1463–1470. doi: 10.1007/s00192-014-2382-1

44. Swift SE, Tate SB, Nicholas J (2003) Correlation of symptoms with degree of pelvic organ support in a general population of women: what is pelvic organ prolapse? Am J Obstet Gynecol 189:372-377-379. doi: 10.1067/S0002-9378(03)00698-7

CHAPTER 3

COMPARATIVE ANATOMY OF THE OVINE AND FEMALE PELVIS

Iva Urbankova, Katarina Vdoviakova, Rita Rynkevic, Nikhil Sindhwani, Dries Deprest, Andrew J. Feola, Paul Herijgers, Ladislav Krofta, Jan Deprest

Centre for Surgical Technologies, Group Biomedical Sciences,

Department of Development and Regeneration, Organ systems cluster, Group Biomedical Sciences & Vesalius Institute of Anatomy, KU Leuven, Leuven, Belgium

Institute for Care of Mother and Child, Third Faculty of Medicine, Charles University, Prague, Czech Republic

Department of Anatomy, Histology, and Physiology, University of Veterinary Medicine and Pharmacy, Košice, Slovak Republic

Pelvic Floor Unit, University Hospitals KU Leuven, Leuven, Belgium

ABSTRACT

Background: Pelvic organ prolapse affects half of vaginally parous women. Several animal models are used to study its pathophysiology and treatment. Sheep are interesting because they develop spontaneously prolapse with similar risk factors as women, and can be used for vaginal surgery. This study describes ovine pelvis anatomy, compares it to women pelvis, and to provides anatomical tools for translational researchers.

Methods: Magnetic resonance imaging, pelvic dissections, and histology were used for detailed macro- and microscopic analysis of relevant anatomical structures in six nulliparous ewes.

Results: Although sheep are quadrupeds the gross and microscopic anatomy are similar to the female pelvis. Principal differences are the shape and its orientation, the absence of the sacrospinous ligament and the internal obturator. The levator ani (except for the puborectalis) and the coccygeus muscle are present, yet the latter is more developed – coinciding with the tail. The dimensions and morphology of the ovine vagina are comparable. The retropubic and the rectovaginal space are accessible transvaginally. There is a wide expression of estrogen receptors with low or absent immunoreactivity in the urethral epithelium, bladder, anus, and internal anal sphincter.

Conclusion: The ovine pelvic floor has many anatomical and ultrastructural similarities to the female pelvic floor.

INTRODUCTION

Pelvic floor dysfunction (PFD) encompass pelvic organ prolapse (POP), urinary, fecal incontinence, as well as sexual dysfunction. PFD drastically reduces the quality of life for women, and this negative impact on a woman's quality of life is comparable to Parkinson's disease or a tension headache [1, 2]. POP is characterized by protrusion of the vaginal wall and descent of organs from their original location. Prolapse affects one in two women who delivered vaginally, half of them being symptomatic [3]. Surgery is the mainstay of therapy with 19% of women undergoing surgery by the age of 80 years [4]. The pathogenesis of POP is multifactorial, which has been depicted by DeLancey et al in an integrated lifespan model [5]. It describes the complex interplay between genetic factors, vaginal birth-induced trauma, aging, lifestyle and other factors [5].

In order to better understand the genesis of POP and preventive measures research utilizing appropriate models are required. Finding an optimal animal model for POP is challenging, since humans are bipedal, the absence of a tail, and the relatively large head-size as compared to pelvic dimensions. This last point makes vaginal delivery relatively traumatic compared with many other species. Further, an animal model should also allow interventions which are clinically used to treat POP. Pragmatically, it should be affordable and available in large numbers, relatively easy to handle and ethically acceptable. Several species *spontaneously* develop POP, including domestic mammals (e.g. dogs and sheep) and non-human primates [6–9]. Genetic models, such as the LOXL1, and FBLN3 and FBLN5 knockout mouse, are attractive because they can be used to study relevant pathways involved in connective tissue metabolism with comprehensive molecular tools [10–12]. Rodents have been used to simulate pelvic floor changes induced by pregnancy and delivery, yet the size of their urogenital tract makes vaginal surgery difficult [13]. Therefore, we and others have moved to larger models, such as the rabbit, yet their gross and microscopic vaginal anatomy are very different from the human, and often do not spontaneously develop POP [14]. The most relevant animal models are non-human primates; such as the squirrel monkey, baboon or rhesus macaque. Their pelvic anatomy is very similar, are semi-bipedal, and spontaneously develop POP after vaginal delivery [9, 15, 16], Further, this animal model has been used to investigate the surgical treatment of POP [17]. However, non-human primates are expensive and ethical and moral concerns make their use in Europe limited.

Another option is a domestic mammal such as the sheep (*Ovis ovis*) [18–22]. Sheep are a relatively large animal (adult weight 45-90kg according to their breed) and up to 15% will spontaneously develop uterovaginal prolapse during pregnancy, after delivery or later in the life [8, 23]. Risk factors for POP in sheep are similar to those in humans, such as increased intra-abdominal pressure, parity or weight [24]. As we and others are increasingly using this model [25–27], we were keen for a more detailed comparison of pelvic anatomy to a woman. Although we identified anatomical descriptions of relevant pelvic structures in veterinarian textbooks, they did

not have sufficient detail for the translational and clinical researcher in this field. Herein, we aimed to describe the detailed anatomy of the ovine pelvis and pelvic floor with relevance to transvaginal mesh surgery, with clinical human anatomy as a reference.

MATERIALS AND METHODS

This research is a part of a wider experimental study on the effects of vaginal birth on the ovine pelvic floor and the use of the ewe as a model for prolapse surgery. Six nulliparous Swifter sheep (50.2 ± 8.0kg, 1-year old) were obtained from the Zoötechnical Institute of the KU Leuven. Ewes were euthanized by intravenous injection of 1.0 mL of a mixture of embutramide 200 mg, mebezonium 50 mg and tetracaine hydrochloride 5 mg (T61; Hoechst Marion Roussel, Brussels, Belgium). This experiment was approved by the Ethics Committee for Animal Experimentation of the Faculty of Medicine of the K.U. Leuven. The aim was to describe the topographic anatomy of muscles, nerves, and vessels relevant to pelvic floor support and function. One ewe underwent detailed post-mortem in vivo magnetic resonance imaging. All underwent detailed post-mortem dissections (n = 6); half fresh and a half following primary fixation. A Phenol-Ethanol-Glycerine-Chloralhydrate mixture with this composition: 500 ml C_6H_5OH (91%) + 500ml C_2H_5OH (95%) + 31.25 ml $C_3H_8O_3$ + 31.25 g $C_2H_3Cl_3O_2$ was used to preserve specimen for later consultation. Specimens were placed for one week in 15l of this solution. Necropsies were photographically documented. One pelvis was silicon plastinated [28]. For the anatomical dissection and systematic reporting, we followed previous textbooks and studies of domestic mammal anatomy [29–33]. As clinicians and translational researchers, we draw comparisons to anatomical findings in women, as published in anatomical textbooks [34–36].

Plastination

Plastination was used to obtain a permanent specimen, including the bony pelvis, ligamentous structures, the deep muscles (*m. obturator externus, mm. gemelli, m. quadratus femoris, m. gluteus profundus, m. piriformis* and *m. pectineus*) In addition as well as the proximal part of the pelvic limbs were preserved, for later documentation and consultation. A freshly dissected specimen was fixed in 3.5% formaldehyde and plastinated using the *silicone10 (S10) impregnation technique* [37]. The specimen was pre-cooled to 4°C and dehydrated in 100% acetone at 25°C for two weeks. Then it was placed in a bath of S10 silicone, 1% S3 catalyst and chain extender at -25°C. Thereafter, impregnation was started
by gradually decreasing ambient pressure in the bath. After 10 days a minimal pressure of 5mmHg was reached and vacuum-forced impregnation was stopped. The excess of silicone was firstly drained at -25°C and the specimen was placed back at room temperature and normal atmospheric pressure. Finally, the specimen was cured in a chamber with vaporized S6 cross-linker [37].

Magnetic Resonance Imaging

A nulliparous ewe (n=1) underwent magnetic resonance (MR) tomography of the pelvis on a 3 Tesla MR device with a spinal coil (Magnetom Trio, Siemens, Erlangen, Germany) in the lateral recumbent position. Anatomic high-resolution T1 images were obtained with a slice thickness 0.9 mm and an interslice gap of 0mm (resolution 1.03 × 1.03 mm,

TE 4.92 ms, TR 10 ms, the field of view 330 mm, bandwidth 446 Hz/pixel). Sagittal scans were used to obtain anatomy and create a 3D model. Mimics Innovation Suite (MIS), v17.0 (Materialise NV, Leuven Belgium) was used to segment the pelvic bones, inner pelvic muscles and pelvic organs. Briefly, the bones and the pelvic organs were segmented using dynamic region growing tools. Afterwards, segmentation was verified visually and manually edited when necessary. 3D models were calculated and further processed (smooth, wrap etc.) to remove any holes, step geometries or spurious structures. The broad sacrotuberous ligament and the levator ani were defined by manually drawing splines on individual axial slices. The splines were exported to Matlab where a custom code generated a point cloud representing the structure of interest. The point cloud was then imported to the 3-matic module of MIS and triangulated to obtain a 3D mesh model. Defects in the resulting model (holes, sharp edges, double triangles etc.) were fixed using inbuilt functions of 3-matic. The accuracy of all resulting 3D models was verified by overlaying their contours on original images and browsing through the slices.

Sagittal and transversal scans were used to measure dimensions of the bony pelvis, including the obstetric conjugate (shortest distance between the cranial aspect of the symphysis and the promontory), the transverse inlet diameter (narrowest horizontal distance at the level of pelvic inlet), the vertical diameter (the shortest distance between the symphysis and the sacrum), the interspinous diameter and the intertuberous diameter (distances between corresponding anatomical structures), the sagittal outlet diameter (distance between the caudal aspect of the symphysis and the caudal end of the sacrum) and the inclination (angle between the cranial pelvic aperture and the front of the 5th lumbar vertebra) [38].

Histology

Specimens were taken at different locations to include representative areas: (1) the levator ani over its entire span between the anus and the tendinous arc on the obturator muscle, (2) the rectovaginal septum one cm above the hymenal remnants, (3) the urethro-vaginal complex one cm above the hymen, (4) the full thickness dorsal vaginal wall one cm below the cervix (5) and midway between 2 and 4. All were fixed with 4% neutral buffered formaldehyde for at least 48 hours, then immersed in phosphate buffered saline (PBS) for one hour, stored in 70% ethanol, embedded in paraffin and cut into 6-µm slices. Slides were stained with hematoxylin & eosin as well as Masson trichrome to allow identification of individual structures and collagen distribution. Images were captured at 25x magnification by an Axioplan 400 microscope (Zeiss, Oberkochen, Germany).

Immunohistochemistry

Immunohistochemistry was done to localize areas expressing estrogen receptor *alpha* (ER-α) and to define smooth muscle tissue. Analysis of these was qualitatively.

Estrogen receptor α (ER-α)

Vaginal wall sections were treated with 0,5% H_2O_2 in methanol for 30 min at room temperature and with Tris-HCl (0.01 M, pH 9,0) with 1 mM of Ethylene-diamine-tetraacetic acid (EDTA) at 78°C for 2 hours. Non-specific binding was minimized by incubating sections in 2% bovine serum albumin (BSA) and 1% milk in PBS-0.1% tween 80 for 30 min. Sections were incubated overnight at 4°C with the primary monoclonal mouse-anti-human antibodies against ER-α at 1:25 dilution (α-ER clone 1D5, 166 µg/ml, DAKO). Following incubation in 1% BSA and 2% milk in PBS-0.1% tween 80 for 15 min; sections were incubated with secondary goat-anti-mouse peroxidase-conjugated antibodies at 1:100 dilution and sheep serum in 1:25 dilution for 30 minutes.

Alpha-smooth muscle actin (α-SMA)

Detection was done on sections treated with 0.5% H_2O_2 in methanol for 30 min at room temperature and protein blocker (2% BSA and 1% milk in PBS-0.1% tween 80, 15 min). Sections were incubated with primary monoclonal mouse anti-human antibodies against smooth muscle actin at 1:200 dilution (α-SMA-clone 1A4, DAKO) for 2 hours. As secondary antibodies, we used Goat-anti-Mouse peroxidase-conjugated antibodies (1:100) with normal rat serum (1:25).

For both, the color reaction was developed with 3,3'-diaminobenzidine (Sigma) and sections were counterstained with Mayer's hematoxylin. Sections were then dehydrated through graded ethanol, cleared in xylene, and mounted in dePex (BDH, VWR international, Belgium).

RESULTS

Table 1 summarizes the most relevant findings. Findings are described in relation to the anatomy of woman, both in terms of similarities and differences. Relevant anatomical structures of the pelvis are described using the official veterinarian nomenclature [32]. Compared to anatomical nomenclature in humans, directions related to body orientation follow the older human anatomical nomenclature (i.e. dorsal rather than posterior, ventral rather than anterior, caudal rather inferior cranial rather than superior).

Bones and ligaments

The bony pelvis serves as a protective shell for the pelvic organs (Figure 1, A 3D reconstruction on MR that can be manipulated, is available as supplementary Figure S1, S2). The cranial pelvic aperture to the pelvis is formed by the *terminal line*, which is dorsally located on the promontory, laterally on the wing of the ilium and ventrally on the pectineal line of the pubis. The caudal pelvic aperture is limited by the sacrum, the caudal aspect of the broad sacrotuberous ligament, the ischial tuberosities and the ischiatic arch.

There are several gross differences with the female bony pelvis, that seem related to the sheep's quadruped nature. In the standing position, the sacrum and pubis are more or less parallel to the ground. The inlet to the pelvic cavity is more elliptic than in woman, where it is nearly round. The ventrodorsal in the ewe has a vertical inlet diameter compared to the transverse diameter in a woman and is smaller than in woman (Table 2). The pelvis is also more flattened dorsoventrally. The axis through the pelvic canal is straighter than in woman. The ovine pelvis is stretched craniocaudally: the promontory is much more cranial along the body axis than the ischiatic arch. All of this is thought to be related to the need for supporting a greater load in the ventral direction [39].

The shape of the pubic bones is to a certain degree comparable to that in woman. However, the caudal ramus of the pubis is much wider. The ischial bone is flattened thereby forming the tabula of the ischium and wide ramus of the ischial bones. The latter is cranially joined with the caudal ramus of the pubis. Together they allow the insertion of strong adductors. The ischial tuberosity is more prominent with its lateral aspects pointing far more laterally. The ischial spine appears more longitudinally stretched so it does not, like in a woman, protrude as a sharp narrow spine into the pelvic canal. The acetabulum is shallow and oriented parallel to the ground. The basis or shaft of the iliac wing is proportionally longer than in woman, from which much smaller iliac wings originate. The ventral cranial iliac spines are present, though less prominent. The obturator foramen is a 2.5 × 3.0 cm oval structure, its shape being comparable to the female. Its craniocaudal axis is parallel to the pelvic symphysis, whereas in woman it is at a 40° angle.

Table 1: *Anatomical differences in the musculoskeletal system between the female and ovine pelvis.*

	Ewe	Human
The obturator foramen	Filled with the intrapelvic part of the obturator externus muscle	Closed by the obturator membrane
Inner surface of the obturator foramen and its surroundings	The intrapelvic part of the obturator externus muscle	The obturator internus muscle
The greater sciatic foramen	Limited by a broad sacrotuberous ligament	Limited by the sacrospinous ligament
The piriformis muscle	The piriformis is merged with the gluteus medius	Splits the greater sciatic foramen into the supra- and infra-piriforme
The lesser sciatic foramen	Contains the caudal gluteal artery and vein	Contains the tendon of the obturator internus, internal pudendal vessels
The obturator internus muscle	Missing, function exerted by other external rotators	inserts around the obturator foramen and on obturator membrane
The levator ani muscle	Appears more as one uniform muscle	Comprises three discernable parts

Figure 1: *A comparison of bones and ligaments of the ovine and human pelvis. Ligaments are displayed in blue; light blue – the inguinal ligament (I), mid blue – the sacrospinous ligament (SS, not present in sheep), dark blue – the broad sacrotuberous ligament (ST). (Illustration by Myrthe Boymans, reproduced with permission from UZ Leuven, Leuven, Belgium.)*
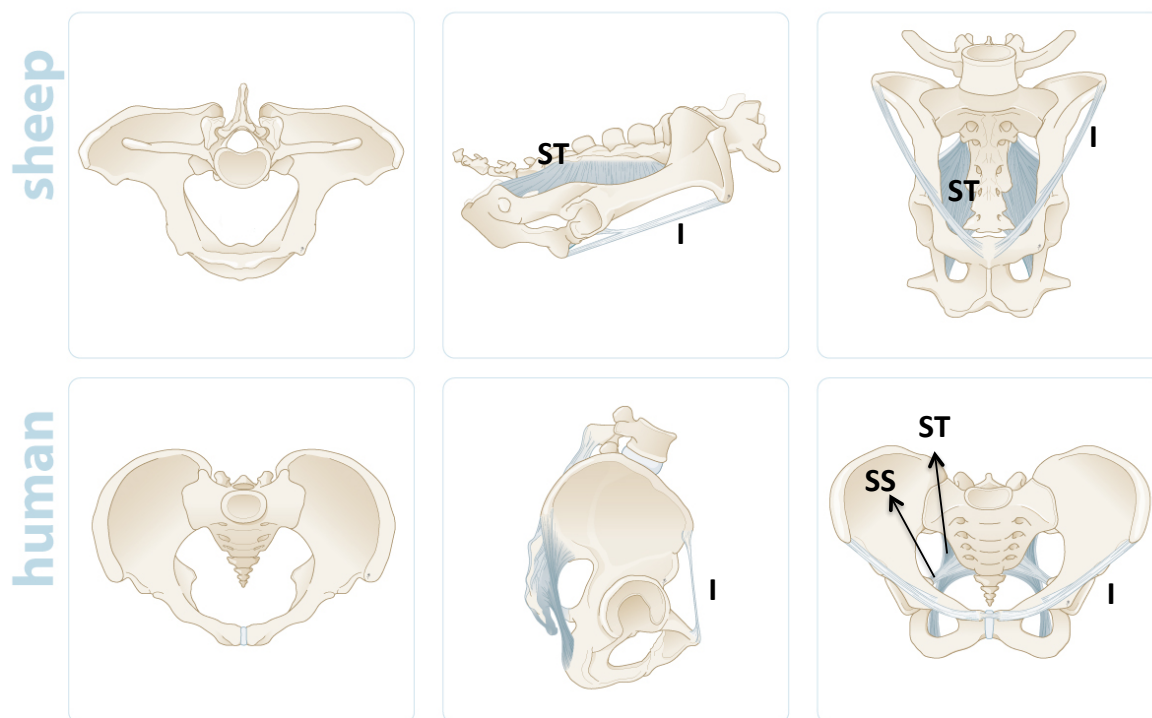
Table 2. *Dimensions of the female pelvis taken from literature [38, 40] compared to MR measurements in one ewe (weight: 60 kg). Obstetric conjugate: shortest distance between the cranial aspect of the symphysis and the promontory; transverse inlet diameter: narrowest horizontal distance at the level of pelvic inlet; vertical diameter: shortest distance between the symphysis and the sacrum; interspinous/intertuberous diameter: distances between corresponding anatomical structures; sagittal outlet diameter: distance between the caudal aspect of the symphysis and the caudal end of the sacrum; inclination: angle between the cranial pelvic aperture and the front of the 5th lumbar vertebra.In woman, the vertical diameter corresponds to the anterior-posterior diameter of the amplitude pelvis.*

	Human (cm)	Sheep (cm)
Obstetric conjugate	12.0 ± 0.9	8.9
Transverse inlet diameter	12.9 ± 0.9	7.8
Vertical diameter [41]	12.5	6.5
Sagittal outlet diameter	12.1 ± 0.9	7.2
Interspinous distance	10.9 ± 0.7	7.6
Intertuberous distance	12.0 ± 0.9	6.8
Inclination of the pelvis	135°	156.3°

Ligaments

The synovial sacroiliac joint in sheep, which is reinforced by a complex of ligaments, is shorter than in woman. The sacrotuberous ligament forms a large trapezoidal sheet, which originates from the sacral and the proximal coccygeal vertebrae and inserts laterally on the opposite side, as a long insertion line on the ischial spine and on the ischial tuberosity. This is usually referred to as *lig. sacrotuberous latum* because of its width. The caudal portion of the broad sacrotuberous ligament is palpable laterally to the tail. Compared to woman, this ligament is thicker and may be stiffer in ewes [33]. The cranial portion appears as a flattened sheet fanning out into the greater and lesser sciatic notches (an insertion that in a woman is not extensive), creating the greater and lesser sciatic foramen. The former contains the sciatic nerve and the cranial gluteal vessels. The sciatic nerve then continues caudally close to the dorsal aspect of the body of the ilium and passes behind the greater trochanter to the pelvic limb. The cranial gluteal vessel supplies the gluteal and gluteofemoral muscles. The lesser sciatic foramen contains only the caudal gluteal vessel and nerve, yet no part of the internal obturator muscle, which is missing in sheep [42]. Therefore there is neither a formal obturator membrane. However, the obturator nerve and vessels are just as in man, passing through the cranial part of the foramen. Sheep neither have a sacrospinous ligament [42]. The pelvic symphysis joint consists of a pubic and an ischiatic symphysis, the latter may become ossified in older animals. Between them is the *lamina fibrocartilaginea intercoxalis* that corresponds to interpubic disc [42, 43]. The joint has a fibrous capsule formed with the cranial pubic ligament and ischiatic arch ligament.

Pelvic diaphragm and muscles
M. obturatorius externus

Again, sheep have no internal obturator muscle. Its function (exo-rotation) is exerted by other rotators (*obturatorius externus, mm. gemelli* and *quadratus femoris*) in the region [42]. However, there is a discernible intrapelvic part of the external obturator muscle, which inserts on the inner aspects of the pubis and ischium, and can be considered as the counterpart of the internal obturator muscle in a woman. That intrapelvic part is passing through the obturator foramen to join the extrapelvic part which originates on the ventral surface around the obturator foramen. The distal insertion of the external obturator muscle terminates as a tendon in the trochanteric fossa. It is innervated by the obturator nerve. The intrapelvic part of the external obturator is covered by the obturator fascia. This fascia is locally reinforced where the levator muscle inserts, referred to as the *arcus tendineus musculi levatoris ani*.

M. Levator ani

The caudal aperture of the lesser pelvic cavity is closed by the *pelvic diaphragm*, which comprises both the coccygeus and the levator ani. These muscles are inserted between the internal and external pelvic diaphragmatic fascia (Figure 2, S2). The *levator ani* is a paired muscle plate, with different shape and insertions than in women (Table 3). Roughly spoken, the levator spans the pelvic floor much less obliquely than in women,

in whom the fibers run predominantly from the front to the back. It is proportionally also much smaller than in humans. In sheep, the levator muscle is divided into three parts based on their medial insertions (Figure 3, view from below):

- Its perineal or ventral part runs towards the midline-located *centrum tendineum* with some fibers to the anus and vagina.

- Its anal or intermediate portion inserts on the longitudinal layer of the rectal muscularis and engages further between the internal and external anal sphincter.

- A coccygeal or dorsal bundle stretches medially towards the area behind the anus towards the coccyx.

The lateral insertion on the tendinous arch of the levator ani is thinner, weaker and shorter than in woman [29]. Thus overall, the levator ani is very different from that in woman, which has five distinct parts [44]. Comparison of the relevant structures is displayed in Table 3. In ruminants, the ventral and dorsal parts are very limited whereas the bulk of the muscle inserts into the anus. The levator pulls the perineum and the anus cranially whereas in woman it elevates the anus. Therefore anatomists earlier proposed to use the name "*musculus retractor ani*", which would apply to all species [45].

Musculus coccygeus

The *musculus coccygeus* is responsible for the abduction of the tail. It is a fan-shaped muscle that originates laterally on the dorsal surface of the ischial spine (hence also called ischiococcygeus muscle) (Figure 2). There its dorsal surface is laterally covered with the broad sacrotuberous ligament and medially with the gluteal fascia. The medial insertion of the muscle is to the transversal processes of the first three coccygeal vertebrae. The coccygeus muscle is palpable through the skin laterally on the basis of the tail.

The innervation of the above muscles comes via the pudendal and caudal rectal nerves. When the tail is docked, a common practice, this muscle as well as the levator may undergo anatomical and functional deterioration [46].

Figure 2: Craniolateral view on the ovine and human pelvic floor. (A) Side-view of the ovine pelvic floor at necropsy. The rectum (R) and the urethro-vaginal complex (V) were pulled down to display the course of the levator ani (LAM) and coccygeus (CM) muscle. Selected nerves and vessels are outlined by dashed lines.

(B) Schematic drawing of the same area. (C) Schematic drawing of the clinical correlate of figure B, and positioned similarly, to facilitate reading. In the areas marked with a blue dashed line, the pelvic membrane was removed to visualize the following anatomical structures:

    1: The inner surface of the broad sacrotuberous ligament (pudendal nerve – yellow, inner pudendal artery, and vein – red, blue);

    2: the intrapelvic part of the external obturator muscle, which is in sheep attached around the obturator foramen (dashed black line) with the obturator artery and nerve entering in its craniolateral part;

    3: the intrapelvic part of the external obturator muscle bellow the tendinous arch of the levator ani (red line) with the pudendal vessels and nerve running through the ischiorectal fossa to the perineum.

(C) Schematic illustration of human pelvis showing similar structures as in sheep. Human pelvis is positioned similarly to the sheep natural stand.

LAM - Levator Ani Muscle, CM - Coccygeus Muscle, IOM - Internal Obturator Muscle EOM – External Obturator Muscle, R - Rectum, V - Vagina, P - Pubis, RVS – Rectovaginal Septum, S1, S5, Co1 – spinal vertebrae

(Illustration by Myrthe Boymans, reproduced with permission from UZ Leuven, Leuven, Belgium.)
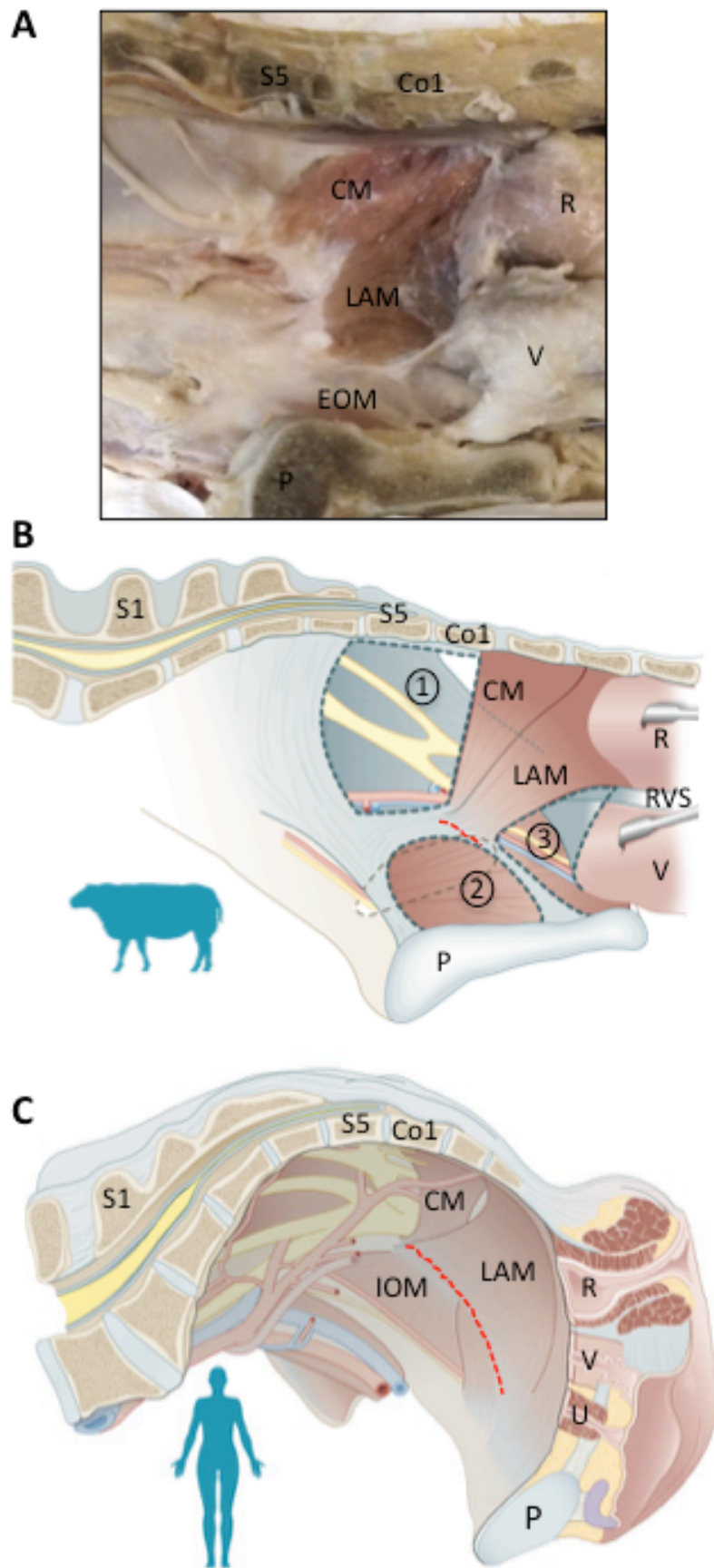
Table 3: *Components and insertion points of the levator ani in sheep and woman [44]. * The levator complex muscles in woman contains 5 divisions named on their insertion points, i.e. puboviseral complex (pubo-vaginal, pubo-perineal and pubo-anal), the puborectal and iliococcygeal muscle [44].*

Sheep Name	Sheep Ventrolateral insertion	Sheep Dorsomedial insertion	Female Name	Female Ventrolateral insertion	Female Dorso.medial insertion
Perineal	Fascia obturatoria	Centrum tendineum, vagina,	Puboperinealis* Pubovaginalis*	Dorsal aspect of the pubis	Insertion, to the perineal body and vaginal wall
Anal	Fascia obturatoria	Intersphincteric insertion	Puboanalis*	Dorsal aspect of the pubic bone	Intersphincteric insertion
Could not identify correlate			Puboanalis*	Dorsolateral aspect of the pubis	Sling around the rectum
Coccygeal	Dorsal aspect of the sciatic spine	Anococcygeal raphe, contralateral caudal vertebra	Puboanalis*	Fascia obturatoria, ilium	Iliococcygeal raphe (coccyx)
M. Coccygeus	Dorsal aspect of the ischial spine	Transversal processes of caudal vertebrae	Puboanalis*	Dorsal aspect of the sciatic spine	Coccyx

Perineum

On caudal inspection, the ewe has longer and deeper *vaginal vestibulum*, with the opening of the urethra on the ventral vaginal wall 3 - 4 cm cranially of the clitoris. The more caudal part of the vagina and the vestibulum are surrounded with the striated *musculus constrictor vulvae* and deeper, the *constrictor vestibuli* (Figure 3), with fibers intermingling with the external anal sphincter [47]. The constrictor muscles correlate to the bulbospongiosus muscles [47]. In the midline between the anal opening (Figure 4C) and the vagina is a short perineal body. Deeper down it consists of connective tissue and attachments of the perineal and perianal muscles (the *external anal sphincte*r, the *constrictor vulvae*, the *transversus perinei*, and the *retractor clitoridis*). The *retractor clitoridis* is quite unique, as it spans from the clitoris to the lower part of the spine, for which we do not see a human equivalent.

Lateral from the vaginal vestibulum and constricting muscles, there is a fibromuscular structure referred to as perineal membrane, and inserting laterally to the rami of the ischium (Figure 3). Its dorsal border is the poorly developed superficial transversal perineal muscle. Cranial to the perineal membrane yet caudal to the levator muscle complex is the ischiorectal space (Figure 3). Dorsally it is delineated by the broad sacrotuberous ligament. The ischiorectal fossa is filled with areolar fatty tissue. The pudendal nerve and vessels exit the peritoneal cavity dorsally to the levator ani and coccygeus muscle, and medially from the intrapelvic part of the obturator muscle, to enter the ischiorectal fossa.

Connective tissue support and vagina

The lower urinary tract, the uterus, and vagina are attached to the pelvic side wall by connective tissue that also contains the supplying vessels and nerves. The uterus is completely intraperitoneal. The sheep vagina in sheep stretches higher into the abdomen compared to humans and is 8 – 12 cm long. Conversely, the rectouterine pouch stretches as deep as 4 cm under the level of the cervix. The vesicouterine pouch is less deep, ending at the level of the cervix. The bladder except its neck is completely intraperitoneal. The pubovesical pouch stretches less deep than dorsally but as far as the bladder neck. The most caudal part of the broad ligament is at the level of the external cervical os and the dorsal vaginal fornix. At that level, the vagina and cervix are attached to the sacrum (S2 - S3) by a fibrous structure, which looks like the sacrouterine ligament (in woman referred to as level I support) [48, 49]. We did not find fibrous or ligamentary structures connecting the vagina to the pelvic sidewall; space is filled with vessels, nerves and loose connective tissue. The caudal third of the vagina is enclosed by the pelvic diaphragm (Figure 5A). The ventral vaginal wall is in tight relation to the urethra, which exits along the ventral vagina 3 - 4 cm above the clitoris (Figure 4). The caudal third of the urethra is surrounded by a horseshoe-shaped striated urethral muscle, inserting both sides of the midline on the ventral vaginal wall. Its bundles are transversely oriented, suggesting it has sphincteric function [50] (Figure 5A).

Figure 3: *Caudal view on the ovine and human dissected perineum.*
(A) Ovine perineum at the time of dissection, after removal of the skin, the most superficial muscles, visualizing the external anal sphincter (EAS), the constrictor vestibuli (CVe). The levator ani is not visible as it is covered with the coccygeus (CM). The perineal membrane (*) was partially removed and the arrow indicates the opening of the ischioanal fossa

(B) Schematic drawing of the ovine perineum with on the left the perineal membrane and superficial muscles removed, and the CM retracted, to expose the levator ani.

(C) Corresponding perineal view of the human pelvic floor, with on the left, part the perineal membrane, transverse perineal muscles, sacrospinous ligament, removed to expose the LAM. * indicates the perineal membrane.

(Illustration by Myrthe Boymans, reproduced with permission from UZ Leuven, Leuven, Belgium.)
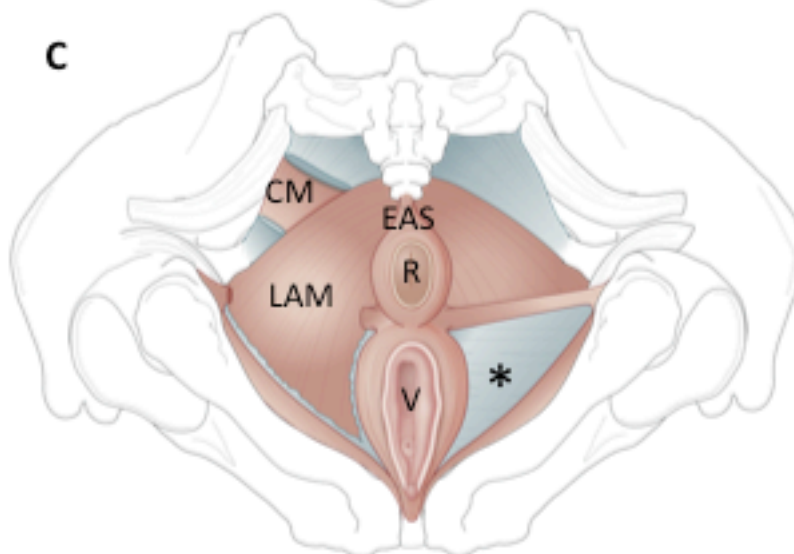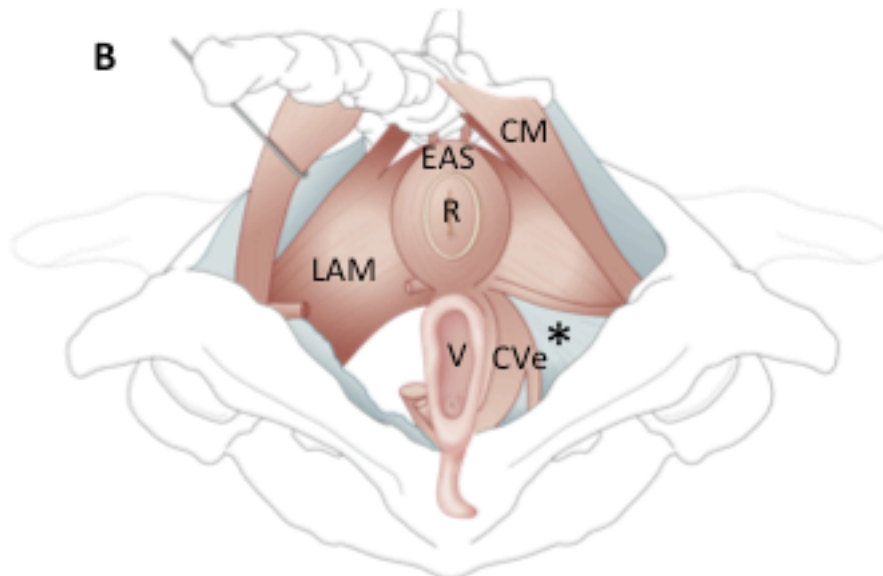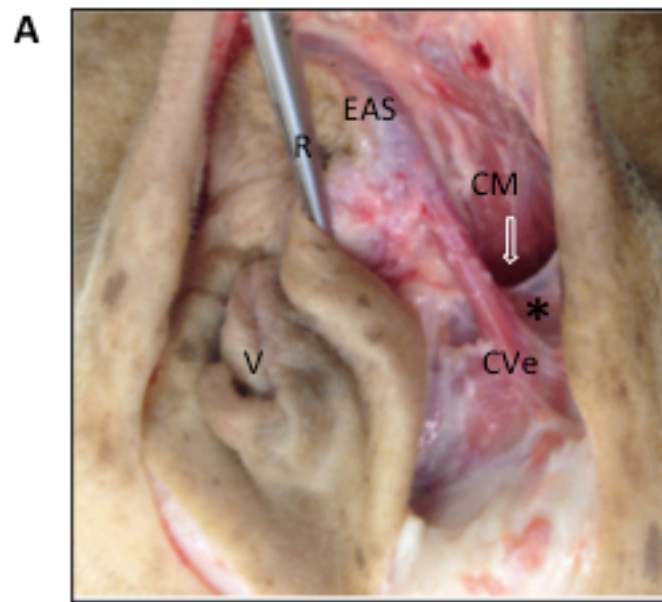
Figure 4: *Mid-sagittal section through the ovine pelvis.*
(A) An overview of a hemi sectioned ovine pelvis. The dashed rectangle indicates the area further magnified in C.

(B) A schematic drawing of hemisection A.

(C) detail of ovine perineum

Abbreviations: AC Anal Canal, B Bladder, C Cervix, RVP Rectovaginal Pouch, EAS External Anal Sphincter, IAS Internal Anal Sphincter, IUS Internal urethral sphincter, LMR Longitudinal muscle of the rectum, P Pubis, PB Perineal body, R Rectum, RE Rectal Epithelium, RVS rectovaginal septum, S Spine, V Vagina, U Urethra, Ur urethralis muscle, CVe Constrictor vestibuli.

(Illustration by Myrthe Boymans, reproduced with permission from UZ Leuven, Leuven, Belgium.)
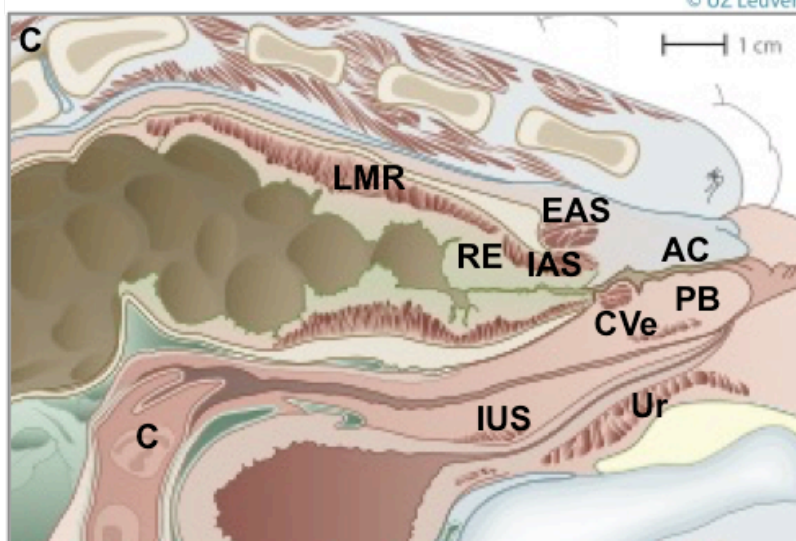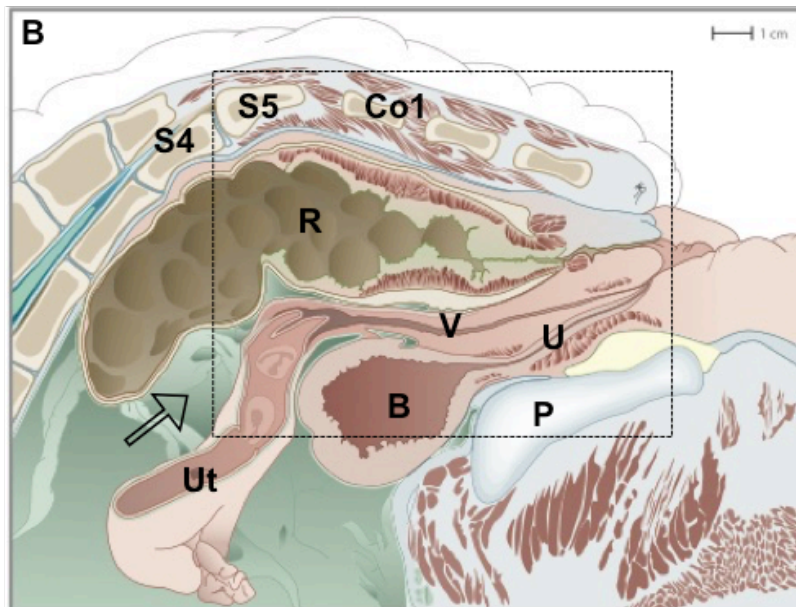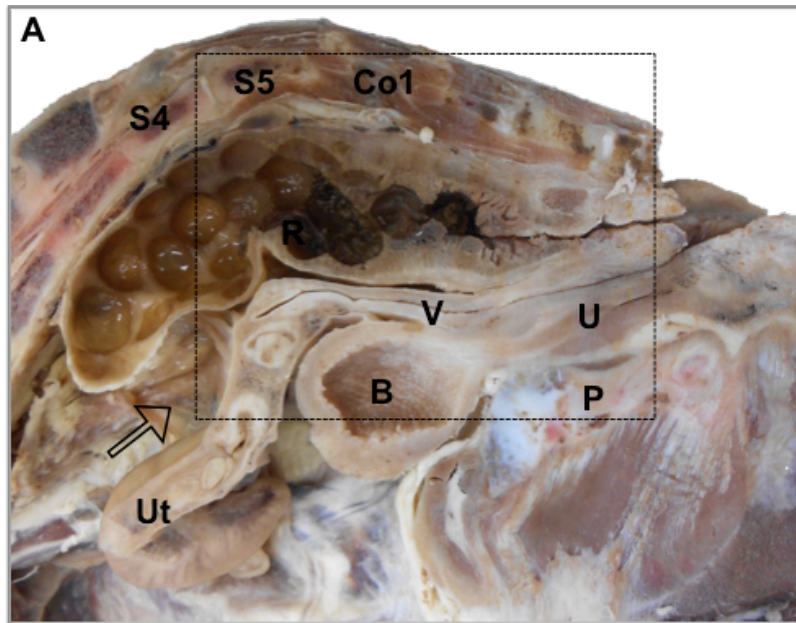
Rectum

The rectum is attached with the mesorectum to the dorsal wall of the pelvic cavity. Ventrally and laterally, there is a deep recto-uterine pouch. The rectum enlarges into the rectal ampulla and continues into the anal canal. It is surrounded by areolar tissue. The anus has an internal smooth and external striated anal sphincter. The latter has three parts; the *deeper* or most cranial part is intimately associated with the levator ani. The more *superficial* part is the strongest part with some fibers passing to the constrictor vulvae (Figure 3). Lastly, there is a *cutaneous* part with thin bundles mainly dorsolateral of the anus.

Vascular supply and innervation

The pelvic floor and organs receive most of their blood supply via the ovarian and the internal iliac artery and its branches. The inner iliac artery gives similar branches as in human. It continues into the inner pudendal artery, which runs dorsal of the coccygeus muscle and caudally through the pudendal canal to supply the structures of the perineum. Venous drainage is through the inner pelvic vein and the caudal vena cava.

Innervation of pelvic organs, pelvic floor and perineum originate from the lumbar nerves and lumbosacral plexus. We only describe those related to vaginal surgery. The obturator nerve originates from the lumbar (L4 - L6) root and runs medially to the iliac shaft. It passes together with the obturator artery and vein through the obturator canal, in the craniolateral part of the obturator foramen. It gives innervation to the entire external obturator muscle.

The sciatic nerve (L5 - S2) is the most robust nerve in the region. It leaves the pelvic cavity through the greater sciatic foramen and continues *behind* the broad sacrotuberous ligament and medially of the greater femoral trochanter. Its branches in this region are responsible for innervation of the deep gluteal muscles, the *gemelli* and the *quadratus femoris muscles*.

The pudendal nerve (S2 - S3) is responsible for motoric innervation of the perineal muscles and sensitive innervation of the perineum and the perianal region. The nerve itself runs *ventrally* of the broad sacrotuberous ligament. At the level of the pelvic diaphragm, it passes together with its accompanying vessels through the pudendal canal. The terminal branches for the perineal structures and organs are irradiating medially. The caudal rectal nerves also innervate muscles of the pelvic diaphragm and external anal sphincter. These are the most caudal branches of the sacral plexus. Their sensitive part innervates the anus.

Internal genitalia

The ovine reproductive tract consists of the ovaries, uterine tubes, a bicornuate uterus, the cervix and the vagina and a well-developed vestibule. The almond-shaped ovaries are attached with a short mesovarium to the dorsal surface of the broad ligament. The uterine tubes are thin (2 – 3 mm) yet 30 cm long tortuous structures. Their infundibula open near the ovaries. The bicornuate uterus has a very small common midline cavity

yet two long dorsolaterally twisted horns that take 80% of the uterine length. The cervix is not a firm anatomical structure yet rather a 4 - 10 cm long zone with a canal lined by interlocking ridges. The cervix protrudes into the vagina; there are left and right cervical lips. The vaginal part of the cervix and the external os of the uterus can be visualized during a vaginal examination.

Histology

The structure of the ovine vagina is similar to human. There is a stratified squamous epithelium, the lamina propria containing a multidirectional network of collagen and elastin fibers and the smooth muscles, which form the inner circular and outer longitudinal layer (Figures 5B, C, F). Finally, there is an adventitia which merges with the adventitia of the bladder and the rectum. The dorsocranial surface of the vagina that is exposed to the abdominal cavity is covered with parietal peritoneum. The muscularis in that area forms a dense band of longitudinally oriented smooth muscle (Figure 5F, asterisk).

ERα staining cells were found through the entire thickness of the vagina as well as its length. Most of them were based on their appearance and localization, fibroblasts and smooth muscle cells. Positive cells were found in the basal layers of the vaginal epithelium and in the vessels of the vaginal wall (Figure 5D, E). In the paravaginal attachment, there were ER-α positive staining fibroblasts and smooth muscle cells with a decreasing concentration when moving away from the vagina.

The urethra has an inner circumferential and outer longitudinal layer of smooth muscles. The cranial third has a pseudostratified columnar epithelium (urothelium), the rest is covered with the non-keratinized stratified squamous epithelium. The *m. urethralis* contains both types of muscle bundles, the majority being striated muscle. Around the urethra, ER-α positivity was found in fibroblasts and few or weakly stained smooth muscles and vessels. We did not find ER-receptors in the urothelium, urethral epithelium, nor in the striated part of the *m. urethralis.* The anus is covered with non-keratinized squamous epithelium which turns at the level of the transition zone into the columnar mucosa of the rectum. In the anal and rectal area, positive cells were scarce, mainly fibroblasts around in the external anal sphincter and few muscular nuclei in the external sphincter. Vessels, anal epithelium or smooth muscles were devoid of ER-positive cells.

The levator ani has a typical striated muscle appearance. It is covered by the *internal diaphragmatic pelvic fascia* which contains longitudinally organized collagen yet also some smooth muscle bundles (Figure 5G, I). There were ER-α positive connective tissue cells around the levator muscle bundles (Figure 5H). The muscle and vessels their selves did not express ER-α.

Figure 5: Histology of the ovine pelvic floor
(A) A cranial view on the ovine pelvic diaphragm. Specimen orientation correlates with its position in a naturally standing animal, i.e. rectum (R) on top. Below are the vagina (V) and urethra (U). The parietal peritoneum and retroperitoneal areolar tissue were removed to expose the levator ani (LAM) and the coccygeus (CM) muscle, the urethralis muscle (UR), and the tendinous arch of the levator ani (red dashed line). Rectangles refer to corresponding microscopic images in panel B, C and G.

(B) The ventral vaginal wall 1 cm above the external urethral os. The vaginal lumen is at the top, partly visible in a vaginal squamous epithelial fold; the urethra is below the section. One can discriminate from top to bottom the epithelium, the vaginal muscularis, en the urethral muscularis.

(C) Caudal part of the dorsal vaginal wall 1 cm above the hymen. The lumen is at the bottom, delineated by the squamous epithelium. Above is a superficial circular oriented muscular layer and a longitudinally oriented second muscular layer, and an adventitial layer. Rectangles indicate the areas further magnified as D and E.

(D) Large magnification (x400) of the vaginal epithelium, with immunohistochemical staining for ER-α. E: same but vaginal muscularis.

(F) Cranial part of the dorsal ovine vaginal wall 1cm below the cervix. The lumen is at the bottom, delineated by the squamous epithelium, and at the top is the peritoneum of the cul-de-sac. The * indicates a more extensive dense smooth muscle than in areas lower in the vagina.

(G) Low magnification of a transverse section from the rectum (left) to the arcus tendineus (right), to which the levator ani muscle (LAM) inserts (#).The dark blue line is a fascia covering the single obturator muscle on its intrapelvic course (OM). The LAM medial insertion is between the external (EAS) and internal (IAS) anal sphincter. The dotted line indicates the retractor clitoridis.
Rectangle H indicates a high magnification of the attachment of the LAM, demonstrating ER-α positive fibroblasts. Rectangle I indicates an area of the fascia pelvis covering the LAM, further magnified indicating its composition of fibrous and smooth muscle tissue.
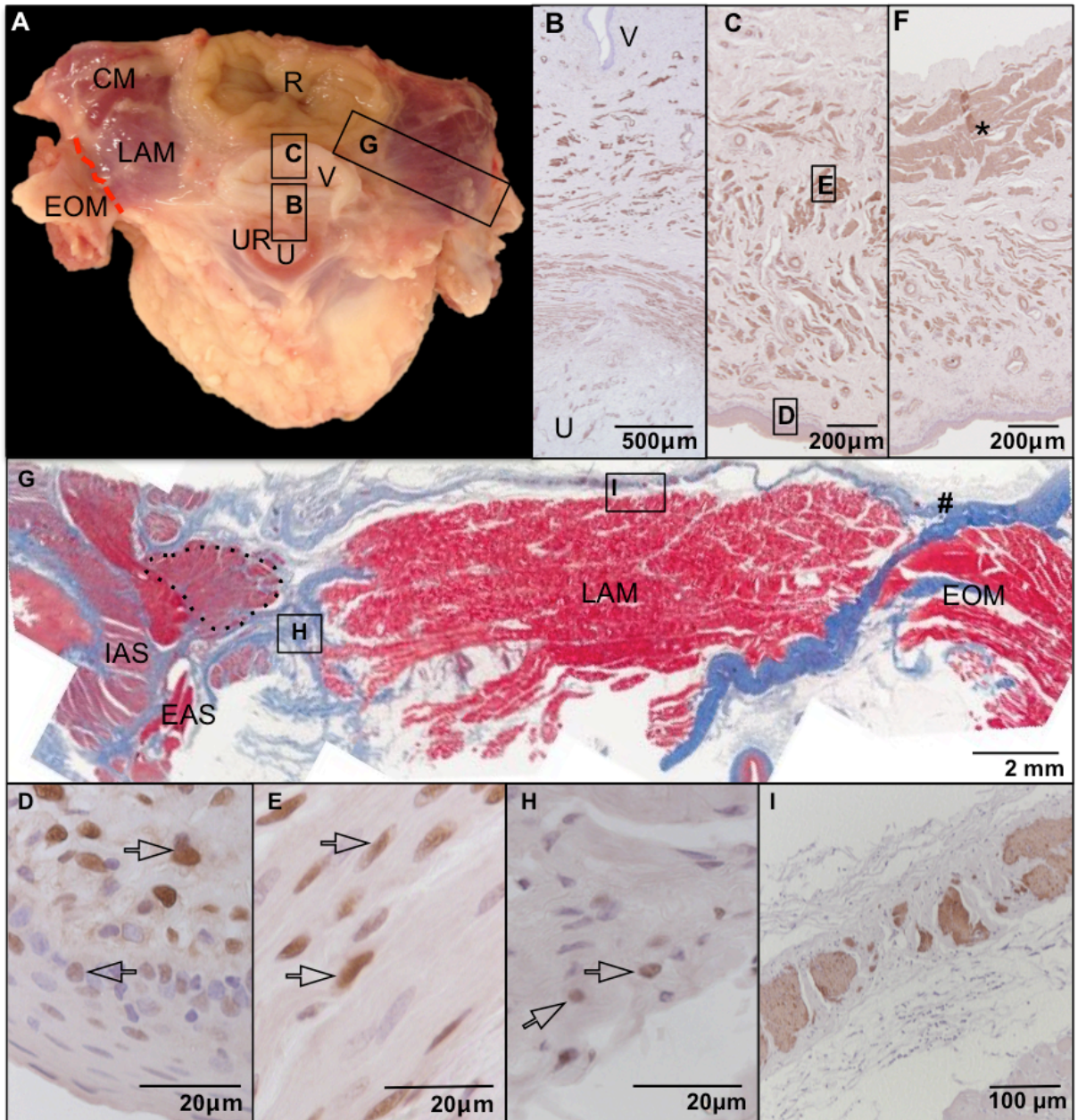
DISCUSSION

Herein we describe the ovine pelvic anatomy relevant to its potential use as an animal model for pelvic floor dysfunction. Although the sheep is a quadruped, we identified many gross and microscopic anatomical similarities to the female human pelvis. The main differences are the shape and orientation of the pelvis, the absence of a sacrospinous ligament, a different structure of the obturator muscle complex and obviously a tail. The levator ani and coccygeus muscle are present and have a very comparable insertion. In sheep, the perineal and vaginal parts of the levator are not separately named, yet lumped into the perineal part of the levator. The puborectal part is however missing. The coccygeus muscle is more developed – coinciding with the presence of a formal tail. Proportionally spoken the ovine vagina and cervix are also very comparable, and to a certain degree also in terms of their attachments, morphology, and dimensions. On the ventral vaginal wall, there is a marked difference between humans, as the urethra inserts 4 cm above the clitoris. Posteriorly, however, the rectovaginal space is very comparable. As in the female, there is a wide expression of ER, though we could not find these in the epithelium lining the urethra, bladder, anus, as well as the internal anal sphincter.

We became interested in sheep as a model for POP because of the many similarities to a woman, as elegantly summarized in the reviews by Couri et al and Abramowitch et al [24, 48]. We were already familiar with the ewe, mainly for reproductive studies [51], yet particularly the similar length and diameter of the vagina drew our interest in this model for vaginal surgery [18, 26, 52]. However, the analogies go much further. First, the ewe has an estrus cycle (17d), the long gestation period for 147 days, an average birth weight of a lamb is 3,6 - 3,9 kg (Swifter). Pelvic support structures are also organized at three levels [48, 53]. There is a standardized prolapse quantification system that can be used in ewes, very much in line with the Baden-Walker system [24]. In addition, 15% of sheep spontaneously develop POP [8, 54]. Obstetrical risk factors for POP, such as pregnancy and number of vaginal deliveries, high birth weight and dystocia [8, 55] are similar between ewes and women. Other predisposing factors are elevated intra-abdominal pressure, intra-abdominal fat, advancing age, multiplets and a history of POP [56]. Ewes with prolapse also display changes in collagen metabolism, however, the role of estrogens in development of POP remains unclear [23]. Another analogy is that there are certain, yet unidentified, genetic factors, causing certain pedigrees to be more likely to have POP [54, 55]. Sheep are cheaper, more easily accessible, and there are less ethical constraints than non-human primates. Consequently, our group and other researchers have started to use this model for biomechanical testing and vaginal surgery [19, 22, 25, 26, 57].

In view of future applications, we embarked on formal anatomical and histological comparison of sheep to human pelvic morphology. The anatomy of quadrupeds, as opposed to bipeds, corresponds to differently oriented loads. In ewes, the gravity is oriented perpendicular to the sacrum whereas in human it is vertical. Conversely, the erect position of women and

resulting loads led to changes in bone mass and bone architecture [39]. Strong muscles that keep the trunk erect, such as the *gluteus maximus* or *erector spinae* muscles require enlargement and different orientation of the iliac wings. The downward facing load results in a wider sacrum, spinal lordosis and kyphosis, orientation and a well-developed pelvic diaphragm, next to others [58]. In quadrupeds the main load is facing the ventral side of the pelvic cavity, which is associated with more developed pubic bones, creating a *bony* pelvic floor rather than a diaphragm [32, 39]. Conversely, the loads towards the pelvic diaphragm are low[59].

We were able to easily identify relevant structures such as the levator ani muscle and a three-level support system [53]. At the level I we found fibromuscular structures containing vessels on gross anatomy inspection, yet nerves and lymphatic vessels were also demonstrated in earlier anatomical studies [60, 61]. Level II reportedly includes the pubocervical and rectovaginal fascia originating from the tendinous arch of the pelvic fascia and of the tendinous arc of the rectovaginal fascia, respectively [61]. Both fasciae fuse with the fascia of the vagina and rectum, which makes it difficult to separate this anatomic structure. According to veterinarian textbooks, ruminants have also two tendinous arches, yet we had difficulties to identify a white line corresponding to the tendinous arc of the rectovaginal septum. However, we identified an obvious tendinous arch of the pelvic fascia and confirmed it by histology (Fig. 5). In women, level III comprises perineal support structures. The ovine caudal vagina is surrounded by similarly organized structures and there is a fibromuscular fascia that corresponds to the perineal membrane. The correlate of the *m. bulbospongiosus* is actually two muscles, which surround the vestibulum (*m. constrictor vestibuli*) and vulva (*m. constrictor vulvae*). According to veterinarian textbooks, they originate from a single structure [62]. Lastly, the function of the levator ani muscle in sheep seems to be confined to retract the anus yet not truly supporting pelvic organs, which rest rather on the bony pelvic floor. Our dissections indeed confirmed the existence of extravaginal spaces of relevance to surgical experimentation. Given the different urethral insertion point, dissection of the ventral vaginal wall is more difficult in its lower part, yet feasible above the urethra. The posterior compartment is easily accessible and is a relatively large and avascular space [26].

We did not perform a formal histological comparison, however, microscopic images of the vagina, urethra, bladder, rectum, anus and the levator ani look very similar to human. The epithelium is of the same type as in human. Smooth muscle tissue is present in the *lamina muscularis* around the vagina, urethra, and bladder. Reportedly, the thickness of the vaginal epithelium is dependent on the ovarian cycle similar to what has been observed in women, though we did not test this in this experiment [63, 64]. The external and internal anal sphincters contain striated and smooth muscle, respectively. Similarly to humans, the anus is surrounded with perianal glands and lymphatic tissue.

In view of future experimentation, we also documented the distribution of estrogen receptors, which is to a certain extent similar to that in women.

In the vagina, the distribution looked very much the same as in women [65, 66], with demonstrable nuclear receptors in both the epithelium, smooth muscle, vessels, and fibroblasts. In the levator muscle, we could only identify ER-α in the fibroblasts between the muscle fibers. For the urethra, bladder, and anus we identified receptors in fibroblasts, and rarely in the smooth muscle cells. In women squamous epithelial cells of the urethra and the anus and the internal anal sphincter have also been shown to express ER-α [66–68]. However, the apparent difference in the regional distribution of ER-α cells may also in part be wrongly estimated due to the uniform dilution on immunostaining used.

In conclusion, we found sufficient analogy between pelvic floor structures of ewes and women. Ewes spontaneously develop POP, have similar risk factors of POP and have parallel anatomical structures to women. This opens the door to use this model further for studies pelvic floor reconstruction, as well as to study more in detail the impact of life events such as pregnancy, vaginal delivery, aging, menopause and therapeutic treatments or interventions for pelvic organ prolapse

ADDITIONAL MATERIAL

Figure S1. 3D reconstruction of the ovine pelvis with relevant structures, which can be added or removed at convenience (3D PDF file). Grey – bones, violet - broad sacrotuberous ligament, red – intrapelvic part of the obturator externus muscle, purple – coccygeus muscle, pink – levator ani muscle, solid pink – external and internal anal sphincter, yellow – urinary bladder and urethra, brown – rectum and anus, levander – vagina and uterus. Copyright: UZ Leuven.

Figure S2: T1 weighted MRI of the ovine pelvis:
(1): Sagittal midline section. P pubis, S spine. Yellow dashed lines mark section in which panel 2, 3, 4 and 5 were made.
(2): Coronal section. Attachments of the levator ani muscle (arrows) to the tendinous arch of the levator ani (asterisk) and to the perineal body (PB). B bladder, U urethra, UH uterine horn, V vagina
(3): Coronal section. Attachment of the levator ani muscle (circle) to the rectum (R).
(4): Transversal section. Attachment of the levator ani (asterisk) to the tendinous arc on the fascia of the intrapelvic part of the external obturator muscle (EOM). The muscle visible more dorsally is the coccygeus muscle (CM). The CM originates on the lateral aspects of the coccygeal vertebrae (Co).
(5): Transversal section. Arrows indicate the levator ani muscle, with its attachment (circle) to the rectum (R). The most dorsal part of the muscle is also attached to the coccygeal vertebrae (Co).

Ethical approval: The experiment was approved by the Ethics Committee for Animal Experimentation of the Faculty of Medicine of the K.U. Leuven. All applicable international, national and institutional guidelines for the housing, care and use of animals were followed. Procedures performed in this study were in accordance with the ethical standards of the institution at which they were conducted.

Author Contribution: I.U.: protocol development, data collection, and analysis, manuscript writing. K.V., P.H., and L.K.: data analysis and manuscript editing. R.R. and N.S.: 3D model development. D.D.: data collection. A.F.: protocol development, data collection, manuscript editing. J.D.: data analysis, manuscript writing, and editing.

REFERENCES:

1. Hunskaar S, Vinsnes A (1991) The quality of life in women with urinary incontinence as measured by the sickness impact profile. J Am Geriatr Soc 40:976–7.

2. Svihrova V, Svihra J, Luptak J, et al. (2014) Disability-adjusted life years (DALYs) in general population with pelvic organ prolapse: a study based on the prolapse quality-of-life questionnaire (P-QOL). Eur J Obstet Gynecol Reprod Biol 182:22–6. doi: 10.1016/j.ejogrb.2014.08.024

3. Glazener C, Elders A, MacArthur C, et al. (2013) Childbirth and prolapse: Long-term associations with the symptoms and objective measurement of pelvic organ prolapse. BJOG An Int J Obstet Gynaecol 120:161–168. doi: 10.1111/1471-0528.12075

4. Løwenstein E, Ottesen B, Gimbel H (2014) Incidence and lifetime risk of pelvic organ prolapse surgery in Denmark from 1977 to 2009. Int Urogynecol J. doi: 10.1007/s00192-014-2413-y

5. DeLancey JOL, Kane Low L, Miller JM, et al. (2008) Graphic integration of causal factors of pelvic floor disorders: an integrated life span model. Am J Obstet Gynecol 199:610.e1-5. doi: 10.1016/j.ajog.2008.04.001

6. Alan M, Cetin Y, Sendag S, Eski F (2007) True vaginal prolapse in a bitch. Anim Reprod Sci 100:411–4. doi: 10.1016/j.anireprosci.2006.10.022

7. Miesner MD, Anderson DE (2008) Management of Uterine and Vaginal Prolapse in the Bovine. Vet Clin North Am Food Anim Pract 24:409–419. doi: http://dx.doi.org/10.1016/j.cvfa.2008.02.008

8. Scott PR (2005) The management and welfare of some common ovine obstetrical problems in the United Kingdom. Vet J 170:33–40. doi: 10.1016/j.tvjl.2004.03.010

9. Coates KW, Gibson S, Williams LE, et al. (1995) The squirrel monkey as an animal model of pelvic relaxation: An evaluation of a large breeding colony. Am J Obstet Gynecol 172:1664–1670. doi: 10.1016/0002-9378(95)90577-4

10. Liu X, Zhao Y, Pawlyk B, et al. (2006) Failure of elastic fiber homeostasis leads to pelvic floor disorders. Am J Pathol 168:519–28. doi: 10.2353/ajpath.2006.050399

11. Rahn DD, Acevedo JF, Roshanravan S, et al. (2009) Failure of Pelvic Organ Support in Mice Deficient In Fibulin-3. Am J Pathol 174:206–215. doi: http://dx.doi.org/10.2353/ajpath.2009.080212

12. Drewes PG, Yanagisawa H, Starcher B, et al. (2007) Pelvic organ prolapse in fibulin-5 knockout mice: pregnancy-induced changes in elastic fiber homeostasis in mouse vagina. Am J Pathol 170:578–89. doi: 10.2353/ajpath.2007.060662

13. Moalli P a, Howden NS, Lowder JL, et al. (2005) A rat model to study the structural properties of the vagina and its supportive tissues. Am J Obstet Gynecol 192:80–8. doi: 10.1016/j.ajog.2004.07.008

14. Van Herck H, Hesp AM., Vessluis A, et al. (1989) Prolapsus vaginae in the IIIVO/JU rabbit. Lab Anim 333–336.

15. Otto L, Slayden DO, Clark A (2002) The rhesus macaque as an animal model for pelvic organ prolapse. Am J Obstet Gynecol 186:416–421. doi: 10.1067/mob.2002.121723

16. Mattson J a, Kuehl TJ, Yandell PM, et al. (2005) Evaluation of the aged female baboon as a model of pelvic organ prolapse and pelvic reconstructive surgery. Am J Obstet Gynecol 192:1395–8. doi: 10.1016/j.ajog.2004.12.046

17. Feola A, Abramowitch S, Jallah Z, et al. (2013) Deterioration in biomechanical properties of the vagina following implantation of a high-stiffness prolapse mesh. BJOG 120:224–32. doi: 10.1111/1471-0528.12077.

18. Krause H, Goh J (2009) Sheep and rabbit genital tracts and abdominal wall as an implantation model for the study of surgical mesh. J Obstet Gynaecol Res 35:219–224. doi: 10.1111/j.1447-0756.2008.00930.x

19. de Tayrac R, Alves A, Thérin M (2007) Collagen-coated vs noncoated low-weight polypropylene meshes in a sheep model for vaginal surgery. A pilot study. Int Urogynecol J Pelvic Floor Dysfunct 18:513–20. doi: 10.1007/s00192-006-0176-9

20. Chen X, Creed KE (2004) Histochemical and contractile properties of striated muscles of urethra and levator ani of dogs and sheep. Neurourol Urodyn 23:702–8. doi: 10.1002/nau.20053

21. Rezapour M, Novara G, Meier P a, et al. (2007) A 3-month preclinical trial to assess the performance of a new TVT-like mesh (TVTx) in a sheep model. Int Urogynecol J Pelvic Floor Dysfunct 18:183–7. doi: 10.1007/s00192-006-0130-x

22. Ulrich D, Edwards SL, Su K, et al. (2014) Influence of reproductive status on tissue composition and biomechanical properties of ovine vagina. PLoS One 9:e93172. doi: 10.1371/journal.pone.0093172

23. Ennen S, Kloss S, Scheiner-Bobis G, et al. (2011) Histological, hormonal and biomolecular analysis of the pathogenesis of ovine Prolapsus vaginae ante partum. Theriogenology 75:212–9. doi: 10.1016/j.theriogenology.2010.08.007

24. Couri B, Lenis A, Borazjani A, et al. (2012) Animal models of female pelvic organ prolapse: lessons learned. Expert Rev Obs Gynecol 7:249–260. doi: 10.1586/eog.12.24.Animal

25. Endo M, Urbankova I, Vlacil J, et al. (2015) Cross-linked xenogenic collagen implantation in the sheep model for vaginal surgery. Gynecol Surg 113–122. doi: 10.1007/s10397-015-0883-7

26. Manodoro S, Endo M, Uvin P, et al. (2013) Graft-related complications and biaxial tensiometry following experimental vaginal implantation of flat mesh of variable dimensions. BJOG 120:244–50. doi: 10.1111/1471-0528.12081

27. Feola A, Endo M, Urbankova I, et al. (2015) Host reaction to vaginally inserted collagen containing polypropylene implants in sheep. Am J Obstet Gynecol 212:474.e1-474.e8. doi:

10.1016/j.ajog.2014.11.008

28. von Hagens G, Tiedemann K, Kriz W (1987) The current potential of plastination. Anat Embryol 4:411–21.

29. König HE, Liebich HG (2007) Veterinary Anatomy of Domestic Mammals, 3rd ed. Schattauer, Stuttgart

30. König H, Liebich H (2003) Anatomie domacich savcu, 2. dil, 2nd ed. Hájko & Hájková, Bratislava

31. König H, Liebich H (2003) Anatomie domacich savcu, 1+2. dil, 2nd ed. Hájko & Hájková, Bratislava

32. Schaller O, Constantinescu G, Habel E, et al. (2007) Illustrated Veterinary Anatomical Nomenclature, 2nd editio. Verlag Enke, Stuttgart, Germany

33. Barone R (2009) Anatomie Compare des Mammiferes Domestiques, 4th ed. VIGOT, Paris

34. Drutz HP, Herschorn S, Diamant NE (2003) Female Pelvic Medicine and Reconstructive Pelvic Surgery, 1st ed. Springer London, London

35. Herschorn S (2004) Female pelvic floor anatomy: the pelvic floor, supporting structures, and pelvic organs. Rev Urol 6 Suppl 5:S2–S10.

36. Stoker J, Taylor S, DeLancey J (2008) Anatomy. In: Baert A, Knauth M (eds) Imaging pelvic floor Disord., 2nd ed. Springer Berlin Heidelberg, Berlin, Heidelberg, pp 5–10

37. DeJnog K, Henry RW (2007) Silicon Plastination of Biological tissue: Cold-temperature Technique Biodur Technique and Products. J Int Soc Plast 22:2–14.

38. Lenhard MS, Johnson TRC, Weckbach S, et al. (2010) Pelvimetry revisited: analyzing cephalopelvic disproportion. Eur J Radiol 74:e107-11. doi: 10.1016/j.ejrad.2009.04.042

39. Hogervorst T, Bouma HW, Vos J De (2009) Evolution of the hip and pelvis. Acta Orthop 80:1–38.

40. Malpas P, Hamilton C (1939) The Effect of the Inclination of the Pelvic Brim and the Shape and Inclination of the Upper Sacrum on the Passage of the Head through the Upper Pelvis. J R Soc Med 1597–1612.

41. Cihák R (2001) Panev jako celek. Anat. 1, 2nd ed. Grada, Prague, pp 284–7

42. König H, Liebich H (2003) Zadní neboli panevni koncetiny (membra pelvina). In: Míšek I, Danko J (eds) Anat. Domac. savcu, 1.díl, 2nd ed. Hájko & Hájková, Bratislava, pp 224–249

43. Becker I, Woodley SJ, Stringer MD (2010) The adult human pubic symphysis: a systematic review. J Anat 217:475–87. doi: 10.1111/j.1469-7580.2010.01300.x

44. Kearney R, Sawhney R, DeLancey JOL (2004) Levator Ani Muscle Anatomy Evaluated by Origin-Insertion Pairs. Obstet Gynecol 104:168–173. doi: 10.1016/j.micinf.2011.07.011.Innate

45. Barone R (2009) Tome 3, Splanchnologie I: appareil disetif. In: Barone R (ed) Anat. Comparée des Mammiferes Domest., 4th ed. VIGOT, Paris, pp 447–453

46. Thomas D., Waldron D., Lowe G., et al. (2003) Length of docked tail and the incidence of rectal prolapse in lambs. J Anim Sci 2725–2732.

47. Schaller O, Constantinescu G, Habel E, et al. (2007) Splanchnology: Perineum. In: Schaller O (ed) Illus. Vet. Anat. Nomencl., 2nd ed. Verlag Enke, Stuttgart, Germany, Germany, pp 224–225

48. Abramowitch SD, Feola A, Jallah Z, Moalli PA (2009) Tissue mechanics, animal models, and pelvic organ prolapse: a review. Eur J Obstet Gynecol Reprod Biol 144 Suppl:S146-58. doi: 10.1016/j.ejogrb.2009.02.022

49. König H, Liebich H (2003) Telni dutiny. In: Míšek I, Danko J (eds) Anat. Domac. savcu, 2.díl, 2nd ed. Hájko & Hájková, Bratislava, pp 13–14

50. Barone R (2001) Tome 4, Splanchnologie II: appareil uro-génital. In: Barone R (ed) Anat. Comparée des Mammiferes Domest., 3rd ed. VIGOT, Paris, p 169

51. Deprest JA, Luks FI, Peers KH, et al. (1995) Intrauterine endoscopic creation of urinary tract obstruction in the fetal lamb: a model for fetal surgery. Am J Obs Gynecol 172:1422–1426. doi: 0002-9378(95)90472-7 [pii]

52. Barnhart KT, Izquierdo A, Pretorius ES, et al. (2006) Baseline dimensions of the human vagina. Hum Reprod 21:1618–22. doi: 10.1093/humrep/del022

53. Ashton-Miller J a, DeLancey JOL (2007) Functional anatomy of the female pelvic floor. Ann N Y Acad Sci 1101:266–96. doi: 10.1196/annals.1389.034

54. Low J, Sutherland H (1987) A census of the prevalence of vaginal prolapse in sheep flocks in the Borders region of Scotland. Vet Rec 120:571–5.

55. Speijers MHM, Carson AF, Dawson LER, et al. (2010) Effects of sire breed on ewe dystocia, lamb survival and weaned lamb output in hill sheep systems. Animal 4:486–96. doi: 10.1017/S1751731109991236

56. Scott PR (2015) Lambing, part 3 - Vaginal and Uterine Prolapse. In: http://www.nadis.org.uk/bulletins/lambing/lambing-part-3-vaginal-and-uterine-prolapse.aspx. http://www.nadis.org.uk/bulletins/lambing/lambing-part-3-vaginal-and-uterine-prolapse.aspx.

57. Liang R, Abramowitch S, Knight K, et al. (2013) Vaginal degeneration following implantation of synthetic mesh with increased stiffness. BJOG An Int J Obstet Gynaecol 120:233–243. doi: 10.1111/1471-0528.12085

58. Ishida H, Tuttle R, Pickford M, et al. (2006) Morphological adaptation of rat femora to difference mechanical environments. In: Ishiada H, Tuttle RH, Pickfor M (eds) Hum. Orig. enviromental backgrounds, 1st ed. Springer, Kyoto, Japan, pp 123–134

59. McLean JW, Claxton JH (1960) Vaginal prolapse in ewes. Part VII: The measurement and effect of intra-abdominal pressure. New Zeal Vet 8:51–61.

60. Ramanah R, Berger MB, Parratte BM, Delancey JOL (2012) Anatomy and histology of apical support: a literature review concerning cardinal and uterosacral ligaments. Int Urogynecol J 23:1483–94. doi: 10.1007/s00192-012-1819-7

61. Ercoli A, Delmas V, Fanfani F, et al. (2005) Terminologia Anatomica versus unofficial descriptions and nomenclature of the fasciae and ligaments of the female pelvis: a dissection-based comparative study. Am J Obstet Gynecol 193:1565–73. doi: 10.1016/j.ajog.2005.05.007

62. König H, Liebich H (2003) Samici pohlavni organy (organa genitalia feminina). Anat. domáacich savcu, 2. díl, 2nd ed., C. Hájko & Hájková, Bratislava, pp 148–155

63. Vincent KL, Bourne N, Bell AB, et al. (2009) High resolution imaging of epithelial injury in the sheep cervicovaginal tract: a promising model for testing safety of candidate micorobicedes. Sex Transm Dis 36:312–318. doi: 10.1097/OLQ.0b013e31819496e4.HIGH

64. Vincent KL, Vargas G, Wei J, et al. (2013) Monitoring vaginal epithelial thickness changes noninvasively in sheep using optical coherence tomography. Am J Obstet Gynecol 208:282.e1-282.e7. doi: 10.1016/j.ajog.2013.01.025

65. Pelletier G, El-Alfy M (2000) Immunocytochemical localization of estrogen receptors alpha and beta in the human reproductive organs. J Clin Endocrinol Metab 85:4835–4840. doi: 10.1210/jcem.85.12.7029

66. Copas P, Bukovsky A, Asbury B, et al. (2001) Estrogen, progesterone, and androgen receptor expression in levator ani muscle and fascia. J Womens Heal Gend Based Med 10:785–95.

67. Blakeman PJ, Hilton P, Bulmer JN (2000) Oestrogen and progesterone receptor expression in the female lower urinary tract, with reference to oestrogen status. BJU Int 86:32–38. doi: 10.1046/j.1464-410X.2000.00724.x

68. Oettling G, Franz HB (1998) Mapping of androgen, estrogen and progesterone receptors in the anal continence organ. Eur J Obstet Gynecol Reprod Biol 77:211–6.

CHAPTER 4

FIRST DELIVERY AND OVARIECTOMY AFFECT BIOMECHANICAL AND STRUCTURAL VAGINAL PROPERTIES IN THE OVINE MODEL.

Iva Urbankova, Geertje Callewaert, Silvia Blacher, Dries Deprest, Lucie Hympanova, Andrew Feola, Laurent De Landsheere, Jan Deprest

Centre for Surgical Technologies, Department of Development and Regeneration, Clinical Specialties Research Groups, Faculty of Medicine & Pelvic Floor Unit, Departments of Obstetrics & Gynecology and Urology, University Hospitals KU Leuven, Leuven, Belgium

Department of Obstetrics and Gynaecology & Laboratory of Tumor and Development Biology, GIGA-Cancer, Institute of Pathology, University of Liège, Belgium

Institute for the Care of Mother and Child and Third Faculty of Medicine, Charles University, Prague, Czech Republic

ABSTRACT:

Introduction & Hypothesis: Animal models are useful for understanding the genesis as well as the development of novel therapies for pelvic floor dysfunction. There is a need for an alternative large animal model to the non-human primate. Therefore we studied the effect of the first vaginal delivery, ovariectomy and systemic hormonal replacement therapy (HRT) on the biomechanical and structural properties of the ovine vagina.

Methods: We examined the gross anatomical properties of nulliparous, primiparous, ovariectomized multiparous, and ovariectomized hormone replaced multiparous sheep (n = 6/group). We also harvested mid- and distal vaginal tissue to determine smooth muscle contractility, passive biomechanical properties and performed morphometric assessment of vaginal wall layers, collagen and elastin content and immunostained for α-smooth muscle actin and estrogen receptor-α.

Results: There were no regional differences in the nulliparous vagina. One year after first vaginal delivery, distal vaginal stiffness and contractility were decreased, whereas elastin increased. The ovariectomized sheep mid-vagina was stiff, its epithelium thin and lacking glycogen. HRT decreased mid-vaginal stiffness by 45% without measurable effect on contractility or elastin content and increased epithelial thickness and glycogen. The latter occurred also in the distal vagina. At this location, there were no changes in morphology neither in stiffness.

Conclusion: In sheep, life phase events like delivery and ovariectomy impact the biomechanical properties of the vagina in a region-specific way. Vaginal delivery mainly affects the distal region by decreasing stiffness and contractility. HRT can reverse the stiffness of the mid-vagina observed after surgical menopause. These observations are in line with scanty biomechanical measurements in comparable clinical specimens.

Keywords: animal model, biomechanics, contractility, sheep vagina, vaginal delivery

INTRODUCTION

Pelvic floor dysfunction (PFD) is a multifactorial disease, with vaginal delivery, age and menopause as important inciting factors [1]. Recent data from the PROLONG study show that 12 years after vaginal delivery, 54% of women have measurable pelvic organ prolapse (POP) with half of them being symptomatic [2]. Along the same lines, urinary and fecal incontinence occur as frequent as 53% and 13%, respectively. PFD impairs the quality of life of women as much as stroke or dementia. The longer life expectancy and increased physical activity in the elder have raised the need for therapy [3]. Surgery remains the mainstay of therapy, with a variety of surgical procedures, using either native tissues or implants. Each has their limitations, including recurrence or local complications. Given the prevalence and the impact of PFD, and the limitations of current therapeutic solutions, there is a need for preclinical research to investigate the pathophysiology of PFD, more efficient or less invasive therapies as well as potential preventive strategies [4].

On way to do so is by using appropriate animal models [5] which should mimic the anatomical and biological vaginal environment. Ideally, these models should undergo comparable structural and functional changes in the pelvic floor by those lifespan events considered as risk factors in women [1]. The leading factors for PFD are vaginal birth and age, and menopause is considered an additional trigger [1]. Several groups are now embracing the sheep as such animal model because of the similarities in pelvic anatomy and reproductive tract to humans [6–8]. The model permits vaginal surgery and mesh insertion, as first described by De Tayrac [7]. Moreover, sheep frequently have complicated vaginal deliveries, and around 15% have antepartum POP. Similar to women, the risk factors for PFD in sheep include multiparity, previous history of POP, increased intra-abdominal pressure, or intake of (fyto)estrogens [5]. In Europe, sheep are an alternative large animal model, as research on the non-human primate has become nearly impossible. Currently, most experiments in sheep were to study therapeutic interventions, yet there is only limited research available on the inciting factors for PFD. The primary aim of this study was to describe the biomechanical effects in two specific conditions: (1) medium-term effects of first vaginal delivery, and (2) following hormone replacement therapy (HRT) in previously ovariectomized sheep.

MATERIAL AND METHODS

This study included six nulliparous, six primiparous, and 12 multiparous reproductive Swifter sheep, which were obtained from the Zoötechnical Institute of the KU Leuven. Primiparous and multiparous ewes were of the same age, and one year after their last lambing hence not nursing anymore. The ovarian cycle of the nulli- and primiparous was synchronized by a vaginal medroxyprogesterone acetate sponge (Veramix, Pfizer, IJsel, The Netherlands). Five days after sponge removal these animals were euthanized. Multiparous sheep underwent bilateral ovariectomy under an earlier described operative and anesthetic protocol [8]. After 60 days half of the sheep were euthanized and the remaining animals received HRT for another 60 days [9, 10]. HRT was by estradiol sustained release, as described by Brasted et al. [11]. Ten mg of 17-β-estradiol (Estradiol, Sigma-Aldrich, Diegem, Belgium) powder was inserted in a cylindrical container (30 × 1.6mm; Dow Corning, Seneffe, Belgium), which was implanted subcutaneously under local anesthesia in a restriction cage. Prior to implantation, the containers were incubated overnight in PBS with 5% fetal calf serum at 37°C. Of these multiparous sheep, there were in both the ovariectomy and HRT group two ewes with two vaginal deliveries, the other four had three prior deliveries.

Outcome measures

Animals were euthanized by i.v. injection of 100 mg/kg of phenobarbital (Release, Ecuphar). First, the vagina and surrounding tissue were removed *"en bloc"* and the vagina was opened longitudinally along the urethra. Length and width were measured using a micrometer (Horex, Helios Preisser, Gammertingen, Germany). The vaginal length was defined as the distance between the cervix and the hymen and the width was measured in the narrowest part of the vagina. The posterior vaginal wall was divided into thirds. The aim was to test biomechanics with the plunger placed 1 cm cranially to the hymenal ring (distal vagina). Suitable sample (30 × 30 mm) to biomechanics was obtained, thereafter we took another 30 × 30 mm sample with the area of interest in the middle third (Figure 1).

Biomechanics

We previously described our testing protocol in detail [8]. Briefly, we used a ball burst test on a 500N Zwicki tensiometer (Zwick GmbH&Co. KG, Ulm, Germany) with a spherical plunger (diameter: 11.5 mm) and a 20 mm aperture. Specimens were trimmed to 30 × 30mm and stored in saline soaked gauzes at -20°C till testing. Prior to testing each specimen was thawed at room temperature for six hours and then clamped with the epithelial side facing upward. The plunger was centered over the aperture and the specimen was preloaded to 0.1 N at a rate of 5 mm/min. Afterwards, the specimen was loaded at a rate of 10 mm/min until disruption or reaching the maximal cell load of 200 N. Load-elongation curves were analyzed using Excel (Microsoft Office, Redmond, Washington, USA) and divided into a comfort and stress zone, as earlier described [12].

The method of contractility measurements is reported in detail elsewhere [8]. Briefly, distal and mid-vaginal strips (~10 × 8 mm) oriented along the circumferential axis of the vagina, were freshly harvested and placed into a 37°C physiological Krebs solution. Samples were preloaded (0.1mN) and allowed to equilibrate for one hour and then subjected to 80 mM KCl. The length, width, and thickness of each sample were measured using a micrometer to estimate the volume of each specimen. The contractile force measurements were normalized to tissue volume (mN/mm^3).

Histology and Immunohistochemistry.

Biopsies were fixed in 4% paraformoldehyde, embedded in paraffin, cut into 6 µm sections and stained with Hematoxylin and Eosin (H&E), Masson trichrome, Miller's pentachrome, periodic acid-Shiff (PAS) and by immunohistochemistry for α-smooth muscle actin (α-SMA-clone 1A4, 1:200 dilution DAKO). The thickness of the epithelium, lamina propria, and muscularis was measured in ZEN2 lite software (Carl Zeiss. Microscopy, GmbH, 2011) on Axioplan 40 microscope (Zeiss, Oberkochen, Germany). PAS-stained sections of the vagina were evaluated qualitatively for the presence of glycogen in the epithelium.

Image evaluation

Virtual images were first acquired with the fully automated digital microscopy system dotSlide (Olympus, BX51TF, Aartselaar, Belgium) coupled with a Peltier-cooled high-resolution digital color camera (1376x1032 pixels; XC10, Olympus). Digital images of the whole tissue sections were digitized at high magnification (100×), producing virtual images in which the pixel size was 0.65 µm.

Image processing and measurements were performed using the image analysis toolbox of MATLAB R2016a (9.0.0.341360; Mathworks, Inc., Natick, MA, USA) according to the methodology described previously [13]. Figure 2 shows original stained images and the corresponding binary images in which the detected αSMA, collagen, and elastin regions are white (pixel value equal to 1) and the background is black (pixel value equal to 0). On those binary images, we measured the elastin density (area occupied by elastin fibers per unit surface), the total collagen density (area occupied by the collagen fibers per unit surface) and the density of smooth muscle cells in the whole tissue section. Densities were first calculated for each animal at each considered location. Mean densities were determined by each location and expressed as the means ± standard error of the mean (SEM).

ER-α immunohistochemistry and evaluation

On deparaffinized vaginal wall slices, endogenous peroxidase activity was blocked with 0.5% H_2O_2 in methanol for 30 min at room temperature. Sections were then heated at 78°C for 2 hours in Tris-HCl buffer (0.01 M, pH 9.0) with 1 mM of EDTA to enhance antigen retrieval. Non-specific binding was minimized by incubating sections in 2% BSA and 1% milk in PBS 0.1% tween 80 for 30 min. Sections were incubated overnight at 4°C with the primary monoclonal antibody against estrogen receptor α (ER-α)

at 1:25 dilution (α-ER clone 1D5, 166µg/mL, DAKO, Glostrup, Denmark). Specific secondary antibodies were used. The color reaction was developed with 3,3'-diaminobenzidine (Sigma). For ER-α analysis, images were captured at a 400× magnification at the epithelium, subepithelium, and muscularis in five randomly chosen fields [8]. The total amount of positively stained cells (brown reaction product) were measured with the particle analysis tool in ImageJ [14] and expressed as a ratio of the total amount of cell nuclei (brown reaction product + blue hematoxylin).

Statistics and ethics committee approval

Normal distribution was tested with the Kolmogorov–Smirnov test. Presence of outliers was tested with a Grubb's test and where appropriate excluded. Parametric data are reported as the mean ± standard deviation (SD) and nonparametric data are represented as a median and interquartile range (IQR).

To compare samples obtained from the distal and middle vagina within a single group we used a paired t-test or Mann-Whitney tests as appropriate. Groups were compared as follows: the effect of first delivery to that of nulliparous, and the effect of HRT on ovariectomized animals (unpaired t-test or Mann-Whitney test). Analyses were performed with Prism 5 (GraphPad Software, Inc., La Jolla, CA, USA). The results were considered significant at $p < 0.05$. Figures display individual data points. Animals were treated in accordance with current national guidelines on animal welfare. This experiment was approved by the Ethics Committee for Animal Experimentation of the Faculty of Medicine of the KU Leuven (P005 – 2013).

Figure 1: Schematic representation of the localization of explanted specimens used for histological, biomechanical and biochemical analysis.
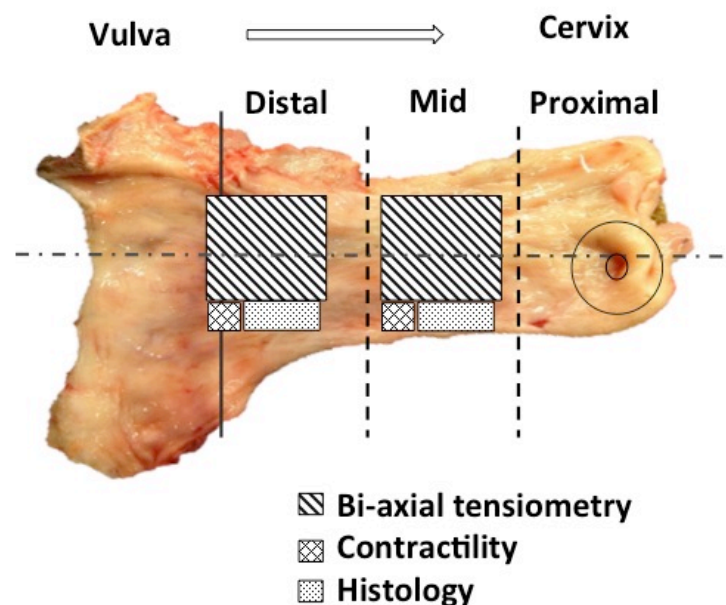
Figure 2: *Image processing for density evaluation. Originally stained images are converted to the binary (black & white) images. The density is determined as the area occupied by designated tissue component (white product).*
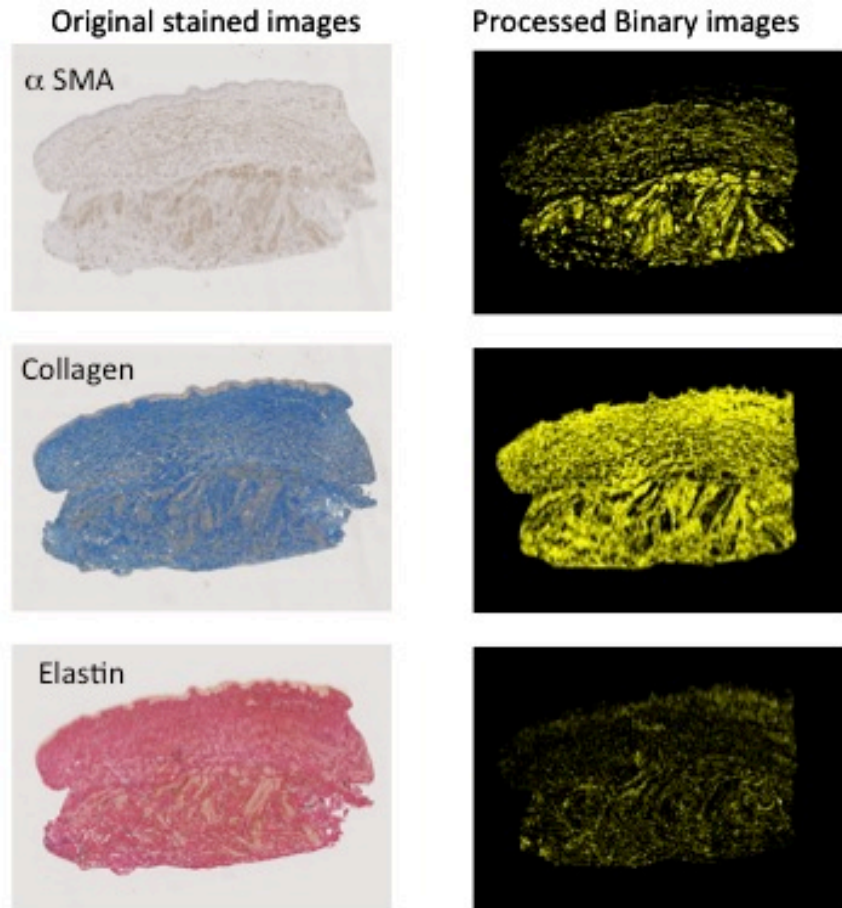
RESULTS

The demographic data are displayed in Table 1. The effects of the studied life phase events are first described in terms of regional differences within each group. Comparisons between nullips and primips, and between ovariectomized and hormone replaced animals follow.

Table 1: Biometry and gross anatomical findings. Data are displayed as median (IQR 25th – 75th) or as mean ± standard deviation according to their distribution. P values: a = >0.0001, b p = 0.04, c p = 0.002, d p = 0.006

	Nulliparous	**Primiparous**	**Multiparous, Menopausal**	**Multiparous, HRT**
Number	6	6	6	6
Biometry				
Weight (kg)	49.0 (43.7–56.2)	53.5 (44.3-73.5)	68.1 (58.8-72.6)	62.2 (53.8-66.3)
Age (months)	12.6 (10.5-14.6)[a]	34.2 (33.4-43.0)[a]	36.2 (35.6-44.5)	42.5 (34.5-43.0)
Macroscopy				
Vaginal length (cm)	9.4 (8.4-10.7)[b]	11.0 (10.3-11.6)[b]	8 .0 (7.2-10.2)	8.2 (7.9-9.0)
Vaginal circumference (cm)	4.5 (3.9-4.7)[c]	6.0 (5.2-6.1)[c]	3.3 (3.5-4.1)[d]	5.5 (4.4-6.0)[d]

Nulliparous animals and effect of first pregnancy and vaginal birth.

The *nulliparous* vagina was 9.4 cm (IQR 25th–75th: 8.4 - 10.7) long. The narrowest was its distal third with a circumference of 4.5 cm (IQR 25th–75th: 3.9 - 4.7; Table 1). The vaginal epithelium is multilayered and rich in glycogen. The lamina propria is globally very thin. In the distal vagina, the lamina muscularis is not very well organized; muscular bundles varied in dimensions and orientation. In the mid-vagina, the lamina muscularis is organized in an inner longitudinal and outer circular layer. There were no regional (distal vs. mid- vagina) differences in vaginal wall stiffness, contractility or histological measurements (Table 2; Figure 3,4).

The *primiparous* distal vagina was 52% less stiff than the mid-vagina (p = 0.007) and had a 63% lower contractility, but that did not reach statistical significance (p = 0.074). The distal vaginal epithelium was 20% thicker and it contained 85% more elastin than the mid-vagina (p = 0.006, p = 0.015, respectively).

When comparing *primiparae* to *nulliparae*, the circumference of the narrowest part of primips was 25% wider and the vagina was 15% longer (p = 0.0097, p = 0.04; respectively). The distal vagina of primips was most affected by first delivery. It was 61% less stiff (p = 0.014) with a 32% longer comfort zone (p = 0.002) compared to nullips. Vaginal

smooth muscle activity in primips generated 64% less force (p = 0.008). Morphologically the distal vaginal lamina propria was 31% thinner (p = 0.004). It contained 79% more elastin and 29% less collagen (p = 0.015, p = 0.041, respectively). The proportion of nuclei staining for ER-α was much lower in the distal vaginal epithelium one year after first delivery compared to nullips. The mid-vagina underwent more limited changes; i.e. only thinning of the lamina propria in the primips. The other variables were not different from measurements in nulliparous ewes.

Effect of HRT on the vagina of ovariectomized sheep

In the *ovariectomized s*heep, the vaginal epithelium was thin and it was lacking PAS-positivity (Figure 4). In half of the menopausal sheep, it was difficult to identify the muscularis in the distal vagina, with sporadically α-SMA positive cells spread over the tissue. In others, the muscularis was qualitative comparable to that of nulliparous sheep. Their mid-vagina was 47.5% stiffer than the distal vagina (p = 0.0004). There were no other regional differences in elastin, collagen or α-SMA density (Figure 3, 4).

Animals on *HRT* displayed regional differences in vaginal tissue. Mid-vaginal contractility was 91% higher than that of the distal vagina (p = 0.045). The mid-vagina contained 56% less elastin (p = 0.065). Similar to the ovariectomized group, no muscularis could be identified in the distal vagina in four of the six animals.

Compared to *ovariectomized* sheep, *HRT* was associated with a 32% larger vaginal circumference (p=0.006) without a difference in vaginal length (Table 1). The biologic effect of HRT became obvious in all animals with widespread PAS-positivity of the epithelium, accompanied with a higher number of ER-α expressing cells mainly in the mid-vagina (Table 2, Figure 4). There were no detectable histomorphological changes in the distal vagina. Sheep on HRT had a 45% lower mid-vaginal stiffness (p = 0.005) compared to ovariectomized sheep, yet there was no difference in contractility. The other variables were not affected by HRT.

Figure 3: *Biomechanics (left column; Comfort zone stiffness, Comfort zone length and Contractility) and histology (right column; Density of Elastin, Collagen and Smooth muscle actin (SMA) of distal and mid-vagina in nulliparous, primiparous and parous sheep following ovariectomy (Parous+OVX) and estrogen replacement therapy (Parous+OVX+HRT). The vertical line in each slope divides the distal (left) and mid- (right) vaginal readings. Data are displayed as individual values, the box plot behind represents the median and the interquartile range. The outlier is displayed as an empty ring. Significant differences between vaginal regions are marked with "#"*
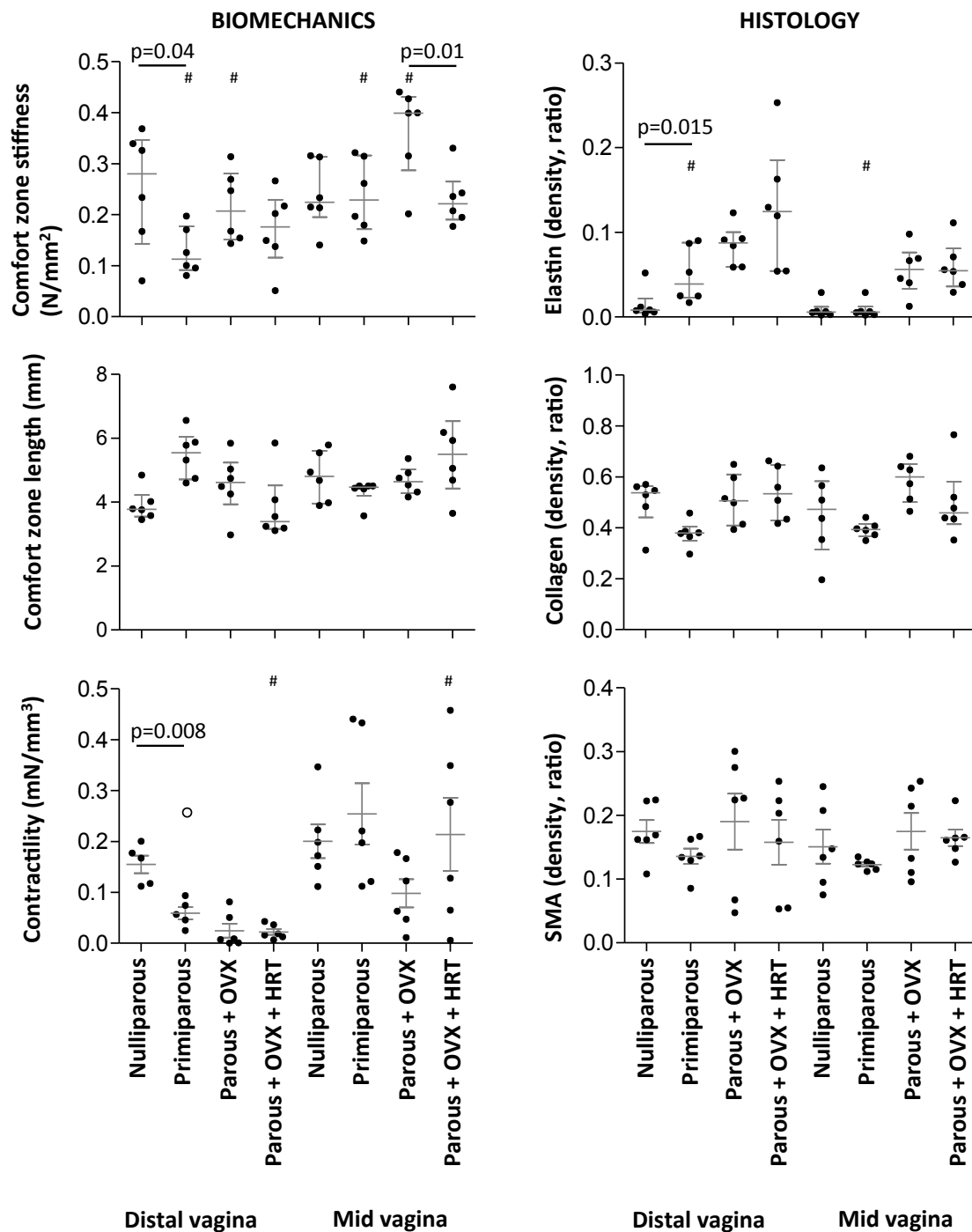
Figure 4: *Representative histological images of collagen content, smooth muscles, elastin and ER-α in the distal and mid-vagina, and glycogen in the mid-vagina in nulliparous, primiparous and parous sheep following ovariectomy (OVX) and estrogen replacement therapy (OVX+HRT). Elastin fibers, ER-α-positively stained nuclei, and glycogen are marked with an arrow. Vaginal epithelium is always at the top of the image.*
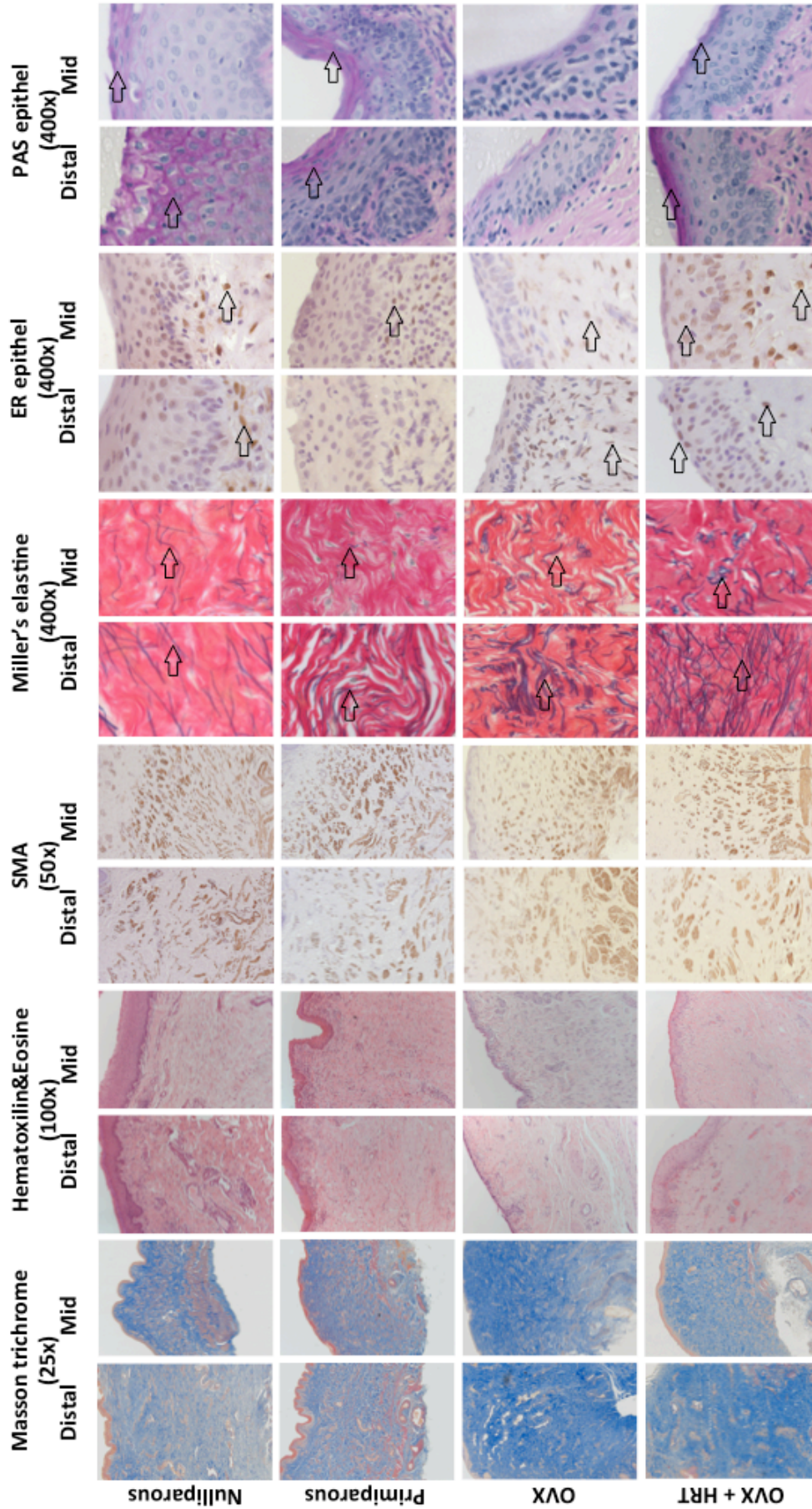
Table 2: *Active and passive biomechanical properties of the distal and mid part of the ovine vagina and lower abdominal wall. Thickness and distribution of ER-α positive nuclei in vaginal epithelium, subepithelium, and muscularis. Data are displayed as median (IQR) or as mean ± standard deviation according to their distribution. Significant differences between vaginal regions are marked with "#".*
Comfort zone stiffness: a p = 0.04, b p = 0.01. Comfort zone length: c p = 0.002.
Contractility: d p = 0.008
Epithelial thickness: f p = 0.017, h p = 0.017; Subepithelial thickness: g p = 0,004,
i p = 0.023; * muscularis was identifiable only in 3 and 4 sheep, respectively
ERα in the epithelium: j p = 0.043, k p = 0.008, l p = 0.005; Subepithelium:
m p = 0.02; Muscularis: n p = 0.007.

	Nulliparous		Primiparous		Multiparous, Ovariectomized		Multiparous, HRT	
	distal	*mid*	*distal*	*mid*	*distal*	*mid*	*distal*	*mid*
Passive biomechanical properties of the vagina; median (IQR 25th – 75th)								
Comfort zone stiffness (N/mm²)	0.28 (0.14-0.35)[a]	0.22 (0.20-0.31)	0.11 (0.09-0.18)[a,#]	0.23 (0.17-0.32)[#]	0.21 (0.15-0.28)[#]	0.40 (0-29-0.43)[b,#]	0.18 (0.12-0.23)	0.22 (0.19-0.26)[b]
Comfort zone length (mm)	3.78 (3.55-4.23)[c]	4.84 (3.96-5.61)	5.55 (4.71-6.05)[c]	4.47 (4.20-4.51)	4.62 (3.93-5.24)	4.53 (4.28-5.03)	3.39 (3.16-4.52)	5.50 (4.43-6.53)
Contractility of vaginal strips; median (IQR 25th – 75th)								
Contractility (mN/mm³)	0.167 (0.115 - 0.189)[d]	0.185 (0.141.0.254)	0.065 (0.035-0.084)[d]	0.209 (0.119-0.435)	0.008 (0.001-0.058)	0.093 (0.038-0.169)	0.017 (0.141-0.254)[#]	0.202 (0.050-0.376)[#]
Vaginal wall thickness (µm); median (IQR 25th – 75th)								
Epithelium	46.5 (36.9-51.6)	38.7 (34.2-54.5)	35.8 30.0-54.7)[#]	28.1 (24.8-43.1)[#]	14.8 (13.5-23.9)[f]	18.7 (14.6-24.8)[g]	30.0 (24.5-33.8)[f]	32.6 (28.2-37.9)[g]
Lamina propria	1408.0 (1396.0 - 1553.0)[h]	1312.0 (1090.0 - 1420.0)[i]	1020.0 (880.4-1085.0)[h]	953.0 (680.5-1137.0)[i]	1575.0 (804.6-1805.0)	1666.0 (1437.0 - 1730.0)	1062.4 (746.0-1481.0)	1355.0 (1121.0 - 1441.0)
Muscularis	1421.0 (1038.0 - 2085.0)	1321.0 (1103.0 - 1868.0)	1077.0 (624.7-1300.0)	1261.0 (1137.0 - 1297.0)	1679.0 (989.0-1881.0)[*]	1012.0 (708.6-2327.0)	1513,7 (1260.0 - 1767.0)[*]	1333.8 (1169.0 - 1797.0)
Estrogen receptor α distribution (%); mean ±SD								
Epithelial	20.7 ±10.8[j]	11.0 ±8.3	4.3 ±4.0[j]	4.3 ±3.9	14.3 ±9.0[k]	9.6 ±6.6[l]	35.2 ±8.0[k]	48.7 ±16.9[l]
Lamina propria	47.7 ±11.0	46.1 ±8.1	42.4 ±21.9	49.0 ±14.3	32.8 ±14.7	41.2 ±16[m]	43.2 ±7.6[#]	72.4 ±6.4[m,#]
Muscularis	56.3 ±18.9[#]	30.4 ±10.6[#]	32.7 ±18.2	24.9 ±10.1	33.4 ±14.2	39.2 ±5.5[n]	36.6 ±25.9	65.7 ±14.8[n]

DISCUSSION

The principal outcome measures in this study were vaginal active and passive biomechanical properties. The effects of phases like delivery or menopause in the lifespan on passive biomechanics are regionally different, as previously observed in other species [1, 6, 15]. Compared to nullips, first vaginal delivery decreases distal vaginal stiffness by 62% but does not affect the mid-vagina. Also, active contractility was decreased in the distal vagina, yet not in the mid-vagina. This was paralleled by an increased distal vaginal elastin and decreased collagen content. Estrogen exposure decreases the stiffness of the mid-vagina compared to ovariectomized ewes, without a change in contractility. This did not coincide with morphometric elastin or collagen changes.

To compare the above to clinical data is challenging. First one can look at data from postmortem studies, but obviously, data on young nulli- or primiparous women are scarce. Conversely available data on elder women may have several confounding factors. Second not much is available on regional differences as it requires the collection of large specimens. Another source of information could be specimens taken at the time of surgery. Those taken on the occasion of hysterectomy are however usually taken at the apex of the vagina. Lower vaginal biopsies would be from prolapse surgeries, hence clearly pathologic specimens. Surgical biopsies obviously may not be large enough for appropriate biomechanical testing. Despite all these shortcomings, the current literature suggests that menopausal aged women indeed have stiffer vaginal tissue compared to younger ones [16, 17]. This is in line with our observations yet in biologically younger surgically castrated animals. To our knowledge, no clinical data are available which could be used to benchmark our findings in young primips. The data we obtained in sheep are in line with the trends observed in other species such as rats and non-human primates [18, 19]. More recently, other sheep studies [6, 20] became available. Our results parallel the trends, though the exact values are different most probably because different testing methodology and regions were used [6].

In terms of the effect of ovariectomy, there has been one earlier study in ovariectomized sheep. It focused on the comparison of the biochemical composition and ultrastructure to that of menopausal women [21]. Of relevance to our study, it included biomechanical testing yet by uniaxial tensiometry. When comparing the passive biomechanical properties of the distal to the middle vagina, Ulrich *et al* did not identify differences. Since the vagina is anisotropic this may well be the case in our samples as well if tested using the same method [22]. In both that, and our study, no regional differences in composition were found, yet, again, not using similar methodologies. One caveat is that in both experiments, relatively young sheep who were castrated were used. Elder sheep are more difficult to get as they are usually only kept for a limited time (<7 - 8 years, depending on the breed) in breeding programs. The effects may be different if the same experiment would have been done in elder sheep around menopausal age. Indeed, in rats, the biomechanical properties of the pelvic supportive

structures following surgical menopause were different in *young* (four months) than in old (nine months) animals [23]. Also, other investigators have shown that age has an additional effect to that of menopause [24]. Clinically, the *functional* vaginal effects of surgical menopause in young women are also more obvious than in naturally on setting menopause in elder individuals [25].

We herein also performed a morphologic study, under the assumption that structural changes would in some way be representative for biomechanical measurements. That relationship is, however, unclear. For instance, we observed higher elastin levels in the stiff vaginas of ovariectomized sheep, which may seem paradoxical. However, a higher elastin content on light microscopy observed in specimens from elder women may as well represent elevated elastin degradation and matrix turnover, which can coincide with higher tissue stiffness [26]. This demonstrates one must be careful in extrapolating morphologic to biomechanical findings. We also observed a low density of elastin mainly in nulliparous and primiparous animals as compared to women. The latter was measured with the same technique [13]. Interestingly, our results also show a much lower density compared to biochemically determined elastin in sheep [6, 21]. The latter difference may be explained by changes in elastin appearance in light microscopy as mentioned above (Figure 4). The used morphologic methods are not truly quantitative yet cannot differentiate between relevant subtypes and organization of extracellular matrix proteins. Unfortunately, we did not have biochemical or more other quantitative measures such as quantification of collagen subtypes and/or elastin [6]. Those may help better understand the relationship between morphology and biomechanics.

The other principal outcome measure was vaginal contractility. Contractility data are scarce in the translational research literature, with to our knowledge none available in sheep. In 6-months old castrated rats, vaginal contractility decreased [27]. There is also a rat study in 3 months old rats, investigating the impact of vaginal delivery. It showed an increased sensitivity to KCl without a change in vaginal contractility [19]. At a closer look, that study examined longitudinal strips of the entire vagina. This is different from the circumferential strips we used, as well did we look into regional differences. Again, for active biomechanical properties, we investigated the potential relationship with morphology, with, again not a true parallel pattern. Only in menopausal distal vaginal tissue, we found a paucity of muscular tissue coinciding with poor contractility.

Our experiments have several limitations. The most obvious one is that we were limited to a cross-sectional study design, hence not collecting samples in a longitudinal fashion through the life phases. Further, we could not, due to the availability of similarly aged ewes, standardize completely the number of deliveries in the ovariectomized groups. Last, it could be suggested that we should have measured estrogen levels in hormone replaced animals. We did not do so since this was well documented before for the given HRT scheme [9, 10]. However, we did document the biological end-organ effects (which were what we targeted for), such as atrophic epithelial changes, glycogen absence and a change in ER-α expression [28].

Another criticism may be that we waited for only 60 d following ovariectomy, as described before [9, 10]. In smaller species, tissue changes are already detected after two weeks of hypo-estrogenism [29]. Clinically many tissue changes take place over the course of years. Though we documented measurable changes after 60 days, it would have been interesting to extend the interval after ovariectomy hence potentially observe more pronounced changes. Our experiment despite its limitations provides new data on the impact of two major events in the female lifespan which in women contribute to the pathogenesis of PFD. To our knowledge, these are the first ovine biomechanical data on the effect of artificial menopause and HRT. This might prove useful as there is now a renewed interest in the local treatment of those changes [30]. It further expands our knowledge of the ovine model, which is increasingly being used both for pathophysiologic or surgical studies [20, 31].

CONCLUSION

In sheep, vaginal delivery and simulated menopause impact the biomechanical properties of the vagina in a region-specific way. The first vaginal delivery affects mainly the distal vagina, decreasing its stiffness and contractility. This coincides with an increase in elastin and decrease in collagen. HRT reverses the effects of ovariectomy on mid-vaginal stiffness with a trend for increased contractility. The distal vagina underwent no changes following HRT. The few available biomechanical findings in clinical specimens are in line with these observations in sheep, supporting its role as a large animal model.

Ethical approval: The experiment was approved by the Ethics Committee for Animal Experimentation of the Faculty of Medicine of the K.U. Leuven. All applicable international, national and institutional guidelines for the housing, care and use of animals were followed. Procedures performed in this study were in accordance with the ethical standards of the institution at which they were conducted.

Contribution to the authorship I Urbankova did study design, biomechanical testing, histology, surgery, data collection, evaluation and manuscript writing, Geertje Callewaert and Andrew Feola did study design, biomechanical testing, Dries Deprest, Lucie Hympanova, Laurent De Landsheere and Silvia Blacher did histological evaluation, Jan Deprest did study design and manuscript writing. All authors contributed to manuscript editing.

REFERENCES:

1. DeLancey JOL, Kane Low L, Miller JM, et al. (2008) Graphic integration of causal factors of pelvic floor disorders: an integrated life span model. Am J Obstet Gynecol 199:610.e1-5. doi: 10.1016/j.ajog.2008.04.001

2. Glazener C, Elders A, MacArthur C, et al. (2013) Childbirth and prolapse: Long-term associations with the symptoms and objective measurement of pelvic organ prolapse. BJOG An Int J Obstet Gynaecol 120:161–168. doi: 10.1111/1471-0528.12075

3. Smith FJ, Holman CDJ, Moorin RE, Tsokos N (2010) Lifetime risk of undergoing surgery for pelvic organ prolapse. Obstet Gynecol 116:1096–1100. doi: 10.1097/AOG.0b013e3181f73729

4. Callewaert G, Albersen M, Janssen K, et al. (2015) The impact of vaginal delivery on pelvic floor function - delivery as a time point for secondary prevention: A commentary. BJOG An Int J Obstet Gynaecol 678–681. doi: 10.1111/1471-0528.13505

5. Couri B, Lenis A, Borazjani A, et al. (2012) Animal models of female pelvic organ prolapse: lessons learned. Expert Rev Obs Gynecol 7:249–260. doi: 10.1586/eog.12.24.Animal

6. Ulrich D, Edwards SL, Su K, et al. (2014) Influence of reproductive status on tissue composition and biomechanical properties of ovine vagina. PLoS One 9:e93172. doi: 10.1371/journal.pone.0093172

7. de Tayrac R, Alves A, Thérin M (2007) Collagen-coated vs noncoated low-weight polypropylene meshes in a sheep model for vaginal surgery. A pilot study. Int Urogynecol J Pelvic Floor Dysfunct 18:513–20. doi: 10.1007/s00192-006-0176-9

8. Feola A, Endo M, Urbankova I, et al. (2015) Host reaction to vaginally inserted collagen containing polypropylene implants in sheep. Am J Obstet Gynecol 212:474.e1-474.e8. doi: 10.1016/j.ajog.2014.11.008

9. Barron AM, Cake M, Verdile G, Martins RN (2009) Ovariectomy and 17beta-estradiol replacement do not alter beta-amyloid levels in sheep brain. Endocrinology 150:3228–36. doi: 10.1210/en.2008-1252

10. Ayen E, Noakes DE, Baker SJ (1998) Changes in the capacity of the vagina and the compliance of the vaginal wall in ovariectomized, normal cyclical and pregnant ewes, before and after treatment with exogenous oestradiol and progesterone. Vet J 156:133–43.

11. Brasted M, White C, Kennedy T, Salamonsen L (2003) Mimicking the events of menstruation in the murine uterus. Biol Reprod 69:1273–80. doi: 10.1095/biolreprod.103.016550

12. Ozog Y, Konstantinovic ML, Werbrouck E, et al. (2011) Shrinkage and biomechanical evaluation of lightweight synthetics in a rabbit model for primary fascial repair. Int Urogynecol J 22:1099–108. doi: 10.1007/s00192-011-1440-1

13. de Landsheere L, Blacher S, Munaut C, et al. (2014) Changes in elastin density in different locations of the vaginal wall in women with pelvic organ prolapse. Int Urogynecol J. doi: 10.1007/s00192-014-2431-9

14. Söderberg MW, Johansson B, Masironi B, et al. (2007) Pelvic floor sex steroid hormone receptors, distribution and expression in pre- and postmenopausal stress urinary incontinent women. Acta Obstet Gynecol Scand 86:1377–1384. doi: 10.1080/00016340701625446

15. Feola A, Endo M, Deprest J (2014) Biomechanics of the rat vagina during pregnancy and postpartum: A 3-dimensional ultrasound approach. Int Urogynecol J Pelvic Floor Dysfunct 25:915–920. doi: 10.1007/s00192-013-2313-6

16. Chantereau P, Brieu M, Kammal M, et al. (2014) Mechanical properties of pelvic soft tissue of young women and impact of aging. Int Urogynecol J 25:1547–53. doi: 10.1007/s00192-014-2439-1

17. Gandhi J, Chen A, Dagur G, et al. (2016) Genitourinary syndrome of menopause: evaluation, sequelae, and management. Am J Obstet Gynecol 1–8. doi: 10.1016/j.ajog.2016.07.045

18. Feola A, Abramowitch S, Jones K, et al. (2010) Parity negatively impacts vaginal mechanical properties and collagen structure in rhesus macaques. Am J Obstet Gynecol 203:595.e1-8. doi: 10.1016/j.ajog.2010.06.035

19. Feola A, Moalli P, Alperin M, et al. (2011) Impact of pregnancy and vaginal delivery on the passive and active mechanics of the rat vagina. Ann Biomed Eng 39:549–58. doi: 10.1007/s10439-010-0153-9

20. Knight KM, Moalli PA, Nolfi A, et al. (2016) Impact of parity on ewe vaginal mechanical properties relative to the nonhuman primate and rodent. Int Urogynecol J. doi: 10.1007/s00192-016-2963-2

21. Ulrich D, Edwards SL, Letouzey V, et al. (2014) Regional Variation in Tissue Composition and Biomechanical Properties of Postmenopausal Ovine and Human Vagina. PLoS One 9:e104972. doi: 10.1371/journal.pone.0104972

22. Rubod C, Boukerrou M, Brieu M, et al. (2007) Biomechanical properties of vaginal tissue. Part 1: new experimental protocol. J Urol 178:320–5; discussion 325. doi: 10.1016/j.juro.2007.03.040

23. Moalli P a, Debes KM, Meyn LA, et al. (2008) Hormones restore biomechanical properties of the vagina and supportive tissues after surgical menopause in young rats. Am J Obstet Gynecol 199:161.e1-8. doi: 10.1016/j.ajog.2008.01.042

24. Rizk DEE, Fahim M a., Hassan H a., et al. (2007) The effect of ovariectomy on biomarkers of urogenital ageing in old versus young adult rats. Int Urogynecol J Pelvic Floor Dysfunct 18:1077–1085. doi: 10.1007/s00192-006-0278-4

25. Shuster L, Gostout B, Grossardt B, Rooca W a. (2009) Prophylactic oophorectomy in pre-menopausal women and long term health - a review. NIH Public Access 14:111–116. doi:

10.1258/mi.2008.008016.Prophylactic

26. Robert C, Lesty C, Robert A (1988) Ageing of the skin: study of elastic fiber network modifications by computerized image analysis. Gerontology 34:291–6.

27. Onol FF, Ercan F, Tarcan T (2006) The effect of ovariectomy on rat vaginal tissue contractility and histomorphology. J Sex Med 3:233–241. doi: 10.1111/j.1743-6109.2006.00216.x

28. Fuermetz A, Schoenfeld M, Ennemoser S, et al. (2015) Change of steroid receptor expression in the posterior vaginal wall after local estrogen therapy. Eur J Obstet Gynecol Reprod Biol 187:45–50. doi: 10.1016/j.ejogrb.2015.02.021

29. Kim N, Min K, Pessina M, et al. (2004) Effects of ovariectomy and steroid hormones on vaginal smooth muscle contractility. Int J Impot Res 16:43–50. doi: 10.1038/sj.ijir.3901138

30. Zdenko Vizintin, Mario Rivera, Ivan Fistonić, Ferit Saraçoğlu, Paolo Guimares, Jorge Gaviria, Victor Garcia, Matjaz Lukac, Tadej Perhavec LM (2012) Novel Minimally Invasive VSP Er:YAG Laser Treatments in Gynecology. J Laser Heal Acad 1:46–58.

31. Urbankova I, Callewaert G, Sindhwani N, et al. (2017) Transvaginal mesh insertion in the ovine model. J Vis Exp. doi: doi: 10.3791/55706.

CHAPTER 5

XENOGENIC COLLAGEN IMPLANTATION IN THE SHEEP MODEL FOR VAGINAL SURGERY

Masayuki Endo, Iva Urbankova, Jaromir Vlacil, Siddarth Sengupta, Thomas Deprest, Bernd Klosterhalfen, Andrew Feola, Jan Deprest

Centre for Surgical Technologies, Faculty of Medicine, Department of Development and Regeneration, Organ systems cluster, Faculty of Medicine &, Pelvic Floor Unit, University Hospitals KU Leuven, KU Leuven, Leuven, Belgium

Institute for the Care of Mother and Child, Third Faculty of Medicine, Charles University, Prague, Czech Republic

Institute of Pathology, Düren, Germany

ABSTRACT:

Background: The properties of meshes used in reconstructive surgery affect the host response and biomechanical characteristics of the grafted tissue. Whereas durable synthetics induce a chronic inflammation, biological grafts ACM are usually considered as more biocompatible. The location of implantation is another determinant of the host response: the vagina has a specific function, anatomy, and environment. Herein we evaluated a cross-linked acellular collagen matrix (ACM), pretreated by the anti-calcification procedure ADAPT, in a sheep model for vaginal surgery.

Methods: 10 sheep were implanted with a cross-linked ACM, and 6 controls were implanted with a polypropylene (PP) mesh control. One implant was inserted in the lower rectovaginal septum and one was used for abdominal wall defect reconstruction. Grafts were removed after 180 days; all graft-related complications were recorded and explants underwent bi-axial tensiometry and contractility testing.

Results: One-half of ACM implanted animals showed local induration in the vagina, in two of them also on the abdominal implant. One animal had a vaginal exposure. Many ACM explants showed areas of graft degradation. Vaginal ACMs were 63% less stiff compared to abdominal ACM explants (p = 0.01) but comparable to vaginal PP explants. There was no overall difference in vaginal contractility, yet explants with degradation of the ACM had a 60% reduced contractility as compared to PP (p = 0.048).

Conclusion: Vaginal implantation with ACM led to GRCs and comparable biomechanical properties to PP and decreased vaginal contractility when the ACM was locally degraded.

Keywords: graft-related complication, biological graft, prolapse, biomechanics

INTRODUCTION

Pelvic organ prolapse (POP) develops in half of parous women over 50 years, half of them being symptomatic with only 20% of them seeking medical help [1, 2]. Lifetime risk of POP surgery is 19% [3] and up to 25% require later re-operation [4]. It was suggested that this may be reduced by using synthetic or biological implants [4, 5]. Although durable synthetic meshes are known to achieve good anatomical and functional results for cystocele repair, they may cause graft-related complications (GRCs) in over 10% of women [4]. Alternative grafts that may reduce the number of GRC yet still provide durable results, could be contemplated [6–10].

Biological grafts are derived from either human (auto- or allografts) or animal material (xenografts). Autografts, such as fascia lata, inherently have donor site-related morbidity and also have unpredictable durability [11, 12]. Allografts are retrieved from cadaveric tissue and although fastidious steps are taken in preparation, concerns regarding transmission of possible prion disease or viruses remained. Xenografts are acellular collagen matrices (ACM) that are either derived from the dermis, pericardium or small intestinal submucosa of animals that are purposely bred in strictly controlled conditions. Most ACM is of bovine or porcine origin, which during their production undergo various chemical procedures (cross-linking, sterilization). After implantation ACM are remodeled and/or replaced by connective tissue within variable time periods. The latter can be modified using e.g. cross-linking agents which leads to the formation of excessive intra- and intermolecular chemical bonds preventing decomposition by endogenous collagenases [13]. This alters the properties of the ACM either physically or chemically. A commonly used cross-linking agent is glutaraldehyde (GAD) [13] resulting in durable grafts that are slowly integrated and remodeled. However, residual GAD is cytotoxic and may cause calcification. To prevent this, Neethling et al. developed a multi-step anti-mineralization process called ADAPT® [14]. This enhances crosslink stability, removes residual GAD, with modification of the non-bifunctionally reacted GAD residues, it reduces lipid content and restores tissue elasticity [14]. ADAPT® treated bovine pericardial patches have been successfully used in surgery of congenital heart defects without demonstrable calcification in a 36 month follow-up period [15]. These promising results demonstrating longterm stability in challenging circumstances are worthwhile considering for translation in pelvic floor surgery. Herein, we used ADAPT® treated xenografts in a sheep model for transvaginal surgery, studying both the occurrence of GRCs and active and passive biomechanical properties of the vaginal wall. As a reference, we compared outcomes to repairs with lightweight polypropylene (PP) implants.

MATERIALS AND METHODS

Implants and surgery

This study compares outcomes following vaginal and abdominal mesh insertion of either a xenogenic or synthetic implant in a sheep model. The xenogenic graft was a non-perforated acellular collagen matrix (ACM) derived from bovine pericardium which was cross-linked with an ultra-low concentration (0.05%) of monomeric GAD. Further preimplantation processing included the so-called ADAPT® anti-calcification procedure and sterilization with propylene oxide [14, 16] (Material donated by Prof WML Neethling, Fremantle, Australia). As a control, we used a commercially available monofilament polypropylene (PP) mesh used for vaginal prolapse repair (PP) (Avaulta Solo; 56 g/m^2, Bard Medical, Covington, GA, USA). The latter was purchased and delivered sterile via the hospital pharmacy. Observations of these animals were earlier reported on elsewhere [17].

The anesthetic, surgical technique, and methodology used for outcome evaluation have been described in detail previously [18, 19]. Briefly, 16 parous Texel sheep (mean weight 68 ± 3.5 kg) were obtained from the Zootechnical Centre of the KU Leuven. They underwent simultaneous vaginal and abdominal implantation with either ACM (n = 10) or PP (n = 6). Surgery was conducted in sterile conditions under general anesthesia with prophylactic antibiotics at induction and 3 days of postoperative analgesia. Following aqua-dissection, a single incision was made in the recto-vaginal septum that was then dissected to create a suitable space for a 35x35mm suture fixed prosthesis (posterior implant) (Figure 1). Additionally, a 10x20 mm graft was inserted into the anterior vaginal wall (anterior implant). Finally, a 50 mm longitudinal paramedian cutaneous incision was made in the anterior abdominal wall and a 40 mm primarily suture repaired full-thickness fascial incision was overlaid with the same graft as used vaginally (Figure 1). All implants were fixed with interrupted polypropylene 4/0 Prolene sutures (Ethicon). Postoperatively, animals were allowed to move, drink and eat *ad libitum*, and were clinically followed by a veterinarian.

Outcome measures

On average 180 days later, animals were euthanized and during necropsy, GRCs or the presence of herniation were noted at each of the three implantation sites. Thereafter the original implant together with the adjacent and ingrown tissue (further referred to as explant) was removed "en bloc" and its dimensions and thickness were determined as an average of three random measurements with a digital micrometer (Mitutoyo, Japan, accuracy 0.01 mm). Contraction of the explant was defined as the explant area over initial graft area (1225 mm^2 for vaginal, 2500 mm^2 for abdominal implant respectively). Explants were then divided to obtain specimens for histology and biomechanical testing as shown in Figure 1. For vaginal explants, the anterior specimens were used for histology while the posterior explants were used for active and passive biomechanical testing. The larger abdominal explants were divided for both histology and passive biomechanics.

Histology quantified the inflammatory response and connective tissue formation on 5μm thick sections, stained with hematoxylin and eosin (H&E) and Movat pentachrome, using an ordinal scoring system [20, 21]. Two operators blinded to the initial treatment counted foreign body giant cell (FBGC), polymorphonuclear cells (PMN), newly formed vessels and collagen organization, composition and amount in five randomly chosen areas at the implant-host tissue interface at a magnification x400 (Zeiss Axioplan 400, Oberkochen, Germany). Infection was classified as either low grade (≥ 15 PMN per HPF and no clinical evidence of infection) or high grade (presence of micro-abscesses, dense inflammatory infiltrate, fibrin exudation, bleeding, and necrosis as well as clinical signs of infection – if any) [22]. All histological scores (FBGCs, PMN, vessel and collagen scores) were at least done in duplicate and averaged.

Passive biomechanics were tested using bi-axial tensiometry by a plunger test on a 500-N Zwick tensiometer with a 200-N cell load (Zwick GmbH & Co. KG, Ulm, Germany) using a protocol defined earlier [18]. A spherical 11.5 mm plunger was passed through an aperture ∅ 20 mm that exposing the explant compressed in ∅ 30 mm rings. All explants were placed with the graft facing upward. Records of the force-elongation relationship allow defining the stiffness (N/mm) of the tested material, which we measured in the low-stress area also called as the "comfort" zone, the average slope of the force-elongation curve and the length of the former zone. These values were determined by TestXpert II software (Zwick GmbH & Co). Active biomechanics of a circumferential oriented posterior vaginal explant, as well as control strip (10 × 8 mm), were assessed by a contractility assay (Figure 1) [23]. This is an ex vivo assessment quantifying the ability of tissue strips to contract by immersing them in an organ bath at 80 mM KCl concentration (mN/mm^3).

Statistical analysis and ethics committee approval
Data are reported as the mean and standard deviation or as median and interquartile range depending on the distribution. Either a Student-t test or a Mann–Whitney U test was performed to compare PP and ACM. Chi-square was used for categorical data. Pairs of abdominal and vaginal explants from the same animal were also tested using a paired t-test or Wilcoxon signed rank test. All analyses were performed with Prism 5 (GraphPad Software, Inc., La Jolla, CA, USA) and the significance level was set up to $p < 0.05$. Animals were housed in controlled conditions and treated in accordance with current national guidelines on animal welfare. The experiment was approved by the Ethics Committee for Animal Experimentation of the Faculty of Medicine of the K.U. Leuven.

Figure 1: *Schematic drawing of abdominal (a) and vaginal (b) implantation in the sheep model. Specimens explanted (c) from the abdomen, anterior (ant), posterior (post) vaginal wall were divided according to their respective testing method. (Illustration by Myrthe Boymans)*
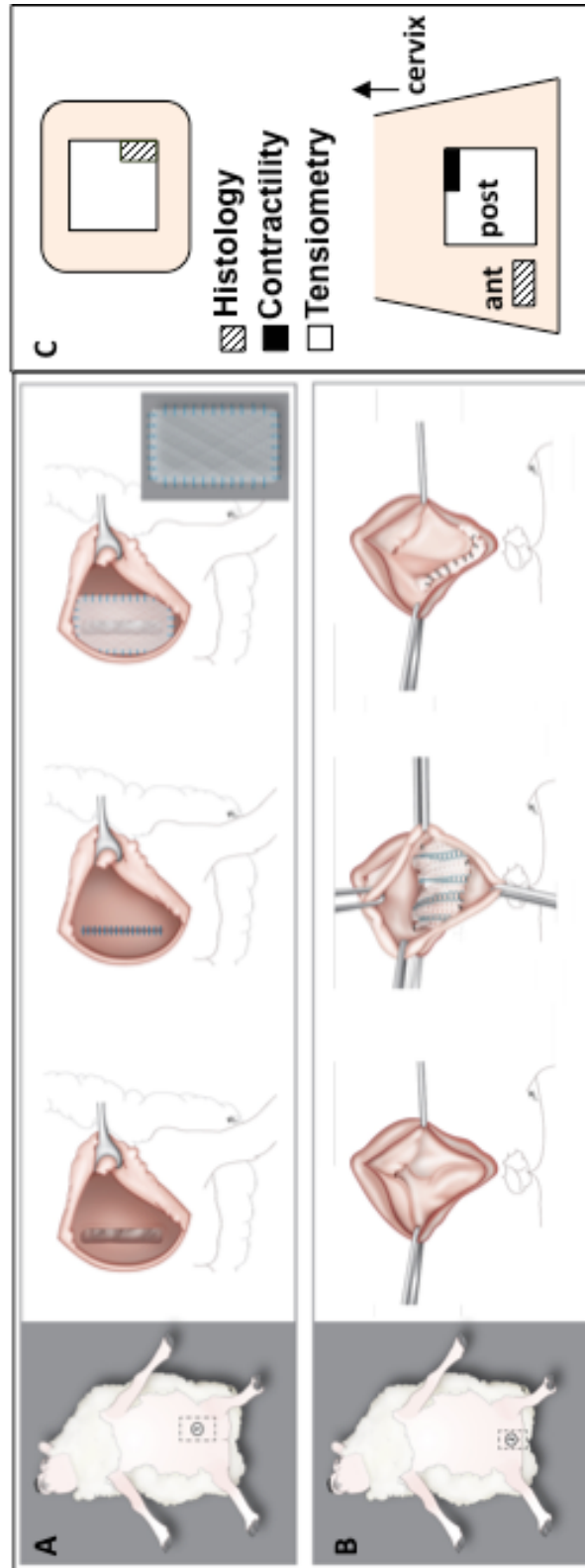
RESULTS

Vaginal versus abdominal implantation of ACM.

Five out of ten sheep implanted with ACM developed GRCs at the vaginal implantation site (50%; Table 1). There was one exposure, two implants showed obvious folding (Figure 2) and two showed remarkable induration. The total GRC rate for xenogenic implants in the abdominal wall was 30%. Animals that had induration in their vaginal implants also showed induration of their abdominal implants.

In one vaginal explant, there was macroscopically no visible implant in between the fixation sutures anymore. Vaginal and abdominal explants were of comparable thickness, though the contraction rate was almost three times higher in vaginal explants ($p = 0.0008$). There were significant differences between implantation sites for passive biomechanics: vaginal explants were 63% less stiff than their abdominal counterparts ($p = 0.01$), though the length of the comfort zone was comparable (Figure 3a).

Histology of vaginal explants was scored on smaller anterior vaginal implants, (Table 2). One must remember that this is a different location than the rectovaginal area described above. ACM abdominal explants had higher scores for FBGC ($p = 0.0078$) yet similar amounts of PMN and vascularization as vaginal ACM explants. Scores for collagen organization and composition were similar for both sites but the amount of collagen was higher in the abdominal ACM explants ($p = 0.0201$). All the above scores were averages. At a closer look, explants fall apart in two categories. In 70% of the anterior vaginal and 30% of the abdominal explants, we could not trace the typically dense structure of the ACM on histology (Figure 2c,d). In these cases, there was no measurable inflammation but limited areas of organized and mature connective tissue. Isolated pockets of inflammation were visible only when a suture was accidentally caught in the section. In the other cases, the ACM could be identified. In that case, there was an abundance of inflammatory cells, both FBGC and PMN, as evidenced by their score, as well as connective tissue deposition. In five ACM sections, we observed precipitated material compatible with calcification (Figure 2e). Four were abdominal explants; three of them were macroscopically categorized as indurated. In one of these ewes, also the anterior and posterior vaginal explants were indurated. The anterior explant showed calcification on histology, which coincided with histologic signs of infection).

Vaginal contractility and further comparison to PP vaginal implants

Figure 3 displays the vaginal contractility findings. ACM explants where no graft was recognizable on histology (n = 7) had a 68% lower contractile response than those with the recognizable material (n = 3; Figure 3b). In view of the very low numbers, no statistics were attempted.

We compared the vaginal findings to observations made earlier when using a PP vaginal implant (Table 3). There was one case of GRC (folding), yet this apparently lower number was not significant. However, the 17% contraction rate of PP explants was significantly less than for ACM

(p = 0.0009). Passive biomechanics of vaginal ACM were comparable to PP explants. For active biomechanics, the values of 3 samples with recognizable ACM were in the range of with samples PP. Conversely, the forces generated by the seven samples without visible ACM were 60% lower than those of PP explants (p = 0.048) (Figure 3b).

The histology of vaginal explants with PP differed completely from those with recognizable ACM (Figure 2f). PP induced a mild inflammation, with few cells, nearly all macrophages or FBGC, and less collagen deposition. These specimens showed no histologic signs of infection.

Table 1: *Paired comparison of outcomes of vaginally and abdominally implanted ACMs. Biomechanical findings are displayed for all animals as well as results without the outlier, and contraction without those with unidentifiable or extruded material.*

	ACM		Paired comparison
	Abdomen	**Posterior vagina**	
Graft Related Complication	3/10 (30%)	5/10 (50%)	ns
Exposure	0/10 (0%)	1/10 (10%)	
Folding	0/10 (0%)	2/10 (20%)	
Induration	3/10 (30%)	2/10 (20%)	
Other gross anatomical findings			
Thickness (mm)	8.22 ± 3.90	6.78 ± 2.27	ns
Material not identifiable	0/10 (0%)	1/10 (10%)	ns
Contraction of identifiable mesh	-20.28% ± 18.24	-61.18% ± 17.25	0.0008
Biomechanics			
All ewes			
Comfort zone stiffness (N/mm)	0.68 ± 0.2	0.41 ± 0.46	ns
Comfort zone length (mm)	7.18 ± 2.00	8.52 ± 3.22	ns
Exclusion of outlier (n=9)			
Comfort zone Stiffness (N/mm, n=9)	0.73 ± 0.29	0.27 ± 0.19	0.0101
Comfort zone length (mm, n=9)	7.30 ± 2.00	8.90 ± 3.17	ns

Figure 2: *Gross anatomy: Explants from in the posterior vaginal wall (a) and the abdomen (b) with induration and folding visible in the below-placed selections. The dark area (arrows) below the vaginal epithelium and above the abdominal muscles is the location of the implant, which looks complete. In these cases, the material was hard on palpation and surrounded by an excessive amount of connective tissue.*

Histology showed variable host response; (c) gradual degradation of ACM with FBGC (arrow) on graft–tissue interface, (d) complete ACM degradation where just sutures (S) were identifiable; or (e) mineral precipitation or calcifications (*) in the acellular collagen matrix (ACM). Polypropylene implant (PP) showed a uniform response (f). (H&E, 200x, 25x, 40x, 100x, respectively)
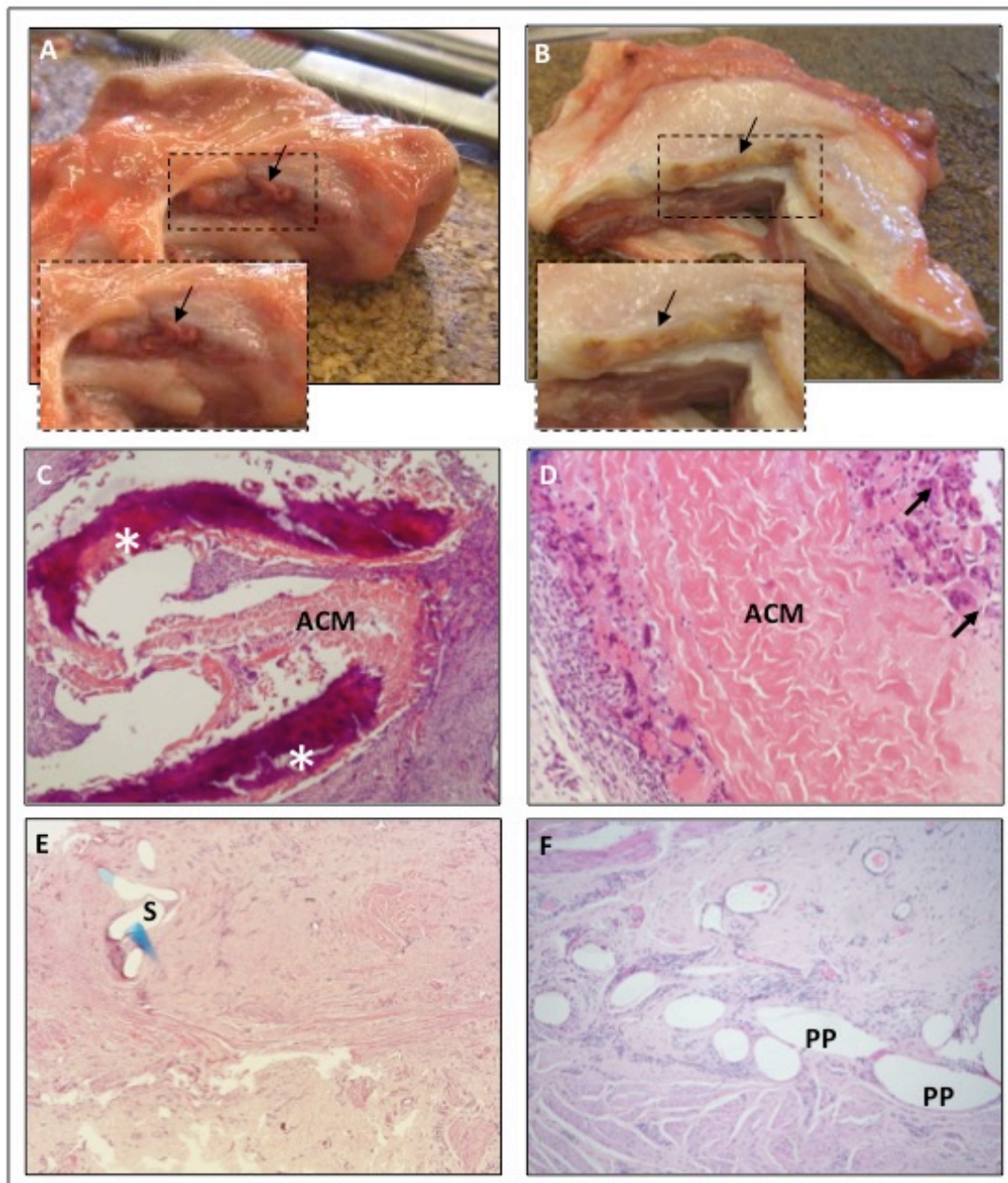
Table 2: *Histological scores of host response and connective tissue formation following insertion of ACM and PP in the vagina and abdominal wall. Scores are displayed for all explanted specimens and also for those with identifiable ACM. For later, statistics were not carried out due to a few specimens. FBGC - Foreign Body Giant Cell, PMN – Polymorphonuclears. (Data for vaginal PP implants were previously published by Feola et al, 2014 [17]*

	Abdomen	Anterior vagina	Pair comparison	Anterior vagina	Unpaired comparison
	ACM			**PP**	
	N=10	**N=10**		**N=6**	
FBGC	**0.8 (0.88)**	**0.1 (0.53)**	**0.0078**	0.40 (0.25)	
PMN	0.15 (0.38)	0.2 (0.67)		0.05 (0.23)	
Vascularity	1.0 (0.4)	1.15 (0.3)		2.05 (0.55)	**0.0023**
Collagen organization	1.5 (1.4)	1.4 (0.35)		1.3 (0.55)	
Collagen composition	1.8 (0.4)	2.1 (0.4)		2.3 (0.55)	
Collagen Amount	2.7 (0.2)	2.5 (0.2)	**0.0201**	1.9 (0.35)	**0.0061**
Calcification	4/10	1/10		0/6	
Scores at the interface with identifiable material on histology	**N=7**	**N=3**		**N=6**	
FBGC	1.1 (0.7)	0.8 (0.35)		0.40 (0.25)	
PMN	0.1 (0.45)	1.8 (0.85)		0.05 (0.23)	
Vascularity	0.7 (0.45)	1.5 (0.45)		2.05 (0.55)	
Collagen organization	1.4 (1.0)	0.8 (0.5)		1.3 (0.55)	
Collagen composition	1.8 (0.3)	2.4 (0.3)		2.3 (0.55)	
Collagen Amount	2.8 (0.3)	2.8 (0.1)		1.9 (0.35)	

Figure 3: *Box plots and individual data of passive (a) and active (b) biomechanical tests. Individual data are plotted as black dots with median and inter-quartile range marked with a gray-lines. The not identifiable implant is marked with an empty circle and outlier red circle.*
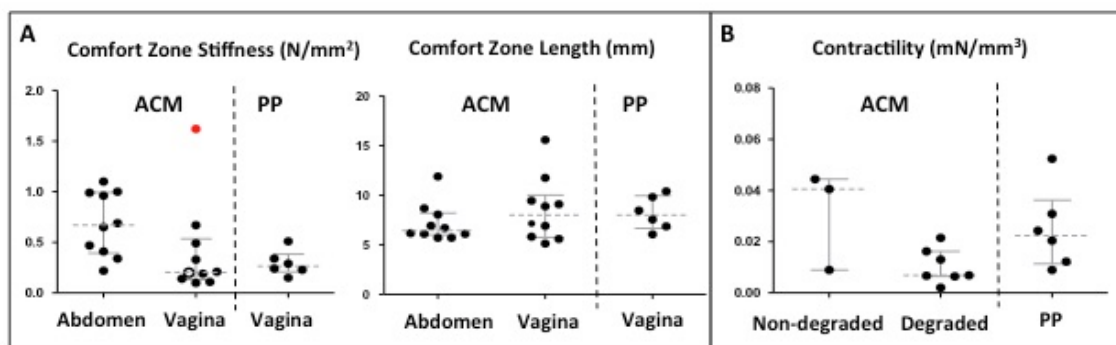
Table 3: *Outcomes and test results of vaginally implanted ACM and PP, and their unpaired comparison (significance level p < 0.05).*

	ACM	PP	Unpaired Comparison
	Posterior vagina	**Posterior vagina**	
	N=10	N=6	
Graft Related Complication	5/10 (50%)	1/6 (16.6%)	0.0367
Exposure	1/10 (10%)	0/6(0%)	
Folding	2/10 (20%)	1/6 (16.6%)	
Induration	2/10 (20%)	0/6(0%)	
Contraction of identifiable mesh	-53,82% ± 10.20 (n=7)	-23.06% ± 16.63	0.0009
Biomechanics			
Comfort zone Stiffness (N/mm)	0.27 ± 0.19 (n=9)	0.29 ± 0.12	ns
Comfort zone length (mm)	8.89 ± 3.17 (n=9)	8.18 ± 1.67	ns
Contractility (mN/mm^3)	0.017 ±0.015 (n=10)	0.025 ± 0.016	ns
Degraded (n=7)	0.010 ± 0.007	0.025 ± 0.016	0.0481
Non-degraded (n=3)	0.031 ± 0.019	-	-

DISCUSSION

In this study, we used the ovine model to document outcomes following insertion of a cross-linked ACM in the rectovaginal septum. We used an investigational product that was treated with the ADAPT® procedure to prevent calcification, reduce lipid content and restore tissue flexibility. We used a double control, i.e. an internal control by implantation of the same material at a control site (the abdominal wall) and an external control by implantation of a durable polypropylene implant at the same (vaginal) site.

Conceptually ACM is the ideal matrix for gradual integration into the host. In order to avoid adverse reactions, ACM is made free of allergens, DNA, and other pathogens. Cross-linking should make them resistant to endogenous collagenase activity. However, several experimental and clinical studies report unfavorable outcomes with the use of a variety of ACM. Clinically both GRC and failure were reported [24–27]. Also, our experiment revealed a number of GRC. The first striking observation was the presence of calcification on histology. This happened at both anatomical locations and not in the control group. Calcification of GA cross-linked grafts has been tied to residual non-viable cells and cellular debris that was not removed during GAD pretreatment. They serve as nucleation sites for calcium phosphate minerals. GAD modifies phosphorous rich cell membranes that are capable of mineralization using calcium present in the extracellular fluid [28, 29]. This adverse effect was meant to be prevented by the ADAPT procedure, which has been earlier shown to work in previous experimental studies in rats and sheep [30–32]. Clinical studies on the use of the same material for cardiac defects showed minimal or no mineral precipitation in the matrices [15]. This was reassuring because pathological calcification is a feared complication in cardiac surgery, certainly in young patients [33, 34]. To our knowledge, no previous studies have looked at the use of this material for surgical repair of the abdominal wall or a vaginal environment,

The most common local observation was palpable induration at the implant site. Histologically, this did not always coincide with calcification, but may also with contraction, folding and wrinkling. There are no published data on contraction rates following insertion of cross-linked ACM in the vagina. Studies on abdominal insertion showed various results. Ozog et al. reported minimal or unchanged dimensions in 180 days with Pelvicol in rats; however without visible deformation [35]. Conversely, Jenkins et al reported a 50% area reduction and wrinkling for abdominal wall reconstruction after three months in minipigs using Collamend (another crosslinked porcine dermis; Bard, Davol, RI) [36]. They explained the process by the presence of encapsulation, though we observed that process also in non-contracted ACM[35]. Contraction is however not the privilege of ACM, as significant contraction rates have been reported following polypropylene implantation both in the vagina (45%) in the vagina and abdomen (10%) 90 days after surgery [18].

We also observed various stages of graft degradation in 30% of abdominal and 70% of vaginal explants. The occurrence of degradation

of crosslinked ACM has been reported by several groups in different models [37–40]. Claerhout et al documented degradation in rabbit abdominal Pelvicol (Bard, Haasrode, Belgium) implants from 180 days onwards [38] and Pierce documented the same for vaginal Pelvisoft implants [39]. In a clinical study, we saw the same when Pelvicol was used for laparoscopic sacrocolpopexy, leading to recurrence [24]. Graft degradation coincided in 8 out of 9 cases with an abundance of foreign body (giant) cells on biopsy [41]. Description of the exact time course of degradation is currently impossible since clinical as experimental studies usually involve only one-time point. Interestingly, degradation does not occur in the same way at both locations. Pierce et al. showed more degradation of Pelvisoft (Bard, Covington, GA) 270 days following vaginal than abdominal implantation [42]. The same difference was present in our study. It is not possible to determine whether this is a faster or more vigorous process. However, Abramov et al showed differences between the wound healing response in the vagina and in the abdomen, which may lead to another remodeling process [43].

Vaginal ACM explants were around 2.7-fold less stiff than their abdominal counterparts. To our knowledge, there are no studies on biomechanics following simultaneous ACM implantation in both locations, so we do not have references to compare to. However, differences in biomechanics for these two environments were studied following insertion of PP (Gynemesh; Ethicon, Somerville, NJ) in a rabbit [42], Vaginal explants were 1.5-fold less stiff than abdominal explants. Both observations follow a trend reported on the biomechanics of cadaverous native tissue from the vagina and abdominal aponeurosis [44]. Gabriel et al. reported the vaginal wall being four times less stiff than abdominal aponeurosis. There are to our knowledge no published reference data on the biomechanics of native vaginal tissue and abdominal wall.

Graft degradation is another factor of relevance as it interferes with the biomechanical properties. For that reason, so we compared the stiffness of those implant sites where no ACM was visible anymore versus those where the material was conserved (abdominal degraded vs. non-degraded 0.44 vs. 0.79, vaginal degraded vs. non-degraded 0.33 vs. 0.15).

Smooth muscle contractility showed at the first glance no difference for the explants using different implant materials. Further analysis into two subgroups revealed a 67% decline of forces in the group without visible ACM. When there was still detectable ACM findings were comparable to PP implanted tissues. In other words, the absence of material coincides with a reduction in contractility. In line with other studies, we further demonstrated that ACM implants affect smooth muscle contractility [45]. This is somewhat counter-intuitive unless one assumes that earlier in time the implant may have already compromised contractility e.g. by a process of stress shielding, as described by others [45–47]. To elucidate that one would, however, need a study with several time points and appropriate native tissue controls, and the mechanisms remain therefore unexplained.

Our study has several limitations. Again, we only studied one-time point, precluding insight into the time course of the host response, hence it cannot learn the processes driving the adverse events neither. Another is the use of a semi-quantitative histological scoring system and limited staining methods. Though they are descriptive, it would be much more informative to also have biochemical and molecular readouts to document details on the nature of the immune response, neovascularization, collagen metabolism and nerve ingrowth [48]. This might be difficult to do, as those tools are not readily available in sheep, and also add significantly to the cost. Further, we had to resort to using a second vaginal location for implantation so that we could obtain sufficient tissue for histology, without compromising the availability of tissue for biomechanical testing. Further, there are the limitations of the model; even though sheep can be used as a model for vaginal surgery as well as prolapse [18] it remains mostly an asymptomatic quadruped, with clinically different anatomical and pelvic floor loads, hence not an ideal disease model. It has, however, several advantages: apparently sheep may clinically develop obvious pelvic floor relaxation and some degree of prolapse after delivery; further, this is a widely available, affordable alternative to the primate, which would be the closest model we could think of.

In conclusion, we demonstrated despite treatment with ADAPT, acellular collagen matrix insertion into the rectovaginal septum was associated with a number of local adverse effects. Apart from that, the passive biomechanical properties were not better than what was obtained when a polypropylene mesh was used. Following degradation of the ACM, there was a decrease in smooth muscle contractility. The ideal implant material has apparently not yet been identified.

Ethical approval: The experiment was approved by the Ethics Committee for Animal Experimentation of the Faculty of Medicine of the K.U. Leuven. All applicable international, national and institutional guidelines for the housing, care and use of animals were followed. Procedures performed in this study were in accordance with the ethical standards of the institution at which they were conducted.

Contribution to the authorship: ME contributed to protocol development, experimental surgery, data collection and data analysis. IU contributed to the histological analysis, data collection and data analysis. IU and JD were responsible for manuscript writing. JV and AF contributed to protocol development, experimental surgery, data collection, and analysis. JV, SS, TD, and BK contributed to histological analysis and data collection. ME, AF, BK, LN and JD contributed to manuscript editing.

REFERENCES:

1. Barber MD, Maher C (2013) Epidemiology and outcome assessment of pelvic organ prolapse. Int Urogynecol J 24:1783–90. doi: 10.1007/s00192-013-2169-9

2. Milsom I, Altman D, Lapitan MC, et al. (2009) Epidemiology of urinary (UI) and faecal (FI) incontinence and pelvic organ prolapse (POP). Health Publication Ltd, Paris

3. Wu JM, Matthews CA, Conover MM, et al. (2014) Lifetime risk of stress urinary incontinence or pelvic organ prolapse surgery. Obstet Gynecol 123:1201–6. doi: 10.1097/AOG.0000000000000286

4. Maher CM, Feiner B, Baessler K, Glazener CMA (2011) Surgical management of pelvic organ prolapse in women: the updated summary version Cochrane review. Int Urogynecol J 22:1445–57. doi: 10.1007/s00192-011-1542-9

5. Keys T, Campeau L, Badlani G (2012) Synthetic mesh in the surgical repair of pelvic organ prolapse: current status and future directions. Urology 80:237–43. doi: 10.1016/j.urology.2012.04.008

6. Mangera A, Bullock A, Chapple CR, MacNeil S (2012) Are biomechanical properties predictive of the success of prostheses used in stress urinary incontinence and pelvic organ prolapse? A systematic review. Neurourol Urodyn 21:13–21. doi: 10.1002/nau

7. Salomon LJ, Detchev R, Barranger E, et al. (2004) Treatment of Anterior Vaginal Wall Prolapse with Porcine Skin Collagen Implant by the Transobturator Route: Preliminary Results. Eur Urol 45:219–225. doi: 10.1016/j.eururo.2003.09.005

8. Meschia M, Pifarotti P, Bernasconi F, et al. (2007) Porcine skin collagen implants to prevent anterior vaginal wall prolapse recurrence: a multicenter, randomized study. J Urol 177:192–5. doi: 10.1016/j.juro.2006.08.100

9. Botros SM, Sand PK, Beaumont JL, et al. (2009) Arcus-anchored acellular dermal graft compared to anterior colporrhaphy for stage II cystoceles and beyond. Int Urogynecol J Pelvic Floor Dysfunct 20:1265–71. doi: 10.1007/s00192-009-0933-7

10. Mangera A, Bullock AJ, Roman S, et al. (2013) Comparison of candidate scaffolds for tissue engineering for stress urinary incontinence and pelvic organ prolapse repair. BJU Int 112:674–85. doi: 10.1111/bju.12186

11. Trabuco EC, Klingele CJ, Weaver AL, et al. (2009) Medium-term comparison of continence rates after rectus fascia or midurethral sling placement. Am J Obstet Gynecol 200:300.e1-6. doi: 10.1016/j.ajog.2008.10.017

12. Jeon M-J, Jung H-J, Chung S-M, et al. (2008) Comparison of the treatment outcome of pubovaginal sling, tension-free vaginal tape, and transobturator tape for stress urinary incontinence with intrinsic sphincter deficiency. Am J Obstet Gynecol 199:76.e1-4. doi: 10.1016/j.ajog.2007.11.060

13. Dunn RM (2012) Cross-linking in biomaterials: a primer for clinicians. Plast Reconstr Surg 130:18S–26S. doi: 10.1097/PRS.0b013e31825efea6

14. Neethling WML, Glancy R, Hodge AJ (2004) ADAPT-treated porcine valve tissue (cusp and wall) versus Medtronic Freestyle and Prima Plus: crosslink stability and calcification behavior in the subcutaneous rat model. J Heart Valve Dis 13:689–96.

15. Neethling WML, Strange G, Firth L, Smit FE (2013) Evaluation of a tissue-engineered bovine pericardial patch in paediatric patients with congenital cardiac anomalies: initial experience with the ADAPT-treated CardioCel(R) patch. Interact Cardiovasc Thorac Surg 17:698–702. doi: 10.1093/icvts/ivt268

16. Neethling WML, Hodge a J, Clode P, Glancy R (2006) A multi-step approach in anti-calcification of glutaraldehyde-preserved bovine pericardium. J Cardiovasc Surg (Torino) 47:711–8.

17. Feola AJ, Endo M, Urbankova I, et al. (2013) Abstracts of the 38th Annual IUGA (International Urogynecological Association) Meeting. Dublin, Ireland. May 28-June 1, 2013. Int Urogynecol J 24 Suppl 1:S1-152. doi: 10.1007/s00192-013-2101-3

18. Manodoro S, Endo M, Uvin P, et al. (2013) Graft-related complications and biaxial tensiometry following experimental vaginal implantation of flat mesh of variable dimensions. BJOG 120:244–50. doi: 10.1111/1471-0528.12081

19. de Tayrac R, Alves A, Thérin M (2007) Collagen-coated vs noncoated low-weight polypropylene meshes in a sheep model for vaginal surgery. A pilot study. Int Urogynecol J Pelvic Floor Dysfunct 18:513–20. doi: 10.1007/s00192-006-0176-9

20. Badylak S, Kokini K, Tullius B, et al. (2002) Morphologic study of small intestinal submucosa as a body wall repair device. J Surg Res 103:190–202. doi: 10.1006/jsre.2001.6349

21. Zheng F, Lin Y, Verbeken E, et al. (2004) Host response after reconstruction of abdominal wall defects with porcine dermal collagen in a rat model. Am J Obstet Gynecol 191:1961–70. doi: 10.1016/j.ajog.2004.01.091

22. Morawietz L, Tiddens O, Mueller M, et al. (2009) Twenty-three neutrophil granulocytes in 10 high-power fields is the best histopathological threshold to differentiate between aseptic and septic endoprosthesis loosening. Histopathology 54:847–53. doi: 10.1111/j.1365-2559.2009.03313.x

23. Feola A, Moalli P, Alperin M, et al. (2011) Impact of pregnancy and vaginal delivery on the passive and active mechanics of the rat vagina. Ann Biomed Eng 39:549–58. doi: 10.1007/s10439-010-0153-9

24. Claerhout F, De Ridder D, Roovers JP, et al. (2009) Medium-term anatomic and functional results of laparoscopic sacrocolpopexy beyond the learning curve. Eur Urol 55:1459–67. doi: 10.1016/j.eururo.2008.12.008

25. Deprest J, De Ridder D, Roovers J-P, et al. (2009) Medium term outcome of laparoscopic sacrocolpopexy with xenografts compared to synthetic grafts. J Urol 182:2362–8. doi: 10.1016/j.juro.2009.07.043

26. Quiroz LH, Gutman RE, Shippey S, et al. (2008) Abdominal sacrocolpopexy: anatomic outcomes and complications with Pelvicol, autologous and synthetic graft materials. Am J Obstet Gynecol 198:557.e1-5. doi: 10.1016/j.ajog.2008.01.050

27. Hviid U, Hviid TVF, Rudnicki M (2010) Porcine skin collagen implants for anterior vaginal wall prolapse: a randomised prospective controlled study. Int Urogynecol J 21:529–34. doi: 10.1007/s00192-009-1018-3

28. Jorge-Herrero E, Garcia Paez JM, Del Castillo-Olivares Ramos JL (2005) Tissue heart valve mineralization: Review of calcification mechanisms and strategies for prevention. J Appl Biomater Biomech 3:67–82.

29. Schoen FJ, Levy RJ (2005) Calcification of tissue heart valve substitutes: progress toward understanding and prevention. Ann Thorac Surg 79:1072–80. doi: 10.1016/j.athoracsur.2004.06.033

30. van den Heever JJ, Neethling WML, Smit FE, et al. (2013) The effect of different treatment modalities on the calcification potential and cross-linking stability of bovine pericardium. Cell Tissue Bank 14:53–63. doi: 10.1007/s10561-012-9299-z

31. Neethling WML, Glancy R, Hodge AJ (2010) Mitigation of calcification and cytotoxicity of a glutaraldehyde-preserved bovine pericardial matrix: improved biocompatibility after extended implantation in the subcutaneous rat model. J Heart Valve Dis 19:778–85.

32. Neethling WML, Yadav S, Hodge AJ, Glancy R (2008) Enhanced biostability and biocompatibility of decellularized bovine pericardium, crosslinked with an ultra-low concentration monomeric aldehyde and treated with ADAPT. J Heart Valve Dis 17:456–63.

33. Schoen FJ, Hobson CE (1985) Anatomic Analysis of Removed Prosthetic Heart Valves: Causes of Failure of 33 Mechanical Valves and 58 Bioprostheses, 1980 to 1983. Hum Pathol 16:549–59.

34. Butany J, Leong SW, Cunningham KS, et al. (2007) A 10-year comparison of explanted Hancock-II and Carpentier-Edwards supraannular bioprostheses. Cardiovasc Pathol 16:4–13. doi: 10.1016/j.carpath.2006.06.003

35. Ozog Y, Konstantinovic M, Zheng F, et al. (2009) Porous acellular porcine dermal collagen implants to repair fascial defects in a rat model: biomechanical evaluation up to 180 days. Gynecol Obstet Invest 68:205–12. doi: 10.1159/000235852

36. Jenkins ED, Melman L, Deeken CR, et al. (2011) Biomechanical and histologic evaluation of fenestrated and nonfenestrated biologic mesh in a porcine model of ventral hernia repair. J Am Coll Surg 212:327–39. doi: 10.1016/j.jamcollsurg.2010.12.006

37. Deeken CRC, Melman L, Jenkins EED, et al. (2011) Histologic and biomechanical evaluation of crosslinked and non-crosslinked biologic meshes in a porcine model of ventral incisional hernia repair. J Am Coll Surg 212:880–8. doi: 10.1016/j.jamcollsurg.2011.01.006.Histologic

38. Claerhout F, Verbist G, Verbeken E, et al. (2008) Fate of collagen-based implants used in pelvic floor surgery: A 2-year follow-up study in a rabbit model. Am J Obstet Gynecol 198:94.e1-94.e6.

39. Pierce LM, Rao A, Baumann SS, et al. (2009) Long-term histologic response to synthetic and biologic graft materials implanted in the vagina and abdomen of a rabbit model. Am J Obstet Gynecol 200:546.e1-8. doi: 10.1016/j.ajog.2008.12.040

40. Melman L, Jenkins ED, Hamilton N a, et al. (2011) Early biocompatibility of crosslinked and non-crosslinked biologic meshes in a porcine model of ventral hernia repair. Hernia 15:157–64. doi: 10.1007/s10029-010-0770-0

41. Deprest J, Klosterhalfen B, Schreurs A, et al. (2010) Clinicopathological study of patients requiring reintervention after sacrocolpopexy with xenogenic acellular collagen grafts. J Urol 183:2249–55. doi: 10.1016/j.juro.2010.02.008

42. Pierce LM, Grunlan MA, Hou Y, et al. (2009) Biomechanical properties of synthetic and biologic graft materials following long-term implantation in the rabbit abdomen and vagina. Am J Obstet Gynecol 200:549.e1-8. doi: 10.1016/j.ajog.2008.12.041

43. Abramov Y, Golden B, Sullivan M, et al. (2007) Histologic characterization of vaginal vs. abdominal surgical wound healing in a rabbit model. Wound Repair Regen 15:80–6. doi: 10.1111/j.1524-475X.2006.00188.x

44. Gabriel B, Rubod C, Brieu M (2011) Vagina, abdominal skin, and aponeurosis: do they have similar biomechanical properties? Int Urogynecol J 22:23–27. doi: 10.1007/s00192-010-1237-7

45. Feola A, Abramowitch S, Jallah Z, et al. (2013) Deterioration in biomechanical properties of the vagina following implantation of a high-stiffness prolapse mesh. BJOG 120:224–32. doi: 10.1111/1471-0528.12077.

46. Majima T, Yasuda K, Tsuchida T, et al. (2003) Stress shielding of patellar tendon: effect on small-diameter collagen fibrils in a rabbit model. J Orthop Sci 8:836–41. doi: 10.1007/s00776-003-0707-x

47. Lo IKY, Marchuk L, Majima T, et al. (2003) Medial collateral ligament and partial anterior cruciate ligament transection: mRNA changes in uninjured ligaments of the sheep knee. J Orthop Sci 8:707–13. doi: 10.1007/s00776-003-0695-x

48. Liang R, Zong W, Palcsey S, et al. (2014) Impact of prolapse meshes on the metabolism of vaginal extracellular matrix in rhesus macaque. Am J Obstet Gynecol 212:174.e1-174.e7. doi: 10.1016/j.ajog.2014.08.008

CHAPTER 6

TRANSVAGINAL MESH INSERTION IN THE OVINE MODEL

Iva Urbankova, Geertje Callewaert, Nikhil Sindhwani, Alice Turri, Lucie Hympanova, Andrew Feola, Jan Deprest

Centrum for Surgical Technologies, Department of Development and Regeneration, Clinical Specialties Research Groups, Faculty of Medicine, KU Leuven, Leuven, Belgium

Institute for the Care of Mother and Child and Third Faculty of Medicine, Charles University, Prague, Czech Republic

Pelvic Floor Unit, University Hospitals KU Leuven, Leuven, Belgium

ABSTRACT

This protocol describes mesh insertion in the rectovaginal septum in sheep using a single vaginal incision technique with/without trocar-guided insertion of anchoring arms. Parous sheep underwent dissection of the rectovaginal septum, followed by insertion of an implant with/without four anchoring arms, both designed to fit the sheep anatomy. The anchoring arms were put in place using a trocar and an "outside-in" technique. The cranial arms were passed through the obturator, gracilis, and adductor magnus muscles. The caudal arms were fixed near to the sacrotuberous ligament through the coccygeus muscles. This technique allows for mimicking of surgical procedures performed in women suffering from pelvic organ prolapse. The anatomical spaces and elements are easily identified. The most critical part of the procedure is the insertion of the cranial trocar, that may easily penetrate the peritoneal cavity or surrounding pelvic organs. This could be avoided by more extensive retroperitoneal dissection and guidance of the trocar more laterally. This approach is designed only for experimental testing of novel implants in large animal models as the trocar guided insertion is currently not used clinically.

INTRODUCTION

Pelvic organ prolapse is clinically diagnosed in half of the women who had at least one vaginal delivery, but subjectively it bothers half of them[1]. The mainstay of therapy is surgical reconstruction, using either native tissue or implant materials, but each of these has their limitations, including recurrence or local complications [2–4]. The ideal implant has not yet been identified, and hence, there is an ongoing demand for product innovation, and for the development of a proper pipeline for preclinical experimentation prior to the introduction of new products and techniques onto the market. One of the steps in this track is an experimental evaluation of suitable animal models [5, 6]. Ideally, they should mimic the anatomical, biomechanical and biological environment. When it comes to experimental evaluation of novel implants, these are typically firstly tested in smaller models, either for biocompatibility or for reconstruction of abdominal wall defects. That type of experiments has been criticized because the implants are not inserted into the area of interest, i.e. the vagina [7]. Vaginal surgery models are more scarce, certainly when the goal of the experiment is to document the biomechanical characteristics of explants. For that reason, there was a move from the rabbit to the sheep [8]. Adult ewes are large animal models with a reasonable sized and accessible vagina. It has been showed that it can be used for mid-term evaluation of novel implants, and it has been possible to reproduce vaginal exposures with given materials [9–13]. Not only the dimensions and anatomy of the ovine vagina and pelvic floor are comparable to human but also the spontaneous occurrence of prolapse in 15% of ewes. Prolapse risk factors are overlapping, i.e. multiparity, previous history of POP and increased intra-abdominal pressure by a higher body weight or when grazing on hills, or comparable effects of (fyto)estrogens [6, 14]. In Europe, sheep are the only reasonable alternative as research on non-human primates has been nearly completely banned. Herein the model was moved one step further, i.e. to mimic transvaginal insertion of implants using trocars and guides for tension free placement of meshes in the recto-vaginal septum, and fix the implant using anchoring by arms through ligaments of muscles that can be considered equivalent to what is done in clinical practice [15, 16]. So far this has not been studied, though many believe that specific complications may be due to the use of these long strips and/or the piercing of anatomical structures.

In an earlier detailed anatomical study, the ovine pelvic floor was compared to the female pelvis [17]. When it comes to the implant anchoring, sheep do not have the sacrospinous ligament, yet a very well developed broad sacrotuberous ligament. The pudendal nerve runs ventrally on it, making it unsafe to use this landmark as a suspension point. Conversely, the coccygeus muscle and its fascia, as well as the obturator membrane, are accessible through the rectovaginal space. Herein the access and position of the anatomical structures for fixation of anchoring arms was proposed, as well as the course of the instruments used to position the mesh, and the relationship of the arms or trocars to adjacent anatomical structures such as vessels and nerves, and potential intraoperative complications.

PROTOCOL

Ethical approval for this experiment was obtained from the Ethics Committee on Animal Experimentation of the KU Leuven (P065/2013). Animals were treated in accordance with current national guidelines on animal welfare.

1 Material and Experimental animal

1.1 Surgery preparation

1.1.1 In the surgical theater cover a table with a sterile drape and prepare one sterile curved trocar (Figure 1A), sterile surgical instruments, sutures and sterile gauze. Perform the entire surgical procedure in sterile conditions if the experiment includes follow-up. Place all instruments on the table to be ready for use during surgery.

1.1.2 Remove a sterile rectangular implant and/or an implant with anchoring arms from their sterile package and put them on the table covered with a sterile drape (Figure 1B,C,D).

1.2 Experimental animal

1.2.1 Administer premedication of 1mL of atropine sulfate 15mg/mL and xylazine HCl 1mL/50 kg intramuscularly (i.m.) 30min before the surgical procedure.

1.2.2 After 30 min, ensure that the premedication has made the sheep lethargic and sleepy.

1.2.3 Insert an intravenous catheter into the jugular vein and administer 0.075 mL/kg of ketamine HCl 100 mg/mL. Confirm deep anesthesia by the animals lack of reactions to painful stimuli.

1.2.4 Move the animal onto the surgical table and secure its airways by intubation. Maintain the anesthesia with 2.5% isoflurane in 5 L/min oxygen.

1.2.5 Keep the intravenous line inserted into the jugular vein and supply 500 mL saline solution at a flow rate of 150 mL/h.

1.2.6 Administer prophylactic antibiotics intramuscularly (amoxicillin-clavulanate, 7mg/kg) and post-operative analgesics (buprenorphine + chlorocresol, 1 mL) or the equivalent according to local protocols.

1.2.7 Place the animal in a lithotomy position on the end of the surgical table, secure its limbs with the hips in hyperflexion with ropes (Figure 2A).

1.2.8 Empty manually the bladder and rectum, by pushing trans-vaginally on the appropriate structures. Shave the perineum, medial part of the thigh and the tail folds and disinfect with polyvidone iodine 7.5% (Figure 2B,C).

Figure 1. A: Schematic drawing of the trocar. B: H-shaped PVDF implant with a detail of the central part (panel C). Its shape is inspired on the four-arm meshes currently available for transvaginal prolapse repair. The rectangular body (30 x 40 mm) is laterally extended by four arms stretching (150 x 10 mm). The dimensions of the arms are designed to be long enough to pierce the relevant suspension structures, based on earlier anatomical studies [17]. D: The rectangular implant (30 x 40 mm). Both implants were made from polyvinylidene fluoride, the textile characteristics and properties are in Table 1.
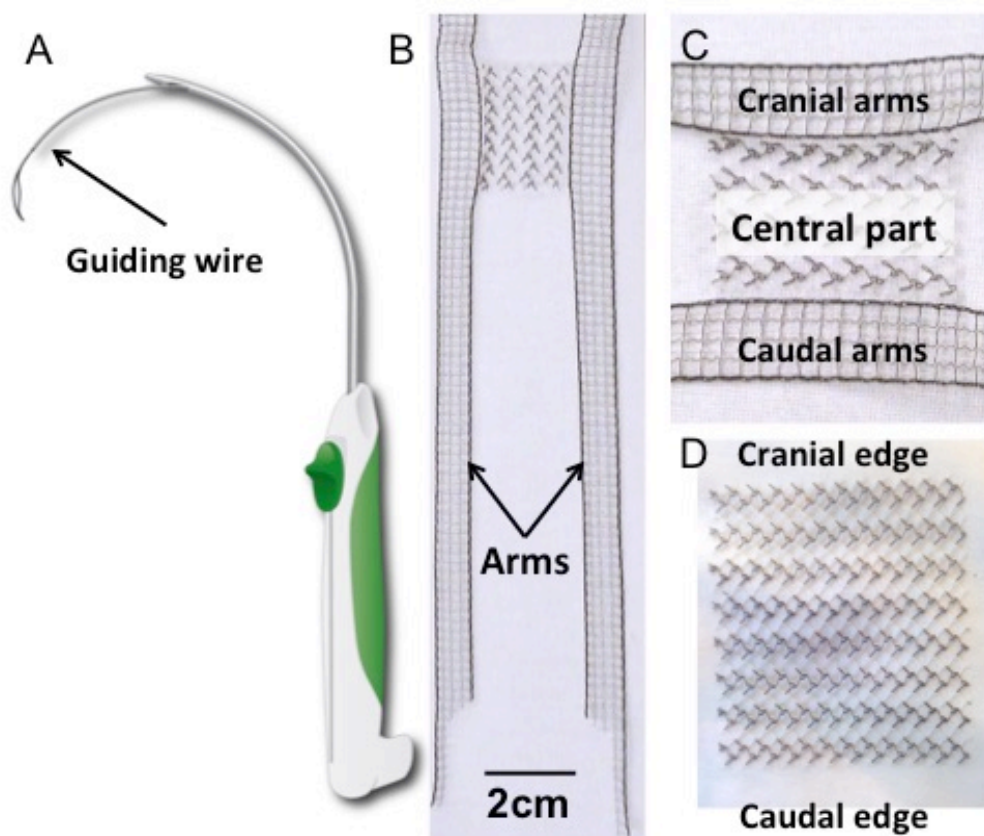
Table 1: Dry material properties. Table showing material properties of the rectangular mesh and mesh with anchoring arms. The stiffness and anisotropic index were obtained from Maurer et al.[18]

	Rectangular mesh	Arm mesh	
		Central body	Arms
Dimensions (mm)	30 × 40	30 × 40	10 × 150
Thickness (mm)	0.54	0.54	0.70
Weight (g/m2)	83.0	83.0	73.0
Pore size (mm)	2.5 × 2.5	2.5 × 2.5	1.0 × 1.4
Stiffness (N/mm)	0.3	0.3	14.7
Anisotropic index	1.3	1.3	7.5

1.2.9 Cover the animal with a sterile drape and make an opening above the genital hiatus.

1.2.10 Prepare personnel for a surgery in sterile conditions. Put on the surgical cap and mouth mask, wash hands for surgery and put on the surgical gown and sterile gloves.

2   Surgical procedure

2.1   Preparation of the rectovaginal septum

2.1.1 Grasp the dorsal vaginal wall 3 cm cranially to the hymeneal ring with Allis forceps.

2.1.2 Take the syringe loaded with 10 mL of saline and a 22 gauge needle. Insert it through the vaginal epithelium (approximately 3 – 4 mm deep) in the midline of the rectovaginal septum 1.5 cm cranially to the hymeneal ring.

2.1.3 Perform "aqua-dissection" by injecting saline the rectovaginal septum [11].

2.1.4 Enter the rectovaginal space through a 3 cm long midline incision through the vaginal epithelium with the scalpel. The incision starts caudally to the Allis forceps (step 2.1.1.) and heads caudally to the hymeneal ring.

2.1.5 Place the self-retaining retractor (see the table of materials) over the perineum and place four sharp stay hooks in the vaginal incision to keep it open.

2.1.6 With forceps and scissors bluntly dissect the rectovaginal fascia from the vaginal wall laterally towards the pelvic side walls and cranially up to the caudal aspect of the cul-de-sac.

2.1.7 Create suitable space for the 30 × 40 mm central part of the mesh (Figure 2D).

2.1.8 Perform hemostasis with hemostatic forceps or a crisscross hemostatic ligature whenever necessary. [1]
Note: At this point, one can either insert the rectangular implant (2.2) or continue with dissection to insert the implant with anchoring arms (2.3).

3   Insertion of rectangular implant

3.1.1 Insert the vaginal retractor into the vaginal incision to allow a better view of the cranial part of the dissected area.

---

[1] The small bleeders could be clamped with the hemostatic forceps. This crushes the vessel and initiates the natural coagulation cascade. For stronger bleeding grasp the bleeding vessel with the forceps and place a crisscross ligature around secured with the square knot.

3.1.2   Suture the left and right cranial corner of the implant with a simple interrupted 3/0 polypropylene suture on the left and right side of the most cranial aspect of the dissected rectovaginal space and cut the residual suture material. The implant is always sutured to the connective tissue comprising the rectovaginal septum. Keep the suture away from the vaginal lumen; in other words, do not penetrate the vaginal wall.[2]

3.1.3   Add one additional simple interrupted suture midway on the cranial aspect of the implant.

3.1.4   Suture the lateral edges of the implant midway onto the surrounding connective tissue with a simple interrupted 3/0 polypropylene. Keep the implant as flat as possible but tension free.

3.1.5   Suture the left and right caudal corner with a simple interrupted 3/0 polypropylene suture on the left and right side of the most caudal aspect of the rectovaginal space.

3.1.6   Add one additional simple interrupted suture midway on the caudal aspect of the implant.

3.1.7   Close the vaginal incisions with a running 3/0 Vicryl suture

4   Insertion of implant with anchoring arms (trocar guided technique)

4.1.1   Continue the dissection of the rectovaginal space created at section 2.1 cranio-ventrally to reach the medial aspect of the obturator foramen which you can easily palpate.

4.1.2   Dissect the space caudolaterally to reach the caudal aspect of the sacrotuberous ligament and the caudally located coccygeus muscle.

4.1.3   With a blade no. 24 make four 1 cm wide incisions on the vulvar side with through the skin and superficial muscular fascia (Figure 2B,C).

4.1.4   Make two "ventral" incisions on the medial aspect of the thigh, 4 cm cranial from the caudal border of the sciatic arch (= inferior border of the symphysis), and 3 cm lateral from the midline (Figure 2C)

4.1.5   Make two "dorsal" incisions at the level of the insertion of the tail folds, 2 cm medial to the ischial tuberosity, which can be easily palpated (Figure 2B).

4.1.6   Place a curved trocar through one of the ventral incisions (Figure 2E).

4.1.7   Pass the trocar through the adductor magnus muscle, the external obturator and finally through the medial aspect of the obturator foramen.

---

[2] The vaginal wall is not penetrated if you cannot see the suture material in the vagina.

4.1.8 Control progression of the trocar with a finger inserted through the vaginal incision. Guide its tip to the tendinous arch of the levator ani muscle (Figure 2E).

4.1.9 Expose the guiding wire in the vaginal wall incision and load it with the corresponding ipsilateral cranial mesh arm (Figure 2F).

4.1.10 Pull the trocar loaded with the mesh arm through the above structures. Keep the arm tension free.

4.1.11 Repeat the process with the second cranial arm through the ventral incision on the other side of the animal.

4.1.12 Through one of the dorsal incisions, pass the trocar through the coccygeus, just distal from the sacrotuberous ligament (Figure 2G).

4.1.13 Expose the guide wire through the vaginal incision, pick the dorsal arm of the mesh and pull it out. Keep the arm tension free and repeat on the other side.

4.1.14 Adjust the position of the mesh by a combination of tension on the arms and flattening, yet keeping it tension free (Figure 2I, Figure 3).

4.1.15 Fix the body of the mesh with a simple interrupted 3/0 polypropylene suture in the middle of its caudal border onto the surrounding connective tissue.

4.1.16 Cut the arms at the level of skin and close all skin incisions with simple interrupted 3/0 poliglecaprone sutures (Figure 2H, Figure 3).

4.1.17 Close the vaginal incision with a running 3/0 poliglecaprone suture

Figure 2. A: A sheep placed in the supine position with the hips hyper flexed by securing the lower limbs. B: The external entrance points for trocar insertion are on the ventral side (empty arrow) and dorsally on the lateral the tail folds (full arrow). C: Position of the ventral insertion points; the dashed line in the middle represents the midsagittal plane of the animal. D: Dissected rectovaginal septum. E: Insertion of the ventral trocar through the muscles on the medial side of the thigh, the obturator foramen and paravaginal space. The trajectory of the piercing trocar is controlled with the finger. F, G: Once the trocar is in place, the wire sling (open arrow) is advanced and loaded with the arm of the vaginal mesh. H: The final position of the ventral (full arrows) and dorsal arms (empty arrow). I: The central part is placed tension free between the vaginal wall and the rectal adventitia.
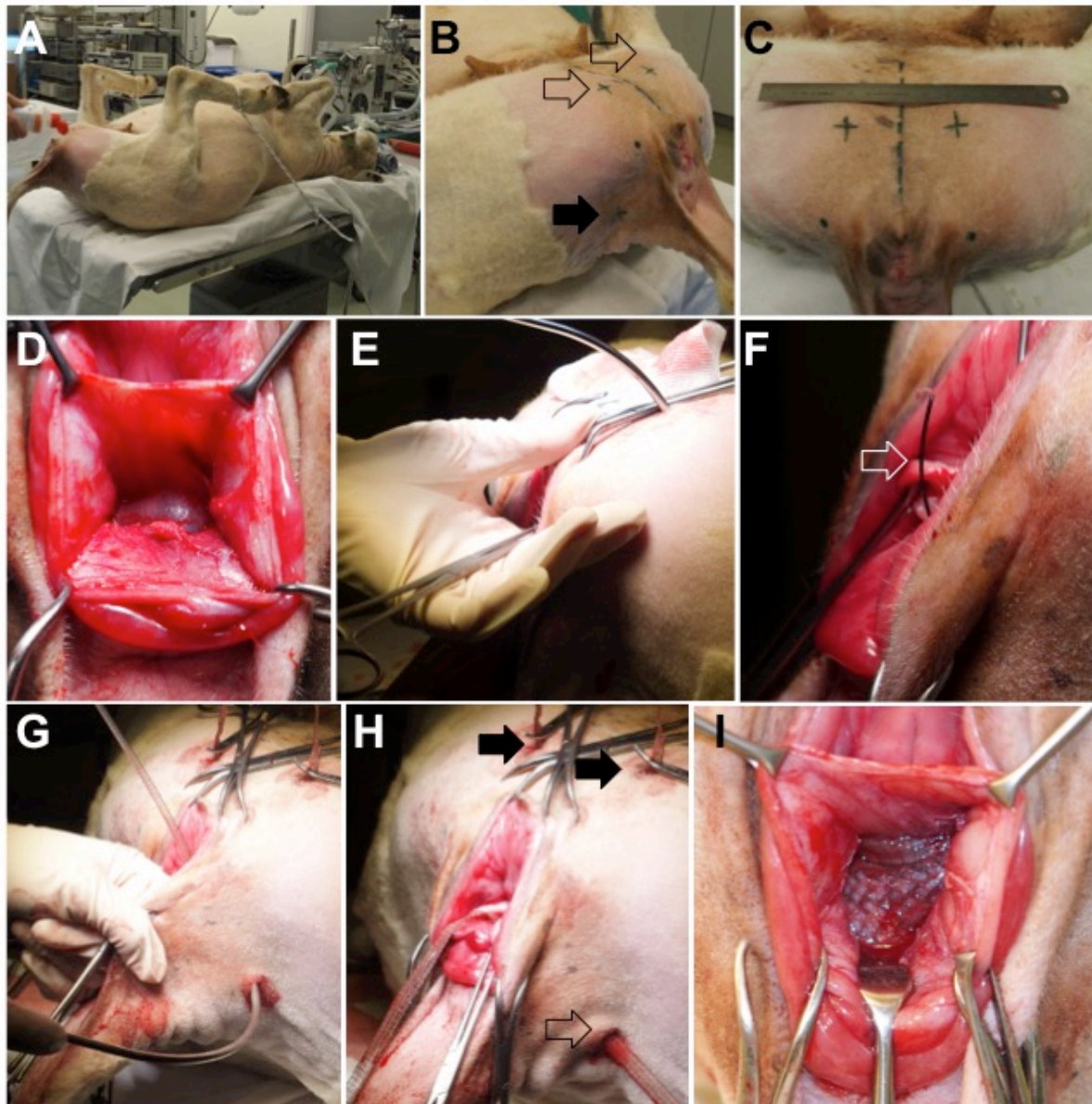
REPRESENTATIVE RESULTS:

Management in longer observation setup

Following the surgical procedure, the vaginal packing [3] may be inserted to secure the implant position for 24 hours. The sheep is placed in a recovery cage and its respiratory function is followed until full recovery. Later it is possible to place the sheep in the stable and allow to move freely, and drink and eat *ad libitum*. The vaginal packing, if present, has to be removed 24 hours after the surgery and the sheep should receive analgesics (buprenorphine + chlorocresol, 1 mL, i.m.) at least for three postoperative days. During the first postoperative week, the animal is checked daily, and then every week until the end of the experiment.

Surgical feasibility

During procedures, there were no problems with mesh insertion in any of the animals. There was almost no bleeding during dissection of the rectovaginal septum and paravaginal spaces. It was possible to identify the medial aspect of the obturator foramen through the dissection. Also, trocar insertion was straightforward with a difference in resistance between more compliant muscles and more resistant fascia of the individual muscles. Though the initial trajectory through the muscles was less controlled, the tip of the trocar became palpable once in contact with the obturator muscle. The dorsal arms were placed without complications or obstacles.

Mesh positioning and findings during subsequent dissection

To investigate the right position of the implant with the anchoring arms, which was considered more difficult, three animals were euthanized by an intravenous injection of 1.0 mL of an embutramide-mebezonium-tetracaine hydrochloride mixture. Following euthanasia, the surgical area was carefully dissected to explore the mesh position and the effect of the insertion of the arms of the mesh through relevant anatomical structures. The shortest distance of the ventral arms from the obturator artery and nerve and the internal pudendal vessel was measured with a ruler and their relationship to the tendinous arch of the levator ani was investigated. Dorsally, the pudendal nerve and internal pudendal artery were identified and the distance between them measured by a standard ruler.

In none of the ewes relevant bleeding was encountered, neither any intra-operative nerve, intestinal or bladder injury. In the first sheep, the cranial arm passed through the caudal aspect of the *cul-de-sac,* but the bowels remained intact. This could be avoided in the next sheep, by paying more attention to guide the tip of the trocar more laterally away from the *cul-de-sac.* The other arm passages could be identified in the anatomical structures previously described and far away from the pelvic nerves and vessels. The cranial arms were passing through the caudal aspect of the obturator foramen (Figure 3, Figure 4A). The entry point of the trocar was at the level of the tendinous arch of the levator ani, 2 - 2.5 cm caudally to the obturator canal and the obturator vessels and nerve (Figure 4B). Once in the paravaginal space, the arm was located 1 – 1.5 cm ventrally

---

[3] Vaginal packing is a saline-solution–soaked gauze package inserted in the vagina immediately after the surgery.

to the pudendal artery and vein and 1 cm laterally to the vaginal artery. The caudal arms passed 1 cm caudally of the caudal aspect of the broad sacrotuberous ligament, right through the coccygeus muscle (Figure 4C). In that location, there are no major vessels or nerves anywhere close. The pudendal nerve is located on the inner surface of the caudal part of the sacrotuberous ligament.

The central part of the mesh was placed flat, with its cranial part stretching retroperitoneal under the caudal end of the cul-de-sac, and its caudal part down along the rectovaginal septum. No rectal perforations occurred (Figure 4B).

Figure 3.: *Schematic illustration of the ovine pelvis with the cranial arms passing through the obturator foramen and caudal arms passing through the tail folds. The broad sacrotuberous ligament is in blue marked with *. The small panel illustrates the position of arms in the animal in recumbent position just before shortening the excessive amount of material. The main panel shows the same but with the skin muscles removed.*
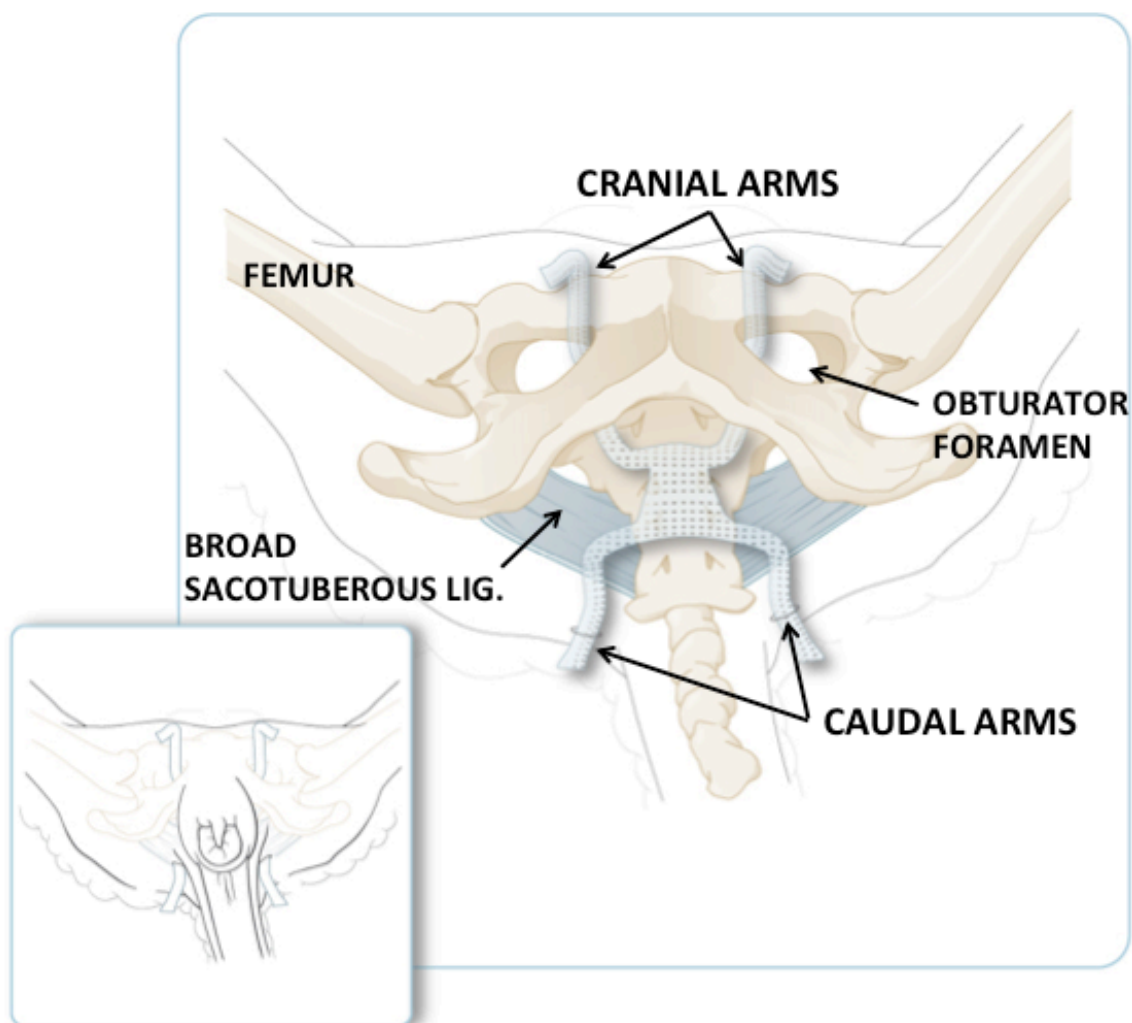
Figure 4.: Anatomical dissection on a pelvic hemisection.
A: The lateral pelvic sidewall after removal of the parietal peritoneum and the retroperitoneal fat tissue. The pubis is at the top of the figure, the vagina is moved medially to reveal the course of the cranial arm (full arrow). The arm is passing through the tendinous arch of the levator ani. The green pin corresponds to the position of the internal pudendal vessels, the blue pin marks the vaginal artery, the yellow pin is placed in the levator ani.
B: The central part of the implant (open arrow) is placed between the vagina, parietal peritoneum and the rectum.
C: The course of the arm (empty arrow) through the medial muscles of the thigh. The gracilis is moved medially to display the course of the arm through the semitendinosus and the adductor magnus muscle.
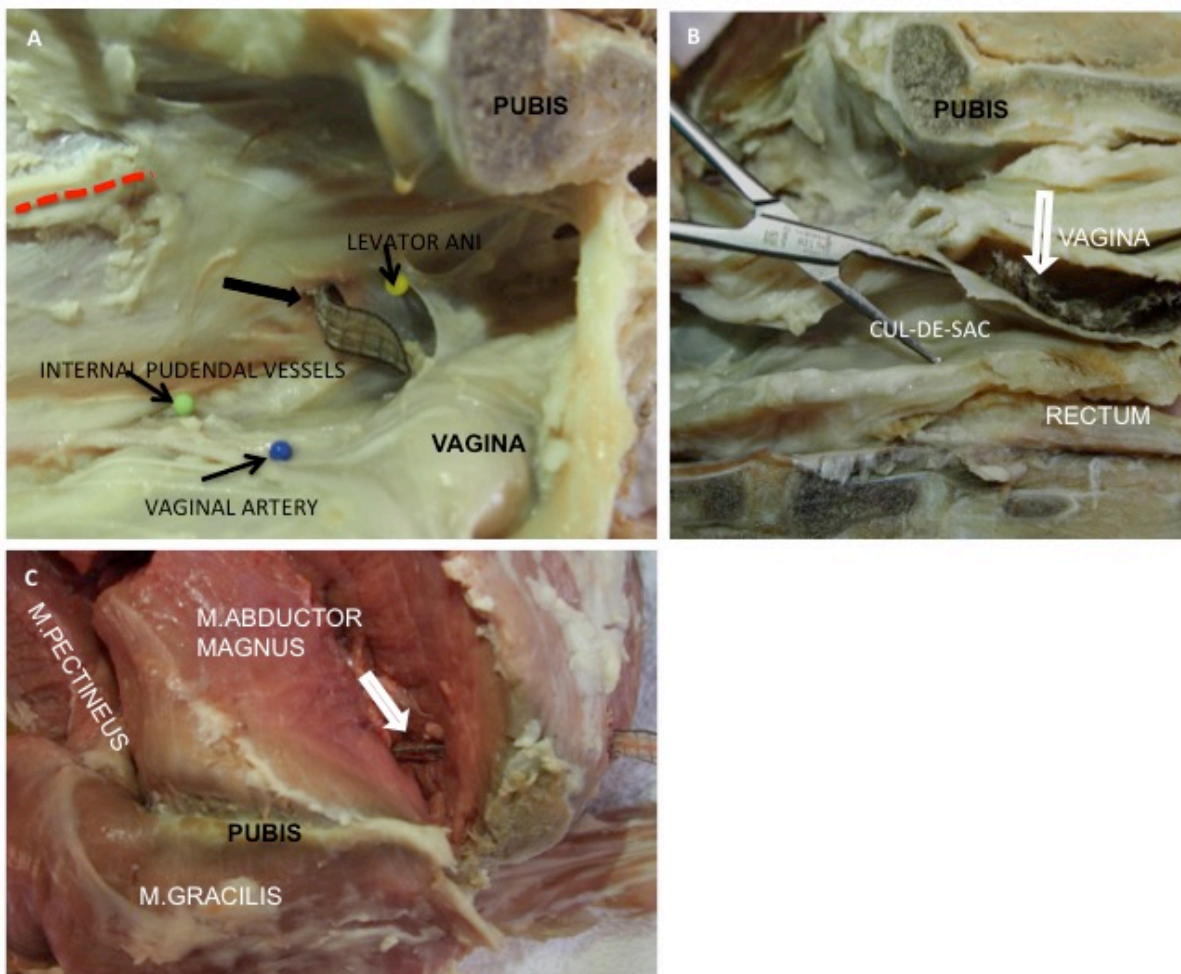
DISCUSSION

This is a description of an experimental procedure in sheep, that aims to mimic vaginal dissection and transvaginal mesh insertion of the implant with or without anchoring arms. The subsequent steps and instruments were inspired by surgical procedures done for POP and stress urinary incontinence [15, 16, 19, 20]. After initial anatomical dissections, there were still some problems during experimental mesh insertion. In the first animal was found a perforation in the peritoneal cavity at the level of the cul-de-sac. This has been previously described clinically in women [21]. In subsequent procedures, this was avoided by guiding the tip of the trocar more laterally (i.e. closer to the pelvic side wall). In later sheep, no other complications were observed.

The most feared anatomical structures were the obturator nerve and artery. In humans, the distance between the trocar/implant and the obturator canal is 1.9 – 3.0 cm [22]. The high variability of the trocar/implant position in women was previously explained by the exact positioning of the legs or needle trajectory. Therefore the hind limbs of the sheep were secured in hyperflexion at the hips to have a wide access to the vagina. In this position, the gracilis muscle is moved cranially. As a consequence, the trocar was passing through the adductor magnus muscle which is undivided but well developed in sheep [23]. A more cranial passage of the trocar is possible yet may harm structures in the obturator canal.

Similar to what is described clinically, the arms were fixing the implant to given anatomical locations, corresponding to natural attachments of the rectovaginal septum in sheep [23]. The implant was lying flat, apparently supporting the posterior vaginal wall without extending more laterally. As a consequence, it did not have a tendency to fold. It may be possible to use larger implants. However as earlier showed in sheep that larger implants are associated with an up to 50% retraction and more local graft-related complications [9].

The previous investigation of novel implants in various animal models included the sheep as a model for vaginal surgery. One part of this work also aimed to fix implants in a way similar to what is done clinically, i.e. by transfixing the arms of meshes to anatomical structures in the pelvis. This procedure was not earlier described in the sheep model. This surgery follows a strategy similar to what was used for introducing new needle- and trocar-assisted surgeries into clinical practice [15]. However, these findings seem to be less relevant than a few years ago, as the use of vaginal implants, hence trocar guided procedures, is quickly dropping due to the consecutive health warnings by the FDA and SCENIHR [24, 25].

Though we describe herein the technique, the number of animals in this experiment was very limited, hence the anatomical variability may not be represented here. Another limitation is that this has described a posterior compartment procedure, which may be less practiced. There are a few reports on surgery in the anterior compartment in sheep [13], yet usually smaller implants were used, and also complications were more frequent. Though these findings may be sufficient to plan further experiments, the feasibility of anterior vaginal mesh placement may also have been informative.

In conclusion, this is a description of safe and feasible surgical technique in the ovine animal model for vaginal surgery, that permits trans-vaginal and trocar guided tension-free vaginal implant insertion. Relevant comparable structures could be blindly pierced without obvious risks for a vessel, nerve or organ injury. This model can of course also be used for simulated vaginal surgery using a native tissue.

Ethical approval: The experiment was approved by the Ethics Committee for Animal Experimentation of the Faculty of Medicine of the K.U. Leuven. All applicable international, national and institutional guidelines for the housing, care and use of animals were followed. Procedures performed in this study were in accordance with the ethical standards of the institution at which they were conducted

Contribution to the authorship: I Urbankova did the study design, surgery, dissection, manuscript writing, G Callewaert, N Sindhwani, A Turri, L Hympanova helped with the surgery and dissections, A Feola did the study design, J Deprest did the study design, manuscript writing. All authors contributed to manuscript editing.

REFERENCES:

1. Glazener C, Elders A, MacArthur C, et al. (2013) Childbirth and prolapse: Long-term associations with the symptoms and objective measurement of pelvic organ prolapse. BJOG An Int J Obstet Gynaecol 120:161–168. doi: 10.1111/1471-0528.12075
2. Jia X, Glazener C, Mowatt G, et al. (2008) Efficacy and safety of using mesh or grafts in surgery for anterior and/or posterior vaginal wall prolapse: systematic review and meta-analysis. BJOG 115:1350–61. doi: 10.1111/j.1471-0528.2008.01845.x
3. Maher C, Feiner B, Baessler K, et al. (2016) Transvaginal mesh or grafts compared with native tissue repair for vaginal prolapse (Review). 10–13. doi: 10.1002/14651858.CD012079
4. Nieminen K, Hiltunen R, Takala T, et al. (2010) Outcomes after anterior vaginal wall repair with mesh: a randomized, controlled trial with a 3 year follow-up. Am J Obstet Gynecol 203:235.e1-8. doi: 10.1016/j.ajog.2010.03.030
5. Abramowitch SD, Feola A, Jallah Z, Moalli PA (2009) Tissue mechanics, animal models, and pelvic organ prolapse: a review. Eur J Obstet Gynecol Reprod Biol 144 Suppl:S146-58. doi: 10.1016/j.ejogrb.2009.02.022
6. Couri B, Lenis A, Borazjani A, et al. (2012) Animal models of female pelvic organ prolapse: lessons learned. Expert Rev Obs Gynecol 7:249–260. doi: 10.1586/eog.12.24.Animal
7. Deprest J, Zheng F, Konstantinovic M, et al. (2006) The biology behind fascial defects and the use of implants in pelvic organ prolapse repair. Int Urogynecol J Pelvic Floor Dysfunct 17 Suppl 1:S16-25. doi: 10.1007/s00192-006-0101-2
8. Ozog Y, Mazza E, De Ridder D, Deprest J (2012) Biomechanical effects of polyglecaprone fibers in a polypropylene mesh after abdominal and rectovaginal implantation in a rabbit. Int Urogynecol J 23:1397–402. doi: 10.1007/s00192-012-1739-6
9. Manodoro S, Endo M, Uvin P, et al. (2013) Graft-related complications and biaxial tensiometry following experimental vaginal implantation of flat mesh of variable dimensions. BJOG 120:244–50. doi: 10.1111/1471-0528.12081
10. Endo M, Urbankova I, Vlacil J, et al. (2015) Cross-linked xenogenic collagen implantation in the sheep model for vaginal surgery. Gynecol Surg 113–122. doi: 10.1007/s10397-015-0883-7
11. Feola A, Endo M, Urbankova I, et al. (2015) Host reaction to vaginally inserted collagen containing polypropylene implants in sheep. Am J Obstet Gynecol 212:474.e1-474.e8. doi: 10.1016/j.ajog.2014.11.008
12. Barnhart KT, Izquierdo A, Pretorius ES, et al. (2006) Baseline dimensions of the human vagina. Hum Reprod 21:1618–22. doi: 10.1093/humrep/del022
13. de Tayrac R, Alves A, Thérin M (2007) Collagen-coated vs noncoated low-weight polypropylene meshes in a sheep model for vaginal surgery. A pilot study. Int Urogynecol J Pelvic Floor Dysfunct 18:513–20. doi: 10.1007/s00192-006-0176-9
14. Sobiraj A, Busse G, I HBOSED (1986) Ivastigation into the blood plasma profiles progesterone in sheep sufferingform vaignal inversion and prolapse antepartum. Br Vet J 218–223.
15. Reisenauer C, Kirschniak A, Drews U, Wallwiener D (2007) Anatomical conditions for pelvic floor reconstruction with polypropylene implant and its application for the treatment of vaginal prolapse. Eur J Obstet Gynecol Reprod Biol 131:214–225. doi: 10.1016/j.ejogrb.2006.03.020
16. Carey M, Slack M, Higgs P, et al. (2008) Vaginal surgery for pelvic organ prolapse using mesh and a vaginal support device. BJOG An Int J Obstet Gynaecol 115:391–397. doi: 10.1111/j.1471-0528.2007.01606.x
17. Urbankova I, Vdoviakova K, Rynkevic R, et al. (2016) Comparative anatomy of the ovine and female pelvis. Gynecol Obstet Invest. doi: 10.1159/000454771
18. Maurer MM, Röhrnbauer B, Feola a., et al. (2014) Mechanical biocompatibility of prosthetic meshes: A comprehensive protocol for mechanical characterization. J Mech Behav Biomed Mater 40:42–58. doi: 10.1016/j.jmbbm.2014.08.005
19. de Leval J (2003) Novel Surgical Technique for the Treatment of Female Stress Urinary Incontinence: Transobturator Vaginal Tape Inside-Out. Eur Urol 44:724–730. doi: 10.1016/j.eururo.2003.09.003
20. Reisenauer C, Kirschniak A, Drews U, Wallwiener D (2006) Transobturator vaginal tape inside-out. Eur J Obstet Gynecol Reprod Biol 127:123–129. doi: 10.1016/j.ejogrb.2005.11.029
21. Bafghi A, Iannelli A, Trastour C, et al. (2005) Bowel perforation as late complication of tension-free vaginal tape. J Gynecol Obs Biol Reprod 34:606–7.
22. Hinoul P, Vanormelingen L, Roovers JP, et al. (2007) Anatomical variability in the trajectory of the inside-out transobturator vaginal tape technique (TVT-O). Int Urogynecol J Pelvic Floor Dysfunct 18:1201–1206. doi: 10.1007/s00192-007-0303-2
23. Schaller O, Constantinescu G, Habel E, et al. (2007) Illustrated Veterinary Anatomical Nomenclature, 2nd editio. Verlag Enke, Stuttgart, Germany
24. FDA (2011) UPDATE on Serious Complications Associated with Transvaginal Placement of Surgical Mesh for Pelvic Organ Prolapse: FDA Safety Communication.
25. Reinier M, Groep G (2016) Final Opinion on the use of meshes in urogynecological surgery (SCENIHR-European Commission) Opinion on. doi: 10.13140/RG.2.1.5108.4883

CHAPTER 7

IN VIVO DOCUMENTATION OF SHAPE AND POSITION CHANGE OF MRI-VISIBLE MESH PLACED IN RECTOVAGINAL SEPTUM

Iva Urbankova, Nikhil Sindhwani, Geertje Callewaert, Alice Turri, Rita Rinkevic, Lucie Hympanova, Andrew Feola, Jan Deprest

Centre for Surgical Technologies, Department of Development and Regeneration, Organ systems cluster, Faculty of Medicine & Pelvic Floor Unit, University Hospitals KU Leuven, KU Leuven, Leuven, Belgium

Institute for the Care of Mother and Child, Third Faculty of Medicine, Charles University, Prague, Czech Republic

ABSTRACT:

Background and Objective: Large deformations in synthetic meshes used in pelvic organ prolapse surgery may lead to suboptimal support for the underlying tissue, graft-related complications as well as recurrence. Our aim was to quantify *in vivo* longitudinal changes in mesh shape and geometry in a large animal model. We compare two commonly used mesh shapes, armed and flat, that are differently affixed. The secondary outcomes were active and passive biomechanical properties.

Methods: A total of 18 animals were used. Six each were implanted with either an arm mesh, a flat mesh or underwent a sham surgery. PVDF meshes loaded with Fe_2O_3 were used to facilitate their visualization in vivo. MR images were taken at 2, 14 and 60 days after implantation and 3D models of the meshes were created at each time point. We calculate the Effective Surface Area (ESA), i.e. the support that the mesh provides to the underlying tissue using custom developed techniques. Longitudinal changes in the mesh shape were studied by comparing the respective 3D models using part comparison analyses. The root means square difference (RMSD) and the modified Hausdorff distance (MHD) was calculated to obtain an objective value for the part comparisons. Wall thickness maps were produced on 3D models. Mesh arm length and their ellipticity profiles were also evaluated. Active and passive biomechanical tests on vaginal tissue overlaying the mesh were conducted using a contractility assay and a uniaxial loading protocol.

Results: MR images of 5 animals in each group were used for longitudinal comparison. Compared to the initial implant size, there was an immediate drop in the ESA measurement at day 2 of almost 32.22 [7.06] % (median [IQR]) for flat meshes, and by 17.59 [6.50] % for arm meshes. After 14 days, the reduction in area was 41.84 [14.89] % and 27.18 [20.44] %, and at day 60 it was 36.61 [6.64] % and 26.43 [14.56] % for the flat and armed meshes respectively. The reduction in area in the two groups was different between the two groups only day 14 (p = 0.046). The ellipticity of the arms was 0.81 [0.08] (median [IQR]) and there was no significant change in the ellipticity profiles over time. The mesh arm length did not change significantly over time.

The part comparison showed a maximum difference of 4.26 [3.29] mm in 3D models according to the MHD measure, which is clinically not relevant. Comparison of high thickness areas on the thickness maps correlated well with the areas of the mesh folding in the arm mesh group observed during postmortem dissection. Thickness maps did not help us understand why the flat meshes had a reduction in the support area.

The comfort zone stiffness of the flat mesh and of the central part of the arm mesh was 2.4 fold and 4.5 times stiffer compared to sham groups, respectively. The arms were 36% stiffer than the central part of the mesh. The comfort zone length of the sham group was 46% longer than the flat mesh group (p= 0.027) and 59% longer than that of the central part of the arm

mesh (p= 0.005). There was no significant difference in vaginal contractile forces generated in samples from the arm, flat mesh, and sham groups.

Conclusions: This is a first longitudinal study observing deformations in vaginally implanted synthetic meshes in a large animal model. A novel methodology is presented to calculate the area of the vaginal tissue effectively supported by the mesh implant. Immediately post-operatively, a reduction in 32% and 17% was noted, which remained stable over the 60 following days of observation. We use thickness maps to analyze the cause of this dramatic immediate reduction. In the armed mesh, we found it to be mesh foldingat the interface between the arms and central part. For the flat mesh, we suggest that pore aggregation during suturing.

Keywords: transvaginal implant, mesh folding, MRI model, sheep

INTRODUCTION

POP is characterized by the descent of one or more of the anterior vaginal wall, posterior vaginal wall, the uterus (cervix), or the apex of the vaginal vault or cuff [1]. Prolapse affects one in two women after first vaginal delivery, half of them being symptomatic [2]. Surgery is the mainstay of therapy with 19% of women operated by the age of 80 years [3]. In analogy to hernia repair, synthetic implants may be used to reduce recurrence. Mesh augmented repair became the preferred surgical method in 10-20% of primary and 34 -75% of recurrent anterior vaginal prolapse repairs [4–6]. There is evidence that repair of the anterior vaginal wall using transvaginal mesh improves anatomical outcomes, yet without superior subjective outcomes [7]. Mesh use is at the expense of an increased risk for graft-related complications (GRC). These include exposure, infection, dyspareunia, and pain, some of them being difficult to treat. GRCs occur in about 10% of cases but relatively little is known about the exact cause [8].

One mechanism for the occurrence of GRCs is that the implants contract *in vivo*. This means a reduction in the size of the implant and is also known as shrinkage [9]. Both wrinkling and folding of the implant may contribute to this apparent reduction in mesh size. Folding may happen either due to surgical handling, or later on, during the time the mesh position adjusts to the underlying anatomy. A secondary mechanism of mesh contraction may be during incorporation of the mesh by the host through secondary inflammatory processes. When mesh contraction becomes symptomatic, it would be ideal to be able to visualize the implant in-vivo using non-invasive medical imaging techniques rather than to have to proceed to surgical exploration [10–13]. This can be achieved by coating or mixing the polymers with contrasting agents. One such agent is Fe_3O_4 microparticles, which when incorporated into the polymer causes a signal void on MR images due to their paramagnetic properties [14–16]. Fe_3O_4 incorporated into polyvinylidene fluoride (PVDF) meshes are commercially available.

We use these meshes to study the mechanisms of mesh contraction. In earlier work, we have demonstrated the feasibility and optimal settings for accurate three-dimensional characterization of such PVDF meshes, in both experimental as well as clinical settings [17, 18]. We found that in rabbits and rat animal models, most of the mesh contraction occurred early on (1-2 days), while dimensions remained stable thereafter. In those studies, however, the implant was inserted in the abdominal wall [16]. Later work on vaginal implantation with a polypropylene material suggested an even larger shrinkage, as measured at dissection 2 months or later [19, 20]. Finally, also clinically we demonstrated a significant smaller mesh size already 6 weeks after implantation [18]. No additional shrinkage occurred by 8 months postoperative.

Herein we aimed to monitor postoperative changes in the mesh shape, size, and position, *in vivo*, using MR visible meshes and non-invasive MR in the ovine model. Secondary outcome measures were histology and biomechanical properties.

MATERIAL AND METHODS

Ethics committee approval

Animals were treated in accordance with current national guidelines on animal welfare. The experiment was approved by the Ethics Committee for Animal Experimentation of the Faculty of Medicine of the K.U. Leuven.

Implants and groups

Two different PVDF mesh geometries, either a "flat" or "arm" mesh, purpose designed to fit the ovine anatomy, were used in this study, see Figure 1 [22]. Both shapes are currently being used in clinical procedures and differ in their mechanism of fixation to the underlying tissues [23, 24]. The meshes were manufactured, packed individually and sterilized by the manufacturer (FEG Textiltechnik GmbH, Aachen, Germany) for this study. The dry material properties of the PVDF mesh are given in Table 1. The constituting fibers of the mesh contain paramagnetic Fe_3O_4 microparticles (0.2 µm) at a concentration of 10 mg/g polymer at the stage of production. The arm mesh was inspired by a four armed-mesh currently available for transvaginal prolapse repair. The dimensions of the main body of this H-shaped implant were the same as the flat mesh at 30 × 40 mm. The arms were 150mm in length and 10 mm in width.

Table 1: Dry material properties

	Flat mesh/Central body of the arm mesh	Arms of the mesh
Thickness (mm)	0.05	0.70
Weight (g/m^2)	83.0	73.0
Pore size (mm)	2.5 × 2.5	1.0 × 1.40
Anisotropic index [21]	1.3	7.5

Figure 1: Geometry of meshes purposely designed for this experiment. A: arm mesh. B: flat mesh.
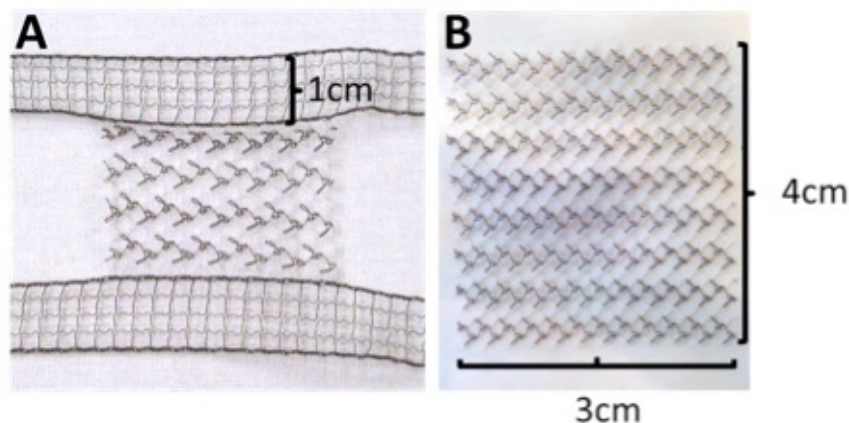
Surgery

18 parous Swifter sheep (mean weight 68 ± 3.5 kg) were obtained from the Zoötechnical Institute of the KU Leuven; animals were randomly assigned to either the (1) vaginal flat mesh, (2) vaginal arm mesh, or (3) vaginal sham group.

Mesh implantation

Surgery was conducted under sterile conditions. The general anesthesia, antibiotic prophylaxis and postoperative analgesia, and the postoperative care protocols have been described in detail previously [19, 25]. In brief, the aqua dissection was followed with a 3 cm long midline incision in the distal vagina. The recto-vaginal septum was then dissected to create a suitable space for the 30 × 40 mm flat mesh or the central part of the arm mesh. The flat mesh was fixed tension free to the underlying tissue, at each corner and then halfway on its borders with 3/0 polypropylene (PP; Prolene, Ethicon, Diegem, Belgium). In the sham group, eight sutures were placed in a similar way to mark dissected area.

In the arm mesh group the recto-vaginal septum was further dissected craniolateral, to reach the medial aspect of the obturator foramen, and caudolateral, to reach the inner surface of the broad sacrotuberous ligament [22]. The arms were placed with a curved trocar (Insnare; Bard, West Sussex, United Kingdom; Figure 2B), that was inserted through ventral and dorsal skin incisions (Figure 2A,C,D). The ventral arms were placed through the obturator foramen and medial thigh muscles. The dorsal arms passed through the coccygeus muscle close to the sacrotuberous ligament. The arms were placed tension free, the position of the body was fixed with a single 3/0 Prolene (Ethicon) suture in the middle of its caudal border to the perineal body. The arms were cut at the level of skin, which was closed with 3/0 polyglactin sutures (Vicryl, Ethicon). All vaginal incisions were closed with a running 3/0 Vicryl suture. Postoperatively, animals were allowed to move, drink and eat ad libitum. They were clinically followed by a veterinarian at the farm until sacrificed 60 days later.

Necropsy

All animals were euthanized at D60 postoperatively using an intravenous injection of 100mg/kg of phenobarbital (Release, Ecuphar, Oostkamp, Belgium). During necropsy, graft-related complications (GRCs) were noted at each of the three implantation sites. Thereafter the original implant together with the adjacent and ingrown tissue (further referred to as explant) was removed *en bloc* and its area was calculated using three longitudinal and horizontal dimensions measured with an analog micrometer (Horex, Helios Preisser, Gammertingen, Germany). Additionally, vaginal tissue samples lateral to the implantation site were taken to obtain control reference measurements for active biomechanics testing.

Observations pertaining to the shape of the implant, as it lay in the embedded tissue were made. Obvious mesh folding or large deformations, if any, were noted. Contraction of the central body of the explanted tissue was defined as the explant over initial graft area

(1200 mm^2). Explants were then divided to obtain specimens for histology and biomechanical testing (Figure 3).

Magnetic resonance imaging

All animals of the implantation groups underwent magnetic resonance (MR) imaging on day 2, 14 and 60 after surgery. Scans were under general inhalation anesthesia in the lateral recumbent position. We used 3T MRI device with a spinal coil (Siemens, Erlangen, Germany). Anatomic high-resolution T1-sequences with a slice thickness and interslice distance of 0.9 mm (resolution 1.03 × 1.03 mm, TE 4.92 ms, TR 10 ms, the field of view 330 mm, bandwidth 446 Hz/pixel) were acquired in the sagittal plane to visualize the entire implant. The implants were visible as a hypointense structure, shown in Figure 4.

Figure 2: *Trocar-guided single incision insertion of vaginal mesh. The ventral side of the animal is always at the top of the image. Panel A: A schematic drawing with a projection of the implant in relation to the ovine pelvic landmarks. The broad sacrotuberous ligament is marked with an asterisk (*). The open arrows showing the ventral arms and full arrows the dorsal arms. Panel B: trocar as used for the surgery. Panel C: External view at the time of vaginal surgery, with the mesh already in place. The open arrows showing the ventral arms and full arrow the dorsal arm. Panel D: Vaginal view at the end of the operation. (Illustration 2A, B by Myrthe Boymans, reproduced with permission from UZ Leuven, Leuven, Belgium.)*
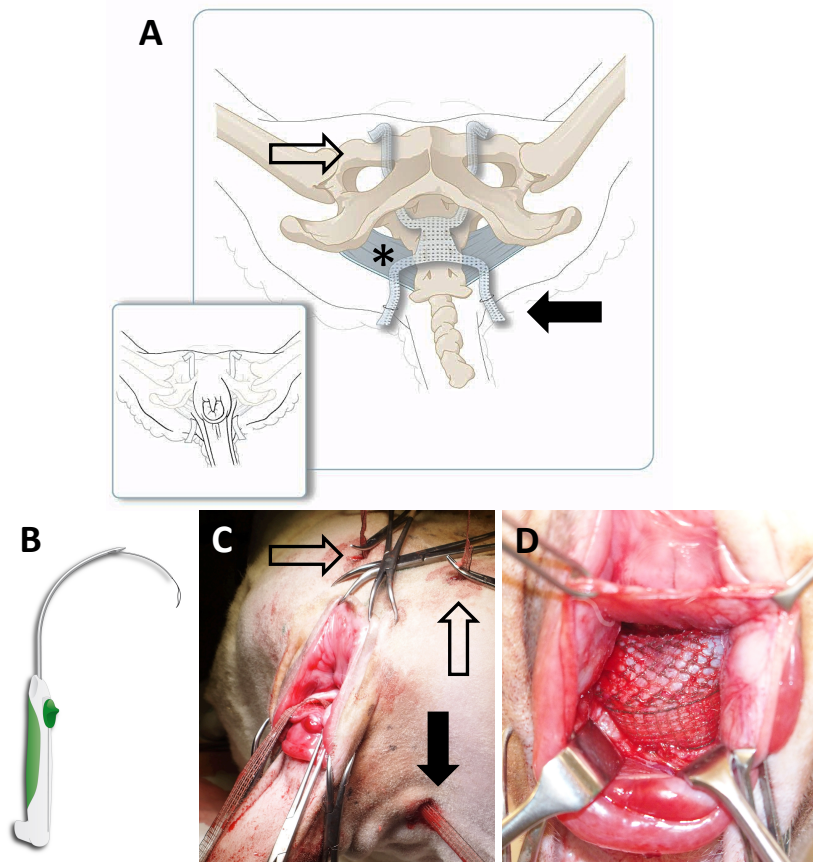
Figure 3: *The example of an arm mesh explant (A) and schematic drawing of explant processing (B) indicating how samples were obtained for passive biomechanics (dotted line, red), and contractility testing (full line, green).For the armed implants, tensiometry was also done on the ventral arms.*
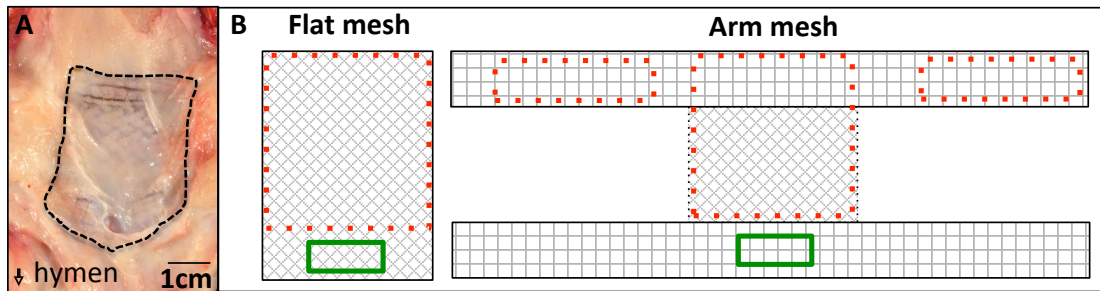
Figure 4: *Mesh is visible as a hypointense structure in T1 weighted MR images. Full white arrows indicate the mesh arms and the empty arrows point to the mesh's main body. The yellow line at sagittal images shows the plane of the transversal section.*
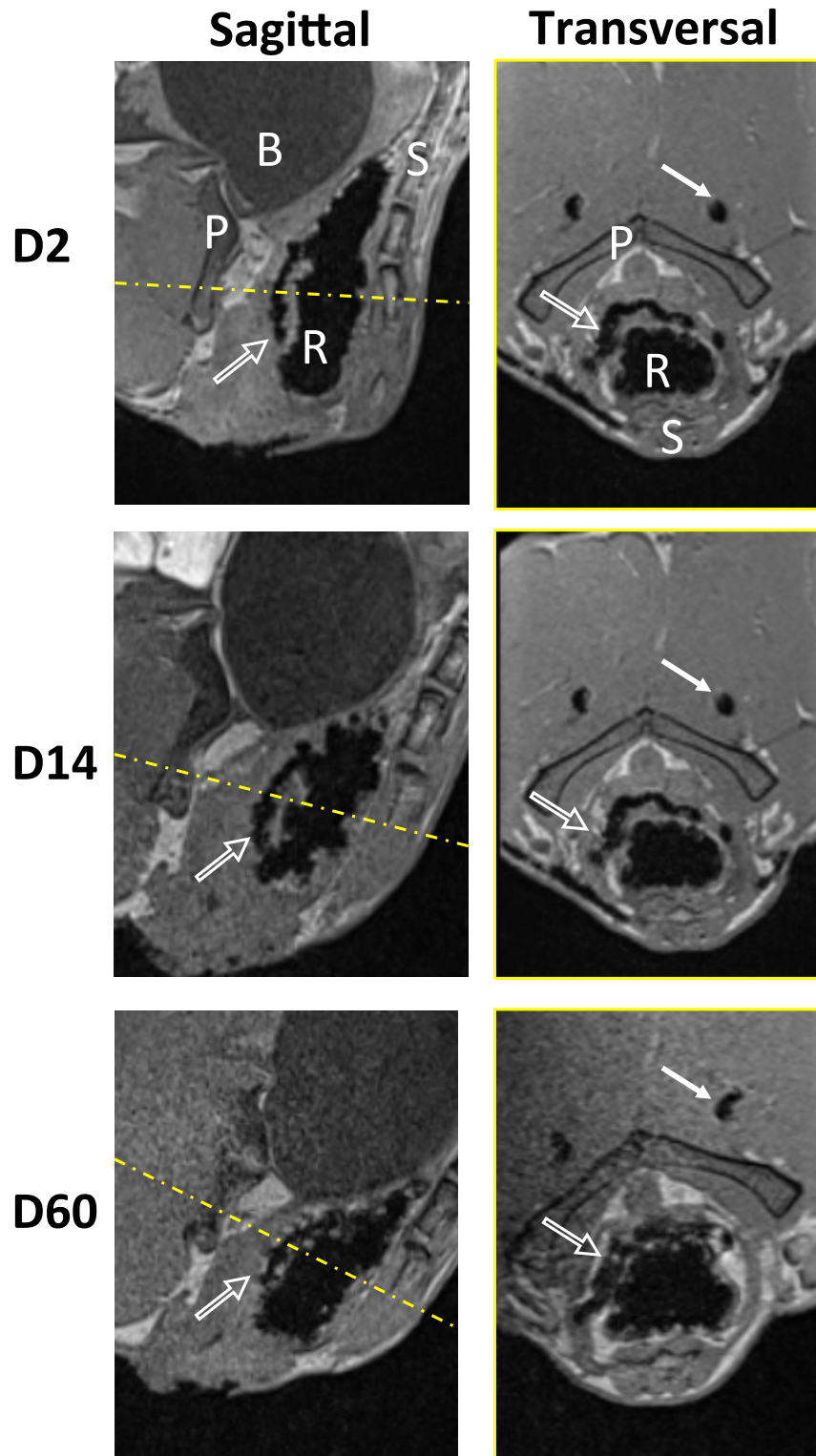
In-vivo mesh measurements

3D models of the mesh

In T2 MR image sequence, the mesh appeared as a continuous hypointense structure. Thus, it can be segmented out to generate a 3D triangulated model of the mesh. The complete process of 3D model generation, processing, and analysis from MR images of visible meshes has been described previously [18]. Briefly, the paramagnetic signal was extracted using the dynamic region growing segmentation technique. To further improve the quality of the 3D model, smoothing and wrapping operations were done. For 3D models of arm meshes, the main body of the mesh was separated from the arms. The process is depicted pictorially in Figure 5.

Figure 5: Left: Segmented mesh outline is indicated with red borders. Right: The 3D model of the mesh along with separated arms and the main body. R rectum, Ventral Arms: LP left posterior, RP right posterior; Dorsal Arms: LA left anterior, LA left anterior
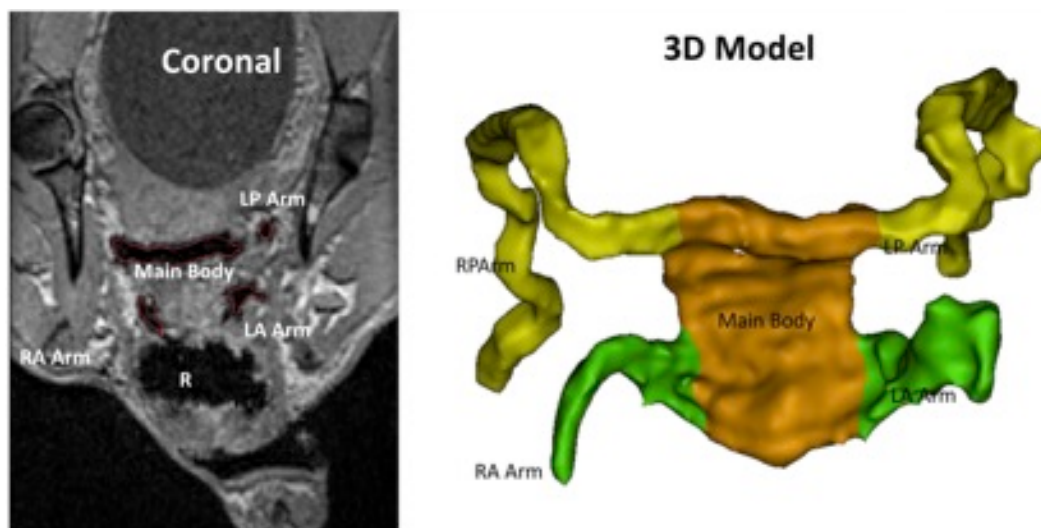
On each MR sequence, the sacral promontory and the ischial tuberosity points were indicated manually. These serve as anatomical bony landmarks for the description of the mesh position. The X-axis is defined as running from left to right side ischial tuberosity points, the Y-axis as that running cranially from the mid-tuberosity towards the sacral promontory and the Z-axis is defined as the cross of between X and Y unit vectors, pointing dorsally.

Image processing, mesh generation, splitting of the model, as well as the assignment of bony landmarks, was done using Mimics Innovation Suite v17 (MIS) (Materialise, Leuven, Belgium). The 3D mesh model generation, 3D model splitting, anatomical landmark placement and mesh arm curves were created by one observer (RR) and verified by two independent assessors (IU and NS).

Wall thickness maps

A wall thickness map was then created for each 3D mesh model using MIS. This operation provides a numerical value to each triangle of the 3D model's surface based on the location of a triangle on the opposite side of the model. The analysis is overlaid on the 3D model's surface and visualized represented as a map. Topological differences in the thickness map may indicate areas where the mesh is folded, as this area should have a larger wall thickness measurement.

Mesh arm measurements

For each arm, a mid-line spline curve was drawn that represented the course of the mesh arms in the sheep, henceforth called as the mesh arm curve. The length of the mesh arm curves is recorded as representative of the length of the mesh arms.

Further, the shape of the mesh arm can be indicated by an ellipticity measure as was first described in Sindhwani et al, 2015 [18]. The ellipticity of the mesh arm at a certain location indicates if it is flat or tubular at that location. It is obtained by obtaining the cross-section of the arm 3D models along the mesh arm curve, and finding the best fit ellipse on the cross-sectional contour to obtain the major and minor axis radii (a, b respectively). Ellipticity is then defined as: $\varepsilon = \sqrt{(a^2 - b^2)/a^2}$. The ellipticity profile of each mesh arm is generated automatically using a custom program implemented in Matlab (v13a, Mathworks Inc., Natick, MA, USA).

Part comparison analysis

Part comparison analyses are done to study longitudinal geometrical changes in the meshes. First, the two 3D models are translated so that their centers of gravity are aligned. Second, the two point clouds are registered using a rigid registration scheme using the iterative closest point search (ICP) algorithm [26, 27]. The ICP algorithm matches every data point in one 3D model to the nearest neighbor in the other, minimizes the root mean square difference (RMSD) between the two point clouds and transforms the data points until the RMSD is minimized.

The part comparison analysis provides a map with a different value at each point, as shown in Figure 6. To quantitatively describe the similarity of the two point clouds we report the RMSD obtained after the registration step. A low value of RMSD shows that overall, the objects are similar [28]. A second measure, the Modified Hausdorff Distance (MHD) is calculated, which represents the maximum difference between two models at any point [29, 30]. The part comparison analysis was done using custom codes using tools in MIS software and Matlab.

Part comparison analysis is done on the 3D models obtained from day 2 to day 14, day 14 to day 60 and day 2 to day 60 MR images. For arm meshes, the part comparison is done only for the main central body of the mesh 3D models.

Figure 6: *The part comparison analysis is done by first overlaying the two objects (Mesh 1 and Mesh 2) onto one another, followed by 3D registration. The part comparison analysis then provides the distance of points on one model to the corresponding points on the other model. These comparison values are represented here as a color map overlay (right).*
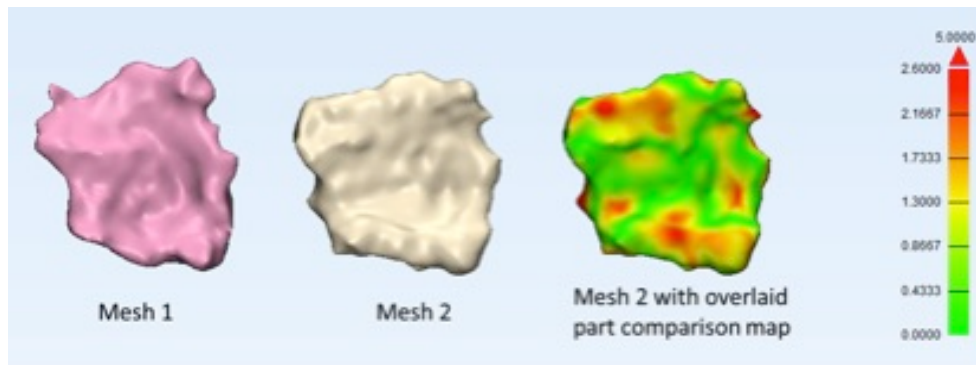
Effective mesh support surface

The effective mesh support surface was obtained by extracting the medial surface of the 3D models of the meshes. For arm meshes, the main body alone was used. We first presented a semi-automated procedure for extracting this surface in [18]. This procedure is here modified to obtain full automation. As in [18], the first step is to obtain a point cloud close to the mid-plane of the 3D model, as in Figure 7A. This is achieved by wall thickness values at each point on the surface of the 3D model, and translating the point by a distance of half the thickness value in the direction opposite to the surface normal. A 3D surface is fitted on this point cloud using the locally weighted scatterplot smoothing (LOWESS) method, to obtain a function of the natural curvature of the mid-plane surface, see Figure 7B. To obtain the area of this mid-plane surface, these points are then projected onto the principal projection plane of the 3D object. and are translated to a structured two-dimensional grid (Figure 7C). A triangulation is then made using the Delaunay method which is projected back to the 3D surface function, giving us the effective support surface as shown in Figure 7D. The area of this support surface is representative of the area of the tissue that is effectively supported by the mesh, or the Effective Support Area (ESA).

The average length and width of the mesh, the right-left, and the craniocaudal direction were marked on the mesh manually by one examiner (NS) and verified by another (IU). The average of 10 sections each in the indicated direction was presumed to the length and the width measurement of the mesh.

Figure 7: Overview of the process to obtain the effective support surface. (A) shows the midplane point cloud (cyan) inside the 3D model of the main body (yellow). (B) shows the LOWESS fit surface function that provides the natural curvature of the mid-plane surface. (C) shows the points from the mid-plane point cloud projected onto their natural projection plane. (D) shows the effective support surface obtained by triangulating in 2D and projecting back onto the LOWESS surface function.
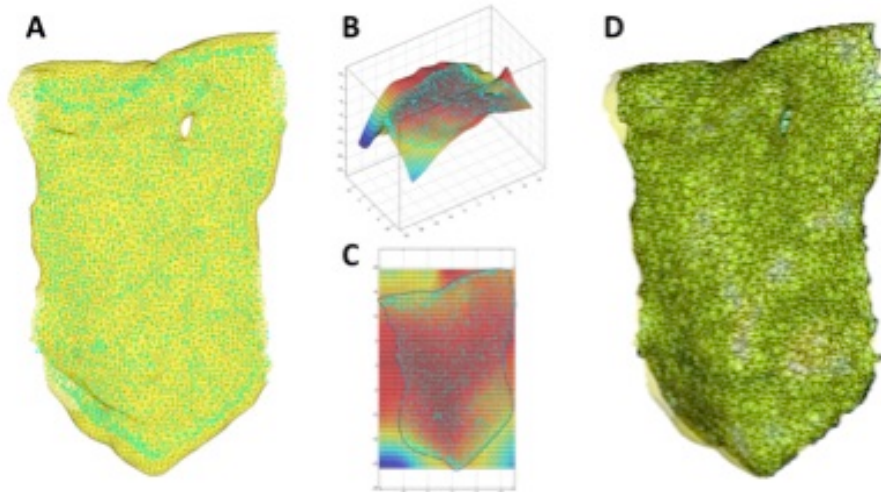
Biomechanics

For biomechanical testing, samples were collected from the explanted mesh-tissue complex, from the main body region of the mesh, from the region of the ventral arms, as shown in Figure 3

The corresponding parts of the dry mesh implants, i.e., the main body and the arms respectively, were used as controls. Passive biomechanics testing was done using a uniaxial Zwick tensiometry apparatus with a 200-N load cell (Zwick GmbH & Co. KG, Ulm, Germany). The sample to be tested was trimmed to a rectangular shape (10x50mm) and gripped perpendicular to the body axis. Specimens were firstly preloaded to 0.1N (speed 10mm/min) and the width, thickness, and grip-to-grip distance were measured with the analog caliper and micrometer (Horex, Helios-Preisser GmbH, Gammertingen, Germany). Following preload, the sample was subjected to a constant displacement 10mm/min in a uniaxial manner up to the rupture. The resulting load-elongation curves were analyzed to determine the structural properties of each mesh. Records of the force-elongation relationship we used for calculation of stiffness (N/mm) of the tested material, which we measured in the low-stress area also called as the "comfort zone", the average slope of the force-elongation curve and the length of the former zone.

To assess active biomechanics, circumferentially oriented vaginal strips (10x8mm) were obtained from the area above the implant and form the non-operated part of the vagina. The active biomechanics of the complete mesh tissue complex could not be tested as it was not

possible to maintain a sufficient oxygen supply to this complete explanted tissue. The tests were conducted in accordance with standard protocols [31]. Each strip was placed into a heated bio-chamber with Krebs solution to 37°C and subjected to a ~10mN preload. Samples were then allowed to equilibrate for an hour before exposing to a 120mM dose of potassium (K+) to determine maximum contractility. Generated forces were normalized by the specimen's wet weight

Statistical analysis

The Kolmogorov–Smirnov test was used to determine data normality. Parametric data are reported as the mean ± standard deviation (SD), whereas nonparametric data are represented as median [interquartile range (IQR)].

Temporal changes in mesh arm length, obtained at different time points, were tested for statistical significance using repeated measures two-way analysis of variance (ANOVA). Changes in the ellipticity profile for each animal were also tested for significance using one-way ANOVA. ANOVA was also done to determine if the ESA, and the length and the width of the meshes were significantly different across the three-time points. Differences in the ESA of the flat mesh and arm mesh group, at each time point, were tested for significance using the two sampled students' t-test.

Biomechanical properties were assessed using a one-way ANOVA with for comparing groups, with a Bonferroni post hoc test. All analyses were performed with Prism 5 (GraphPad Software, Inc., La Jolla, CA, USA). Significance was assumed at $p < 0.05$.

RESULTS

Surgical procedures were uncomplicated in all animals except one in the sham group. It died immediately after surgery due to an anesthesiological complication. There was one subcutaneous abscess in the area of the caudal fixation arm on day 14. Following abscess evacuation, it was treated with i.m. antibiotics for three days and recovered. At day 60 no local complication was observed.

Anatomical findings

Table 2 enlists the anatomical findings. The number of GRC for vaginal implantations were two in the arm group. One sheep had an asymptomatic abscess in the ischioanal fossa at necropsy. One had a subcutaneous abscess day 14 as mentioned above. There were no GRC in the flat mesh group and sham-operated animals.

In the flat mesh group, no obvious mesh deformation was found at explantation (Figure 8A), except one that appeared to be considerably smaller in size than the others (Figure 8C). In the arm mesh group, four animals had the ventral arms folded on top of the main body of the mesh and in one the dorsal arm was folded below the main mesh body (Figure 8B,D,E). The arms themselves lay mostly flat (Figure 8F) but were rolled in a rope-like structure in certain areas (Figure 8G,H).

Passive and active biomechanics

The comfort zone stiffness of the flat mesh and of the central part of the arm mesh were 2.4 fold and 4.5 times stiffer compared to sham groups, respectively. The arms were 36% stiffer than the central part of the mesh.

Explants from the central part of the arm mesh included in all cases both types of mesh as apparent in Figure **1**. In other words, there is a contribution of both types of biomechanics. All explants with the graft were significantly stiffer than explants from sham group.

The comfort zone length of the sham group was 46% longer than the flat mesh group (p= 0.027) and 59% longer than the comfort zone of the central part of the arm mesh (p= 0.005). There was no difference between the central part and the arms in the arm mesh group.

There was no significant difference in contractility testing between the arm, flat mesh, and sham group (ANOVA, p=0.51). Moreover, in neither group, there was a significant difference between vaginal stripes located above the implant and from the non-operated control area.

Table 2: Comparison of outcomes of vaginally implanted meshes.
a p= 0.027, b p= 0.007, c p= 0.002, d p= 0.005, e p= 0.027

	Armed mesh Main body	Armed mesh Arms	Flat mesh	Sham	ANOVA
Graft related complications					
In total	2/6 (33%)		0/6 (0%)	0/5 (0%)	
Exposure	0/6 (0%)		0/6 (0%)	0/5 (0%)	
Deep abscess	1/6 (17%)		0/6 (0%)	0/5 (0%)	
Subcutaneous abscess, re-intervention	1/6 (17%)		0/6 (0%)	0/5 (0%)	
Other gross anatomical findings					
Folding and visible deformation	5/6 (83%)		1/6 (17%)	NA	
Explant contraction	-34.50 (9.0)		-36.8 (6.0)	NA	
Biomechanics	**Main body**	**Arms**			
Comfort zone stiffness (N/mm)	$3.27 \pm 1.08^{a,b}$	5.11 ± 1.57	$1.67 \pm 0.32^{b,c}$	$0.70 \pm 0.56^{a,c}$	0.0002
Comfort zone length (mm)	3.02 ± 1.42^{d}	2.67 ± 1.20	3.91 ± 1.03^{e}	$7.30 \pm 1.66^{d,}$	$p<0.0001$
Comfort zone stiffness dry mesh	0.54 ± 0.15	5.31 ± 0.39	0.54 ± 0.15		
Comfort zone length dry mesh	9.78 ± 0.98	10.45 ± 1.00	9.78 ± 0.98		
Contractility (mN/g)	97.1 ± 42.3	NA	149.5 ± 65.13	144.1 ± 80.2	NS

Figure 8: *Examples of mesh deformation following the explantation and histology. In panels A – D the cranial direction is always at the top, ventral arms are located cranially, dorsal caudally. (A) shows the appearance of a flat mesh where there were no indications of major deformation. (B) shows an arm mesh without any major deformation. (C) shows a flat mesh where there is serious deformation. (D) shows an arm mesh with the ventral (located cranially) arm folded over the main body (*) and the dorsal arm is also quite deformed. (E) shows a mesh arm that appears to be lying flat in the tissue while (F) shows a mesh arm with rolled appearance. (G) and (H) show how a histological section of the mesh arm that lays flat or is rolled over respectively. Histological images are stained with Movat pentachrome (collagen – blue, green, yellow; muscles-red; nuclei – black; elastin - black) and captured at 25x magnification.*
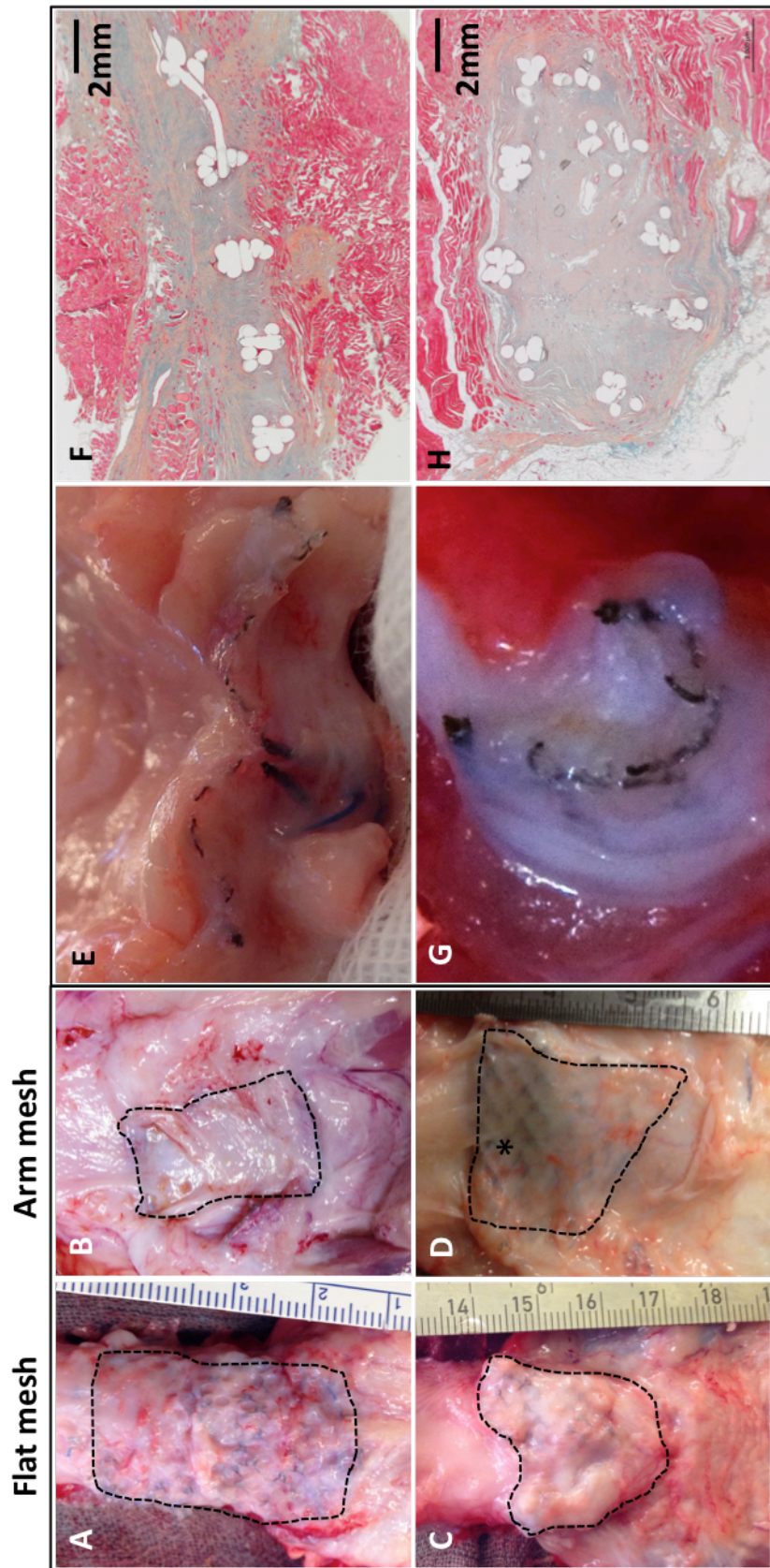
MR imaging

36 MRI scans were recorded on twelve sheep implanted with vaginal mesh. Implants were visible as a hypointense area in the rectovaginal septum and the arms in the soft tissue in the lesser pelvis, obturator foramen and in the muscles of the medial thigh as shown in Figure 4. Extreme movement artifacts were observed in MR images of 1 animal at day 14 in the arm mesh group and 1 animal at day 60 in flat mesh group. These animals were excluded from all longitudinal analyses.

Changes in mesh position

Between the 2nd and the 14th day after implantation, the main body of the arm meshes moved by 6.19 [2.54] mm (median [IQR]), and for the flat meshes that was 6.60 [9.97] mm. On the 60th day, compared to the 14th day, the central body of the arm mesh moved by 4.58 [9.10] mm, and for the flat mesh that was 8.25 [5.15] mm. Compared to the 2nd day, on the 60th day, the arm mesh had moved by 6.34 [4.59] mm, and the flat mesh by 6.08 [6.80] mm. The longitudinal changes in the two groups were not statistically significant.

Overall changes in mesh topology

The part comparison analysis showed that the mesh models of the arm mesh group differed by 1.37 [0.55] mm (median [IQR]), and 3.40 [1.25] according to the RMSD and MHD metrics respectively, between 2 and 14 days after implantation. Between 14 and 60 days after implantation, they differed by 1.41 [0.31] mm (RMSD) and 4.26 [3.29] mm (MHD). Between 2 and 60 days, they differed by 1.51 [0.45] mm and 4.19 [2.46] mm according to the RMSD and the MHD metrics respectively.

For the flat mesh group, the mesh models differed by 1.40 [0.62] mm and 3.85 [3.37] according to the RMSD and MHD metrics respectively, between 2 and 14 after implantation. Between 14 and 60 days, they differed by 1.40 [0.86] mm (RMSD) and 3.66 [3.37] mm (MHD). Between 2 and 60 days, they differed by 1.21 [0.50] mm and 3.53 [1.16] mm according to the RMSD and the MHD metrics respectively. None of the part comparison measures showed statistically significant differences when comparing flat and arm meshes. These differences are also very small and to us clinically not relevant.

Effective surface area

Table 3 shows the ESA measurements of both mesh groups at the three-time points. Relative to initial implantation size (1,200 mm^2), a considerable reduction in mesh area was recorded on day 2. The ESA of arm meshes was 988.87 [152.79] mm^2 (median [IQR]), a reduction of 17.59 [6.50] %, and the ESA for flat meshes was 813.36 [135.05] mm^2, a reduction of 32.22 [7.06] %. However, this initial drop in surface area was statistically similar for both groups at that point in time. At day 14, the ESA was 873.88 [254.41] mm^2 and 697.8654 [234.09] mm^2, a change of 27.18 [20.44] % and 41.84 [14.89] % for the arm and flat mesh group respectively. Here, the differences between the two groups reached statistical

significance (p = 0.046). At day 60, the areas were 882.77 [214.42] mm^2, and 760.72 [133.50] mm^2, a change of 26.43 [14.56] % and 36.61 [6.64] % respectively for an arm and flat mesh groups, and the difference in ESA was not statistically significant. An ANOVA analysis of the ESA measurements of the two groups revealed that the temporal changes in ESA were not statistically significant.

Mesh thickness maps

Mesh thickness maps were evaluated visually to get a sense of the areas that were of higher thickness. Generally, for the arm mesh group, the common regions of high thickness were along the cranial border of the main mesh body and at the location of the mesh arms' attachment to the main body, as shown in Figure 8A. For the flat mesh group, in addition to the cranial and caudal borders, high thickness areas could also be seen in the middle of the mesh for some animals, Figure 8B.

Table 3: In vivo changes on mesh surface area as seen on MRI (median, [IQR])

	Area arm mesh main body (mm^2)	% change	Area Flat mesh (mm^2)	% change
Pre-implantation area	1200		1200	
Day2	988.87 [152.79]	17.59 [6.50]	813.36 [135.05]	32.22 [7.06]
Day 14	873.88 [254.41]	27.18 [20.44]	697.86 [234.09]	41.84 [14.89]
Day 60	882.77 [214.42]	26.43 [14.56]	760.72 [133.50]	36.61 [6.64]
Explant area	786.0 [102.2]	34.5 [8.5]	739.2 [214.42]	36.8 [77.1]
ANOVA	ns		ns	

Figure 9: *(A) shows an example thickness map of an animal in the arm mesh group and (B) shows the thickness maps of an animal in the flat mesh group. The models on the left are that of 2 days after surgery, the middle ones are at day 14 and the right ones are at 60 days after surgery. The red regions represent areas of higher relative thickness. The cranial direction is always on the top.*
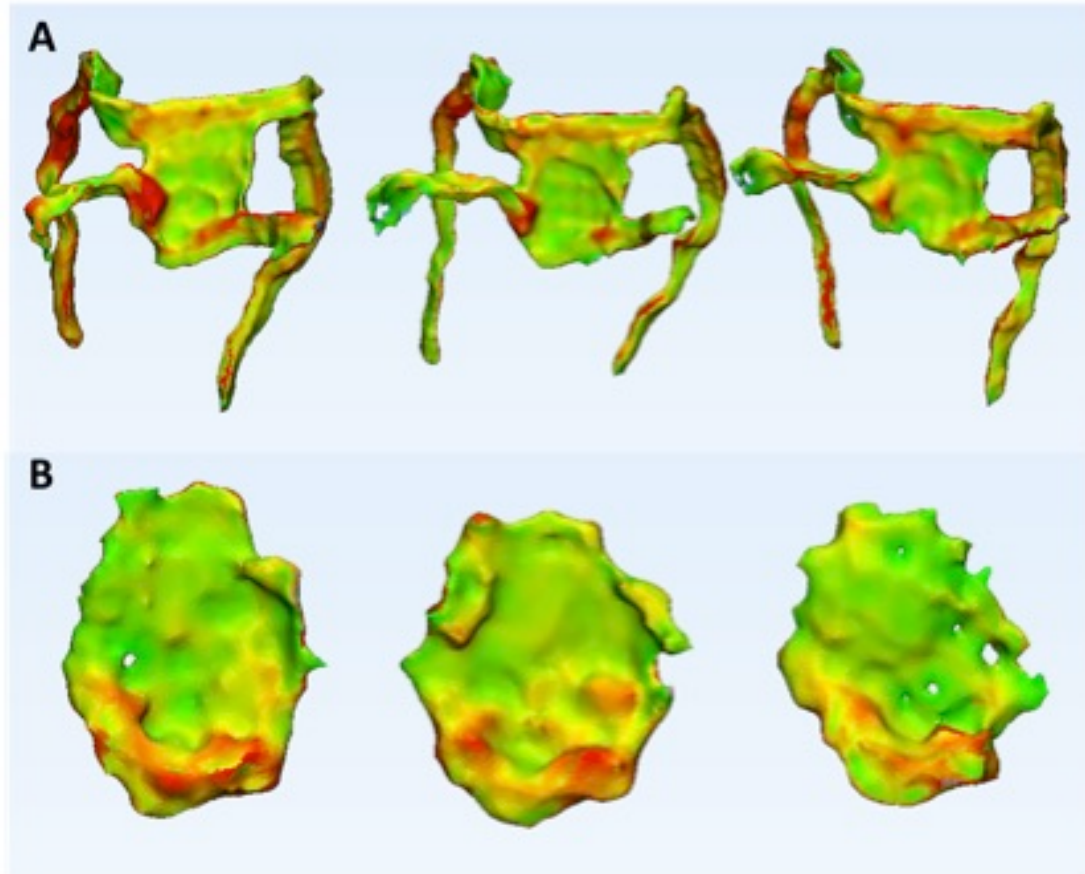
Mesh arm deformation analysis (ellipticity and length)

The lengths of the mesh arms at different time points are summarized in Table 4. The change in length of all the arms was not statistically significant upon an ANOVA analysis.

Ellipticity analysis could only be done on ventral arms, as the dorsal arms were too short to have sufficient values for comparison. Overall, the ellipticity of the arms was 0.81 [0.08] (median [IQR]). This implies that in the majority of the portion, most of the arms lay flat with the long axis of the cross-sectional ellipsoid being 70.5 % greater than the short axis. No obvious patterns could be observed in the averaged ellipticity profiles of the right and left ventral mesh arms. Figure 10 shows averaged ellipticity of the ventral left and right arms, plotted along their minimum common length.

When comparing ellipticity profiles of individual animals over time, only one arm of one animal showed significant deformation between day 14 and day 60 postoperatively (p<0.001).

Table 4: Lengths of the mesh arms at the three-time points given in Median [IQR].

	Ventral right (mm)	Ventral left (mm)	Dorsal right (mm)	Dorsal left (mm)
Pre-implantation length	115.5 [27.4]	118 .8 [5]	36.5 [14]	33.1 [11.5]
Day 2	108.29 [16.14]	103.40 [18.11]	26.17 [4.33]	28.5 [8.34]
Day 14	100.67 [10.40]	105.58 [13.04]	25.80 [2.67]	33.81 [11.38]
Day 60	101.77 [10.71]	107.17 [21.82]	28.89 [9.29]	38.15 [11.65]
Explant	97.5 [6.3]	112 [14.0]	27.5 [6.8]	31 [7.8]

Figure 10: *Ellipticity curves of the ventral left and right arms. Ellipticity value of all animals is averaged at every 0.5mm distance from the main body of the mesh. To draw longitudinal comparisons, ellipticity of the first 8cm (minimum common length) of the arms is shown.*
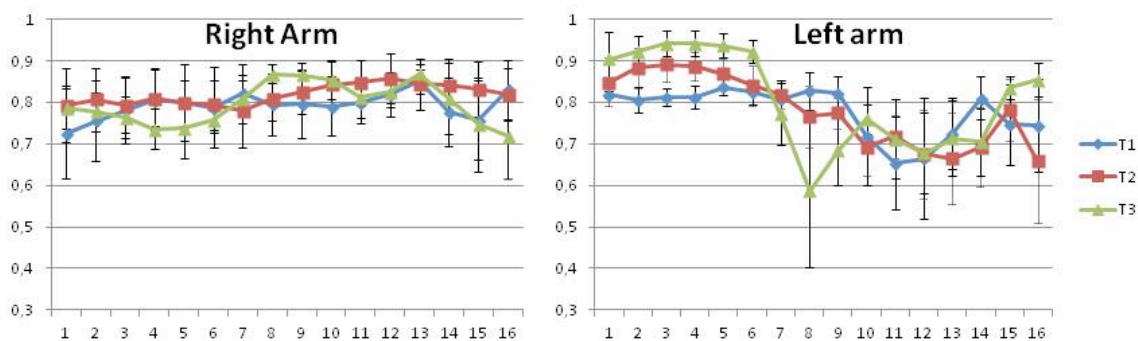
DISCUSSION

Mesh contraction or "shrinkage" is suggested to be one of the reasons for graft-related complications, mainly pain, and dyspareunia. Implant contraction in the vagina may reach up to 50% depending on the implant's size [19, 20, 32]. It is suggested that contraction may explain tenderness or tense areas below the vaginal epithelium [33]. In vivo visualization of the entire implant shape with ultrasound is limited, primarily due to lack of field of view and depth. While transvaginal probes are more useful, the method causes unintentional implant deformation and hence prevents its observation in the normative state [11, 34].

MR-visible mesh implants offer a unique opportunity to study the meshes *in-vivo.* We have previously shown that a wide variety of parameters may be derived from the three-dimensional shape of the implant [18]. Further, we have also shown that in the rabbit abdominal wall model, the mesh area may reduce by almost 17% within two days postoperatively with no further change subsequently [16]. The findings were similar in our recent experiments in the rat animal model where we attempted to find the cause of the deformation at the pore level [35]. While these earlier animal models significantly add to our understanding of the mechanisms of mesh folding and shrinkage, they do not represent the clinical scenario: they are not in the vaginal environment and the dimensions of the implants are different from that used in humans.

To our knowledge, this is the first study documenting *in vivo* longitudinal dimensional and morphological changes of synthetic implants in the vaginal environment of a large animal model. This study allowed us to test the implant in a setting much closer to that of the human.

We compared different mesh suspension techniques and their effectiveness in biomechanically supporting the underlying tissue. We used two types of mesh geometries: the flat meshes, that are fixed with interrupted sutures and the arm mesh that are suspended by anchoring them to ligamentous structures in the pelvis. Nonetheless, there was no significant migration of either of the implant throughout the observation period, indicating that both techniques prevent any significant mesh migration. The overall shape of the mesh, as observed upon part comparison analysis also did not show any clinically relevant changes over time.

The pattern of longitudinal reduction in the ESA of both mesh shapes was the same: a marked decrease immediately postoperatively, with no significant change thereafter. In this study, the flat meshes underwent an initial drop in the area of 32%, and that of arm meshes by 17%. While the flat meshes seemed to undergo a higher reduction in ESA, the difference between the groups was found to be statistically significant only at the 14-day. The mesh arms also showed no change in length over time and the ellipticity profile was different only for one animal in one arm at 60 days.

Observation of the thickness maps from the arm mesh group suggests that high thickness regions were almost always present near the ventral arms of the mesh. Further, this location of high thickness remained relatively stable over time, suggesting the presence of folding in this region. We acknowledge that since both the mesh and the air in surrounding bowels appear hypointense in MR images, we cannot completely discount the possibility that the areas of high thickness may just be segmentation errors. However, upon explantation, we could clearly see that in the arm mesh group, the arms were folded on top of the main body in 5/6 meshes. Four of these folded meshes showed high thickness in the corresponding thickness maps obtained in vivo, see Figure 11. This strongly indicates that the thickness maps are a good way to identify mesh folding in-vivo. In the flat mesh group, high thickness regions are often found around the edges and/or the corners. Unfortunately, such a pattern could not be corroborated reliably in the explants of the flat mesh group. This is likely due to the homogenous nature of pore aggregation during suturing, as we demonstrated in earlier studies [35].

Figure 11: *Left is an image of the mesh explant where the ventral mesh arm is folded onto the main body of the mesh (indicated with *). The same region shows up as a region of high relative thickness in the map on the right.*
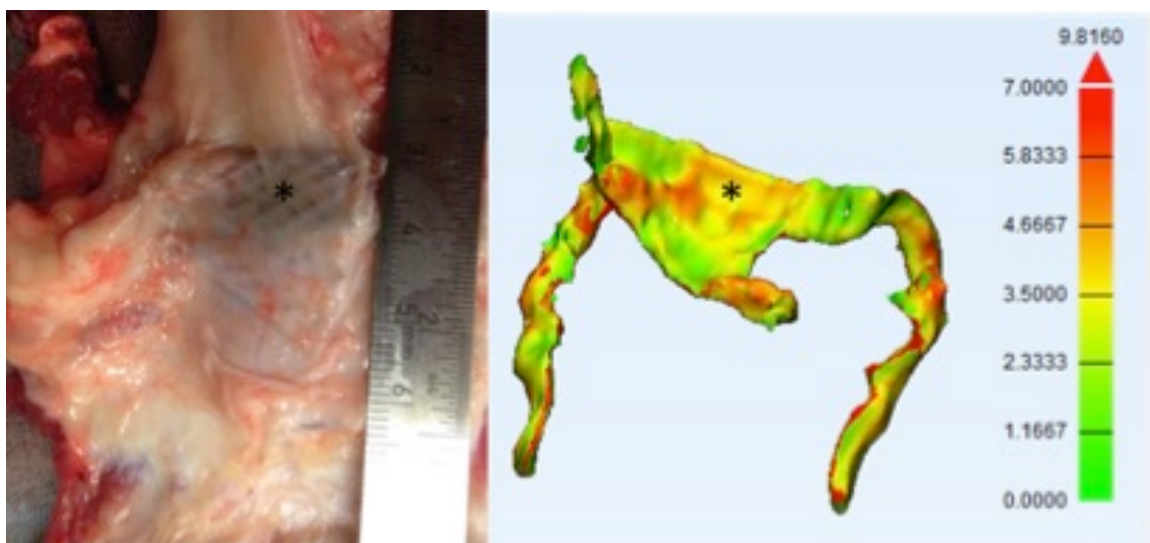
Biomechanical findings showed that the mesh tissue complex around the arms was also stiffer than that from the central part, the flat meshes, and the sham controls. Since the mesh arms were fabricated from a stiffer material than the central part or the flat meshes, this was expected. Active biomechanics tests revealed that the mesh implant did not affect contractility of the vaginal wall, as the forces generated in the explanted tissue were similar to those of controls. This is similar to our previous findings in polypropylene meshes 60-day postoperatively [32].

A limitation of our study was the small number of animals used in each group. However, our previous experiments revealed that there was little

reason to expect longitudinal changes beyond the immediate postoperative period [16, 18, 35]. Thus, it was deemed sufficient to reproduce this effect in 5 consecutive animals to discard any possibility of discrepancies in measurements. A second limitation is that we explanted meshes 60-day postoperatively, thus describing only mid-term outcome and not a longterm outcome. Especially, it would have been interesting to see if any of the animals developed mesh exposure or erosion eventually. However, such a study was not feasible due to the high housing costs. Third, we tested the active biomechanical response by performing smooth muscle contractility experiments on explants-sans-mesh. This decision was made because the complete explant is that thick that reliable in vitro contractility measurements would not be possible. Finally, we acknowledge that the mesh segmentation process may be challenging in certain cases where the recto-vaginal septum is thin and/or there is air in the bowels bordering the mesh. In this study, we verify the segmentations by two independent experienced observers.

CONCLUSION

This is a first longitudinal study observing deformations in vaginally implanted synthetic meshes in a large animal model. A novel methodology is presented to calculate the area of the vaginal tissue effectively supported by the mesh implant. Immediately post-operatively, a reduction in 32% and 17% was noted, which remained stable over the 60 following days of observation. We use thickness maps to analyze the cause of this dramatic immediate reduction. In the arm mesh, we found it to be mesh folding at the interface between the arms and central part. For the flat mesh, we suggest that pore aggregation during suturing.

Ethical approval: The experiment was approved by the Ethics Committee for Animal Experimentation of the Faculty of Medicine of the K.U. Leuven. All applicable international, national and institutional guidelines for the housing, care and use of animals were followed. Procedures performed in this study were in accordance with the ethical standards of the institution at which they were conducted.

Contribution to the authorship I Urbankova did study design, histology, surgery, MRI data collection and evaluation, data collection, evaluation and manuscript writing, Geertje Callewaert, Hympanova Lucie, Turri Alice and Andrew Feola helped with surgery, biomechanical testing, Rinkevic Rita did the biomechanical testing, Sindhwani Nikhil did the MRI data collection and evaluation and manuscript writing. Jan Deprest did study design and manuscript writing. All authors contributed to manuscript editing

REFERENCES:

1. Haylen BT, de Ridder D, Freeman RM, et al. (2009) An international urogynecological association (IUGA)/international continence society (ICS) joint report on the terminology for female pelvic floor dysfunction. Neurourol Urodyn 29:n/a-n/a. doi: 10.1002/nau.20798

2. Glazener C, Elders A, MacArthur C, et al. (2013) Childbirth and prolapse: Long-term associations with the symptoms and objective measurement of pelvic organ prolapse. BJOG An Int J Obstet Gynaecol 120:161–168. doi: 10.1111/1471-0528.12075

3. Løwenstein E, Ottesen B, Gimbel H (2014) Incidence and lifetime risk of pelvic organ prolapse surgery in Denmark from 1977 to 2009. Int Urogynecol J. doi: 10.1007/s00192-014-2413-y

4. Vanspauwen R, Seman E, Dwyer P (2010) Survey of current management of prolapse in Australia and New Zealand. Aust N Z J Obstet Gynaecol 50:262–7. doi: 10.1111/j.1479-828X.2010.01145.x

5. Jha S, Moran P (2007) National survey on the management of prolapse in the UK. Neurourol Urodyn 331:325–331. doi: 10.1002/nau

6. Lensen EJ., Withagen MI., Stoutjesdijk JA, et al. (2012) The use of synthetic mesh in vaginal prolapse surgery : a survey of Dutch urogynaecologists. Eur J Obstet Gynecol Reprod Biol 162:113–115. doi: 10.1016/j.ejogrb.2012.02.004

7. Maher C, Feiner B, Baessler K, et al. (2016) Surgery for women with apical vaginal prolapse (Review) SUMMARY OF FINDINGS FOR THE MAIN COMPARISON. Cochrane Database Syst Rev 10:CD012376. doi: 10.1002/14651858.CD012376.www.cochranelibrary.com

8. Gopinath D, Radley S (2013) Complications of polypropylene mesh in prolapse surgery: an update. Obstet Gynaecol Reprod Med 23:300–306. doi: 10.1016/j.ogrm.2013.07.001

9. Haylen BT, Freeman RM, Swift SE, et al. (2011) An International Urogynecological Association (IUGA) / International Continence Society (ICS) joint terminology and classification of the complications related directly to the insertion of prostheses (meshes , implants , tapes) & grafts in female pe. Int Urogynecol J 22:3–15. doi: 10.1007/s00192-010-1324-9

10. Guillaume O, Blanquer S, Letouzey V, et al. (2012) Permanent Polymer Coating for in vivo MRI Visualization of Tissue Reinforcement Prostheses. Macromol Biosci 12:1364–74. doi: 10.1002/mabi.201200208

11. Svabík K, Martan A, Masata J, et al. (2011) Ultrasound appearances after mesh implantation--evidence of mesh contraction or folding? Int Urogynecol J 22:529–33. doi: 10.1007/s00192-010-1308-9

12. Velemir L, Amblard J, Fatton B, et al. (2010) Transvaginal mesh repair of anterior and posterior vaginal wall prolapse: A clinical and ultrasonographic study. Ultrasound Obstet Gynecol 35:474–480. doi: 10.1002/uog.7485

13. Palma P, Riccetto C, Fraga R, et al. (2010) Dynamic evaluation of pelvic floor reconstructive surgery using radiopaque meshes and Three-dimensional helical CT. Int Braz J Urol 36:209–214. doi: 10.1590/S1677-55382010000200012

14. Conze J, Junge K, Weiss C, et al. (2008) New polymer for intra-abdominal meshes-- PVDF copolymer. J Biomed Mater Res B Appl Biomater 87:321–8. doi: 10.1002/jbm.b.31106

15. Klinge U, Klosterhalfen B, Ottinger a P, et al. (2002) PVDF as a new polymer for the construction of surgical meshes. Biomaterials 23:3487–93.

16. Endo M, Feola A, Sindhwani N, et al. (2014) Mesh contraction: in vivo documentation of changes in apparent surface area utilizing meshes visible on magnetic resonance imaging in the rabbit abdominal wall model. Int Urogynecol J 25:737–43. doi: 10.1007/s00192-013-2293-6

17. Sandaite I, Claus F, Manodoro S, et al. (2011) Experimental MRI-contrast imaging of suture and mesh materials with FE304 –containing polyvinylidenefluoride polymers designed for pelvic floor surgery. Neurourol Urodyn 30:1114–1115.

18. Sindhwani N, Feola A, De Keyzer F, et al. (2015) Three-dimensional analysis of implanted magnetic-resonance-visible meshes. Int Urogynecol J 26:1459–1465. doi: 10.1007/s00192-015-2681-1

19. Manodoro S, Endo M, Uvin P, et al. (2013) Graft-related complications and biaxial tensiometry following experimental vaginal implantation of flat mesh of variable dimensions. BJOG 120:244–50. doi: 10.1111/1471-0528.12081

20. Endo M, Urbankova I, Vlacil J, et al. (2015) Cross-linked xenogenic collagen implantation

in the sheep model for vaginal surgery. Gynecol Surg 113–122. doi: 10.1007/s10397-015-0883-7

21. Maurer MM, Röhrnbauer B, Feola a., et al. (2014) Mechanical biocompatibility of prosthetic meshes: A comprehensive protocol for mechanical characterization. J Mech Behav Biomed Mater 40:42–58. doi: 10.1016/j.jmbbm.2014.08.005

22. Urbankova I, Vdoviakova K, Rynkevic R, et al. (2016) Comparative anatomy of the ovine and female pelvis. Gynecol Obstet Invest. doi: 10.1159/000454771

23. Reisenauer C, Kirschniak A, Drews U, Wallwiener D (2007) Anatomical conditions for pelvic floor reconstruction with polypropylene implant and its application for the treatment of vaginal prolapse. Eur J Obstet Gynecol Reprod Biol 131:214–225. doi: 10.1016/j.ejogrb.2006.03.020

24. Carey M, Higgs P, Goh J, et al. (2009) Vaginal repair with mesh versus colporrhaphy for prolapse: A randomised controlled trial. BJOG An Int J Obstet Gynaecol 116:1380–1386. doi: 10.1111/j.1471-0528.2009.02254.x

25. Urbankova I, Callewaert G, Sindhwani N, et al. (2017) Transvaginal mesh insertion in the ovine model. J Vis Exp accepted.

26. Chen Y, Medioni G (1991) Object modeling by registration of multiple range images. Proceedings 1991 IEEE Int Conf Robot Autom 2724–2729. doi: 10.1109/ROBOT.1991.132043

27. (2016) Iterative Closest Point - File Exchange - MATLAB Central. Mathworks.com

28. Hyndman RJ, Koehler AB (2006) Another look at measures of forecast accuracy. Int J Forecast 22:679–688. doi: 10.1016/j.ijforecast.2006.03.001

29. Dubuisson M-P, Jain a. K (1994) A modified Hausdorff distance for object matching. Proc 12th Int Conf Pattern Recognit 1:566–568. doi: 10.1109/ICPR.1994.576361

30. (2015) Modified Hausdorff Distance - File Exchange - MATLAB Central. Mathworks.com

31. Feola A, Moalli P, Alperin M, et al. (2011) Impact of pregnancy and vaginal delivery on the passive and active mechanics of the rat vagina. Ann Biomed Eng 39:549–58. doi: 10.1007/s10439-010-0153-9

32. Feola A, Endo M, Urbankova I, et al. (2015) Host reaction to vaginally inserted collagen containing polypropylene implants in sheep. Am J Obstet Gynecol 212:474.e1-474.e8. doi: 10.1016/j.ajog.2014.11.008

33. Feiner B, Maher C (2010) Vaginal Mesh Contraction. Definition, Clinical Presentation and Management. Obstet Gynecol 115:325–330.

34. Eisenberg VH, Steinberg M, Weiner Z, et al. (2014) Three-dimensional transperineal ultrasound for imaging mesh implants following sacrocolpopexy. Ultrasound Obstet Gynecol 43:459–465. doi: 10.1002/uog.13303

35. Sindhwani N, Liaquat Z, Urbankova I, et al. (2015) Immediate postoperative changes in synthetic meshes – In vivo measurements. J Mech Behav Biomed Mater 55:228–235. doi: 10.1016/j.jmbbm.2015.10.015

GENERAL DISCUSSION

In the clinical part of this thesis we performed a prospective cohort study, documenting the occurrence of, and the major risk factors for pelvic floor dysfunction among primiparous women one year after delivery. In the wider framework of this thesis, we were in particular interested in the occurrence of Pelvic Organ Prolapse (POP). POP is just one clinical entity out of different bothersome pelvic floor dysfunction (PFD) women may report. According to the lifespan model from DeLancey, POP, or any PFD, are more likely in genetically predisposed women, in women who have given vaginal birth, to which later in life other risk factors such as age, obesity and a variety of medical conditions, may add [1]. The relationship between pregnancy, labor and vaginal delivery on the one hand, and POP (or in the wider sense: PFD) is a complex one. Next, to their generic effect, there are certain maternal characteristics, the nature of labor and the fetal weight which play an important role in the occurrence of PFD after vaginal delivery[2].

For years, physicians and researchers search for preventive approaches before and at the time of delivery, and for long-lasting treatment solutions for women who had developed POP. The most important risk factors are forceps and normal vaginal delivery. The obstetrical practice has changed with a decreased use of mid-pelvic forceps to the advantage of vacuum extraction, which is more friendly to pelvic floor structures [3]. However, other factors such as maternal at first delivery age, the longer life expectancy, and higher patient demands are as important. Currently available conservative and surgical interventions do not meet all clinical and patient expectations.

In the clinical part, we aimed to contribute to the identification of demographical and obstetrical risk factors for PFD development at one year postpartum. To do so, we set up an unselected cohort of women giving their first singleton delivery in one of the largest delivery units in Prague, Czech Republic (Chapter 2). During the observation period, women underwent three consecutive urogynecological assessments, including clinical examination, transperineal ultrasound and subjective evaluation of pelvic floor function. We used a uni- and multivariate regression analysis to determine delivery related risk factors for the development pelvic floor dysfunction 1-year after delivery. The entire cohort included 987 women, whose average age was 30.8 ± 3.5. One-year postpartum women reported UI, AI, and dyspareunia in 31.8%, 1%, and 17% respectively. Since we did not include subjective evaluation of pelvic POP, we used observations of others who have shown that symptomatic is usually prolapsed reaching the level of the hymen and beyond (POPII+) [4]. POP II was identified in 57% of women of which 23% had POP II+. Risk factors for UI and POPII+ similarly included maternal age. For each additional year, women were 9% and 8% more likely to report UI and POPII+, respectively. AI was not investigated due to its low occurrence.

Regression analysis was used to determine delivery related risk factors for levator ani avulsion and over-distension (ballooning). LAM injuries are increasing the risk for UI, POP and recurrent POP [5]. Similarly to others, we

identified forceps delivery as a risk factor for avulsion and maternal age and initial BMI for ballooning. Two other factors were identified yet with surprisingly opposite effects. Epidural analgesia and perineal rupture grade I decreased the likelihood of avulsion but increased it of ballooning. These effects could be explained by on the one hand a relaxation effect on the pelvic floor of the anesthesia, and that is less prone to be injured yet also not protected against muscular over distension [6].

In the experimental part of the thesis work we first studied the effects of a selection of the lifespan events on the ovine pelvic floor. Animal models are important tools in translational research; this is also the case for the study of pelvic floor function. Several animal models to study the pathogenesis of PFD, the effects of pregnancy, labor and delivery or for corrective surgery have been proposed. As we aimed also for a model usable for the study of surgical solutions for POP, large animal models seemed the only suitable option. We discussed the pros and cons of rabbits and primates in the introduction. Yet for vaginal surgery, the rabbit is too small, and to our knowledge, vaginal surgery has not been described in primates [7]. Sheep seem a suitable alternative. They are widely available, relatively easy to handle and there are less financial and ethical constraints than with nonhuman primates [7]. The Zootechnical Center at the KU Leuven has a breeding program with different sheep strains so that we have permanent access to them for long-term experimentation. Their size, their pelvic anatomy, and inner vaginal environment are sufficiently similar to human [8–10]. Encouraged by the work of De Tayrac [11] we first started using them for the study of vaginal mesh insertion in 2011 [12]. In this thesis, we started filling up the gap in our knowledge of the model. We first characterized pelvic floor anatomy and then studied the effects of those events during their lifespan, that are relevant to their pelvic floor function, such as vaginal delivery and menopause[1].

In Chapter 3, we performed a comparative anatomical study of the ovine and female pelvis. We identified those differences that we needed to take into account while attempting to translate observations to the clinical setting (Chapter 3). The obvious difference in pelvic orientation and the presence of a functional tail has its consequences to the pelvic floor and its physiological loads. Pelvic floor muscles participate in tail movement and retraction of the anus. This seems the reason why the iliococcygeus muscle is much more developed than in women. Sheep have similar attachment points of the LAM, similar vaginal dimensions, and a rectovaginal septum, as present in women. Moreover, histologically the vaginal wall is composed of comparable layers, including the stratified squamous epithelium, lamina propria, and lamina muscularis with two layers of smooth muscles. We demonstrated the presence of estrogen receptors in the vagina, yet not in the urethra, bladder or anal sphincters of reproductive sheep. Again, their vaginal dimensions are sufficient for transvaginal surgery and at the same time they provide sufficient tissue to perform a wide range of histological and biomechanical tests [11–13]. Concomitantly, abdominal implantation can be performed to obtain control samples from an anatomically and biomechanically different environment [12, 13]. For future studies, it may be

important to remember that sheep do not have a sacrospinous ligament, an obturator membrane or internal obturator muscle. It is encouraging to see that other teams also have been using the model for urogynaecological studies and surgical training [14, 15].

In Chapter 4 we studied the effect of vaginal delivery, surgical menopause and hormonal replacement therapy on morphological and biomechanical properties of the vaginal wall. One year after the first delivery, the distal ovine vagina was more spacious, more compliant and smooth muscles generated less contractile forces. These changes to a certain extent follow the clinical observations yet the formal comparison is not possible due to lacking data from women. To simulate menopause, ovariectomy was performed and estrogen replacement therapy (HRT) was used to reverse those changes. Estrogen deficit resulted in an increase of estrogen receptor-α, thinning of the vaginal epithelium with the absence of glycogen. HRT restored the presence of glycogen and epithelial thickness, yet also significantly increased mid-vaginal compliance. Obviously, "surgical menopause" in chronologically younger sheep than those naturally going into menopause may not have the same effect on genital tract function, as is the case in women [16]. It would be appropriate to compare at some stage these observations to normally cycling sheep and to very old ones. We did not do so, as we do not have access to that type of sheep. Sheep are usually sacrificed once they near the end of their natural reproductive life. Anyway, we have meanwhile gone on with using this model for the experimental evaluation of laser energy in the treatment of genito-urinary syndrome (Hympanova et al., unpublished).

When comparing primiparous and ovariectomized sheep we observed a large difference in tissue stiffness and smooth muscle contractility. The current literature suggests that menopausal aged women have indeed stiffer vaginal wall compared to the younger ones, underscoring the relevance of the model [17, 18]. On the other hand, we can at this stage only speculate if this was because of their high parity, the effect of aging or estrogen depletion [19]. We also studied the histological changes, mainly in an effort to understand if those microstructural changes would explain changes in the stiffness. The correlation between gross anatomy and tissue biomechanics and ultrastructure is however complex.

Soft tissues (i.e.in this case, the vaginal wall) are interconnected 3D networks composed of cells attached to the extracellular matrix (ECM). In the vagina, the most abundant component is collagen that forms a multi-directional system of fibers to which elastin, proteoglycans, hyaluronic acid and other molecules are attached. The biomechanical behavior is a result of their proportions and interplay. Several studies have described either collagen or elastin as the responsible component [20–23]. However, tissue hydration, temperature or load direction may significantly interfere with results [24]. The biomechanical testing in most of the studies is a uniaxial tensiometry, which is easier to describe than a multi-directional load during the ball burst test, which, on the other side, represents more the loads applied on the vaginal wall [25, 26].

Finding the relationship between the tissue composition and biomechanics may require more complex and sensitive evaluation including i.e. collagen alignment or biochemistry.

Given the sufficient similarities, we proceeded to experimental vaginal surgery. We used the model in two experimental studies with the acellular collagen matrices (Chapter 5) and polyvinidylene meshes (Chapter 6 and 7). In Chapter 5 we evaluated a newly designed acellular xenogenic graft manufactured from cross-linked bovine pericardium (ACM) that was inserted in the rectovaginal septum and in the abdominal wall. In that study, we used a commercially available polypropylene mesh (PP) as a reference, i.e. Avaulta Solo™ (dry weight 56 g/m^2, Bard medical). Xenografts have been proposed as an alternative to PP because they would be better compatible [27, 28]. Bovine pericardium has been clinically used in the field of cardiac surgery in children with congenital heart defects [28]. Unfortunately, during follow-up and explanation, we observed more graft-related complications, including exposure, local induration or infection. Additional histology revealed calcification of exposed grafts and severe inflammation. However, there was actually more calcification in the abdominal grafts, in the absence of exposure and a milder inflammation. Therefore the correlation between macroscopic gross anatomical findings and histology is not strict, yet calcification would seem to be an undesirable process in a vaginal environment. These calcifications were also not expected. Though these ACM matrices were cross-linked with formaldehyde, which is known for causing this, yet they were also treated with a specific anti-calcification procedure called ADAPT, which worked apparently in cardiac surgery patients [29, 30].

Vaginal implantation is associated with faster graft degradation, which confirms the relevance of using a vaginal surgery model. In our hands the number of local complications with this PP mesh was minimal. Vaginal ACM explants had a comparable stiffness and smooth muscle contractility as PP explants, yet once the ACM got completely degraded, the smooth muscle contractility was significantly decreased. Similar observations were made on PP implants with two different types of collagen coating [13]. We speculated that the negative impact of ACM matrix reabsorption on smooth muscle contractility could be (partially) explained by stress shielding [31, 32].

In that paper, however, we failed to compare the biomechanics of the explant to that of native tissues. Though the experiment did not include such a group, we previously have done so in another study using the same PP mesh (Avaulta Solo) and two PP meshes with different types of collagen (Avaulta Plus, Bard, PP with cross-linked collagen sheet derived from porcine dermis; Ugytex, Sofradim, PP coated with atelocollagen). Passive biomechanics of vaginal explants with meshes were comparable among each other, but all were stiffer than native tissue. Once the collagen was resorbed, the forces generated by vaginal smooth muscle activity was 90% below that of native tissue [33]. Since in this experiment; the ACM had comparable properties to that of Avaulta Solo, we would presume that anyway ACM explants were stiffer than native tissue

The conclusion from that particular preclinical experiment was that this graft would not be ideal for clinical use. The unpredictable and heterogeneous graft degradation was previously reported for other cross-linked acellular collagen grafts [34, 35]. Though cross-linked, degradation is theoretically not avoidable, and the degree of reabsorption seems to be dependent on the anatomical location, hence that would not be predictable either by the manufacturer [36]. Again, we observed location specific host responses, yet we did not dwell very deep into the mechanisms and processes behind these observations. This might be food for further research, and actually is relevant – as many of the implants used in vaginal surgery are identical or comparable to meshes used in hernia surgery or abdominal wall reconstruction.

Moreover, the old dream that a biomatrix will be gradually replaced by newly created connective tissue that will be sufficiently strong and compliant ("constructive remodeling" [34]) does not seem achievable with this product. We have earlier made that conclusion for other biometrics in other models [34]. Actually, we confirmed the experimental observations, i.e. in a clinical setup, when we observed a higher recurrence rate and graft-related complications in sacrocolpopexy with a Pelvicol (CR Bard, Covington, GA, USA) [37]. Pelvicol is made from the porcine dermis and is a cross-linked ACM [38].

In clinical practice, "flat" implants are not much used in vaginal POP surgery. Usually, meshes are anchored to anatomical fixation points, both to prevent them from moving, yet also to give a certain degree of suspension, ideally without creating tension. Therefore we had to find the anatomical planes and structures to mimic clinical procedures (Chapter 6). Our approach followed the insertion technique used for Prolift® implant, though today this particular implant is not anymore in clinical use because the manufacturer withdrew it from the market [39, 40]. However, the use of vaginal mesh, needles and/or anchoring devices has not been completely abandoned, so the model would stay relevant for training purposes [41–44]. Also, many women were operated with these reconstruction techniques and such animal model may help to understand the genesis of complications. So we performed trocar guided insertion of a purposely designed transvaginal H-shaped implant to fit the ovine pelvic dimensions. It has two pairs of arms; one pair (cranial) to be anchored through the obturator foramen and muscles on the medial side of the thigh. The second pair (caudal) was placed in close proximity of the broad sacrotuberous ligament. In a small feasibility study, we did not identify any major complication, bleeding, bowel or nerve injury. In one animal the cranial arm punctured the caudal part of the cul-de-sac, therefore in other animals, we guided the trocar more laterally to prevent this. We concluded that this experimental surgical procedure was safe enough to be carried out in more animals in a longitudinal observational study designed for other purposes; while the model could also be used for training vaginal mesh insertion [44]. Two more studies were meanwhile published using a sheep as a training model for transvaginal surgery, supporting that most clinically performed procedures are feasible [14, 15].

In Chapter 7 we report on the in vivo behavior of implants, either inserted as a flat mesh secured with interrupted non-resorbable sutures, or as an H-shaped, anchored mesh, both reinforcing the rectovaginal septum. Mesh visualization may help in understanding the in vivo behavior of mesh as well as it may help in the understanding why graft-related complications occur [45]. In this experiment, visualization of implants on MR permitted longitudinal observations. We reconstructed their in vivo shape, thickness and position. Following a dramatic initial drop in the apparent surface area, none of the implants showed further progressive area reduction or graft migration. This was in line with similar observations in another animal model for abdominal wall reconstruction [46]. We have meanwhile made comparable observations in women undergoing sacrocolpopexy (Sindhwani, unpublished observations; thesis submitted). Thickness mapping revealed areas suspected of folding or major deformation that was confirmed during dissection. The arm anchored meshes displayed an almost a uniform deformation pattern. The cranial or the caudal arms which were made from different material got folded above or below the central part of the construct, probably due to a biomechanical mismatch between them. Anyway, also the flat rectangular mesh showed heterogeneous patterns of deformation and therefore it was almost impossible to predict it based on the MR constructed models. One possible reason for effective area reduction of the flat meshes is pore aggregation due to suturing. This is a process where multiple pores are caught within the same not, hence locally contracting the mesh at the time of implantation. It would seem that the degree of contraction caused by this process is much larger than what is caused by mesh contraction at the pore level. We studied the latter process in rats, using similar flat meshes. We demonstrated that pore contraction is a limited process, that cannot explain the mesh dimensional changes at the macroscale [47, 48]. Again, we have used this technology in clinical studies in women undergoing sacrocolpopexy (Sindhwani, doctoral thesis, submitted 2017; Callewaert, doctoral thesis, final work plan approved 2017).

Apart from polyvinidylene meshes, iron particles have been also used to visualize polypropylene implants for POP [49, 50]. A phantom study has shown that the implant is visible with a negative contrast [50]. Later, during a small clinical study, a similar type of polypropylene implant was used for transvaginal correction of recurrent cystocele. MR 3D reconstruction allowed visualization of the implant and adjacent organs [50]. Hopefully, this approach will help to improve the treatment of women having POP and understanding to graft-related complications.

FUTURE PERSPECTIVES

In terms of the sheep model our immediate future research is characterizing the vaginal wall properties in the missing lifespan stages i.e. juvenile and multiparous sheep, and when finances allow, sheep at advanced non-reproductive age. It would be also useful to describe in detail the (peri)vaginal tissue metabolism and biochemistry to understand differences between the female and ovine vagina, or between the vaginal tissues of ewes at different stages of the lifespan. This information could be useful to define the (patho)physiologic processes induced by aging, vaginal delivery or hormone replacement. Again, we are now using it for testing novel implants that are based on a non-textile, yet electrospun matrix that mimics better the ECM, and that is made of a degradable polymer (Hympanova, final doctoral work plan submitted 10/2017). Though vaginal meshes have become nearly discredited, their use most likely cannot be completely banned [51], yet indeed any novel development in this field should be preceded by proper preclinical evaluation [52]. This will avoid the timely identification of an increased risk for complications or, more likely, materials that are not able to prevent recurrence or compromise normal tissue compliance. Another application in our lab is the evaluation of newly emerging therapies such as laser rejuvenation (Hympanova) or stem cell therapy (Bia Mori, preliminary doctoral plan accepted 2016).

REFERENCES:

1. DeLancey JOL, Kane Low L, Miller JM, et al. (2008) Graphic integration of causal factors of pelvic floor disorders: an integrated life span model. Am J Obstet Gynecol 199:610.e1-5. doi: 10.1016/j.ajog.2008.04.001

2. Gyhagen M, Åkervall S, Milsom I (2015) Clustering of pelvic floor disorders 20 years after one vaginal or one cesarean birth. Int Urogynecol J. doi: 10.1007/s00192-015-2663-3

3. Memon HU, Blomquist JL, Dietz HP, et al. (2015) Comparison of levator ani muscle avulsion injury after forceps-assisted and vacuum-assisted vaginal childbirth. Obstet Gynecol 125:1080–7. doi: 10.1097/AOG.0000000000000825

4. Wiederoder M Mike Wiederoder.

5. Dietz HP, Chantarasorn V, Shek KL (2010) Levator avulsion is a risk factor for cystocele recurrence. Ultrasound Obstet Gynecol 36:76–80. doi: 10.1002/uog.7678

6. Jangö H, Langhoff-Roos J, Rosthøj S, Sakse A (2014) Modifiable risk factors of obstetric anal sphincter injury in primiparous women: A population-based cohort study. Am J Obstet Gynecol 210:59.e1-59.e6. doi: 10.1016/j.ajog.2013.08.043

7. Couri B, Lenis A, Borazjani A, et al. (2012) Animal models of female pelvic organ prolapse: lessons learned. Expert Rev Obs Gynecol 7:249–260. doi: 10.1586/eog.12.24.Animal

8. Vincent KL, Bourne N, Bell AB, et al. (2009) High resolution imaging of epithelial injury in the sheep cervicovaginal tract: a promising model for testing safety of candidate micorobicedes. Sex Transm Dis 36:312–318. doi: 10.1097/OLQ.0b013e31819496e4.HIGH

9. Vincent KL, Vargas G, Wei J, et al. (2013) Monitoring vaginal epithelial thickness changes noninvasively in sheep using optical coherence tomography. Am J Obstet Gynecol 208:282.e1-282.e7. doi: 10.1016/j.ajog.2013.01.025

10. Krause H, Goh J (2009) Sheep and rabbit genital tracts and abdominal wall as an implantation model for the study of surgical mesh. J Obstet Gynaecol Res 35:219–224. doi: 10.1111/j.1447-07562008.00930.x

11. de Tayrac R, Alves A, Thérin M (2007) Collagen-coated vs noncoated low-weight polypropylene meshes in a sheep model for vaginal surgery. A pilot study. Int Urogynecol J Pelvic Floor Dysfunct 18:513–20. doi: 10.1007/s00192-006-0176-9

12. Manodoro S, Endo M, Uvin P, et al. (2013) Graft-related complications and biaxial tensiometry following experimental vaginal implantation of flat mesh of variable dimensions. BJOG 120:244–50. doi: 10.1111/1471-0528.12081

13. Feola A, Endo M, Urbankova I, et al. (2015) Host reaction to vaginally inserted collagen containing polypropylene implants in sheep. Am J Obstet Gynecol 212:474.e1-474.e8. doi: 10.1016/j.ajog.2014.11.008

14. Kerbage Y, Giraudet G, Rubod C, et al. (2017) Feasibility and benefits of the ewe as a model for vaginal surgery training. Int Urogynecol J 1–5. doi: 10.1007/s00192-017-3313-8

15. B. R, A. M, S. CC-L, et al. (2015) Development of an animal model-ewe- for training in vaginal surgery for pelvic organ prolapse. Gynecol Surg 12:S74. doi: 10.1007/s00192-017-3292-9

16. Shuster L, Gostout B, Grossardt B, Rooca W a. (2009) Prophylactic oophorectomy in pre-menopausal women and long term health - a review. NIH Public Access 14:111–116. doi: 10.1258/mi.2008.008016.Prophylactic

17. Chantereau P, Brieu M, Kammal M, et al. (2014) Mechanical properties of pelvic soft tissue of young women and impact of aging. Int Urogynecol J 25:1547–53. doi: 10.1007/s00192-014-2439-1

18. Gandhi J, Chen A, Dagur G, et al. (2016) Genitourinary syndrome of menopause: evaluation, sequelae, and management. Am J Obstet Gynecol 1–8. doi: 10.1016/j.ajog.2016.07.045

19. Rizk DEE, Fahim M a. (2008) Ageing of the female pelvic floor: Towards treatment a la carte of the "geripause." Int Urogynecol J Pelvic Floor Dysfunct 19:455–458. doi: 10.1007/s00192-008-0576-0

20. Rynkevic R, Martins P, Hympanova L, et al. (2017) Biomechanical and morphological properties of the multiparous ovine vagina and effect of subsequent pregnancy. J Biomech 57:94–102. doi: 10.1016/j.jbiomech.2017.03.023

21. Fallah A, Ahmadian MT, Firozbakhsh K, Aghdam MM (2016) Micromechanics and constitutive modeling of connective soft tissues. J Mech Behav Biomed Mater 60:157–176. doi: 10.1016/j.jmbbm.2015.12.029

22. Green EM, Mansfield JC, Bell JS, Winlove CP (2014) The structure and micromechanics of elastic tissue. Interface Focus 4:20130058. doi: 10.1098/rsfs.2013.0058

23. Landsheere L De, Brieu M, Blacher S, et al. (2015) Elastin density : Link between histological and biomechanical properties of vaginal tissue in women with pelvic organ prolapse ? doi: 10.1007/s00192-015-2901-8

24. Rubod C, Boukerrou M, Brieu M, et al. (2007) Biomechanical properties of vaginal tissue. Part 1: new experimental protocol. J Urol 178:320–5; discussion 325. doi: 10.1016/j.juro.2007.03.040

25. Feola AJ (2011) Impact of Vaginal Synthetic Prolapse Meshes on the Mechanics.

26. Feola A, Barone W, Moalli P, Abramowitch S (2012) Characterizing the ex vivo textile and structural properties of synthetic prolapse mesh products. Int Urogynecol J 1–6. doi: 10.1007/s00192-012-1901-1

27. Neethling WML, Yadav S, Hodge AJ, Glancy R (2008) Enhanced biostability and biocompatibility of decellularized bovine pericardium, crosslinked with an ultra-low concentration monomeric aldehyde

and treated with ADAPT. J Heart Valve Dis 17:456–63.

28. Neethling WML, Strange G, Firth L, Smit FE (2013) Evaluation of a tissue-engineered bovine pericardial patch in paediatric patients with congenital cardiac anomalies: initial experience with the ADAPT-treated CardioCel(R) patch. Interact Cardiovasc Thorac Surg 17:698–702. doi: 10.1093/icvts/ivt268

29. van den Heever JJ, Neethling WML, Smit FE, et al. (2013) The effect of different treatment modalities on the calcification potential and cross-linking stability of bovine pericardium. Cell Tissue Bank 14:53–63. doi: 10.1007/s10561-012-9299-z

30. Neethling WML, Glancy R, Hodge AJ (2010) Mitigation of calcification and cytotoxicity of a glutaraldehyde-preserved bovine pericardial matrix: improved biocompatibility after extended implantation in the subcutaneous rat model. J Heart Valve Dis 19:778–85.

31. Feola A, Abramowitch S, Jallah Z, et al. (2013) Deterioration in biomechanical properties of the vagina following implantation of a high-stiffness prolapse mesh. BJOG 120:224–32. doi: 10.1111/1471-0528.12077.

32. Liang R, Abramowitch S, Knight K, et al. (2013) Vaginal degeneration following implantation of synthetic mesh with increased stiffness. BJOG An Int J Obstet Gynaecol 120:233–243. doi: 10.1111/1471-0528.12085

33. Feola A, Endo M, Urbankova I, et al. (2015) Host reaction to vaginally inserted collagen containing polypropylene implants in sheep. Am J Obstet Gynecol 212:474.e1-474.e8. doi: 10.1016/j.ajog.2014.11.008

34. Claerhout F, Verbist G, Verbeken E, et al. (2008) Fate of collagen-based implants used in pelvic floor surgery: A 2-year follow-up study in a rabbit model. Am J Obstet Gynecol 198:94.e1-94.e6.

35. Pierce LM, Rao A, Baumann SS, et al. (2009) Long-term histologic response to synthetic and biologic graft materials implanted in the vagina and abdomen of a rabbit model. Am J Obstet Gynecol 200:546.e1-8. doi: 10.1016/j.ajog.2008.12.040

36. Pierce LM, Grunlan MA, Hou Y, et al. (2009) Biomechanical properties of synthetic and biologic graft materials following long-term implantation in the rabbit abdomen and vagina. Am J Obstet Gynecol 200:549.e1-8. doi: 10.1016/j.ajog.2008.12.041

37. Deprest J, Klosterhalfen B, Schreurs A, et al. (2010) Clinicopathological study of patients requiring reintervention after sacrocolpopexy with xenogenic acellular collagen grafts. J Urol 183:2249–55. doi: 10.1016/j.juro.2010.02.008

38. Herschorn S (2004) The use of biological and synthetic materials in vaginal surgery for prolapse. Rev Urol 17:S2–S10. doi: 10.1097/MOU.0b013e3282f10a2b

39. Koski ME, Rovner ES (2014) Implications of the FDA Statement on Transvaginal Placement of Mesh : The Aftermath. Curr Urol Rep 15:13–17. doi: 10.1007/s11934-013-0380-3

40. Delorme E, Spinosa JP, Riederer BM (2011) New Techniques in Genital Prolapse Surgery. 137–145. doi: 10.1007/978-1-84882-136-1

41. FDA (2011) UPDATE on Serious Complications Associated with Transvaginal Placement of Surgical Mesh for Pelvic Organ Prolapse: FDA Safety Communication.

42. FDA (2011) Urogynecologic Surgical Mesh : Update on the Safety and Effectiveness of Transvaginal Placement for Pelvic Organ Prolapse. Rev. Lit. Arts Am.

43. FDA (2008) Serious complications associated with transvaginal placement of surgical mesh in repair of pelvic organ and stress urinary incontinence. U.S. Food Drug Adm.

44. Riccetto CLZ, Palma PCR, Thiel M, et al. (2007) Experimental animal model for training transobturator and retropubic sling techniques. Urol Int 78:130–4. doi: 10.1159/000098070

45. Svabík K, Martan A, Masata J, et al. (2011) Ultrasound appearances after mesh implantation--evidence of mesh contraction or folding? Int Urogynecol J 22:529–33. doi: 10.1007/s00192-010-1308-9

46. Sindhwani N, Liaquat Z, Urbankova I, et al. (2015) Immediate postoperative changes in synthetic meshes – In vivo measurements. J Mech Behav Biomed Mater 55:228–235. doi: 10.1016/j.jmbbm.2015.10.015

47. Sindhwani N, Feola A, De Keyzer F, et al. (2015) Three-dimensional analysis of implanted magnetic-resonance-visible meshes. Int Urogynecol J 26:1459–1465. doi: 10.1007/s00192-015-2681-1

48. Sindhwani N, Liaquat Z, Urbankova I, et al. (2015) Immediate postoperative changes in synthetic meshes - In vivo measurements. J Mech Behav Biomed Mater 55:228–235. doi: 10.1016/j.jmbbm.2015.10.015

49. Chen L, Lenz F, Alt CD, et al. (2017) MRI visible Fe3O4 polypropylene mesh: 3D reconstruction of spatial relation to bony pelvis and neurovascular structures. Int Urogynecol J 28:1131–1138. doi: 10.1007/s00192-017-3263-1

50. Brocker KA, Lippus F, Alt CD, et al. (2015) Magnetic resonance-visible polypropylene mesh for pelvic organ prolapse repair. Gynecol Obstet Invest 79:101–106. doi: 10.1159/000366442

51. Deprest J, Feola a. (2013) The need for preclinical research on pelvic floor reconstruction. BJOG An Int J Obstet Gynaecol 120:141–143. doi: 10.1111/1471-0528.12088

52. Slack M, Ostergard D, Cervigni M, Deprest J (2012) A standardized description of graft-containing meshes and recommended steps before the introduction of medical devices for prolapse surgery. Consensus of the 2nd IUGA Grafts Roundtable: optimizing safety and appropriateness of graft use

in transvaginal pe. Int Urogynecol J 23 Suppl 1:S15-26. doi: 10.1007/s00192-012-1678-2

SUMMARY

Pelvic organ prolapse is a bothersome condition defined as the abnormal descent of pelvic organs through the vaginal opening. The main risk factors are vaginal delivery and age. We aimed to use modern assessment tools to study selected risk factors related to the development of pelvic organ prolapse in a clinical setting as well as in an experimental model. We performed a clinical study, in which we tried to define the weight of certain risk factors for the later development of pelvic organ prolapse and other pelvic floor dysfunction. In a second, more extensive part, we did experimental studies dedicated to the characterization of a large animal model for the development of pelvic organ prolapse and for its vaginal surgical condition, i.e. the ewe.

The clinical study was conducted in Prague, Czech Republic, and included a cohort of 987 nulliparous women who delivered vaginally. One year after delivery one-third of women reported urinary incontinence, 13% had pelvic organ prolapse reaching down to the level of hymen or beyond and 3.3% reported anorectal dysfunction mainly painful defecation. Following their first delivery, 18% of women sustained levator ani avulsion and 17% had levator hiatus ballooning. Both have been named to be closely related to the further development of symptomatic pelvic organ prolapse and its recurrence after surgical correction. In our study, also age and body mass index increased the likelihood of urinary incontinence, whereas age also increased the risk for pelvic organ prolapse. Risk factors for levator ani avulsion included forceps delivery, whereas epidural analgesia and perineal rupture grade I were 'protective'.

In the sheep model, we first characterized the pelvic floor anatomy of the virgin ewe and compared it to that of women. Second, we documented the effects of certain key lifespan events such as the first delivery, menopause and the changes after hormone replacement therapy. We identified many anatomical and structural similarities such as vaginal dimensions, the composition of the vaginal wall, and the attachments of levator ani muscle. Some anatomical structures present in women are not developed in sheep (i.e. the sacrospinous ligament, internal obturator muscle and obturator membrane) and their pelvic floor anatomy seems to be adapted to their quadruped position and presence of a tail. We demonstrated the effects of specific lifespan events (first vaginal delivery, ovariectomy, hormonal replacement therapy) on active and passive biomechanical properties of the ovine vagina. Following first vaginal delivery, the ovine vagina became more spacious, its distal part becomes less stiff and smooth muscles generate lower contractile forces. Following artificially induced menopause the ovine vagina was narrower and its middle part becomes stiffer. Estradiol hormonal replacement returned the stiffness within the range of the premenopausal animal. Histology showed only a limited amount of changes, comparable to those seen in women, yet to us, these do not sufficiently explain the biomechanical changes.

The experimental work was also dedicated to the study of the effect of novel implants in the treatment of pelvic organ prolapse. In a comparative study, we used a bovine-derived acellular cross-linked collagen matrix (ACM) suggested as an alternative to polypropylene "flat" meshes. Both types of implants were inserted in the ovine rectovaginal septum. After 6 months, ACMs showed more local graft-related complications and biomechanical properties comparable to polypropylene. Moreover, partial degradation of ACM had a negative impact on smooth muscle contractility. We concluded that ACM does not seem to have a better biosafety profile than polypropylene.

To proceed with the experimental study of certain vaginal repairs in sheep, we first needed to further explore the potential and feasibility of an implant that can be anchored via additional arms within the pelvis. In a small study, we performed a trocar guided transvaginal insertion of a purpose made H-shaped implant to fit ovine anatomy and dimensions. No serious complications were identified. We also made the surgical procedure as a video document for educational purposes.

In a subsequent study, the previously described H-shaped mesh and flat mesh were implanted. Both meshes are made from polymeric polyvinidylene fluoride loaded with iron particles which allow its visualization with magnetic resonance (MR). In a longitudinal study, we collected data documenting the stability of the shape and position of the implants. Initially, there was a drop in the effective surface area in both types of implants, where after the area remained stable until the end of the observational period. More detailed analysis of thickness maps obtained from MRI data revealed two deformations patterns, different for the H-shape and flat mesh. Deformation of H-shaped implants was most probably due to distinct biomechanical properties of its central part and arms, whereas flat implants displayed a heterogenic pattern most probably linked with pore aggregation caused by suturing. The implants were well tolerated with a low rate of graft-related complications, the absence of an effect on smooth muscle contractility yet there was an increase in stiffness of the augmented tissue.

In general, this project has shown that pelvic organ prolapse is linked with maternal age and delivery-related injuries. Up to every eight women may have a symptomatic prolapse already one year after their first delivery. Moreover, those with muscle injury have a higher short-term risk of pelvic organ prolapse development. To improve our knowledge we further explored the potential of a large ovine model for prolapse and vaginal surgery. We showed that many anatomical and morphological features and vaginal wall changes induced by specific lifespan factors (first delivery, artificial menopause, and hormonal replacement) are similar to what is observed in women. We further used this model for testing novel implants and mesh visualization techniques. We believe that the ovine model can be used in future research on pelvic organ prolapse pathophysiology and novel treatment modalities.

SAMENVANTTING

Vaginale verzakking (ook prolaps genoemd) wordt gedefinieerd als het abnormaal uitzakken van bekkenbodemorganen doorheen de vaginale opening. Deze aandoening kan erg storend zijn. De voornaamste risico factoren zijn vaginale bevalling en ouderdom. Wij wilden nieuwe methodes evalueren om risicofactoren voor latere verzakking te identificeren zowel in klinische als experimentele omstandigheden. In een klinische studie bepaalden we het impact van het maternele gewicht en leeftijd en enkele arbeids- en bevallingsparameters op latere bekkenbodemdisfuncties, met name prolaps. Daarnaast deden we meerdere experimentele studies in een groot dierenmodel, dat bruikbaar is bij het zoeken naar zowel het ontstaan van prolaps als de chirurgische behandeling.

De klinische studie werd uitgevoerd in Praag (Tsjechië) op een cohorte van 987 nullipara die voor het eerst vaginaal bevielen. Een jaar later had ongeveer één vrouw op drie urinaire incontinentie, 13% vaginale verzakking tot aan de vaginale opening, en 3.3% had anorectale klachten, in het bijzonder pijnlijke ontlasting. 18% van de bevallen vrouwen hielden er een afrukking van de m. levator ani aan over, en 17% vertoonden hiatale "ballooning", d.i. een abnormale rekbaarheid van de damstreek. Beide laatste verschijnselen werden eerder al in verband gebracht met de latere ontwikkeling van verzakkingssymptomen en herval na eerdere chirurgische behandeling. Zowel de leeftijd van de moeder als haar "body mass index" waren gerelateerd aan het optreden van urinaire incontinentie, en voor prolaps speelde enkel de leeftijd een rol. Levator avulsie was gerelateerd aan forcipale extractie, en invers gerelateerd aan epidurale anesthesie en eerste graads ruptuur van de dam.

In het schapenmodel voerden we eerst een vergelijkende anatomische studie uit met het vrouwelijk bekken. Daarna brachten de gevolgen in kaart van bepaalde scharnierpunt gebeurtenissen in het leven van een vrouw, zoals de eerste bevalling, menopause en het artificieel substitueren van het laatste. We konden vele structurele (anatomische) gelijkenissen aantonen, zoals daar zijn de vaginale afmetingen, de samenstelling en de aanhechting van de levator spier. Er zijn wel verschillen, zoals het ontbreken van een sacrospineus ligament, een inwendige obturator spier en ook van het membraan tussen de twee obturator spieren. De bekkenbodem anatomie lijkt aangepast aan dat van een viervoetig dier en het gebruik van een staart. Ook bij het schaap blijken bovenstaande gebeurtenissen een diepgaand effect te hebben op de actieve and passieve biomechanische eigenschappen van de vagina. Na de eerste vaginale bevalling is de vagina wijder, het distale derde lakser, en de vaginale gladde spiercellen kunnen minder kracht ontwikkelen. Na castratie vernauwt de vagina wat en wordt die ook minder compliant. Hormoon vervanging heeft de omgekeerde effecten. De beperkte histologische veranderingen in de gemenopauseerde vagina zijn vergelijkbaar met die bij de vrouw.

We bestudeerden ook de gastheer-respons op nieuwe, alternatieve implantaten die mogelijks naar de markt zouden gebracht worden. Zo vergeleken we de performantie van bovien-gederiveerde acellulare

gecross-linkte collageen matrix (ACM) met polypropylene meshes, wanneer deze gebruikt worden voor een achterwandherstel. Na 6 maanden waren er enerzijds meer lokale mesh complicaties, anderzijds waren de biomechanische testen vergelijkbaar. Meer nog, wanneer er toch resorptie was van het implant, verminderde dit de contractiliteit van de vagina. Dit preklinisch onderzoek deed ons besluiten dat dit type implant geen beter veiligheidsprofiel heeft dan polypropyleen.

Daarna wilden we dit dierenmodel gebruiken om chirurgische procedures mee te testen. We ontwikkelden een schapenmodel voor vaginale implantatie van meshes die verankerd kunnen worden aan spieren of ligamenten (van het type dat ook klinisch gebruikt wordt). In een haalbaarheid studie plantten we op maat gemaakte H-vormige meshes in, waarbij de armen dienen voor verankering. Deze konden zonder intra-operatieve complicaties geplaatst. We stelden een videodemonstratie van het onderzoek ter beschikking. Deze operatietechniek werd dan gebruikt voor een grotere prospectieve vergelijkende studie met twee implantaten, het ene een vlakke mesh die ingehecht wordt, en de andere de H-vormige mesh hierboven beschreven. Beiden zijn van polyvinidylene fluoride filamenten gemaakt. Tijdens de productie worden ijzer micropartikels met het polymeer gemengd, wat visualizatie van het implant bij magnetische resonantie (MR) beeldvorming toelaat. In een longitudinale studie documenteerden we de stabiliteit van de vorm en positie van het implant. Op korte termijn bleken de implantaten te "krimpen", t.t.z. in oppervlakte te verkleinen. Tijdens de verdere ingroei bleeft de oppervlakte constant. De initiele krimp vertoonde twee patronen. De H-vormige, verankerde implantaten plooiden ter hoogte van de intersectie van de armen en het lichaam van de "H". Vlakke, vrije implantaten daarentegen vertoonden een heterogeen patroon van vooral lokale aggregatie van poriën, vermoedelijk t.h.v. de hechtingen. De implantaten werden lokaal goed getolereerd, hadden geen meetbaar effect op de vaginale contractiliteit, maar de reconstructie was toch stijver dan het natieve weefsel.

Samengevat heeft ons studiewerk aangetoond dat vaginale verzakking klinisch gelinkt is aan een hogere leeftijd bij eerste bevalling en aan geboorte-trauma. Een op acht vrouwen had een symptomatische prolaps binnen het eerste jaar na de bevalling. Wanneer er levator avulsie was, waren de gevolgen meer uitgesproken. In het translationeel onderzoeksgedeelte onderzochten we de bruikbaarheid van het schapenmodel voor fysiologisch onderzoek evenals voor experimenteel chirurgische studies. We toonden aan dat er veel anatomische en morfologische gelijkenissen zijn. Bepaalde gebeurtenissen, zoals eerste vaginale bevalling, artificiële menopause en hormoon vervangingstherapie, hebben gelijkaardige effecten op de vagina van de ooi, als wat wordt vastgesteld bij de mens. We hebben dit diermodel gebruikt voor het testen van specifieke vaginale implantaten, zoals PVDF-implanten die op MR zichtbaar zijn. Samengevat denken we dat dit schapenmodel verder gebruikt kan worden in het onderzoek naar oorzaken en oplossingen van bekkenbodemproblemen.

SOUHRN

Sestup pánevních orgánů je definován jako stav, při kterém pánevní orgány vystupují skrze poševní vchod. Nejvýznamnějším rizikovým faktorem je vaginální porod a věk. V této práci jsme se zaměřili na použití moderních metod při vyšetřování specifických rizikových faktorů pro rozvoj sestupu pánevních orgánů a jeho léčby v klinickém a v experimentálním prostředí. V klinické části jsme hodnotili vliv specifických rizikových faktorů jak na vznik sestupu pánevních orgánů, tak na ostatní druhy onemocnění pánevního dna u prvorodiček. V experimentální části, jsme se věnovali podrobnějšímu popisu ovčího modelu pro vznik, rozvoj a chirurgickou léčbu pánevního sestupu.

Klinická studie proběhla v České Republice v Praze a zahrnovala 987 zdravých žen s jednočetnou graviditou, které dokončily svůj první porod vaginální cestou. Při kontrole na urogynekologické ambulanci jeden rok po porodu udávala jedna třetina žen nechtěné úniky moči, 13% mělo sestup pánevních orgánů, jehož vedoucí bod dosahoval oblasti poševního vchodu (hymen) nebo před něj, a 3.3% žen mělo ano-rektální obtíže, které byly spojené hlavně s bolestivou defekací. V důsledku vaginálního porodu došlo u 18% k odtržení části *musculus levator ani* a u 17% k jeho přetažení, které se projevilo nadměrně roztažitelným genitálním hiatem při Valsalvově manévru tzv. ballooningem. Oby typy poranění byly v minulosti označeny jako rizikové pro vznik symptomatického sestupu a pro jeho recidivu po operačním výkonu. V naší studii jsme jako rizikové faktory pro inkontinenci moči identifikovali věk a BMI, a pro sestup pánevních orgánů věk. Nejvýraznějším rizikovým faktorem pro odtržení *musculus levator ani* byl klešťový porod, jako protektivní se ukázalo použití epidurální analgezie a poranění hráze I stupně.

V experimentální části výzkumu jsme se nejprve zaměřili na porovnání anatomie pánevního dna ovce a ženy. Následně jsme studovali změny poševní stěny vyvolané specifickými životními událostmi (první porod, menopausa, náhradní hormonální terapie). Byli jsme schopni identifikovat velké množství anatomických a morfologických podobností, jako jsou rozměry pochvy, složení a organizace poševní stěny či úpony *musculus levator ani*. Některé anatomické struktury, které známe u ženy, nejsou ovcí vyvinuté (*lig. sacrospinosum, musculus obturatotrius internus, membrana obturatoria*). Jejich pánevní dno je přizpůsobeno pozici těla (čtyřnožec) a jeho součástí je ocas. Během studií jsme zjistili, že specifické životní události mají vliv na aktivní a pasivní biomechanické vlastnosti ovčí pochvy. Po prvním vaginálním porodu byla ovčí pochva prostornější, její distální část je poddajnější a hladká svalovina vykazovala nižší kontraktilitu. Po uměle vytvořené menopause se pochva celkově zúžila a její stěny byly tužší. Tyto změny byly částečně vratné pod vlivem náhradní estrogenní terapie, např. pokles tuhosti stěny ve střední části pochvy na úroveň srovnatelnou s premenopausálními ovcemi. Podobnější histologické vyšetření odhalilo minimální změny, které sice odpovídají změnám pozorovaným u žen, ale které dostatečně nevysvětlily pozorované biomechanické změny.

V druhá části jsme se zaměřili na studium vlivu a chování nových implantátů určených k léčbě sestupu. Ve srovnávací studii jsme studovali vliv

a chování nebuněčného "cross-link" kolageního implantátu derivovaného z hovězího perikardu (acellular collagen matrix, ACM), jako alternativy běžně používaného polypropylenu. Oba typy implantátů byly vloženy a obdobným způsobem fixovány v rektovaginálním septu ovce. Po šesti měsících jsme zaznamenali větší množství lokálních komplikací u ovcí s ACM. Biomechanické vlastnosti kompozitu (tkáň-implantát) byly srovnatelné s polypropylenem. A dále jsme také pozorovali částečnou degradaci ACM a jeho negativní vliv na kontraktilitu hladkých svalových buněk v poševní stěně. Došli jsme k závěru, že ACM se nezdá být bezpečnější alternativou k polypropylenu.

Proto abychom mohli provést dlouhodobější observační studii zahrnující specifický typ rekonstrukce poševní stěny, jsme nejprve provedli malou studii ověřující proveditelnost a bezpečnost zavedení implantátu tvaru "H" do rectovaginálního septa pomocí trokarů. Implantát, který byl vyroben, tak aby odpovídal anatomii ovčí pánve, byl pomocí ramen připevněn k pevnějším strukturám. Během operací jsme nezaznamenali závažné komplikace a celý postup jsme zachytili v edukačním videu.

V poslední experimentální studii jsme výše popsaný implantát tvaru „H" porovnávali s obdélníkovým implantátem fixovaným jednotlivými stehy v rektovaginálním septu. Oba implantáty byly vyrobené polyvinidylene flouridu obohaceného o železité částice, které umožnily jejich viditelnost na magnetické rezonanci. V dlouhodobé studii jsme poté sbírali informace změně tvaru a uložení implantátů. Krátce po implantaci jsme u obou typů implantátů zaznamenali výrazné zmenšení efektivní plochy, která však zůstala až do konce observačního období stabilní. Detailní zhodnocení tloušťky rekonstruovaných modelů nám pomohlo odhalit odlišný charakter deformace, který byl závislý na typu implantátu. Ohnutí, které jsme pozorovali u implantátu tvaru „H", bylo pravděpodobně důsledkem rozdílných mechanických vlastností jednotlivých komponent (ramena vs. centrální část). Deformace obdélníkových implantátů byla různorodá a souvisela nejspíše s agregací pórů v důsledku fixace k okolní tkáni. Jinak byly implantáty dobře tolerovány a neměly vliv na kontraktilitu hladké svaloviny.

Celý tento projekt ukázal, že sestup pánevních orgánů spojen jednak s poraněními pánevního dna vzniklými v průběhu vaginálního porodu a jednak s věkem rodičky. Již jeden rok po porodu může mít až každá osmá žena symptomatický sestup. Ženy, které utrpěly poranění svalů pánevního dna, jsou vystaveny riziku časnějšího vzniku sestupu. Proto abychom zlepšili naše znalosti o vzniku, vývoji a chirurgické léčbě sestupu pánevních orgánů, jsme podrobněji studovali ovčí model. Identifikovali jsme velké množství anatomických a morfologických podobností a také popsali změny poševní stěny vyvolané specifickými životními událostmi (první porodu, uměle vytvořená menoupauza či hormonální susbstituční terapie), které jsou podobné změnám popisovaným u žen. Ovčí model jsme dále použili pro testování nových implantátů a zobrazovacích technik. Veříme, že ovčí model je možné v budoucnosti použít pro studium patofyziologie sestupu pánevních orgánů a pro testování nových léčebných metod a postupů.

CURRICULUM VITAE

Name: Iva Urbankova
Adress: V Klidu 2, 40011 Usti nad Labem, Czech Republic
Date and place of birth: 27.6.1984, Usti nad Labem
E-mail :   iva.urbankova@upmd.eu
Nationality: Czech

Education and employment history:

1995 -2002   Gymnazium dr. Vaclava Smejkala (grammar school), Usti nad Labem, Czech Republic

2002 - 2008   Third Medical Faculty, Charles University, Prague, Czech Republic

Since 10/2008   Gynecological - Obstetric department of Institute for the care of mother and child, Prague, Czech Republic

Since 10/2012   Joint doctorate on University of Leuven Belgium and Third Medical Faculty, Prague, Charles University, Czech Republic

Additional information on education:

2006   Course on laparoscopic anatomy

2006   Student scientific activity during pregradual studies
                Topic: Clinical anatomy of the inguinal region

2009   Course in the Fundamentals of Research Work Administered, Academy of science, Prague, Czech Republic

2013/2014   Course on statistics, Scientific writing, Writing for general audience, Email writing, KU Leuven, Belgium

2/2014   Course on Laboratory Animal Science for persons that carry out experiments or take part in them, KU Leuven, Belgium

4/2016   Course on Laparoscopic sacrocolpopexy, Faculty of Medicine in Pilsen, Charles University, Czech Republic

THESIS RELATED PUBLICATION ACTIVITY:

with IF

- <u>Urbankova I</u>, Vdoviakova K, Rynkevic, R, Sindhwani N, Deprest D, Feola A, Herijgers P, Krofta L, Deprest J, Comparative anatomy of the ovine and female pelvis; Gynecol Obstet Invest. 2017; Jan 27; doi: 10.1159/000454771, IF 1.67

- <u>Urbankova I</u>, Callewaert G, Sindhwani N, Turri A, Hympanova L, Feola A, Deprest J, Transvaginal Mesh Insertion in the Ovine Model. J Vis Exp. 2017; Jul (27);(125); doi: 10.3791/55706, IF 1.2

- <u>Urbankova I</u>, Sindhwani N, Callewaert G, Turri A, Rinkijevic R, Hympanova L, Feola A, Deprest J, In vivo documentation of shape and position changes of MRI-visible mesh placed in t rectovaginal septum. J Mech Behav Biomed Mater. 2017 Nov (75), 379 – 89, doi: 10.1016/j.jmbbm.2017.08.005, IF 1.96

without IF

- Endo M, <u>Urbankova I</u>, Vlacil J, Sengupta S, Deprest T, Klosterhalfen B, Feola A, Deprest J. Cross-linked xenogenic collagen implantation in the sheep model for vaginal surgery. Gynecol Surg [Internet]. 2015; 113–22; doi: 10.1007/s10397-015-0883-7, without IF

OTHER PUBLICATIONS:

with IF

- Sindhwani N, Feola A, De Keyzer F, Claus F, Callewaert G, <u>Urbankova I</u>, Ourselin S, D´hooge J, Deprest J. Three-dimensional analysis of implanted magnetic-resonance-visible meshes. Int Urogynecol J [Internet]. 2015;26(10):1459–65. doi: 10.1007/s00192-015-2681, IF 1.96

- Feola A, Endo M, <u>Urbankova I</u>, Vlacil J, Deprest T, Bettin S, Klosterhalfen B, Deprest J. Host reaction to vaginally inserted collagen containing polypropylene implants in sheep. Am J Obstet Gynecol [Internet]. Elsevier; 2015 Dec 11;212(4): 474.e1–474.e8. doi: 10.1016/j.ajog.2014.11.008, IF 4.7

- Sindhwani N, Liaquat Z, <u>Urbankova I</u>, Vande Velde G, Feola A, Deprest J. Immediate postoperative changes in synthetic meshes – In vivo measurements. J Mech Behav Biomed Mater [Internet]. Elsevier; 2015; 55: 228–3; doi: 10.1016/j.jmbbm.2015.10.015, IF 2.87

- Sabiniano R, <u>Urbankova I</u>, Callewaert G, Lesage F, Hillary C, Osman NI, Cappele R, Deprest J, MacNeil S. Evaluating Alternative Materials for the Treatment of Stress Urinary Incontinence and Pelvic Organ Prolapse: A Comparison of the In Vivo Response to Meshes Implanted in Rabbits. J Urol. 2016;196(1):261–9; doi: 10.1016/j.juro.2016.02.067, IF 4.47

- Darzi S, <u>Urbankova I</u>, Su K, White J, Lo C, Werkmeister JA, Gargett CE, Deprest J, Alexander D. Tissue response to collagen containing polypropylene meshes in an ovine vaginal repair model. Acta Biomater. 2016 Jul 15 15;39: 114/123; doi: 10.1012/j.actbio.2016.05.010, IF 6.02

- Krofta L, Havelková L, <u>Urbánková I</u>, Krčmář M, Hynčík L, Feyerreisl J, Finite element model focused on stress distribution in the levator ani muscle during vaginal delivery, Int. Urogynecol J, 2017 Feb;(28)2:275-284.; doi: 10.1007/.00192-016-3126-1; IF 1.96

- Hympanova L, Mori da Cunha MGMC, Rynkevic R, Zündel M, Gallego MR, Vange J, Callewaert G, <u>Urbankova I</u>, Van der Aa F, Mazza E, Deprest J., Physiologic musculofascial compliance following reinforcement with electrospun polycaprolactone-ureidopyrimidinone mesh in rat model. J Mech Behav Biomed Mater 2017, Jun 27(74), 349 – 357; doi:10.1016/j.jmbbm.2017.06.032, IF 1.96

without IF
- Stranák Z, Kucerová I, Urbánková I, Goldová B, Vítková I, Rygl M, Pýcha K, Krofta L, Current options of prenatal diagnosis in congenital diaphragmatic hernia, Stranak Z, Ceska Gynekol. 2009 Jun;74(3):183-7; PMID: 19642516

- Urbankova I, Haaková L, Stranak Z, Krofta L., Prenatal diagnosis and management of fetuses with congenital diaphragmatic hernia, Ceska Gynekol. 2011 Dec;76(6):439-42. PMID: 22312837